University of Alberta

Synthetic Lethal Targeting of Polynucleotide Kinase/Phosphatase and its Potential Role in Directed Cancer Therapies

By

Todd Mereniuk

A thesis submitted to the Faculty of Graduate Studies and Research in partial fulfillment of the requirements for the degree of

Doctor of Philosophy

in

Experimental Oncology

Department of Oncology

Fall 2012
Edmonton, Alberta

ABSTRACT

Synthetic lethality arises when simultaneous disruption of two non-essential, non-allelic genes in the same cell causes lethality. This phenomenon has been shown to occur between proteins involved in DNA repair and much attention to date has focused on poly(ADP-ribose) polymerase and the BRCA proteins. Synthetic lethality holds great promise in the development of tailor-made treatments for each specific patient and as such, there exists a need to expand the repertoire of known synthetic lethal associations in human cells. We intended to identify novel synthetic lethal relationships and show these lethal combinations need not solely rely on the interactions between two DNA repair proteins.

We performed an siRNA screen of Qiagen's druggable genome to identify synthetic lethal partnerships with another DNA repair protein, polynucleotide kinase/phosphatase (PNKP). We identified 14 currently known tumor suppressors showing potential synthetic lethality with PNKP, including the tyrosine-protein phosphatase SHP-1, and the major tumor suppressor PTEN. SHP-1 has been shown to be lost or diminished in ~90% of malignant prostate tissues, 95% of malignant lymphomas and 100% of NK and T cell lymphomas tested, whereas PTEN is the second most frequently lost tumor suppressor in human sporadic cancers. Therefore, targeted disruption of PNKP may be of benefit to a large subset of cancer sufferers.

Further investigation into the mechanisms underlying synthetic lethality revealed that depletion of SHP-1 causes an increase in the production of reactive oxygen species. This finding suggests a possible mechanism for synthetic lethality beyond widely accepted models seen with co-disruption of PARP and the BRCA proteins in which reactive oxygen species enhance the level of unrepaired strand breaks. We also demonstrated that PTEN's cytoplasmic phosphatase function is important to rescue the lethal phenotype upon co-disruption with PNKP. Furthermore, loss of both the 3' phosphatase and 5' kinase function of PNKP in double-strand break repair contribute to synthetic lethality.

Since tumor suppressor proficient cells can withstand PNKP disruption, only the suppressor protein depleted cancer cells should be sensitive to PNKP inhibition. This allows for the development of a highly selective and patient-specific cancer therapy using the targeted disruption of PNKP with either a small molecule inhibitor of PNKP, or siRNA. Furthermore, since normal tissues should be minimally affected by treatment, side effects typically associated with cancer therapies should be minimized.

TABLE OF CONTENTS

LIST OF TABLES

LIST OF FIGURES

LIST OF ABBREVIATIONS

Abbreviation	Full Name
3'OH	3' hydroxyl group
3'P	3' phosphate group
3'PG	3' phosphoglycolate group
5'dRP	5' deoxyribose phosphate
5'P	5' phosphate group
A12B4C3	2-(1-hydroxyundecyl)-1-(4-nitrophenylamino)-6-phenyl-6,7a-dihydro-1H-pyrrolo[3,4-b]pyridine-5,7(2H,4aH)-dione
A549-LZ	Vector control of PolβDN cells
A549-SC	Synonym of A549-Scramble
A549-Scramble	A549 cells expressing a scrambled shRNA
A549δPNKP	A549 cells stably depleted of PNKP
A549δPNKPkin	A549δPNKP cells but PNKP kinase proficient
A549δPNKPphos	A549δPNKP cells but PNKP phosphatase proficient
A549δPNKPphoskin	A549δPNKP with full length PNKP but both kinase and phosphatase deficient
A549δSHP-1	A549 cells stably depleted of SHP-1
ADME	Absorption, distribution, metabolism and excretion
ALCL	Anaplastic large-cell lymphoma
AOA1	Ataxia-oculomotor apraxia 1
AP	Apurinic/apyrimidinic
APE1	AP endonuclease 1
APF	Aminophenyl fluorescein
APTX	Aprataxin
ASN	Negative scrambled control siRNA
AT	Ataxia telangiectasia

ATLD	Ataxia telangiectasia-like disorder
ATLL	Adult T cell lymphoma/leukemia
ATM	Ataxia telangiectasia mutated
BARD1	BRCA1 associated RING domain 1
BER	Base excision repair
BH3I-1	5-(p-bromobenzylidine)-α-isopropyl-4-oxo-2-thioxo-3-t hiozolidineacetic acid
BLM	Bloom syndrome, RecQ helicase-like
BRCA	Breast cancer associated
BRCA1	Breast cancer associated, early onset 1
BRCA2	Breast cancer associated, early onset 2
BRCAness	Behaves as if harbouring dysfunctional BRCA protein(s)
CHAPS	3-[(3-Cholamidopropyl)dimethylammonio]-1 propanesulfonate
CK2	Casein kinase 2
DAPI	4’6-diamidino-2-phenylindole
DMEM/F12	Dulbecco’s modified eagle medium: nutrient mixture F-12
DNA2	DNA replication helicase 2 homolog
DNA-PK_{cs}	DNA dependent protein kinase catalytic subunit
DPQ	3,4-dihydro-5[4-(1-piperindinyl)butoxy]-1(2H)-isoquinoline
DSB(s)	Double-strand break(s)
DSBR	Double-strand break repair
dsDNA	Double-stranded DNA
DSS1	Deleted in split hand/split foot 1
EME1	Essential meiotic endonuclease 1
FBS	Fetal bovine serum
Gy	Gray
FA	Fanconi anemia

FANCA	Fanconi anemia, complementation group A
FANCB	Fanconi anemia, complementation group B
FANCC	Fanconi anemia, complementation group C
FANCD1	Fanconi anemia, complementation group D1 (synonym of BRCA2)
FANCD2	Fanconi anemia, complementation group D2
FANCE	Fanconi anemia, complementation group E
FANCF	Fanconi anemia, complementation group F
FANCG	Fanconi anemia, complementation group G
FANCI	Fanconi anemia, complementation group I
FANCJ	Fanconi anemia, complementation group J
FANCL	Fanconi anemia, complementation group L
FANCM	Fanconi anemia, complementation group M
FANCN	Fanconi anemia, complementation group N
FEN1	Flap endonuclease 1
FHA	Forkhead associated
FITC	Fluorescein isothiocyanate
GPCR	G-protein couple receptor
H9T3-7-1	EM9 expressing wildtype levels of XRCC1
H101	Lab-made mouse monoclonal antibody towards PNKP
HBSS	Hanks balanced salt solution
HD	Hodgkin’s disease
HJ	Holliday junction
HPF	Hydroxyphenyl fluorescein
HR	Homologous recombination
KCND2	potassium voltage-gated channel, Shal-related subfamily, member 2
KRAS	v-Ki-ras2 Kirsten rat sarcoma viral oncogene homolog
LB	Lysogeny broth

Lig3	DNA ligase III
Lig4	DNA ligase IV
M059J	Glioblastoma cells lacking DNA-PK_{cs} activity
M059K	Glioblastoma cells (from same tumour as M059J) but DNA-PK_{cs} active
MCF7δPNKP	MCF7 cells stably depleted of PNKP
MCL	Mantle cell lymphoma
MCSZ	Microcephaly, early-onset, intractable seizures and developmental delay disorder
MLH1	MutL homolog 1
MRN	Mre11-Rad50-Nbs1 complex
MTD	Maximum tolerated dose
MSH2	MutS homolog 2
MSH6	MutS homolog 6
mtBER	Mitochondrial base excision repair
mtLig3	Mitochondrial DNA ligase III
MUS81	Methyl methansulfonate and ultraviolet-sensitive gene clone 81
NBS	Nijmegen breakage syndrome
NHEJ	Non-homologous end joining
PALB2	Partner and localizer of BRCA2
PAR	Poly(ADP-ribose)
PARP	Poly(ADP-ribose) polymerase
PBS	Phosphate buffered saline
PD	Pharmacodynamics
PDK1	Phosphoinositide-dependent kinase-1
PI3K	Phosphoinositide-3-kinase
PINK1	PTEN-induced putative kinase 1
PIP2	Phosphatidylinositol 4,5-bisphosphate
PIP3	Phosphatidylinositol 3,4,5-triphosphate
PK	Pharmacokinetics

PL	Peripheral T cell lymphoma
PNKP	Polynucleotide kinase/phosphatase
Polβ	DNA polymerase β
PolβDN	A549 cells expressing a DNA polymerase β dominant negative
PTEN	Phosphatase and tensin homolog deleted on chromosome 10
PTPN6	Synonym of SHP-1
P-XRCC1	Phosphorylated XRCC1
P-XRCC4	Phosphorylated XRCC4
qRT-PCR	Quantitative real-time reverse transcription polymerase chain reaction
RECQL4	RecQ protein-like 4
Resazurin	7-Hydroxy-3*H*-phenoxazin-3-one-10-oxide
RNAi	RNA interference
ROS	Reactive oxygen species
RPA	Replication protein A
SCAN1	Spinocerebellar ataxia with axonal neuropathy 1
SDS-PAGE	Sodium dodecyl sulfate polyacrylamide gel electrophoresis
S.E.	Standard error
siRNA	Small interfering RNA
SHP-1	Src homology region 2 domain-containing phosphatase-1
ssDNA	Single-stranded DNA
shRNA	Small hairpin RNA
spSSBR	Short-patch single-strand break repair
SSB(s)	Single-strand break(s)
SSBR	Single-strand break repair
ssDNA	Single-stranded DNA

STK33	Serine/threonine kinase 33
TAP1	Transporter 1, ATP-binding cassette, sub-family B (MDR/TAP)
TDP1	Tyrosyl-DNA phosphodiesterase
UV	Ultraviolet
WR1065	2-[(3-aminopropyl)amino] ethanethiol dihydrochloride
WRN	Werner syndrome, RecQ helicase-like
XLF	XRCC4-like factor
XRCC1	X-ray cross complementing group 1
XRCC4	X-ray cross complementing group 4

Chapter 1: Introduction

INTRODUCTION

1.1 DNA REPAIR

Every day, the genomic complement of every single human cell is subjected to tens of thousands of damaging lesions (Lindahl & Nyberg, 1972). An astonishing 18,000 purine residues are lost through the spontaneous hydrolysis of the glycosidic bond (Lindahl & Nyberg, 1972; Nakamura et al, 1998). Furthermore, cytosine undergoes deamination between 100-500 times per day to generate the RNA-specific base uracil in DNA, which must then be recognized and repaired (Frederico et al, 1990; Lindahl & Nyberg, 1974; Shen et al, 1994). Additionally, naturally occurring reactive oxygen species (ROS, see appendix for full list of abbreviations) generated through normal cellular metabolism can interact with the DNA bases or the DNA backbone itself generating base damage, single-strand breaks (SSBs) and/or double-strand breaks (DSBs). All the aforementioned damages must be efficiently and effectively repaired for the successful propagation and segregation of genetic material to subsequent generations.

These examples, however, only highlight the production of *spontaneous* DNA damage and do not include environmental factors such as heat, UV or airborne contaminants that provide a multitude of DNA damage themselves. These factors can increase the rate of deamination (heat), cause base or DNA backbone damage directly (UV and environmental factors, such as vinyl chloride) or generate intra-/inter-strand cross-links (environmental factors, such as UV and ionizing radiation)

putting even more stress on cellular DNA. The consequences to the cell can be catastrophic if it is unable to fully repair this damage and can potentially lead to several adverse outcomes (i.e. neurological disorders, cell death or various cancers) (Ahel et al, 2006; Caldecott, 2003a; Caldecott, 2008; Hartlerode & Scully, 2009; Reynolds et al, 2009). It is therefore imperative that cells are able to rectify these damages, and fortunately, through evolution most organisms including humans have developed a highly coordinated complement of DNA repair pathways capable of restoring genomic integrity.

1.1.1 Base Excision Repair (BER)

BER is a repair pathway active throughout the cell cycle and is responsible for removing DNA bases damaged primarily by ROS, ionizing radiation and alkylating agents. The damaged base is first recognized and excised by a DNA glycosylase. DNA glycosylases fall into one of two categories, monofunctional or bifunctional DNA glycosylases. Monofunctional DNA glycosylases recognize and flip the damaged base out of the double helix before cleaving the glycosidic bond to leave an apurinic/apyrimidinic site (AP site) in the DNA. The DNA backbone at the AP site is then cleaved by an AP endonuclease to generate an SSB. Bifunctional DNA glycosylases, however, also possess an AP lyase activity that can generate the SSB at the site of damage without the need for a separate AP endonuclease. Each AP endonuclease (or bifunctional DNA glycosylase) leaves characteristic DNA ends, which are either competent

for elongation and ligation, or require additional processing to generate correct termini (listed in Figure 1.1). Once end correction occurs, downstream DNA repair proteins access the strand break to continue repair, which proceeds through either the short-patch or long-patch DNA repair pathway.

1.1.2 Short-patch single strand break repair (spSSBR)

spSSBR is the major pathway for repair of SSBs caused by endogenous DNA damaging agents and occurs by the sequential action of several key proteins (Figure 1.2) (Caldecott, 2008; Lindahl & Nyberg, 1972). First, poly(ADP-ribose) polymerase (PARP) recognizes and binds the SSB, which causes PARP to undergo a conformational change to become activated (Lilyestrom et al, 2010). Activated PARP then catalyzes the formation of long poly(ADP-ribose) (PAR) polymers on itself, transcription factors, and histones (H1 and H2B) near the SSB (Allinson et al, 2003; Audebert et al, 2006; El-Khamisy et al, 2003; Kim et al, 2004; Lilyestrom et al, 2010; Masaoka et al, 2009; Mortusewicz et al, 2007; Nusinow et al, 2007; Parsons et al, 2005b; Sukhanova et al, 2009; Woodhouse & Dianov, 2008; Woodhouse et al, 2008; Zaniolo et al, 2007). Charge repulsion between the negatively charged PAR residues and DNA leads to the dissociation of poly(ADP-ribosylated) proteins from the DNA, allowing the SSBR machinery unfettered access to the SSB (Ahel et al, 2009; Ahel et al, 2008; Gagne et al, 2006; Gagne et al, 2008; Kim et al, 2004). The poly(ADP-ribosylation) also serves as a recruitment flag for the

a Types of damaged 3′ termini

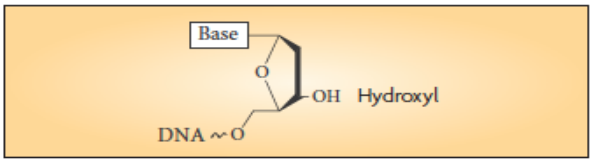

• Undamaged 3′ terminus

Enzyme

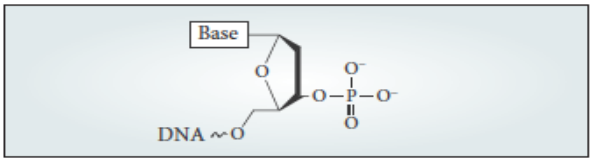

Phosphate
• Direct break; sugar disintegration (ROS)
• Indirect break; BER (ROS, alkylators, spontaneous base damage and/or loss)
• TOP1–SSBs (TOP1 inhibitors, ROS, other genotoxins)

PNKP
(3′-phosphatas

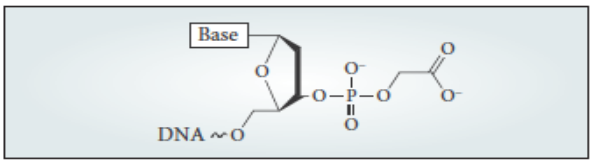

Phosphoglycolate
• Direct break; sugar disintegration (ROS)

APE1

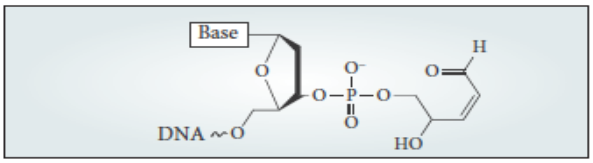

α,β unsaturated aldehyde
• Indirect break; BER (ROS, alkylators, spontaneous base damage and/or loss)

APE1

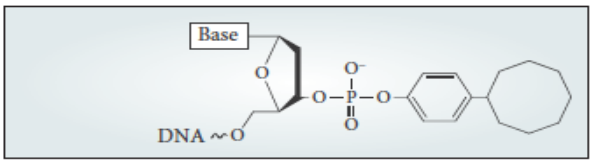

TOP1 peptide
• TOP1–SSBs (TOP1 inhibitors, ROS, other genotoxins)

TDP1

b Types of damaged 5′ termini

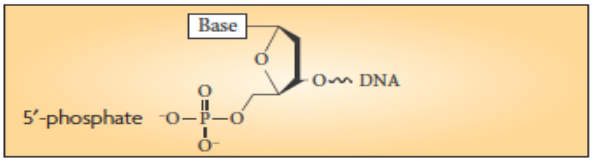

• Undamaged 5′ terminus

Enzyme

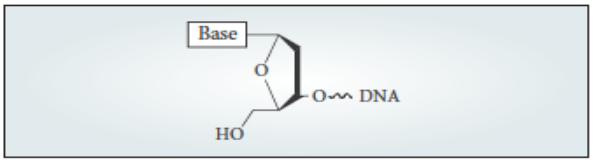

5′-hydroxyl
• TOP1–SSBs (TOP1 inhibitors, ROS, other genotoxins)

PNKP
(5′-kinase)

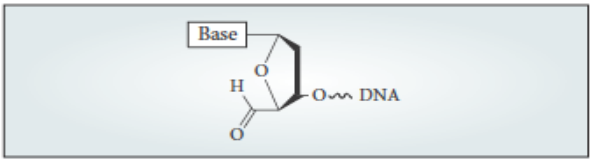

5′-aldehyde
• Direct break; sugar disintegration (ROS)

?

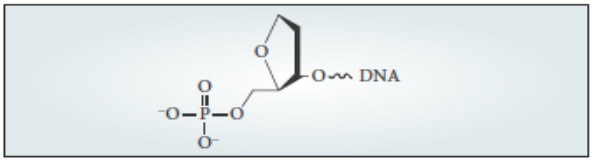

5′-dRP (AP site)
• Indirect break; BER (ROS, alkylators, spontaneous base damage and/or loss)
• Following ROS, this damage can be an oxidized dRP that might require LPR for removal

Pol β

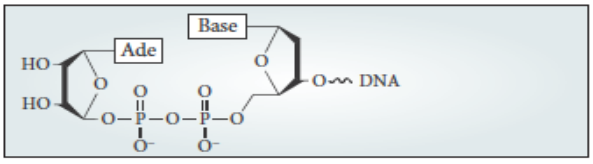

5′-AMP
• Abortive ligase activity (can form at breaks with 5′-P)

APTX

Figure 1.1. Types of DNA damage and their end processing enzymes (Caldecott, 2008). The steps of both spSSBR and lpSSBR are summarized below in Figure 1.2.

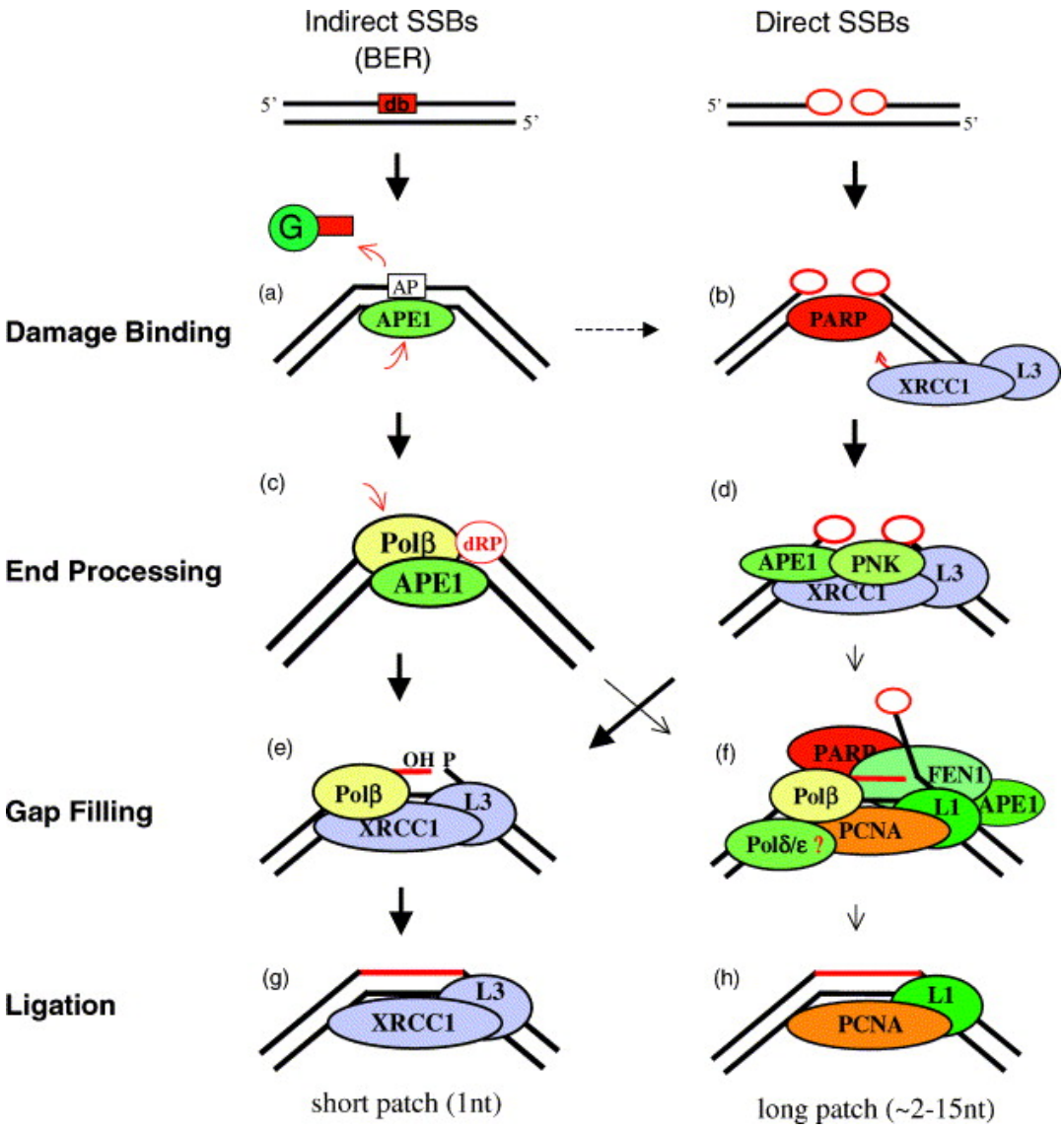

Figure 1.2. spSSBR and lpSSBR (Caldecott, 2003b), the steps of which are outlined in the text. L1 and L3 stand for DNA ligase 1 and DNA ligase 3, respectively.

X-ray cross complementing group 1 (XRCC1), polynucleotide kinase/phosphatase (PNKP), and DNA ligase III (Lig3) heterotrimeric complex (Audebert et al, 2004; Caldecott et al, 1995; El-Khamisy et al, 2003; Horton et al, 2008; Kulkarni et al, 2008; Thompson et al, 1990), which is followed closely by DNA polymerase β (Polβ) (Dianova et al, 2004; Horton et al, 2008; Masaoka et al, 2009; Parsons et al, 2005a; Sukhanova et al, 2009; Vens et al, 2002). XRCC1 mainly serves as a scaffold protein upon which the SSB repair complex is built but it also stimulates the activity and turnover rate of PNKP (Fishel et al, 1994; Mani et al, 2007; Whitehouse et al, 2001). While at the SSB, PNKP utilizes its 3'-phosphatase and 5'-kinase functions to repair damaged DNA end groups to the elongation/ligation competent 3' hydroxyl (3'OH) and 5' phosphate (5'P) groups (Audebert et al, 2006; Bernstein et al, 2005; Dobson & Allinson, 2006; Jilani et al, 1999; Karimi-Busheri et al, 1998; Mani et al, 2001). End damage correction permits Polβ and Lig3 to replace a missing nucleotide if needed and seal the DNA nick, respectively, resulting in error-free repair of DNA (Caldecott, 2007; Caldecott, 2008; Horton et al, 2008; Rass et al, 2007; Thacker & Zdzienicka, 2003).

1.1.3 Long-patch SSBR

The alternative SSBR pathway is termed long-patch SSBR (lpSSBR). The first steps of both branches of SSBR occur in the same fashion, PARP recognizes the SSB and catalyzes poly(ADP-ribosylation) upon itself and other proteins. However, if there is damage that is resistant

to lyase activity of Polβ, but 3'OH groups are restored, repair is fed into lpSSBR (Prasad et al, 2011). Polβ adds several nucleotides onto the 3'OH terminus, and DNA polymerases δ/ε further elongate the DNA if necessary. Elongation occurs beyond the damaged 5' end group generating a DNA flap 2-12 nucleotides long. Flap endonuclease 1 (FEN1) cleaves the flap, including the damaged 5' end, to leave the appropriate 5'P end. Then, DNA ligase I, in conjunction with proliferating cell nuclear antigen, seals the DNA nick, which like spSSBR, results in the error-free repair of DNA (Balakrishnan et al, 2009; Godon et al, 2008; Narayan et al, 2005; Sukhanova et al, 2009; Vens et al, 2002).

DNA end correction is a critical step in SSBR. Without end repair, elongation and ligation cannot occur resulting in the persistence SSBs in the DNA. During subsequent S-phase, as the replication fork traverses the DNA it will encounter these unrepaired SSBs. As the DNA helicase ahead of the replication machinery opens the DNA at the SSB, the SSB would cause a collapse of the replication fork resulting in the formation of DSBs (Figure 1.3). Since there are only 10 naturally occurring DSBs per cell per day, a preponderance of SSBs being converted to DSBs (i.e. tens of thousands per cell per day) could cause an accumulation of DSBs. DSB repair pathways may not be able to cope with the increase in damage, which may eventually lead to cancers, neurological disorders, and cell death (Caldecott, 2008). Therefore, an assortment of DNA end processing enzymes exist in addition to PNKP. Each one is able to repair one or more of the different species of damaged ends produced by genotoxic agents,

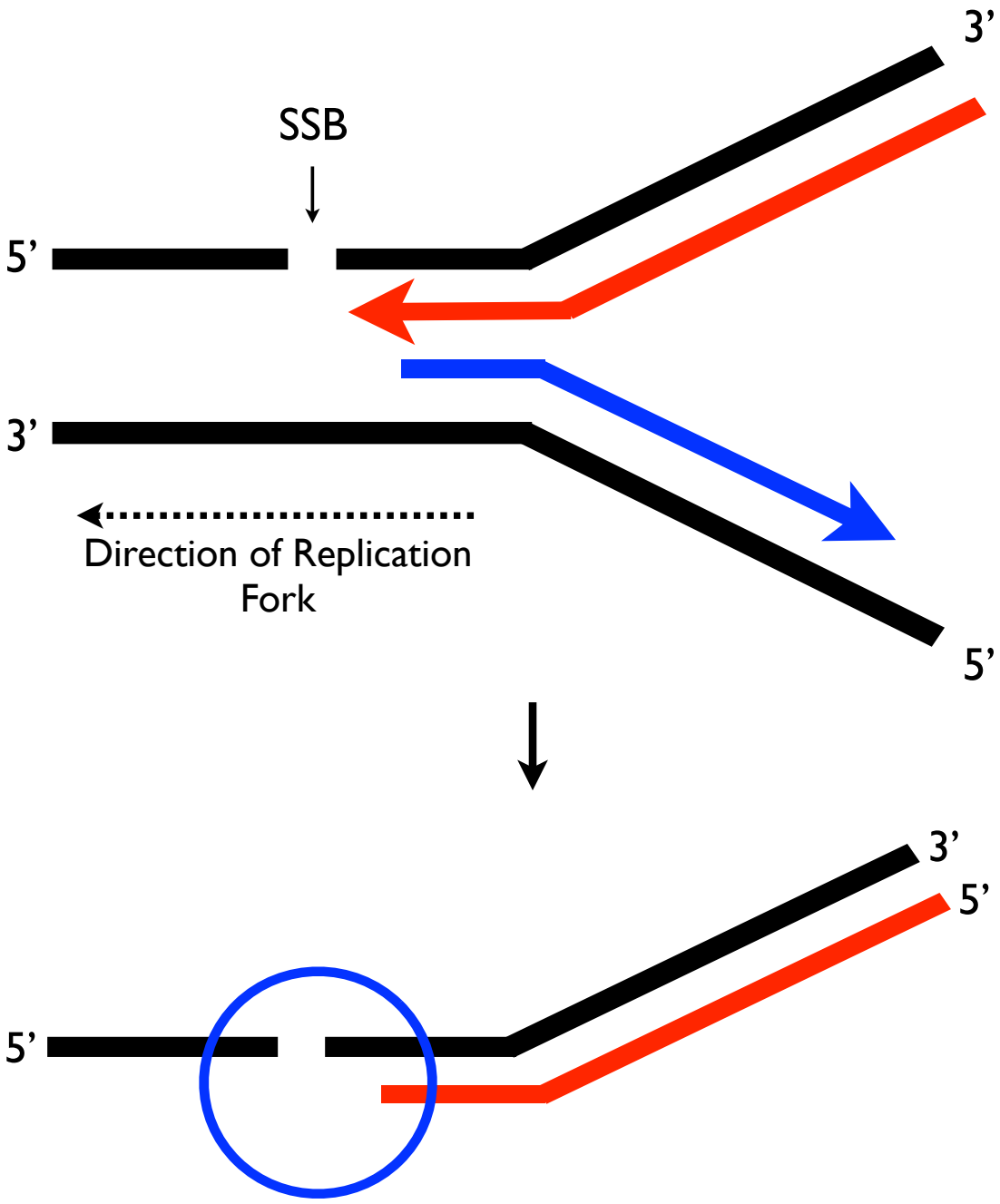

Figure 1.3. Representation of how SSBs can be converted into DSBs through the replication cycle.

thereby helping to restore 3'OH and 5'P termini (listed in Figure 1.1). However, even with all these precautions to repair SSBs, DSBs still occur. They can arise indirectly by the aforementioned avoidance of SSB repair by clastogenic SSBs, or directly from DNA damaging agents. When DSBs occur, one of the two major mammalian DSBR pathways, homologous recombination or non-homologous end joining, act to recognize and repair them.

1.1.4 Homologous recombination (HR)

HR is an error-free DNA DSB repair pathway active during late-S/G_2 phase and utilizes the sister chromatid as a template (Figure 1.4). HR is initiated by the binding of the MRN complex, consisting of Mre11, Rad50, and Nbs1, to the DSB ends (Hopfner et al, 2002; Moreno-Herrero et al, 2005). The DNA ends are kept in close proximity through homodimerization of Rad50 proteins in adjacent MRN complexes (Williams et al, 2008). Next, Nbs1 activates ataxia telangiectasia mutated (ATM) kinase activity through direct interaction, allowing regulatory phosphorylation of several proteins, such as H2AX (Lee & Paull, 2004; Lee & Paull, 2005; Lee & Paull, 2007). ATM phosphorylation also serves to either convert Mre11 into a 5'-3' exonuclease or permit binding of exonuclease 1 thereby inducing DNA resection to create 3'OH overhangs (Matsuoka et al, 2007; Savic et al, 2009). Replication protein A (RPA) rapidly binds the newly forming single-stranded DNA (ssDNA) and serves

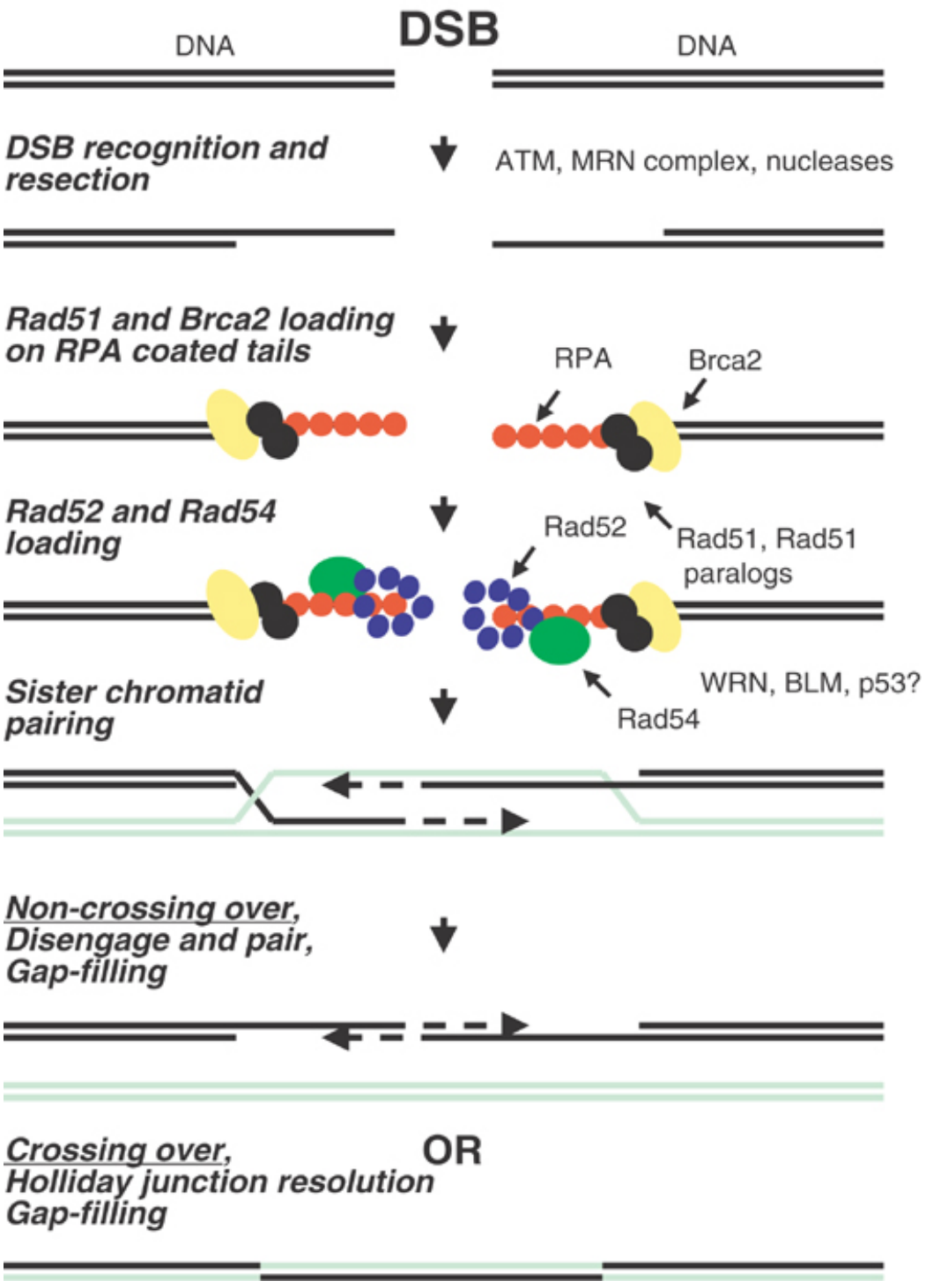

Figure 1.4. Graphical representation of the steps involved in homolgous recombination (Valerie & Povirk, 2003).

to melt DNA secondary structure (Sung & Klein, 2006). Next, multimers of Rad51 are loaded onto the ssDNA, thereby displacing RPA (Bugreev et al, 2009; Hartlerode & Scully, 2009; Pellegrini et al, 2002; Sung & Klein, 2006; Wong et al, 1997). RPA displacement is accomplished through the action of two protein complexes. The first complex, BRCA1/BARD1, promotes the accumulation at the strand break of the second protein complex, BRCA2/DSS1, via PALB2 (partner and localizer of BRCA2) (Hartlerode & Scully, 2009; Sung & Klein, 2006). Once at the DSB, BRCA2/DSS1 promotes loading of Rad51 onto the ssDNA through direct interaction of Rad51 with BRCA2 (Pellegrini et al, 2002; Sharan et al, 1997; Wong et al, 1997). The Rad51 nucleoprotein filament then directs homology search of the sister chromatid, and once a sequence match has been found the invading strand sets up a displacement-loop intermediate (Bugreev et al, 2009; Pellegrini et al, 2002). DNA polymerase η uses the invading strand:sister chromatid DNA duplex as a template to extend DNA (Bolderson et al, 2009; Bryant & Helleday, 2006; Hartlerode & Scully, 2009). The 3' end of the invading strand can then capture the second end of the break, causing the formation of double Holliday Junctions (HJs) (Sung & Klein, 2006).

The next step in HR involves the resolution of HJs. Certain protein complexes exist to complete this important task and each complex generates its own specific type of repair product. For example, Bloom syndrome gene product in complex with topoisomerase IIIα can resolve double HJs to yield non-crossover double-stranded DNA products

(Bachrati & Hickson, 2009; Bugreev et al, 2009; Kikuchi et al, 2009). The MUS81-EME1 complex is also able to resolve HJs, yet produce crossover products (Gaskell et al, 2007; Osman & Whitby, 2007). No matter how the HJs are resolved, the result is error-free repair of DNA.

HR is essential to the conservation and propagation of genetic material, as inherited defects in proteins involved in HR lead to a variety of human disease. For example, inheriting a mutant copy of BRCA1, followed by loss of heterozygosity, accounts for ~40% of inherited breast cancer and ~80% of inherited ovarian cancers (Bolderson et al, 2009; Rass et al, 2007). BRCA1 mutations are inherited as autosomal dominant since one mutant copy leads to ~100% chance of developing breast or ovarian cancer sometime throughout the carrier's life (Bryant et al, 2005; Farmer et al, 2005; Fong et al, 2009; Venkitaraman, 2009). This outlines the importance of HR in resistance to human disease, and represents a possible therapeutic target for directed cancer therapies.

1.1.5 Non-homologous end joining (NHEJ)

NHEJ is the other major DSBR pathway in mammalian cells (Figure 1.5), and is the most common pathway for the resolution of DSBs (Chan et al, 2002; Hartlerode & Scully, 2009; Iliakis, 2009; Lieber, 2010; O'Connor et al, 2007; Pastwa & Blasiak, 2003; Yoo & Dynan, 1999). NHEJ is an iterative process occurring independently of cell cycle, but it is particularly important during G_0, G_1 and early S-phase, when homology directed repair is not an option (Hartlerode & Scully, 2009; Pastwa & Blasiak, 2003). After

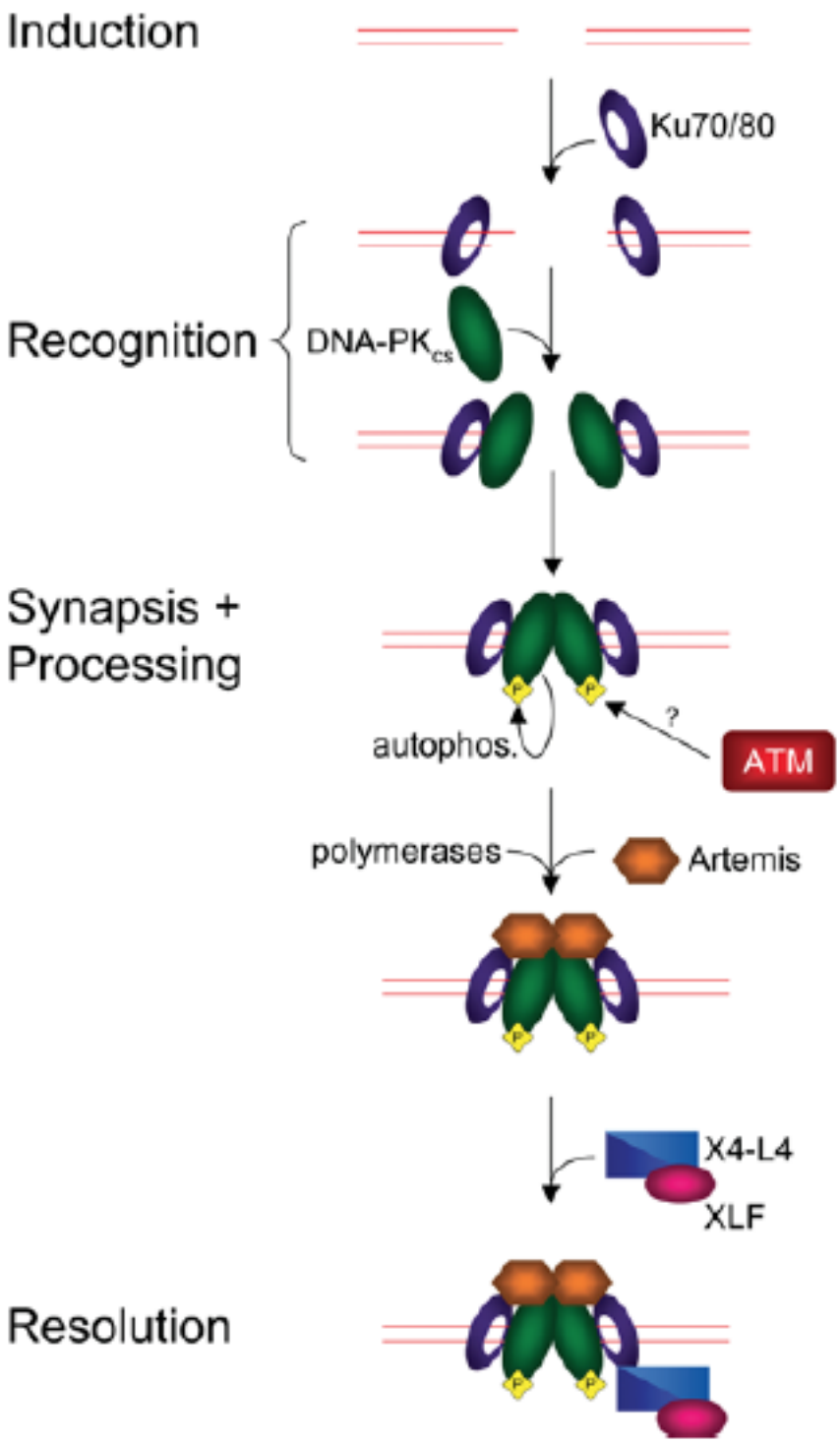

Figure 1.5. Representation of the major steps of nonhomologous end-joining (Hartlerode & Scully, 2009).

the cell suffers a DSB, the first step towards its resolution through NHEJ is the binding of the Ku70/Ku80 heterodimer to the DNA ends. This complex serves as a scaffold upon which the rest of the NHEJ repair complex is built (Hartlerode & Scully, 2009; Iliakis, 2009; Pastwa & Blasiak, 2003). After binding, the Ku70/80 heterodimer moves inwards along the DNA approximately ten base pairs, allowing DNA-dependent protein kinase catalytic subunit (DNA-PK_{cs}) access to the DSB ends (Yoo & Dynan, 1999). DNA-PK_{cs} serves as the end-bridging molecule to keep the two DNA ends in close proximity (Chen et al, 2000; DeFazio et al, 2002). Association with the Ku70/80 heterodimer and DNA activates the serine/threonine kinase activity of DNA-PK_{cs}, which has the ability to phosphorylate many substrates *in vitro*, such as Ku70, Ku80, XRCC4, Cernunnos/XRCC4-like factor (XLF), Artemis and DNA ligase IV (Lig4). However, it is not clear which of these proteins absolutely require phosphorylation *in vivo* (Hartlerode & Scully, 2009; Yaneva et al, 1997). Two possible candidates for critical phosphorylation substrates by DNA-PK_{cs} *in vivo* are Artemis and DNA-PK_{cs} itself (Chan et al, 2002; Chen et al, 2005; Ma et al, 2005). It has been shown that the phosphorylation status of DNA-PK_{cs}, at threonine 2609, influences its conformation and dynamics and could influence its activity *in vivo* (Dobbs et al, 2010; Morris et al, 2011), whereas DNA-PK_{cs}-mediated autophosphorylation at the T2609-T2647 cluster has been proposed to be necessary for the activation of the endonuclease function of Artemis, promoting the formation of blunt, or

near-blunt ended DSBs, which is important for the final resolution of DSBs (Goodarzi et al, 2006).

The next step in NHEJ is DNA end processing. As with SSBR, a diverse set of end processing enzymes can work on damaged DSB termini, including PNKP, aprataxin (APTX) and PNKP-APTX-like factor, a protein that acts as an endonuclease and a 3' exonuclease (Audebert et al, 2006; Lieber, 2010). However, most end processing is performed by Artemis. Artemis, in complex with DNA-PK_{cs}, has 3' endonuclease activity. It binds the four nucleotides after the ssDNA:dsDNA transition and nicks 3' to that four nucleotide stretch (Lieber, 2010; Ma et al, 2005; Yannone et al, 2008). This converts 5' overhangs to blunt ends, and long 3' overhangs to four nucleotide overhangs (Ma et al, 2002). The XLF-XRCC4-Lig4 complex then ligates the DNA ends (Chen et al, 2000; Lieber, 2010; Pastwa & Blasiak, 2003). The main outcome of this pathway is error-prone repair (i.e. microdeletions) because Artemis resects DNA to achieve ligatable termini (Audebert et al, 2006; Ma et al, 2005; Yannone et al, 2008). NHEJ, like HR, is important for resistance to human disease. Approximately 15% of severe combined immunodeficiency cases and a variety of lymphomas result from an inherited defect in NHEJ (Buck et al, 2006; Hartlerode & Scully, 2009; Lieber, 2010).

1.1.6 DNA Repair in Mitochondria

DNA damage and its subsequent repair was first documented to occur in the nucleus, however, it is now known that organellar DNA repair

also occurs and the best characterized pathway to date describes short patch mitochondrial BER (mtBER). One major consideration, though, is that mitochondrial DNA (mtDNA) damage is typically not considered to be phenotypically consequential unless a large number of mitochondria are damaged simultaneously (Friedberg, 2006). However, even in light of this, damage to mitochondria does seem to cause dramatic effects (Druzhyna et al, 2008; Jeppesen et al, 2011; Wallace et al, 1995).

Due to the proximity to the electron transport chain and lack of nucleosomal structure, mitochondrial DNA is actually particularly susceptible to oxidative attack from ROS when compared to the DNA in the nucleus (O'Rourke et al, 2002). It has been suggested that mtDNA accumulates mutations at a rate that is 10 times that of nuclear DNA and therefore the presence of DNA repair pathways similar to those found in the nucleus are expected (Wallace et al, 1995; Yakes & Van Houten, 1997). It is therefore of critical importance that mtDNA be repaired as efficiently and effectively as DNA found in the nucleus. Without this repair, accumulation of mtDNA damage can lead to increased aging rate (Harman, 1972; Miquel et al, 1980), neurodegenerative disorders and cancer (Druzhyna et al, 2008).

The damage caused by ROS parallels that seen in nuclear DNA, the major products of which are repaired by mtBER (Maynard et al, 2010). The key steps of mtBER resemble that of nuclear BER; first, a DNA glycosylase removes the damaged base (uracil-DNA glycosylase and MYH-DNA glycosylase have been identified in mitochondria), after which a protein

with endonuclease activity incises the DNA at the AP site (Maynard et al, 2010). There are several proteins identified in the mitochondria that possess AP lyase activity, such as APE1 (Szczesny et al, 2008), an Nth-like AP lyase, AP lyase associated with 8-oxoguanine DNA glycosylase, and finally an AP lyase function has also been attributed to the mitochondrial DNA polymerase γ (Maynard et al, 2010). After incision, 5'OH and/or 3'P DNA ends are cleaned by mitochondrial PNKP, or 5'-deoxyribose phosphate (5'dRP) ends are cleaned by the 5'dRP-lyase activity of DNA polymerase γ, to the elongation and ligation competent 5'P and 3'OH groups. DNA polymerase γ then fills in the missing nucleotide and mitochondrial DNA ligase III (mtLig3) seals the nick (Maynard et al, 2010). Unlike nuclear Lig3, mtLig3 does not require XRCC1 or a mitochondrial XRCC1-like protein for stability and function (Simsek et al, 2011). The end result of short patch mtBER, like nuclear BER, is error-free repair of DNA.

Another DNA repair pathway postulated to be active in the mitochondrial genome is long patch mtBER. The hotly contested presence of FEN1 (Akbari et al, 2008; Szczesny et al, 2008) and the presence of the replication associated DNA helicase, DNA2, suggest the activity of such a pathway, but definitive results are pending (Maynard et al, 2010).

ROS can directly attack the DNA backbone to generate single and double strand breaks directly. As such, it is reasonable to assume that mitochondria possess DNA double-strand break repair pathways. To date, evidence has been collected outlining both homology-directed and

homology-independent DSB repair in mitochondria (Bacman et al, 2009; Coffey et al, 1999; Kajander et al, 2001; Lakshmipathy & Campbell, 1999; Thyagarajan et al, 1996). For example, human Rad51, a protein central to the function of HR in the nucleus, has been shown to localize to the mitochondria (Sage et al, 2010). However, most of the evidence collected describes repair in lower mammals and definitive evidence for a HR- or NHEJ-like pathway in human cells has yet to be discovered.

1.2 DNA REPAIR AND CANCER

1.2.1 Single-Strand Break Repair, Cancer and Neurological Disorders

Many DNA repair proteins, when aberrant, are implicated in the increase in cancer susceptibility. While this may be true of DSB repair proteins as a general rule, few proteins involved in SSB repair have been associated with an increase in the incidence of cancer. Only XRCC1 (lung, endometrial (Cincin et al, 2012), head and neck, thyroid, sporadic breast, and cervical (Settheetham-Ishida et al, 2011) cancers), Polβ (gastric cancer (Mello et al, 1996) and APE1 (lung and endometrial (Cincin et al, 2012) cancers) when mutated cause an increase in the incidence of cancer.

More common in individuals harbouring defective SSB repair is the prevalence of neurological disorders. For example, mutations in PNKP cause an autosomal recessive disorder characterized by microcephaly, early-onset, intractable seizures and developmental delay (MCSZ) (Shen et al, 2010). Additionally, mice lacking functional XRCC1 showed similar

symptoms as PNKP-deficient humans in that they also show delay in development and seizure-like activity, however, XRCC1 deficient mice possess normal brain size (Schmutte et al, 1998). Furthermore, ataxia-oculomotor apraxia 1 (AOA1), characterized by variable onset (between 1 and 16 years), cerebellar atrophy and ataxia, late axonal peripheral neuropathy, oculomotor apraxia, cognitive impairment, hypercholesterolaemia, hypoalbuminaemia and involuntary movements, and spinocerebellar ataxia with axonal neuropathy 1 (SCAN1), characterized by cerebellar atrophy, peripheral neuropathy, mild hypercholesterolaemia and hypoalbuminaemia, are caused by defects in the SSBR proteins APTX and tyrosyl-DNA phosphodiesterase (TDP1), respectively (Caldecott, 2008). SCAN1, however, has a later onset than AOA1 (after 15 years) and does not involve the subsequent decline in cognitive faculties (Caldecott, 2008). Interestingly, MCSZ, AOA1 and SCAN1 correspond to a defect in one of the many DNA end-processing enzymes indicating the importance of this step to the fidelity of SSB repair.

1.2.2 Homologous Recombination, Cancer and Neurological Disorders

One of the striking features of a lack of HR is the presence of neurological disorders. When the ATM protein is mutated, a syndrome called ataxia telangiectasia (AT) presents in patients early on in life (i.e. 2-3 years old) and is followed by neurodegeneration, such that by the age of 10 AT sufferers are confined to a wheelchair (Anheim, 2011). This disease

is characterized by uncoordinated movements, such as unsteady gait, mental retardation, dilated blood vessels, skin discoloration, seizures, sensitivity to radiation and susceptibility to cancer, and an average life-span of 20 years (Anheim, 2011). There also exists an AT-like disorder (ATLD), which is found in people with mutated Mre11. This disease presents itself much like AT, however, there is a noticeable lack of telangiectasia (Jeppesen et al, 2011). Furthermore, a mutation in NBS1 causes a disorder called Nijmegen breakage syndrome (NBS). This is characterized by microcephaly, but the extraneurological features of NBS mimic those of AT, including the susceptibility to the development of cancer (Jeppesen et al, 2011).

The increased susceptibility to cancer is a salient feature of patients suffering from defective HR. Many cancers show familial predisposition due to the inheritance of a mutated copy of an HR allele. For example, an increase in the incidence of lymphoma (Gumy-Pause et al, 2004), leukemia (Gumy-Pause et al, 2004) and breast cancers (Angele et al, 2003; Thorstenson et al, 2003) are seen in ATM deficient people. Furthermore, germline mutations in XRCC3 (endometrial (Cincin et al, 2012)), NBS1 (lymphomas (Williams et al, 2002)), BRCA1 (breast and ovarian (Miki et al, 1994)), and BRCA2 (breast, ovarian and prostate (Lancaster et al, 1996; Tischkowitz et al, 2003; Wooster et al, 1995)) confer an increased predisposition to the indicated cancers.

Similarly, the Fanconi anemia (FA) pathway, which also operates during HR and interacts with BRCA1, BRCA2 and Rad51 (Digweed et al,

2002; Garcia-Higuera et al, 2001; Howlett et al, 2002; Hussain et al, 2004; Taniguchi et al, 2002) to form DNA repair structures, causes an increase in the incidence of cancer when aberrant. Mutations in 1 of the 11 FA (FANCA, FANCB, FANCC, FANCD1 (BRCA gene (Howlett et al, 2002)), FANCD2, FANCE, FANCF, FANCG, FANCI, FANCJ, FANCL, FANCM, FANCN) genes can cause vulvar, esophageal, head and neck cancer and most importantly leukemia, which is a 1000-fold more prevalent in individuals bearing germline FA mutations than the non-mutated population (Alter, 2003; Rosenberg et al, 2008; Rosenberg et al, 2003).

A number of other syndromes associated with aberrant HR proteins expression have been described, including; Werner Syndrome (WRN), Bloom Syndrome (BLM), and Rothmund-Thompson Syndrome (RECQL4). All of these syndromes are characterized by an increase in the incidence of cancer. HR, therefore, plays a critical role in the maintenance of genomic integrity and plays a tumour suppressive role in human cells.

1.2.3 Nonhomologous End-Joining and Cancer and Neurological Disorders

As with SSBR, faulty NHEJ does not seem to be associated with an increase in cancers, except for Artemis, which when disrupted causes an increase in the occurrence of lymphoma (Moshous et al, 2003). NHEJ mutations also share another aspect in common with SSBR mutations, and that is an increase in the incidence of neurological disorders. Disruptions to DNA ligase IV (Barnes et al, 1998; Frank et al, 1998; O'Driscoll et al,

2001), Cernunnos (Buck et al, 2006), XRCC4 (Gao et al, 1998), Ku70 (Gu et al, 2000), Ku80 (Gu et al, 2000) and DNA-PK_{cs} (Vemuri et al, 2001) all result in a severe combined immunodeficiency and microcephaly. Disruption of NHEJ, however, does not seem to cause the severe seizures seen with the disruption of PNKP in MCSZ (Shen et al, 2010).

1.3 DNA END PROCESSING ENZYMES WITH AN EMPHASIS ON PNKP

1.3.1 Types of DNA end damage and their repair

A critical step in DNA damage resolution is the repair of incompatible DNA ends. Without the correct 5'-phosphate and 3'-hydroxyl groups, elongation and ligation of the DNA cannot be performed and the strand break will persist in the DNA. Several DNA end processing enzymes have evolved, each with their own respective type(s) of damage they correct. Listed previously are the types of DNA damage, along with their causes and designated DNA end-processing enzyme (Figure 1.1).

1.3.2 Structure and function of PNKP

Mammalian PNKP (57 kDa) possesses three well characterized domains, an N-terminal forkhead–associated (FHA) domain (green, Figure 1.6), and a C-terminal fused catalytic domain consisting of kinase (yellow, Figure 1.6) and phosphatase (blue, Figure 1.6) domains (Bernstein et al, 2005). The protein's catalytic domain is connected to the FHA domain

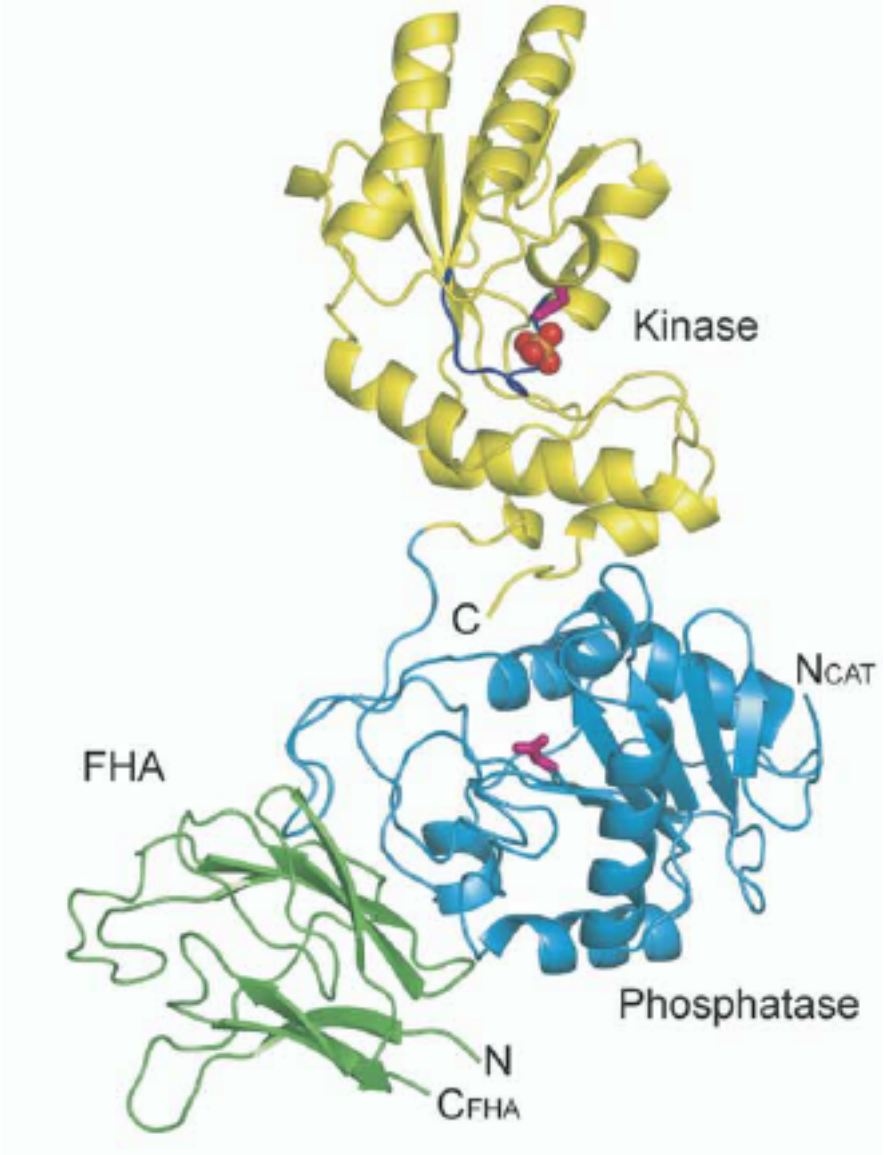

Figure 1.6. Molecular structure of mammalian PNKP (Bernstein et al, 2005). Specifically depicted here is murine PNKP, which shares ~80% similarity with human PNKP.

through a flexible polypeptide linker. The linker has recently been shown to be phosphorylated by ATM and DNA-PK_{cs}, but the cellular consequences of this phosphorylation have yet to be fully elucidated (Segal-Raz et al, 2011; Zolner et al, 2011). The FHA domain binds casein kinase 2 (CK2)-mediated phosphorylation sites found in the scaffold proteins XRCC1 (Loizou et al, 2004) and XRCC4 (Koch et al, 2004). This interaction with XRCC1 and XRCC4 with the FHA domain allows an increase in the turnover rate thereby stimulating an increased rate of end processing (Lu et al, 2010; Mani et al, 2010; Weinfeld et al, 2011).

The phosphatase domain of PNKP is a member of the haloacid dehalogenase superfamily (Aravind & Koonin, 1998; Bernstein et al, 2005) and contains a conserved DxDGT motif. The first aspartate residue of this motif covalently bonds to the substrate to generate a phosphoaspartate intermediate. Figure 1.7 shows the mechanism of PNKP 3'-phosphatase activity, where Asp179 binds the substrate to facilitate reaction progression (Bernstein et al, 2008).

The kinase domain of PNKP consists of a 5-stranded parallel β-sheet belonging to the adenylate family of kinases and binds the DNA strand termini on the same side as the phosphatase active site (Bernstein et al, 2005; Coquelle et al, 2011; Garces et al, 2011).

Binding of ATP is required for kinase function of PNKP and is characterized by two Walker motifs, A and B (Bernstein et al, 2005). Walker motif A interacts with the β- and γ-phosphates of ATP and two amino acid residues in Walker motif B,

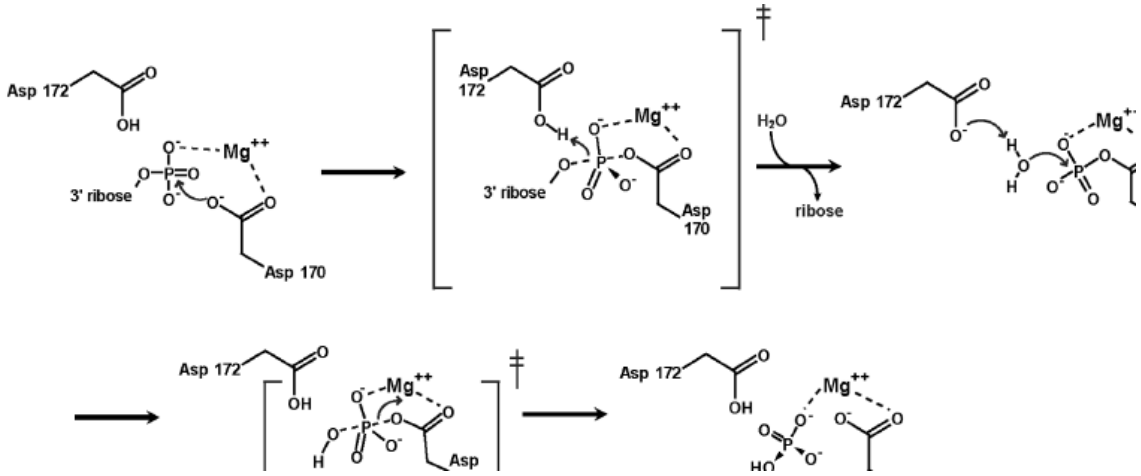

Figure 1.7. Mechanism of 3'-dephosphorylation by PNKP (Bernstein et al, 2008). Transition states are indicated by the double dagger.

Asp421 and Ser378, hydrogen bond and aid in the positioning of Mg^{2+} (Bernstein et al, 2005). Figure 1.8 shows the mechanism of PNKP kinase action where Asp396 activates the 5'-OH for nucleophilic attack (Bernstein et al, 2008)

PNKP phosphatase is active in both SSB and DSB repair, but the crystal structure reveals that the active site accommodates only single-stranded DNA (Coquelle et al, 2011). SSBs thus situate in the active site easily, where the 3'-most base stacks with phenylalanine 305 in PNKP (Coquelle et al, 2011). PNKP, however, does not directly interact with the 3' base at the DNA terminus (Coquelle et al, 2011). Instead it utilizes a water molecule that is present as part of the octahedral coordination shell of the Mg^{2+} present in PNKP (Coquelle et al, 2011). Thus, PNKP is able to bind 3'-termini in a sequence-independent manner.

Double-stranded DNA substrates need to undergo melting to fit into the active site. PNKP facilitates DNA melting utilizing phenylalanine 184 to destabilize base pairing through hydrophobic interactions with the two to six terminal base pairs (Coquelle et al, 2011; Garces et al, 2011). After DNA melting, phenylalanine 305 could help to stabilize the newly formed open complex of DNA (Coquelle et al, 2011). A consequence of bound double-stranded DNA to PNKP is a pronounced bend of approximately 70° in the DNA, allowing recognition of DNA ends (Garces et al, 2011). Ultimately PNKP converts 3'P and 5'OH groups to the correct 3'OH and 5'P ends allowing repair to continue unabated.

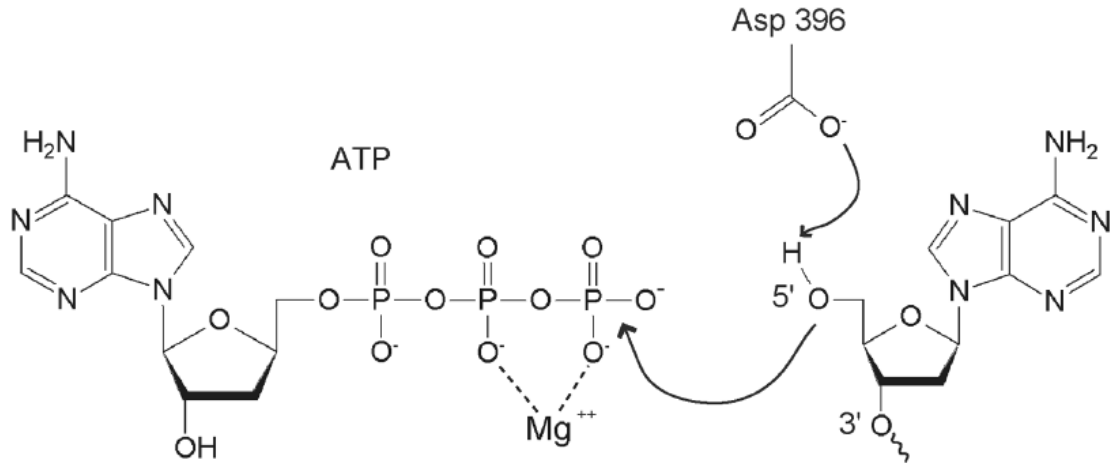

Figure 1.8. Mechanism of 5'-phosphorylation by PNKP (Bernstein et al, 2008). Asp396 in this murine model is analogous to Asp397 in human PNKP.

1.4 SYNTHETIC LETHALITY

The major challenge faced by medical oncology has always related to the identification and implementation of therapeutics selectively targeted to cancer cells yet simultaneously non-toxic to normal cells (Kaelin, 2009). To date, the majority of chemotherapeutic drugs were identified based on their ability to kill rapidly dividing cells, however, this lead to complications (Overington et al, 2006). Certain normal tissues are also rapidly dividing; bone marrow hematopoietic precursors, cells lining the stomach and intestine, and hair follicle cells are all non-selectively targeted by the majority of chemotherapeutic agents, which leads to the side effects typically associated with such treatment regimens (Kaelin, 2005; Kaelin, 2009; Overington et al, 2006). In fact, the lack of specific targeting of cancerous cells is one of the major causes of treatment failure (Overington et al, 2006). There is thus a need to implement treatment paradigms designed to specifically target cancer cells for death, yet leave normal cells intact, ultimately minimizing side effects and maximizing therapeutic benefit. One potential route for achieving selective targeting of cancer cells is based on the concept of synthetic lethality.

Synthetic lethality occurs when the simultaneous disruption of two non-allelic, non-essential genes or the proteins they code for in the same cell is lethal (Dobzhansky, 1946; Iglehart & Silver, 2009; Lucchesi, 1968). Recently, this phenomenon has been shown to occur between combinations of DNA repair genes/proteins, and much attention has focused on the co-disruptions of the SSB repair protein PARP and the

breast cancer associated (BRCA) proteins (Bryant et al, 2005; Comen & Robson, 2010; Farmer et al, 2005; Fong et al, 2009). The BRCA proteins are putative tumour suppressors, naturally lost or mutated in tumour cells of people afflicted with familial breast cancer, and have a role in DSB repair as discussed above (Bryant et al, 2005; Comen & Robson, 2010; Farmer et al, 2005). It has been hypothesized that PARP inhibition serves as a means to inhibit SSBR thus generating DSBs (Bolderson et al, 2009). This occurs during DNA synthesis when SSBs collapse the replication fork to generate DSBs (O'Connor et al, 2007). Therefore, in $BRCA^{-/-}$ breast cancer cells, PARP inhibition would induce simultaneous disruption of SSB repair and DSB repair, allowing highly genotoxic DSBs to accumulate and eventually lead to specific cancer cell death (Bolderson et al, 2009) (Figure 1.9). It has been shown that NHEJ proteins, DNA-PK_{cs}, Ku and Lig4, all play a role in the replication stress response (Allen et al, 2011), and that cells lacking critical NHEJ proteins are sensitive to agents causing replication stress (e.g. camptothecin (Arnaudeau et al, 2001), hydroxyurea and excess thymidine (Lundin et al, 2002)). However, the sensitivity to these compounds in an NHEJ-deficient background is far less than that of cells lacking HR (Allen et al, 2011). This implies that NHEJ may play a lesser role in the restarting of stalled replication forks and that it may not be able to handle the increase of damage caused under synthetic lethal conditions described.

Alternative explanations for the synthetic lethality seen with PARP and BRCA proteins have been proposed. For example, PARP

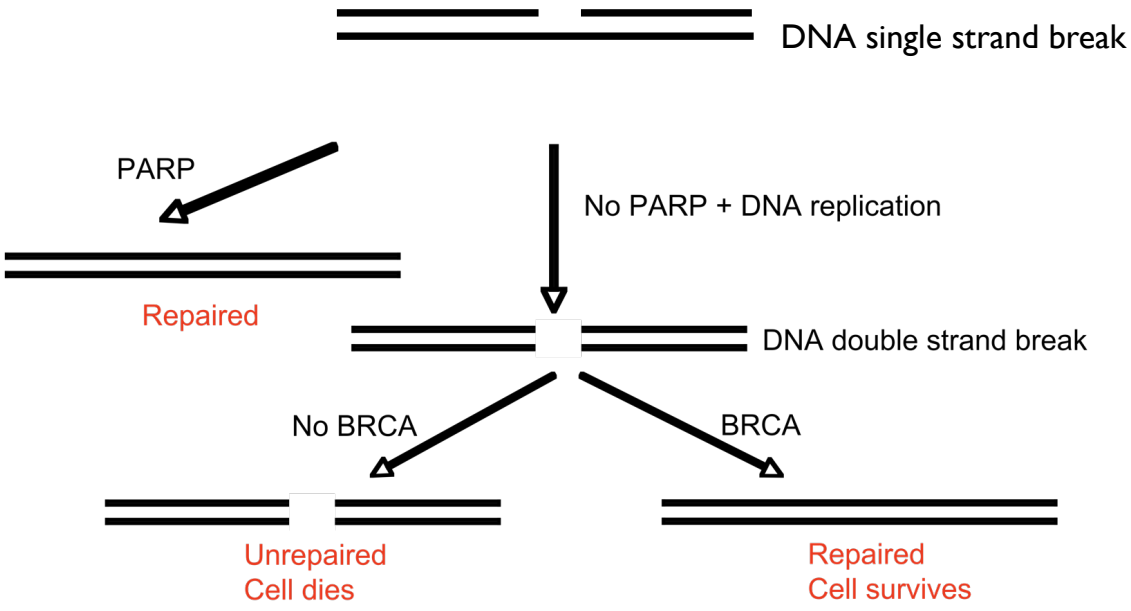

Figure 1.9. Proposed model for the accumulation of DSBs upon simultaneous PARP and BRCA disruption.

inhibition may lead to a trapping of PARP on the SSB due to prevention of PAR formation on PARP itself, not necessarily due to the increased formation of SSB or inhibition of SSB repair (Helleday, 2011). The trapped PARP:DNA damage complex may then be converted to a more toxic lesion during replication, similar to what is seen using the topoisomerase I poison camptothecin, where topoisomerase I is trapped on the DNA itself (Strumberg et al, 2000). This in turn may lead to damage requiring BRCA-dependent repair, which is unavailable in BRCA deficient cells (Helleday, 2011). A second explanation comes from the observation that BRCA-deficient cells display a hyperactive PARP, when cells are in S-phase (Helleday, 2011). PARP has been shown to be involved in the restarting of stalled replication forks (Bryant et al, 2009; Yang et al, 2004) in a pathway distinct from HR. In this way inhibition of PARP activity in an HR-deficient background would prevent restart of stalled replication forks, leading to the generation and accumulation of highly cytotoxic DSBs that would eventually lead to cell death (Helleday, 2011).

Interestingly it has been found that the clinical success of PARP inhibitors BSI-201 (2009; Pal & Mortimer, 2009) and Olaparib (Dungey et al, 2009; Evers et al, 2010; Fong et al, 2009; O'Brien & Stokoe, 2009; Pal & Mortimer, 2009; Stefansson et al, 2009; Venkitaraman, 2009; Williamson et al, 2010; Zander et al, 2010) in treating breast cancers associated with BRCA (or BRCA-like) mutations depended solely on the synthetic lethal association between PARP and BRCA proteins.

Importantly, synthetic lethality seen in PARP inhibited BRCA-mutated cells occurs in the absence of exogenous DNA damaging agents, and is presumed to be caused by the large number of SSBs produced per cell per day by endogenous ROS (Lindahl & Nyberg, 1972). For this reason, any critical SSBR protein could be synthetically lethal when co-disrupted with a core DSBR protein.

Since the lack of specific targeting of neoplastic tissue is a major cause of failure of chemotherapy (Overington et al, 2006), there is an urgent need to develop approaches to induce selective toxicity in cancer cells, while simultaneously leaving normal cells unharmed. Work described in this thesis examines the possibility of exploiting synthetic lethal relationships between the DNA repair protein polynucleotide kinase/phosphatase (PNKP) and its partners in the development of a directed cancer therapy. We do not, however, solely rely on endogenous rates of SSB formation and selective protein disruption to kill only cells deficient in PNKP or its partner protein (i.e. cancer cells). We also investigate the use of “synthetic sickness”, a process in which the simultaneous disruption of two genes/proteins weakens cells thereby rendering them hypersensitive to treatments combining conventional chemo- or radiotherapy with targeted protein disruptors. This should enhance the cancer cell killing potential of standard doses of chemo- or radiotherapy, or perhaps more importantly allow for the use of lower drug or radiation doses so as to reduce adverse responses in normal tissue.

1.4.1 Clinical significance of synthetic lethality

We can theoretically take advantage of the fact that the human genome is subjected to a large number of insults per day (Lindahl & Nyberg, 1972) as well as the fact that many familial predispositions to cancer result from inheritance of a defective copy of a DNA repair protein (Comen & Robson, 2010; Dungey et al, 2009; Gien & Mackay, 2010; Iglehart & Silver, 2009; Mendes-Pereira et al, 2009; Pal & Mortimer, 2009; Williamson et al, 2010) to design treatments using synthetic lethal approaches. Furthermore, we may also be able to take advantage of the large number of sporadic cancers harbouring defective tumour suppressor activity to tailor-make treatment paradigms using the knowledge of synthetic lethal partnerships. These therapies do away with the need to induce DNA damage and rely solely on the natural formation of DNA damage.

Synthetic lethality as it relates to DNA repair exploded onto the cancer research scene in 2005. The Ashworth and Helleday groups published back-to-back papers in *Nature* outlining synthetic lethality between PARP and BRCA proteins (Bryant et al, 2005; Farmer et al, 2005) (proposed mechanism of lethality is outlined in Figure 1.9). Most work on synthetic lethality in cancer research to date has focused on associations between PARP and the BRCA proteins. Normally, DSBR can cope with the number of naturally occurring DSBs (~10 per cell per day), but, when PARP is inhibited, few of the >10,000 naturally occurring daily SSBs can be repaired (Lieber, 2010; Lindahl & Nyberg, 1972). In non-cancerous

tissues, the cells retain both NHEJ and HR and can thus handle the increase in formation of DSBs. However, this potential three log-fold difference in the number of DSBs formed due to replication fork collapse, coupled with the lack of functional HR in the cancer cells (the pathway primarily responsible for resolving collapsed replication forks (Arnaudeau et al, 2001), forces these cells to funnel all DSBR through NHEJ. This vast increase in DSBs saturates NHEJ, allowing many DSBs to elude repair. As the cell continues to progress through cell cycles, there is an accumulation of DSBs, which eventually leads to cell death (O'Brien & Stokoe, 2009) (Figure 1.9). In this model, only those cells with naturally occurring HR-deficiency (i.e. cancer cells) will be affected because normal cells (wildtype and heterozygous) are proficient in HR and can tolerate the increased DSB formation through PARP inhibition (Comen & Robson, 2010; Iglehart & Silver, 2009; O'Brien & Stokoe, 2009; O'Connor et al, 2007). The proteins involved in this relationship have since been expanded to include most proteins involved in HR, and thus cancers showing 'BRCAness' (similar defect as that seen in BRCA-deficient cells) are undergoing clinical trials using PARP inhibitors.

However, in 2008, Turner *et al*. found a synthetic lethal relationship between PNKP and PARP, providing the first evidence of synthetic lethality related to DNA repair but not involving the BRCA proteins (Turner et al, 2008). Furthermore, in 2009, Mendes-Pereira *et al.* discovered that PARP also shows synthetic lethality with phosphatase and tensin homolog (PTEN) (Mendes-Pereira et al, 2009). PTEN is a potent tumour

suppressor, acting in the phosphoinositide-3-kinase signaling pathway and the cell-cycle checkpoint, and is not considered a canonical DNA repair protein (Cantley & Neel, 1999; Simpson & Parsons, 2001; Yin & Shen, 2008). These findings have led research on synthetic lethality in a new direction, in which synthetic lethality need not rely solely on PARP inhibition in a DNA repair defective background.

The concept of synthetic lethality has great clinical significance. For example, cancers such as those harbouring homozygous BRCA1, BRCA2, and PTEN mutations could be selectively killed using Olaparib, whereas wildtype/heterozygous cells, i.e. normal cells, would be unaffected (Bryant et al, 2005; Farmer et al, 2005; Mendes-Pereira et al, 2009). It is possible that we can take advantage of synthetically lethal relationships using disruption of other DNA repair proteins to benefit a wider spectrum of cancers. Additionally, discovery of novel protein targets to use in synthetic lethal treatments would provide greater clinical benefit as those patients who have developed a resistance to PARP inhibitors may be able to be further treated using another protein inhibitor.

1.5 WORKING HYPOTHESIS AND SPECIFIC AIMS

The main objective of this project is the determination of synthetic lethal associations with PNKP and its potential application in targeted cancer therapies. The major hypotheses were as follows:

1) PNKP will be synthetically lethal with many proteins, including DNA repair and non-DNA repair proteins.

2) Given that PNKP is both a SSBR and a DSBR protein (NHEJ), we hypothesize that the role of PNKP in DSBR is critical in synthetic lethality involving PNKP.

3) Inhibition of PNKP in certain cancers will have value as a directed therapy.

The specific aims of this project were:

1) To identify synthetic lethal partnerships of PNKP

2) To apply of the information gained in the development of a highly directed and cancer specific therapy.

1.6 CHAPTER SUMMARIES

1.6.1 Chapter 2

Many cells lose function of key proteins during their transformation into a cancerous cell. It may be possible to target these loss-of-function cells for selective cell death yet simultaneously leave normal, non-cancerous tissues unaffected.

A library of 6961 siRNAs was used to identify genes/proteins that are potentially synthetic lethal when co-disrupted with the DNA repair protein polynucleotide kinase/phosphatase (PNKP) using human lung adenocarcinoma A549 cell lines in which PNKP has been stably knocked down by shRNA (A549δPNKP) or expressing a scrambled shRNA (A549-Scramble). Confirmatory experiments were conducted using various concentrations of siRNA, stable knockdown cell lines or protein inhibitors as well as several distinct cell lines in both cell proliferation assays and

clonogenic survival assays. Cell proliferation was measured using an Alamar Blue-based fluorescence detection assay and surviving cells were stained with crystal violet and counted to determine survival. A549δPNKP, A549-Scramble or a cell line stably depleted of SHP-1 (A549δSHP-1) were used to test for protein function in response to DNA damage (comet assays), reactive oxygen species (ROS) production using a hypochlorite, hydroxyl radical and peroxynitrite detection kit, cellular protection using the ROS scavenger WR1065 and determination of mode of cell death using a triple stain of Hoescht 33342, Ethidium Homodimer III and Annexin V-FITC. All statistical tests were two-sided.

A genetic screen using a library of 6961 siRNAs led to the identification of SHP-1, a tumour suppressor frequently mutated in malignant lymphomas and leukemias and prostate cancer, as a potential synthetic lethal partner PNKP. After confirming the partnership with SHP-1, we observed that co-depletion of PNKP and SHP-1 induced apoptosis. A T-cell lymphoma cell line naturally SHP-$1^{-/-}$ (Karpas 299) was shown to be sensitive to a chemical inhibitor of PNKP, but resistance was restored by expression of wild-type SHP-1 in these cells. We determined that while SHP-1 depletion does not significantly impact DNA strand-break repair, it does amplify the level of ROS and elevated endogenous DNA damage. The ROS scavenger WR1065 afforded protection to SHP-1 depleted cells treated with the PNKP inhibitor. We propose that co-disruption of SHP-1 and PNKP leads to an increase in DNA damage that escapes repair, resulting in the accumulation of cytotoxic double-strand breaks and

induction of apoptosis. This supports an alternative paradigm for synthetic lethal partnerships that could be exploited therapeutically.

PNKP may be a viable therapeutic target of importance to synthetic lethal treatment paradigms. We investigated the tumour suppressor SHP-1 further as it may benefit a large number of lymphoma and leukemia sufferers, however, this is just one of the fourteen known tumour suppressors identified through screening, implying that targeted disruption of PNKP function may potentially benefit many more forms of cancer.

1.6.2 Chapter 3

Recently we performed a genetic screen of 6961 siRNAs to identify possible synthetic lethal partners of PNKP. One of the genes identified was the potent tumour suppressor phosphatase and tensin homolog deleted on chromosome 10 (*PTEN*). Here we have confirmed the PNKP/PTEN synthetic lethal partnership in a variety of different cell lines including the PC3 prostate cancer cell line naturally deficient in PTEN. Complementation of PC3 cells with several well characterized *PTEN* mutants revealed that the critical function of PTEN required to prevent toxicity induced by an inhibitor of PNKP is its cytoplasmic lipid phosphatase activity. In the cytoplasm PTEN acts to antagonize the PI3K/Akt pathway by dephosphorylating the second messenger phosphatidylinositol 3,4,5-triphosphate to the inactive form phosphatidylinositol 4,5-bisphosphate. In this way, signals allowing cell growth and proliferation are abated. Furthermore, since there is evidence linking this function of PTEN to the

regulation of homologous recombination through RAD51, we tested the ectopic expression of RAD51 in PC3 cells, but found this had no effect on the response to PNKP inhibition. Finally, we show that modest inhibition of PNKP in a PTEN knockout background results in a marked increase in radiosensitivity, suggesting that such a “synthetic sickness” approach involving the combination of PNKP inhibition with radiotherapy may be applicable to PTEN-deficient tumours.

1.6.3 Chapter 4

PNKP is a bifunctional DNA repair protein possessing both 5’-kinase and 3’-phosphatase functions. This versatile protein is involved in multiple DNA repair pathways, including BER, SSBR and the DSBR pathway NHEJ. We sought to determine if it was the single-strand or the double-strand repair function of PNKP that was essential in synthetic lethal relationships.

We performed both proliferation and clonogenic survival assays using artificially generated and naturally occurring DNA repair protein deficient cell lines, siRNA, and protein inhibitors to impair target protein function. Again, to determine cell survival for proliferation assays, an Alamar Blue-based reduction assay was used, whereas surviving colonies in clonogenic assays were stained with crystal violet and counted to determine survival. All statistical tests were two-sided.

We postulated that since PNKP shows synthetic lethality with both PARP and DNA polymerase β, it was likely the DSBR function of PNKP

that was important for synthetic lethality. We further tested this hypothesis by co-disrupting PNKP with an essential NHEJ protein, DNA-PK_{cs} and found that there was no lethality seen. This is expected if PNKP's DSBR capacity is important as it functions in the same pathway as DNA-PK_{cs}. Thus, co-disruption of both PNKP and DNA-PK_{cs} would be knocking out only NHEJ, leaving both SSBR and HR active and able to compensate for the increase in damage. However, it may be simply that a co-disruption of SSBR and NHEJ is not lethal. To test this, we examined the sensitivity of DNA-PK_{cs} negative cells with a PARP inhibitor and showed that these cells are indeed sensitive to PARP inhibition. Together, these results implicate PNKP involvement in DSBR as the essential repair pathway for synthetic lethality. Furthermore, we examined the enzymatic function of PNKP (5'-kinase or 3'-phosphatase) to see which was necessary to rescue cell death under synthetic lethal conditions. PNKP-depleted cells were reconstituted with various forms of full-length mutant PNKP, including kinase-dead but phosphatase active, phosphatase-dead but kinase active, or completely inactive protein. When subjected to PARP inhibition, both the kinase-dead and phosphatase-dead cell lines rescued lethality, but not to wild type levels, whereas the completely inactive mutant did not rescue lethality at all. This shows that both the kinase and phosphatase functions of PNKP are important in synthetic lethal relationships.

These findings may be of significant value for the discovery of treatment regimens targeting the synthetic lethal partners of PNKP. Drugs targeting either the kinase or phosphatase function alone, such as

A12B4C3, which is a PNKP phosphatase inhibitor alone, should be effective to an extent, but ideally a drug affecting both functional domains of PNKP, such as one that disrupts the three-dimensional folding of PNKP, would be most beneficial.

1.7 REFERENCES

(2009) BiPar Sciences presents interim phase 2 results for PARP inhibitor BSI-201 at San Antonio Breast Cancer Symposium. *Cancer Biol Ther* **8:** 2-3

Ahel D, Horejsi Z, Wiechens N, Polo SE, Garcia-Wilson E, Ahel I, Flynn H, Skehel M, West SC, Jackson SP, Owen-Hughes T, Boulton SJ (2009) Poly(ADP-ribose)-dependent regulation of DNA repair by the chromatin remodeling enzyme ALC1. *Science* **325:** 1240-1243

Ahel I, Ahel D, Matsusaka T, Clark AJ, Pines J, Boulton SJ, West SC (2008) Poly(ADP-ribose)-binding zinc finger motifs in DNA repair/checkpoint proteins. *Nature* **451:** 81-85

Ahel I, Rass U, El-Khamisy SF, Katyal S, Clements PM, McKinnon PJ, Caldecott KW, West SC (2006) The neurodegenerative disease protein aprataxin resolves abortive DNA ligation intermediates. *Nature* **443:** 713-716

Akbari M, Visnes T, Krokan HE, Otterlei M (2008) Mitochondrial base excision repair of uracil and AP sites takes place by single-nucleotide insertion and long-patch DNA synthesis. *DNA Repair (Amst)* **7:** 605-616

Allen C, Ashley AK, Hromas R, Nickoloff JA (2011) More forks on the road to replication stress recovery. *J Mol Cell Biol* **3:** 4-12

Allinson SL, Dianova, II, Dianov GL (2003) Poly(ADP-ribose) polymerase in base excision repair: always engaged, but not essential for DNA damage processing. *Acta Biochim Pol* **50:** 169-179

Alter BP (2003) Cancer in Fanconi anemia, 1927-2001. *Cancer* **97:** 425-440

Angele S, Lauge A, Fernet M, Moullan N, Beauvais P, Couturier J, Stoppa-Lyonnet D, Hall J (2003) Phenotypic cellular characterization of an ataxia telangiectasia patient carrying a causal homozygous missense mutation. *Hum Mutat* **21:** 169-170

Anheim M (2011) [Autosomal recessive cerebellar ataxias]. *Rev Neurol (Paris)* **167:** 372-384

Aravind L, Koonin EV (1998) The HD domain defines a new superfamily of metal-dependent phosphohydrolases. *Trends Biochem Sci* **23:** 469-472

Arnaudeau C, Lundin C, Helleday T (2001) DNA double-strand breaks associated with replication forks are predominantly repaired by

homologous recombination involving an exchange mechanism in mammalian cells. *J Mol Biol* **307:** 1235-1245

Audebert M, Salles B, Calsou P (2004) Involvement of poly(ADP-ribose) polymerase-1 and XRCC1/DNA ligase III in an alternative route for DNA double-strand breaks rejoining. *J Biol Chem* **279:** 55117-55126

Audebert M, Salles B, Weinfeld M, Calsou P (2006) Involvement of polynucleotide kinase in a poly(ADP-ribose) polymerase-1-dependent DNA double-strand breaks rejoining pathway. *J Mol Biol* **356:** 257-265

Bachrati CZ, Hickson ID (2009) Dissolution of double Holliday junctions by the concerted action of BLM and topoisomerase IIIalpha. *Methods Mol Biol* **582:** 91-102

Bacman SR, Williams SL, Moraes CT (2009) Intra- and inter-molecular recombination of mitochondrial DNA after in vivo induction of multiple double-strand breaks. *Nucleic Acids Res* **37:** 4218-4226

Balakrishnan L, Brandt PD, Lindsey-Boltz LA, Sancar A, Bambara RA (2009) Long patch base excision repair proceeds via coordinated stimulation of the multienzyme DNA repair complex. *J Biol Chem* **284:** 15158-15172

Barnes DE, Stamp G, Rosewell I, Denzel A, Lindahl T (1998) Targeted disruption of the gene encoding DNA ligase IV leads to lethality in embryonic mice. *Curr Biol* **8:** 1395-1398

Bernstein NK, Karimi-Busheri F, Rasouli-Nia A, Mani R, Dianov G, Glover JN, Weinfeld M (2008) Polynucleotide kinase as a potential target for enhancing cytotoxicity by ionizing radiation and topoisomerase I inhibitors. *Anticancer Agents Med Chem* **8:** 358-367

Bernstein NK, Williams RS, Rakovszky ML, Cui D, Green R, Karimi-Busheri F, Mani RS, Galicia S, Koch CA, Cass CE, Durocher D, Weinfeld M, Glover JN (2005) The molecular architecture of the mammalian DNA repair enzyme, polynucleotide kinase. *Mol Cell* **17:** 657-670

Bolderson E, Richard DJ, Zhou BB, Khanna KK (2009) Recent advances in cancer therapy targeting proteins involved in DNA double-strand break repair. *Clin Cancer Res* **15:** 6314-6320

Bryant HE, Helleday T (2006) Inhibition of poly (ADP-ribose) polymerase activates ATM which is required for subsequent homologous recombination repair. *Nucleic Acids Res* **34:** 1685-1691

Bryant HE, Petermann E, Schultz N, Jemth AS, Loseva O, Issaeva N, Johansson F, Fernandez S, McGlynn P, Helleday T (2009) PARP is

activated at stalled forks to mediate Mre11-dependent replication restart and recombination. *EMBO J* **28:** 2601-2615

Bryant HE, Schultz N, Thomas HD, Parker KM, Flower D, Lopez E, Kyle S, Meuth M, Curtin NJ, Helleday T (2005) Specific killing of BRCA2-deficient tumours with inhibitors of poly(ADP-ribose) polymerase. *Nature* **434:** 913-917

Buck D, Malivert L, de Chasseval R, Barraud A, Fondaneche MC, Sanal O, Plebani A, Stephan JL, Hufnagel M, le Deist F, Fischer A, Durandy A, de Villartay JP, Revy P (2006) Cernunnos, a novel nonhomologous end-joining factor, is mutated in human immunodeficiency with microcephaly. *Cell* **124:** 287-299

Bugreev DV, Mazina OM, Mazin AV (2009) Bloom syndrome helicase stimulates RAD51 DNA strand exchange activity through a novel mechanism. *J Biol Chem* **284:** 26349-26359

Caldecott KW (2003a) DNA single-strand break repair and spinocerebellar ataxia. *Cell* **112:** 7-10

Caldecott KW (2003b) XRCC1 and DNA strand break repair. *DNA Repair (Amst)* **2:** 955-969

Caldecott KW (2007) Mammalian single-strand break repair: mechanisms and links with chromatin. *DNA Repair (Amst)* **6:** 443-453

Caldecott KW (2008) Single-strand break repair and genetic disease. *Nat Rev Genet* **9:** 619-631

Caldecott KW, Tucker JD, Stanker LH, Thompson LH (1995) Characterization of the XRCC1-DNA ligase III complex in vitro and its absence from mutant hamster cells. *Nucleic Acids Res* **23:** 4836-4843

Cantley LC, Neel BG (1999) New insights into tumour suppression: PTEN suppresses tumour formation by restraining the phosphoinositide 3-kinase/AKT pathway. *Proc Natl Acad Sci U S A* **96:** 4240-4245

Chan DW, Chen BP, Prithivirajsingh S, Kurimasa A, Story MD, Qin J, Chen DJ (2002) Autophosphorylation of the DNA-dependent protein kinase catalytic subunit is required for rejoining of DNA double-strand breaks. *Genes Dev* **16:** 2333-2338

Chen BP, Chan DW, Kobayashi J, Burma S, Asaithamby A, Morotomi-Yano K, Botvinick E, Qin J, Chen DJ (2005) Cell cycle dependence of DNA-dependent protein kinase phosphorylation in response to DNA double strand breaks. *J Biol Chem* **280:** 14709-14715

Chen L, Trujillo K, Sung P, Tomkinson AE (2000) Interactions of the DNA ligase IV-XRCC4 complex with DNA ends and the DNA-dependent protein kinase. *J Biol Chem* **275:** 26196-26205

Cincin ZB, Iyibozkurt AC, Kuran SB, Cakmakoglu B (2012) DNA repair gene variants in endometrial carcinoma. *Med Oncol*

Coffey G, Lakshmipathy U, Campbell C (1999) Mammalian mitochondrial extracts possess DNA end-binding activity. *Nucleic Acids Res* **27:** 3348-3354

Comen EA, Robson M (2010) Poly(ADP-ribose) polymerase inhibitors in triple-negative breast cancer. *Cancer J* **16:** 48-52

Coquelle N, Havali-Shahriari Z, Bernstein N, Green R, Glover JN (2011) Structural basis for the phosphatase activity of polynucleotide kinase/phosphatase on single- and double-stranded DNA substrates. *Proc Natl Acad Sci U S A* **108:** 21022-21027

DeFazio LG, Stansel RM, Griffith JD, Chu G (2002) Synapsis of DNA ends by DNA-dependent protein kinase. *EMBO J* **21:** 3192-3200

Dianova, II, Sleeth KM, Allinson SL, Parsons JL, Breslin C, Caldecott KW, Dianov GL (2004) XRCC1-DNA polymerase beta interaction is required for efficient base excision repair. *Nucleic Acids Res* **32:** 2550-2555

Digweed M, Rothe S, Demuth I, Scholz R, Schindler D, Stumm M, Grompe M, Jordan A, Sperling K (2002) Attenuation of the formation of DNA-repair foci containing RAD51 in Fanconi anaemia. *Carcinogenesis* **23:** 1121-1126

Dobbs TA, Tainer JA, Lees-Miller SP (2010) A structural model for regulation of NHEJ by DNA-PKcs autophosphorylation. *DNA Repair (Amst)* **9:** 1307-1314

Dobson CJ, Allinson SL (2006) The phosphatase activity of mammalian polynucleotide kinase takes precedence over its kinase activity in repair of single strand breaks. *Nucleic Acids Res* **34:** 2230-2237

Dobzhansky T (1946) Genetics of Natural Populations. Xiii. Recombination and Variability in Populations of Drosophila Pseudoobscura. *Genetics* **31:** 269-290

Druzhyna NM, Wilson GL, LeDoux SP (2008) Mitochondrial DNA repair in aging and disease. *Mech Ageing Dev* **129:** 383-390

Dungey FA, Caldecott KW, Chalmers AJ (2009) Enhanced radiosensitization of human glioma cells by combining inhibition of poly(ADP-ribose) polymerase with inhibition of heat shock protein 90. *Mol Cancer Ther* **8:** 2243-2254

El-Khamisy SF, Masutani M, Suzuki H, Caldecott KW (2003) A requirement for PARP-1 for the assembly or stability of XRCC1 nuclear foci at sites of oxidative DNA damage. *Nucleic Acids Res* **31:** 5526-5533

Evers B, Schut E, van der Burg E, Braumuller TM, Egan DA, Holstege H, Edser P, Adams DJ, Wade-Martins R, Bouwman P, Jonkers J (2010) A high-throughput pharmaceutical screen identifies compounds with specific toxicity against BRCA2-deficient tumours. *Clin Cancer Res* **16:** 99-108

Farmer H, McCabe N, Lord CJ, Tutt AN, Johnson DA, Richardson TB, Santarosa M, Dillon KJ, Hickson I, Knights C, Martin NM, Jackson SP, Smith GC, Ashworth A (2005) Targeting the DNA repair defect in BRCA mutant cells as a therapeutic strategy. *Nature* **434:** 917-921

Fishel R, Ewel A, Lee S, Lescoe MK, Griffith J (1994) Binding of mismatched microsatellite DNA sequences by the human MSH2 protein. *Science* **266:** 1403-1405

Fong PC, Boss DS, Yap TA, Tutt A, Wu P, Mergui-Roelvink M, Mortimer P, Swaisland H, Lau A, O'Connor MJ, Ashworth A, Carmichael J, Kaye SB, Schellens JH, de Bono JS (2009) Inhibition of poly(ADP-ribose) polymerase in tumours from BRCA mutation carriers. *N Engl J Med* **361:** 123-134

Frank KM, Sekiguchi JM, Seidl KJ, Swat W, Rathbun GA, Cheng HL, Davidson L, Kangaloo L, Alt FW (1998) Late embryonic lethality and impaired V(D)J recombination in mice lacking DNA ligase IV. *Nature* **396:** 173-177

Frederico LA, Kunkel TA, Shaw BR (1990) A sensitive genetic assay for the detection of cytosine deamination: determination of rate constants and the activation energy. *Biochemistry* **29:** 2532-2537

Friedberg EC (2006) *DNA repair and mutagenesis*, 2nd edn. Washington, D.C.: ASM Press.

Friedberg EC, Aguilera A, Gellert M, Hanawalt PC, Hays JB, Lehmann AR, Lindahl T, Lowndes N, Sarasin A, Wood RD (2006) DNA repair: from molecular mechanism to human disease. *DNA Repair (Amst)* **5:** 986-996

Gagne JP, Hendzel MJ, Droit A, Poirier GG (2006) The expanding role of poly(ADP-ribose) metabolism: current challenges and new perspectives. *Curr Opin Cell Biol* **18:** 145-151

Gagne JP, Isabelle M, Lo KS, Bourassa S, Hendzel MJ, Dawson VL, Dawson TM, Poirier GG (2008) Proteome-wide identification of poly(ADP-ribose) binding proteins and poly(ADP-ribose)-associated protein complexes. *Nucleic Acids Res* **36:** 6959-6976

Gao Y, Sun Y, Frank KM, Dikkes P, Fujiwara Y, Seidl KJ, Sekiguchi JM, Rathbun GA, Swat W, Wang J, Bronson RT, Malynn BA, Bryans M, Zhu C, Chaudhuri J, Davidson L, Ferrini R, Stamato T, Orkin SH, Greenberg ME, Alt FW (1998) A critical role for DNA end-joining proteins in both lymphogenesis and neurogenesis. *Cell* **95:** 891-902

Garces F, Pearl LH, Oliver AW (2011) The structural basis for substrate recognition by mammalian polynucleotide kinase 3' phosphatase. *Mol Cell* **44:** 385-396

Garcia-Higuera I, Taniguchi T, Ganesan S, Meyn MS, Timmers C, Hejna J, Grompe M, D'Andrea AD (2001) Interaction of the Fanconi anemia proteins and BRCA1 in a common pathway. *Mol Cell* **7:** 249-262

Gaskell LJ, Osman F, Gilbert RJ, Whitby MC (2007) Mus81 cleavage of Holliday junctions: a failsafe for processing meiotic recombination intermediates? *EMBO J* **26:** 1891-1901

Gien LT, Mackay HJ (2010) The Emerging Role of PARP Inhibitors in the Treatment of Epithelial Ovarian Cancer. *J Oncol* **2010:** 151750

Godon C, Cordelieres FP, Biard D, Giocanti N, Megnin-Chanet F, Hall J, Favaudon V (2008) PARP inhibition versus PARP-1 silencing: different outcomes in terms of single-strand break repair and radiation susceptibility. *Nucleic Acids Res* **36:** 4454-4464

Goodarzi AA, Yu Y, Riballo E, Douglas P, Walker SA, Ye R, Harer C, Marchetti C, Morrice N, Jeggo PA, Lees-Miller SP (2006) DNA-PK autophosphorylation facilitates Artemis endonuclease activity. *EMBO J* **25:** 3880-3889

Gu Y, Sekiguchi J, Gao Y, Dikkes P, Frank K, Ferguson D, Hasty P, Chun J, Alt FW (2000) Defective embryonic neurogenesis in Ku-deficient but not DNA-dependent protein kinase catalytic subunit-deficient mice. *Proc Natl Acad Sci U S A* **97:** 2668-2673

Gumy-Pause F, Wacker P, Sappino AP (2004) ATM gene and lymphoid malignancies. *Leukemia* **18:** 238-242

Harman D (1972) The biologic clock: the mitochondria? *J Am Geriatr Soc* **20:** 145-147

Hartlerode AJ, Scully R (2009) Mechanisms of double-strand break repair in somatic mammalian cells. *Biochem J* **423:** 157-168

Helleday T (2011) The underlying mechanism for the PARP and BRCA synthetic lethality: clearing up the misunderstandings. *Mol Oncol* **5:** 387-393

Hopfner KP, Craig L, Moncalian G, Zinkel RA, Usui T, Owen BA, Karcher A, Henderson B, Bodmer JL, McMurray CT, Carney JP, Petrini JH, Tainer JA (2002) The Rad50 zinc-hook is a structure joining Mre11 complexes in DNA recombination and repair. *Nature* **418:** 562-566

Horton JK, Watson M, Stefanick DF, Shaughnessy DT, Taylor JA, Wilson SH (2008) XRCC1 and DNA polymerase beta in cellular protection against cytotoxic DNA single-strand breaks. *Cell Res* **18:** 48-63

Howlett NG, Taniguchi T, Olson S, Cox B, Waisfisz Q, De Die-Smulders C, Persky N, Grompe M, Joenje H, Pals G, Ikeda H, Fox EA, D'Andrea AD (2002) Biallelic inactivation of BRCA2 in Fanconi anemia. *Science* **297:** 606-609

Hussain S, Wilson JB, Medhurst AL, Hejna J, Witt E, Ananth S, Davies A, Masson JY, Moses R, West SC, de Winter JP, Ashworth A, Jones NJ, Mathew CG (2004) Direct interaction of FANCD2 with BRCA2 in DNA damage response pathways. *Hum Mol Genet* **13:** 1241-1248

Iglehart JD, Silver DP (2009) Synthetic lethality--a new direction in cancer-drug development. *N Engl J Med* **361:** 189-191

Iliakis G (2009) Backup pathways of NHEJ in cells of higher eukaryotes: cell cycle dependence. *Radiother Oncol* **92:** 310-315

Jeppesen DK, Bohr VA, Stevnsner T (2011) DNA repair deficiency in neurodegeneration. *Prog Neurobiol* **94:** 166-200

Jilani A, Ramotar D, Slack C, Ong C, Yang XM, Scherer SW, Lasko DD (1999) Molecular cloning of the human gene, PNKP, encoding a polynucleotide kinase 3'-phosphatase and evidence for its role in repair of DNA strand breaks caused by oxidative damage. *J Biol Chem* **274:** 24176-24186

Kaelin WG, Jr. (2005) The concept of synthetic lethality in the context of anticancer therapy. *Nat Rev Cancer* **5:** 689-698

Kaelin WG, Jr. (2009) Synthetic lethality: a framework for the development of wiser cancer therapeutics. *Genome Med* **1:** 99

Kajander OA, Karhunen PJ, Holt IJ, Jacobs HT (2001) Prominent mitochondrial DNA recombination intermediates in human heart muscle. *EMBO Rep* **2:** 1007-1012

Karimi-Busheri F, Lee J, Tomkinson AE, Weinfeld M (1998) Repair of DNA strand gaps and nicks containing 3'-phosphate and 5'-hydroxyl termini by purified mammalian enzymes. *Nucleic Acids Res* **26:** 4395-4400

Kikuchi K, Abdel-Aziz HI, Taniguchi Y, Yamazoe M, Takeda S, Hirota K (2009) Bloom DNA helicase facilitates homologous recombination between diverged homologous sequences. *J Biol Chem* **284:** 26360-26367

Kim MY, Mauro S, Gevry N, Lis JT, Kraus WL (2004) NAD+-dependent modulation of chromatin structure and transcription by nucleosome binding properties of PARP-1. *Cell* **119:** 803-814

Koch CA, Agyei R, Galicia S, Metalnikov P, O'Donnell P, Starostine A, Weinfeld M, Durocher D (2004) Xrcc4 physically links DNA end processing by polynucleotide kinase to DNA ligation by DNA ligase IV. *EMBO J* **23:** 3874-3885

Kulkarni A, McNeill DR, Gleichmann M, Mattson MP, Wilson DM, 3rd (2008) XRCC1 protects against the lethality of induced oxidative DNA damage in nondividing neural cells. *Nucleic Acids Res* **36:** 5111-5121

Lakshmipathy U, Campbell C (1999) Double strand break rejoining by mammalian mitochondrial extracts. *Nucleic Acids Res* **27:** 1198-1204

Lancaster JM, Wooster R, Mangion J, Phelan CM, Cochran C, Gumbs C, Seal S, Barfoot R, Collins N, Bignell G, Patel S, Hamoudi R, Larsson C, Wiseman RW, Berchuck A, Iglehart JD, Marks JR, Ashworth A, Stratton MR, Futreal PA (1996) BRCA2 mutations in primary breast and ovarian cancers. *Nat Genet* **13:** 238-240

Lee JH, Paull TT (2004) Direct activation of the ATM protein kinase by the Mre11/Rad50/Nbs1 complex. *Science* **304:** 93-96

Lee JH, Paull TT (2005) ATM activation by DNA double-strand breaks through the Mre11-Rad50-Nbs1 complex. *Science* **308:** 551-554

Lee JH, Paull TT (2007) Activation and regulation of ATM kinase activity in response to DNA double-strand breaks. *Oncogene* **26:** 7741-7748

Lieber MR (2010) The Mechanism of Double-Strand DNA Break Repair by the Nonhomologous DNA End-Joining Pathway. *Annu Rev Biochem*

Lilyestrom W, van der Woerd MJ, Clark N, Luger K (2010) Structural and biophysical studies of human PARP-1 in complex with damaged DNA. *J Mol Biol* **395:** 983-994

Lindahl T, Nyberg B (1972) Rate of depurination of native deoxyribonucleic acid. *Biochemistry* **11:** 3610-3618

Lindahl T, Nyberg B (1974) Heat-induced deamination of cytosine residues in deoxyribonucleic acid. *Biochemistry* **13:** 3405-3410

Loizou JI, El-Khamisy SF, Zlatanou A, Moore DJ, Chan DW, Qin J, Sarno S, Meggio F, Pinna LA, Caldecott KW (2004) The protein kinase CK2 facilitates repair of chromosomal DNA single-strand breaks. *Cell* **117:** 17-28

Lucchesi JC (1968) Synthetic lethality and semi-lethality among functionally related mutants of Drosophila melanfgaster. *Genetics* **59:** 37-44

Lundin C, Erixon K, Arnaudeau C, Schultz N, Jenssen D, Meuth M, Helleday T (2002) Different roles for nonhomologous end joining and homologous recombination following replication arrest in mammalian cells. *Mol Cell Biol* **22:** 5869-5878

Ma Y, Pannicke U, Lu H, Niewolik D, Schwarz K, Lieber MR (2005) The DNA-dependent protein kinase catalytic subunit phosphorylation sites in human Artemis. *J Biol Chem* **280:** 33839-33846

Ma Y, Pannicke U, Schwarz K, Lieber MR (2002) Hairpin opening and overhang processing by an Artemis/DNA-dependent protein kinase complex in nonhomologous end joining and V(D)J recombination. *Cell* **108:** 781-794

Mani RS, Fanta M, Karimi-Busheri F, Silver E, Virgen CA, Caldecott KW, Cass CE, Weinfeld M (2007) XRCC1 stimulates polynucleotide kinase by enhancing its damage discrimination and displacement from DNA repair intermediates. *J Biol Chem* **282:** 28004-28013

Mani RS, Karimi-Busheri F, Cass CE, Weinfeld M (2001) Physical properties of human polynucleotide kinase: hydrodynamic and spectroscopic studies. *Biochemistry* **40:** 12967-12973

Mani RS, Yu Y, Fang S, Lu M, Fanta M, Zolner AE, Tahbaz N, Ramsden DA, Litchfield DW, Lees-Miller SP, Weinfeld M (2010) Dual modes of interaction between XRCC4 and polynucleotide kinase/phosphatase: implications for nonhomologous end joining. *J Biol Chem* **285:** 37619-37629

Martin SA, Hewish M, Sims D, Lord CJ, Ashworth A (2011) Parallel high-throughput RNA interference screens identify PINK1 as a potential therapeutic target for the treatment of DNA mismatch repair-deficient cancers. *Cancer Res* **71:** 1836-1848

Masaoka A, Horton JK, Beard WA, Wilson SH (2009) DNA polymerase beta and PARP activities in base excision repair in living cells. *DNA Repair (Amst)* **8:** 1290-1299

Matsuoka S, Ballif BA, Smogorzewska A, McDonald ER, 3rd, Hurov KE, Luo J, Bakalarski CE, Zhao Z, Solimini N, Lerenthal Y, Shiloh Y, Gygi SP, Elledge SJ (2007) ATM and ATR substrate analysis reveals extensive protein networks responsive to DNA damage. *Science* **316:** 1160-1166

Maynard S, de Souza-Pinto NC, Scheibye-Knudsen M, Bohr VA (2010) Mitochondrial base excision repair assays. *Methods* **51:** 416-425

Mello JA, Acharya S, Fishel R, Essigmann JM (1996) The mismatch-repair protein hMSH2 binds selectively to DNA adducts of the anticancer drug cisplatin. *Chem Biol* **3:** 579-589

Mendes-Pereira AM, Martin SA, Brough R, McCarthy A, Taylor JR, Kim JS, Waldman T, Lord CJ, Ashworth A (2009) Synthetic lethal targeting of PTEN mutant cells with PARP inhibitors. *EMBO Mol Med* **1:** 315-322

Miki Y, Swensen J, Shattuck-Eidens D, Futreal PA, Harshman K, Tavtigian S, Liu Q, Cochran C, Bennett LM, Ding W, et al. (1994) A strong candidate for the breast and ovarian cancer susceptibility gene BRCA1. *Science* **266:** 66-71

Miquel J, Economos AC, Fleming J, Johnson JE, Jr. (1980) Mitochondrial role in cell aging. *Exp Gerontol* **15:** 575-591

Moreno-Herrero F, de Jager M, Dekker NH, Kanaar R, Wyman C, Dekker C (2005) Mesoscale conformational changes in the DNA-repair complex Rad50/Mre11/Nbs1 upon binding DNA. *Nature* **437:** 440-443

Morris EP, Rivera-Calzada A, da Fonseca PC, Llorca O, Pearl LH, Spagnolo L (2011) Evidence for a remodelling of DNA-PK upon autophosphorylation from electron microscopy studies. *Nucleic Acids Res* **39:** 5757-5767

Mortusewicz O, Ame JC, Schreiber V, Leonhardt H (2007) Feedback-regulated poly(ADP-ribosyl)ation by PARP-1 is required for rapid response to DNA damage in living cells. *Nucleic Acids Res* **35:** 7665-7675

Moshous D, Pannetier C, Chasseval Rd R, Deist Fl F, Cavazzana-Calvo M, Romana S, Macintyre E, Canioni D, Brousse N, Fischer A, Casanova JL, Villartay JP (2003) Partial T and B lymphocyte immunodeficiency and predisposition to lymphoma in patients with hypomorphic mutations in Artemis. *J Clin Invest* **111:** 381-387

Nakamura J, Walker VE, Upton PB, Chiang SY, Kow YW, Swenberg JA (1998) Highly sensitive apurinic/apyrimidinic site assay can detect spontaneous and chemically induced depurination under physiological conditions. *Cancer Res* **58:** 222-225

Narayan S, Jaiswal AS, Balusu R (2005) Tumour suppressor APC blocks DNA polymerase beta-dependent strand displacement synthesis during long patch but not short patch base excision repair and increases sensitivity to methylmethane sulfonate. *J Biol Chem* **280:** 6942-6949

Nusinow DA, Hernandez-Munoz I, Fazzio TG, Shah GM, Kraus WL, Panning B (2007) Poly(ADP-ribose) polymerase 1 is inhibited by a histone H2A variant, MacroH2A, and contributes to silencing of the inactive X chromosome. *J Biol Chem* **282:** 12851-12859

O'Brien T, Stokoe D (2009) Converting cancer mutations into therapeutic opportunities. *EMBO Mol Med* **1:** 297-299

O'Connor MJ, Martin NM, Smith GC (2007) Targeted cancer therapies based on the inhibition of DNA strand break repair. *Oncogene* **26:** 7816-7824

O'Driscoll M, Cerosaletti KM, Girard PM, Dai Y, Stumm M, Kysela B, Hirsch B, Gennery A, Palmer SE, Seidel J, Gatti RA, Varon R, Oettinger MA, Neitzel H, Jeggo PA, Concannon P (2001) DNA ligase IV mutations identified in patients exhibiting developmental delay and immunodeficiency. *Mol Cell* **8:** 1175-1185

O'Rourke TW, Doudican NA, Mackereth MD, Doetsch PW, Shadel GS (2002) Mitochondrial dysfunction due to oxidative mitochondrial DNA damage is reduced through cooperative actions of diverse proteins. *Mol Cell Biol* **22:** 4086-4093

Osman F, Whitby MC (2007) Exploring the roles of Mus81-Eme1/Mms4 at perturbed replication forks. *DNA Repair (Amst)* **6:** 1004-1017

Overington JP, Al-Lazikani B, Hopkins AL (2006) How many drug targets are there? *Nat Rev Drug Discov* **5:** 993-996

Pal SK, Mortimer J (2009) Triple-negative breast cancer: novel therapies and new directions. *Maturitas* **63:** 269-274

Parsons JL, Dianova, II, Allinson SL, Dianov GL (2005a) DNA polymerase beta promotes recruitment of DNA ligase III alpha-XRCC1 to sites of base excision repair. *Biochemistry* **44:** 10613-10619

Parsons JL, Dianova, II, Allinson SL, Dianov GL (2005b) Poly(ADP-ribose) polymerase-1 protects excessive DNA strand breaks from deterioration during repair in human cell extracts. *FEBS J* **272:** 2012-2021

Pastwa E, Blasiak J (2003) Non-homologous DNA end joining. *Acta Biochim Pol* **50:** 891-908

Pellegrini L, Yu DS, Lo T, Anand S, Lee M, Blundell TL, Venkitaraman AR (2002) Insights into DNA recombination from the structure of a RAD51-BRCA2 complex. *Nature* **420:** 287-293

Prasad R, Beard WA, Batra VK, Liu Y, Shock DD, Wilson SH (2011) A review of recent experiments on step-to-step "hand-off" of the DNA intermediates in mammalian base excision repair pathways. *Mol Biol (Mosk)* **45:** 586-600

Rasouli-Nia A, Karimi-Busheri F, Weinfeld M (2004) Stable down-regulation of human polynucleotide kinase enhances spontaneous

mutation frequency and sensitizes cells to genotoxic agents. *Proc Natl Acad Sci U S A* **101:** 6905-6910

Rass U, Ahel I, West SC (2007) Defective DNA repair and neurodegenerative disease. *Cell* **130:** 991-1004

Reynolds JJ, El-Khamisy SF, Katyal S, Clements P, McKinnon PJ, Caldecott KW (2009) Defective DNA ligation during short-patch single-strand break repair in ataxia oculomotor apraxia 1. *Mol Cell Biol* **29:** 1354-1362

Rosenberg PS, Alter BP, Ebell W (2008) Cancer risks in Fanconi anemia: findings from the German Fanconi Anemia Registry. *Haematologica* **93:** 511-517

Rosenberg PS, Greene MH, Alter BP (2003) Cancer incidence in persons with Fanconi anemia. *Blood* **101:** 822-826

Sage JM, Gildemeister OS, Knight KL (2010) Discovery of a novel function for human Rad51: maintenance of the mitochondrial genome. *J Biol Chem* **285:** 18984-18990

Savic V, Yin B, Maas NL, Bredemeyer AL, Carpenter AC, Helmink BA, Yang-Iott KS, Sleckman BP, Bassing CH (2009) Formation of dynamic

gamma-H2AX domains along broken DNA strands is distinctly regulated by ATM and MDC1 and dependent upon H2AX densities in chromatin. *Mol Cell* **34:** 298-310

Schmutte C, Marinescu RC, Sadoff MM, Guerrette S, Overhauser J, Fishel R (1998) Human exonuclease I interacts with the mismatch repair protein hMSH2. *Cancer Res* **58:** 4537-4542

Settheetham-Ishida W, Yuenyao P, Natphopsuk S, Settheetham D, Ishida T (2011) Genetic risk of DNA repair gene polymorphisms (XRCC1 and XRCC3) for high risk human papillomavirus negative cervical cancer in Northeast Thailand. *Asian Pac J Cancer Prev* **12:** 963-966

Sharan SK, Morimatsu M, Albrecht U, Lim DS, Regel E, Dinh C, Sands A, Eichele G, Hasty P, Bradley A (1997) Embryonic lethality and radiation hypersensitivity mediated by Rad51 in mice lacking Brca2. *Nature* **386:** 804-810

Shen J, Gilmore EC, Marshall CA, Haddadin M, Reynolds JJ, Eyaid W, Bodell A, Barry B, Gleason D, Allen K, Ganesh VS, Chang BS, Grix A, Hill RS, Topcu M, Caldecott KW, Barkovich AJ, Walsh CA (2010) Mutations in PNKP cause microcephaly, seizures and defects in DNA repair. *Nat Genet* **42:** 245-249

Shen JC, Rideout WM, 3rd, Jones PA (1994) The rate of hydrolytic deamination of 5-methylcytosine in double-stranded DNA. *Nucleic Acids Res* **22:** 972-976

Simpson L, Parsons R (2001) PTEN: life as a tumour suppressor. *Exp Cell Res* **264:** 29-41

Simsek D, Furda A, Gao Y, Artus J, Brunet E, Hadjantonakis AK, Van Houten B, Shuman S, McKinnon PJ, Jasin M (2011) Crucial role for DNA ligase III in mitochondria but not in Xrcc1-dependent repair. *Nature* **471:** 245-248

Stefansson OA, Jonasson JG, Johannsson OT, Olafsdottir K, Steinarsdottir M, Valgeirsdottir S, Eyfjord JE (2009) Genomic profiling of breast tumours in relation to BRCA abnormalities and phenotypes. *Breast Cancer Res* **11:** R47

Strumberg D, Pilon AA, Smith M, Hickey R, Malkas L, Pommier Y (2000) Conversion of topoisomerase I cleavage complexes on the leading strand of ribosomal DNA into 5'-phosphorylated DNA double-strand breaks by replication runoff. *Mol Cell Biol* **20:** 3977-3987

Sukhanova M, Khodyreva S, Lavrik O (2009) Poly(ADP-ribose) polymerase 1 regulates activity of DNA polymerase beta in long patch base excision repair. *Mutat Res* **685:** 80-89

Sung P, Klein H (2006) Mechanism of homologous recombination: mediators and helicases take on regulatory functions. *Nat Rev Mol Cell Biol* **7:** 739-750

Szczesny B, Tann AW, Longley MJ, Copeland WC, Mitra S (2008) Long patch base excision repair in mammalian mitochondrial genomes. *J Biol Chem* **283:** 26349-26356

Taniguchi T, Garcia-Higuera I, Andreassen PR, Gregory RC, Grompe M, D'Andrea AD (2002) S-phase-specific interaction of the Fanconi anemia protein, FANCD2, with BRCA1 and RAD51. *Blood* **100:** 2414-2420

Thacker J, Zdzienicka MZ (2003) The mammalian XRCC genes: their roles in DNA repair and genetic stability. *DNA Repair (Amst)* **2:** 655-672

Thompson LH, Brookman KW, Jones NJ, Allen SA, Carrano AV (1990) Molecular cloning of the human XRCC1 gene, which corrects defective DNA strand break repair and sister chromatid exchange. *Mol Cell Biol* **10:** 6160-6171

Thorstenson YR, Roxas A, Kroiss R, Jenkins MA, Yu KM, Bachrich T, Muhr D, Wayne TL, Chu G, Davis RW, Wagner TM, Oefner PJ (2003) Contributions of ATM mutations to familial breast and ovarian cancer. *Cancer Res* **63:** 3325-3333

Thyagarajan B, Padua RA, Campbell C (1996) Mammalian mitochondria possess homologous DNA recombination activity. *J Biol Chem* **271:** 27536-27543

Tischkowitz M, Eeles R, Cancer IsIoMwgptP, its Clinical Treatment c (2003) Mutations in BRCA1 and BRCA2 and predisposition to prostate cancer. *Lancet* **362:** 80; author reply 80

Turner NC, Lord CJ, Iorns E, Brough R, Swift S, Elliott R, Rayter S, Tutt AN, Ashworth A (2008) A synthetic lethal siRNA screen identifying genes mediating sensitivity to a PARP inhibitor. *EMBO J* **27:** 1368-1377

Valerie K, Povirk LF (2003) Regulation and mechanisms of mammalian double-strand break repair. *Oncogene* **22:** 5792-5812

Vemuri MC, Schiller E, Naegele JR (2001) Elevated DNA double strand breaks and apoptosis in the CNS of scid mutant mice. *Cell Death Differ* **8:** 245-255

Venkitaraman AR (2009) Targeting the molecular defect in BRCA-deficient tumours for cancer therapy. *Cancer Cell* **16:** 89-90

Vens C, Dahmen-Mooren E, Verwijs-Janssen M, Blyweert W, Graversen L, Bartelink H, Begg AC (2002) The role of DNA polymerase beta in determining sensitivity to ionizing radiation in human tumour cells. *Nucleic Acids Res* **30:** 2995-3004

Wallace DC, Shoffner JM, Trounce I, Brown MD, Ballinger SW, Corral-Debrinski M, Horton T, Jun AS, Lott MT (1995) Mitochondrial DNA mutations in human degenerative diseases and aging. *Biochim Biophys Acta* **1271:** 141-151

Weinfeld M, Mani RS, Abdou I, Aceytuno RD, Glover JN (2011) Tidying up loose ends: the role of polynucleotide kinase/phosphatase in DNA strand break repair. *Trends Biochem Sci*

Whitehouse CJ, Taylor RM, Thistlethwaite A, Zhang H, Karimi-Busheri F, Lasko DD, Weinfeld M, Caldecott KW (2001) XRCC1 stimulates human polynucleotide kinase activity at damaged DNA termini and accelerates DNA single-strand break repair. *Cell* **104:** 107-117

Wickliffe JK, Herring SM, Hallberg LM, Galbert LA, Masters OE, 3rd, Ammenheuser MM, Xie J, Friedberg EC, Lloyd RS, Abdel-Rahman SZ,

Ward JB, Jr. (2007) Detoxification of olefinic epoxides and nucleotide excision repair of epoxide-mediated DNA damage: Insights from animal models examining human sensitivity to 1,3-butadiene. *Chem Biol Interact* **166:** 226-231

Williams BR, Mirzoeva OK, Morgan WF, Lin J, Dunnick W, Petrini JH (2002) A murine model of Nijmegen breakage syndrome. *Curr Biol* **12:** 648-653

Williams RS, Moncalian G, Williams JS, Yamada Y, Limbo O, Shin DS, Groocock LM, Cahill D, Hitomi C, Guenther G, Moiani D, Carney JP, Russell P, Tainer JA (2008) Mre11 dimers coordinate DNA end bridging and nuclease processing in double-strand-break repair. *Cell* **135:** 97-109

Williamson CT, Muzik H, Turhan AG, Zamo A, O'Connor MJ, Bebb DG, Lees-Miller SP (2010) ATM deficiency sensitizes mantle cell lymphoma cells to poly(ADP-ribose) polymerase-1 inhibitors. *Mol Cancer Ther* **9:** 347-357

Wong AK, Pero R, Ormonde PA, Tavtigian SV, Bartel PL (1997) RAD51 interacts with the evolutionarily conserved BRC motifs in the human breast cancer susceptibility gene brca2. *J Biol Chem* **272:** 31941-31944

Woodhouse BC, Dianov GL (2008) Poly ADP-ribose polymerase-1: an international molecule of mystery. *DNA Repair (Amst)* **7:** 1077-1086

Woodhouse BC, Dianova, II, Parsons JL, Dianov GL (2008) Poly(ADP-ribose) polymerase-1 modulates DNA repair capacity and prevents formation of DNA double strand breaks. *DNA Repair (Amst)* **7:** 932-940

Wooster R, Bignell G, Lancaster J, Swift S, Seal S, Mangion J, Collins N, Gregory S, Gumbs C, Micklem G (1995) Identification of the breast cancer susceptibility gene BRCA2. *Nature* **378:** 789-792

Yakes FM, Van Houten B (1997) Mitochondrial DNA damage is more extensive and persists longer than nuclear DNA damage in human cells following oxidative stress. *Proc Natl Acad Sci U S A* **94:** 514-519

Yaneva M, Kowalewski T, Lieber MR (1997) Interaction of DNA-dependent protein kinase with DNA and with Ku: biochemical and atomic-force microscopy studies. *EMBO J* **16:** 5098-5112

Yang YG, Cortes U, Patnaik S, Jasin M, Wang ZQ (2004) Ablation of PARP-1 does not interfere with the repair of DNA double-strand breaks, but compromises the reactivation of stalled replication forks. *Oncogene* **23:** 3872-3882

Yannone SM, Khan IS, Zhou RZ, Zhou T, Valerie K, Povirk LF (2008) Coordinate 5' and 3' endonucleolytic trimming of terminally blocked blunt DNA double-strand break ends by Artemis nuclease and DNA-dependent protein kinase. *Nucleic Acids Res* **36:** 3354-3365

Yin Y, Shen WH (2008) PTEN: a new guardian of the genome. *Oncogene* **27:** 5443-5453

Yoo S, Dynan WS (1999) Geometry of a complex formed by double strand break repair proteins at a single DNA end: recruitment of DNA-PKcs induces inward translocation of Ku protein. *Nucleic Acids Res* **27:** 4679-4686

Zander SA, Kersbergen A, van der Burg E, de Water N, van Tellingen O, Gunnarsdottir S, Jaspers JE, Pajic M, Nygren AO, Jonkers J, Borst P, Rottenberg S (2010) Sensitivity and acquired resistance of BRCA1;p53-deficient mouse mammary tumours to the topoisomerase I inhibitor topotecan. *Cancer Res* **70:** 1700-1710

Zaniolo K, Desnoyers S, Leclerc S, Guerin SL (2007) Regulation of poly(ADP-ribose) polymerase-1 (PARP-1) gene expression through the post-translational modification of Sp1: a nuclear target protein of PARP-1. *BMC Mol Biol* **8:** 96

Chapter 2: Genetic screening for synthetic lethal partners of polynucleotide kinase/phosphatase: potential for targeting SHP-1 depleted cancers

Genetic screening for synthetic lethal partners of polynucleotide kinase/phosphatase: potential for targeting SHP-1 depleted cancers

[1]Todd R. Mereniuk, [2]Robert A. Maranchuk, [2]Anja Schindler, [1]Jonathan C. Penner, [1]Gary K. Freschauf, [3]Samar Hegazy, [3]Raymond Lai, [2]Edan Foley, and [1]Michael Weinfeld

Affiliations of authors:
[1]Experimental Oncology, Department of Oncology, University of Alberta, Edmonton, AB, Canada T6G 1Z2
[2]Department of Medical Microbiology and Immunology, University of Alberta, Edmonton, AB, Canada T6G 2S2
[3]Department of Laboratory Medicine and Pathology, University of Alberta, Edmonton, AB, Canada T6G 1Z2

Correspondence to: Michael Weinfeld
Cross Cancer Institute
University of Alberta
11560 University Ave
Edmonton, AB, Canada, T6G 1Z2
Tel: 780 432 8438
Fax: 780 432 8428
E-mail: michael.weinfeld@albertahealthservices.ca.

Running title: Synthetic lethal partnership between PNKP and SHP-1

Total number of Figures in main text - 7
Total number of Tables in main text - 1
Total number of Figures in Supplementary material - 6
Total number Tables in Supplementary material - 1

Key words: Synthetic lethality, genetic screen, reactive oxygen species, polynucleotide kinase/phosphatase, SHP-1

A version of this chapter has been submitted for publication. Cancer Research.

2.1 INTRODUCTION

A recent exciting development in cancer treatment is the potential utilization of synthetic lethality as a patient and cancer-specific therapy. Synthetic lethality arises when the simultaneous disruption of two non-allelic, non-essential genes or their proteins in the same cell induces lethality (Iglehart & Silver, 2009; Lucchesi, 1968). Recently this phenomenon has been shown to occur between combinations of DNA repair genes and much attention has focused on the co-disruption of the single-strand break repair (SSBR) protein poly(ADP-ribose) polymerase (PARP) and the breast cancer associated (BRCA) proteins (Bryant et al, 2005; Farmer et al, 2005; Fong et al, 2009). The BRCA proteins are putative tumour suppressors naturally lost or mutated in tumour cells of women afflicted with hereditary breast and ovarian cancer and have roles in DNA double-strand break repair (DSBR). One proposed explanation for this synthetic lethality is that chemical inhibition of PARP causes the generation of double-strand breaks (DSBs) by preventing SSBR (Bolderson et al, 2009; Helleday, 2011). As cells progress through S-phase, naturally occurring SSBs collapse the replication fork to give rise to DSBs, which in $BRCA^{-/-}$ cancer cells accumulate, eventually leading to specific cancer cell death. Normal cells in BRCA patients retain BRCA heterozygosity and therefore possess the capacity to fully repair DSBs and so are not appreciably affected by PARP inhibitors during the treatment, and thus the deleterious side effects typically associated with cancer therapy are greatly reduced (Amir et al, 2010).

It has been argued that the clinical success of PARP inhibitors BSI-201 (Pal & Mortimer, 2009) and Olaparib (Evers et al, 2010; Stefansson et al, 2009) in treating breast and ovarian cancers associated with BRCA and BRCA-like mutations depended primarily on the synthetic lethal relationship between PARP and dysfunctional DSBR. Interestingly, recent evidence has suggested that there also exists a synthetic lethal relationship between PARP and the major tumour suppressor PTEN (Mendes-Pereira et al, 2009). This finding shows that the clinical potential of PARP inhibitors need not solely rely on the effectiveness in treating BRCA-related cancers.

It has been estimated that there are approximately 10^4 SSBs formed per cell per day probably as a result of the generation of reactive oxygen species (ROS) during normal metabolism (Lindahl & Nyberg, 1972). Many of these breaks harbour unligatable termini such as 3'-phosphates and 5'-hydroxyls that must be processed for repair of DNA to proceed. Polynucleotide kinase/phosphatase (PNKP) is a bifunctional repair enzyme whose role is to process these termini during SSBR and DSBR by catalyzing the dephosphorylation of 3'-phosphate termini and the phosphorylation of 5'-hydroxyl termini to yield elongation and ligation-competent 5'-phosphate and 3'-hydroxyl ends (Weinfeld et al, 2011). PNKP is a versatile protein acting in many DNA repair pathways, including base excision repair (BER), SSBR and DSBR (Weinfeld et al, 2011). Cells stably depleted of PNKP show marked sensitization to γ-radiation and the topoisomerase I inhibitor camptothecin (Rasouli-Nia et al, 2004).

Given the potential to target PNKP by small molecule inhibitors (Freschauf et al, 2009), we sought to identify synthetic lethal relationships of PNKP in order to expand the repertoire of targeted therapy taking advantage of this approach. By screening ~7000 genes targeting the "druggable" genome, we have identified a variety of proteins potentially synthetic lethal with PNKP including several that are either known or are implicated as tumour suppressors, such as the protein tyrosine phosphatase SHP-1 (PTPN6). We also show that SHP-1 is not directly involved in DNA repair and therefore cell death based on DSB accumulation caused by inhibition of two distinct but interacting DNA repair pathways, i.e. SSBR and DSBR as previously described, is not the only explanation for the occurrence of synthetic lethality involving a DNA repair protein partner (Bolderson et al, 2009; Helleday, 2011). Instead, the observation that SHP-1 depletion causes an increase in ROS production supports an alternative paradigm for synthetic lethality that combines increased DNA damage production with limited DNA repair capacity, as was previously shown for the interaction between PTEN-induced putative kinase 1 (PINK1) and the mismatch repair proteins MSH2, MLH1 and MSH6 (Martin et al, 2011). This suggests that we can broaden the potential for clinical application of synthetic lethality.

2.2 MATERIALS AND METHODS

2.2.1 Cells

A549 (human lung carcinoma) and MCF7 (human breast adenocarcinoma) cell lines were obtained from the American Type Culture Collection (Manassas, VA). These cells and their transfected derivatives were cultured at 37°C and 5% CO_2 in a humidified incubator in a 1:1 mixture of Dulbecco's Modified Eagle's Medium and F12 (DMEM/F12) supplemented with 10% fetal bovine serum (FBS), L-glutamine (2 mM), non-essential amino acids (0.1 mM) and sodium pyruvate (1 mM). All culture supplements were purchased from Invitrogen (Carlsbad, CA). For comet assays and apoptosis/necrosis detection penicillin (50 U/mL) and streptomycin (50 µg/mL) were added to the DMEM/F12 (complete DMEM/F12). SUPM2 (DCMZ, Braunschweig, Germany) and Karpas 299 (obtained as a gift from Dr. M. Kadin, Boston, MA) human anaplastic large cell lymphoma cell lines were cultured in RPMI-1640 medium (Sigma-Aldrich, Oakville, ON) supplemented with 10% FBS, 0.3 g/L L-glutamine and 2 g/L $NaHCO_3$. Both SUP-M2 and Karpas 299 cells were recently confirmed to carry monoclonal T-cell rearrangements by polymerase chain reaction and express the NPM-ALK fusion protein by western blots.

2.2.2 Plasmids for stable transfections

All cell lines were generated by stable transfection of pSUPER.neo constructs (Oligoengine, Seattle, WA) into A549 or MCF7 cells yielding several distinct cell lines. An shRNA directed against nucleotides 1391-1410 of PNKP (Rasouli-Nia et al, 2004) was used to stably deplete PNKP in A549 and MCF7 cells (A549δPNKP and MCF7δPNKP, respectively),

and another shRNA expression vector targeting nucleotides 1313-1333 of SHP-1 was used to generate A549δSHP-1 cells. A control cell line was also generated in which an shRNA to no known gene target (a scrambled shRNA, pSUPER.neo.Mamm-X, Oligoengine) was expressed in A549 cells (A549-Scramble).

2.2.3 Stable transfections

Approximately 20,000 A549 or MCF7 cells were plated and allowed to adhere overnight in a 24-well dish at 37°C and 5% CO_2. The transfection mixture was prepared from two separate solutions, the first containing 1 µg of pSUPER.neo plasmid DNA dissolved in 50 µL total of Opti-MEM (Invitrogen), and the second 3 µL of Lipofectamine2000 (Invitrogen) in 50 µL total Opti-MEM. The two solutions were incubated at room temperature for 5 min before combination, mixed and then held at room temperature for 20 min. The media from the pre-plated A549 cells was removed and the transfection mixture was added and the cells were incubated for 24 h at 37°C and 5% CO_2. The cells were then trypsinized and replated into 6 x 100-mm plates in DMEM/F12 without antibiotics and incubated overnight at 37°C and 5% CO_2. The following day, media was removed and replaced with complete DMEM/F12 containing 500 µg/mL G418. After single-clone colonies were formed (10-18 days) the colonies were picked and expanded prior to protein analysis.

2.2.4 Transient transfections

Approximately 4,000 A549δPNKP, A549-Scramble, MCF7δPNKP or MCF7 cells were plated per well in a 96-well plate, and allowed 24 h to adhere in a humidified incubator at 37°C and 5% CO_2. All wells surrounding samples were filled with 100 µL distilled water to control for evaporation effects. For protocol optimization and initial verification of selected hits, 56 nM final concentration of siRNA was added to 50 µL total reaction volume in Opti-MEM (Invitrogen). At the same time as siRNA-Opti-MEM incubation, a 1:25 dilution of Dharmafect Transfection Reagent 1 (Dharmacon, Lafayette, CO) in Opti-MEM was allowed to incubate at room temperature for 5 min, to provide a final volume of 0.23 µL transfection reagent per well. The two transfection solutions were then combined and held at room temperature for 20 min. The media was then removed from the cells and 100 µL of the transfection mixture was added per well and the plate was incubated at 37°C and 5% CO_2 for 72 h. All siRNAs used here were purchased from Qiagen (Mississauga, ON).

2.2.5 Protein analysis

Approximately 10^6 stably transfected cells were washed twice with ice cold PBS, trypsinized, and spun down at 600 *g* for 10 min at 4°C. The supernatant was aspirated and the cell pellet was resuspended in 200 µL of CHAPS buffer (0.5% CHAPS, 137 mM NaCl, 50 mM Tris-HCl, pH 7.5, and 1 mM EDTA) and rocked for 1 h at 4°C, after which cell debris was spun down at 17,500 *g* for 20 min at 4°C. Determination of whole cell lysate concentration was conducted using the Bradford Assay (Bio-Rad,

Hercules, CA).

Western blots were conducted using 50 µg of whole cell lysate. Monoclonal antibody towards PNKP (H101) was used as previously described (Fanta et al, 2001) and was incubated at 1:1000 in 5% PBSMT (PBS with 5% w/v skim milk) overnight at 4°C. Polyclonal primary antibodies (SHP-1 and β-actin) were incubated (1:4000 dilution) in 5% PBSMT for 1 h at room temperature (SantaCruz Biotechnology, Santa Cruz, CA). All secondary antibodies were incubated (1:5000 dilution) for 45 min at room temperature (Jackson ImmunoResearch Laboratories, Inc. West Grove, PA).

2.2.6 siRNA library screen

Qiagen's "Druggable" genome siRNA library is comprised of four sub-classifications: phosphatases, kinases, G-protein coupled receptors and uncategorized proteins consisting of 205, 696, 490 and 5570 mRNA targets, respectively. The library was first distributed into 89 x 96-well plates at a total siRNA concentration of 1 µM, each well containing a pool of four separate siRNAs to the same mRNA target. Also added to the plates were three additional control wells (C12, D12 and E12) of AllStars Negative (ASN) scrambled siRNA (Qiagen). Then, utilizing a JANUS Automated Workstation (PerkinElmer, Waltham, MA), 4,000 A549δPNKP or A549-Scramble cells were seeded into each well of a 96-well plate in a final volume of 100 µL DMEM/F12 without penicillin/streptomycin and allowed to adhere overnight in a humidified incubator. The following day,

transfection mixture was generated as described above (56 nM siRNA and a total of 0.23 µL Dharmafect transfection reagent 1 per well), media was aspirated from the plates containing cells, and 100 µL of the mixture was added to each well and allowed to incubate for 72 h. Then 10% v/v of 440 µM Alamar Blue (Sigma-Aldrich, Oakville, ON) was added to each well and the cells were incubated for 50-90 min after which the fluorescence in each well was determined using an EnVision 2104 Multilabel Reader (PerkinElmer) with an excitation wavelength of 563 nm and emission wavelength of 587 nm (Schindler & Foley, 2010). Each screen was performed in duplicate.

Transient transfections of siRNAs for synthetic lethal partners were used for confirmatory assays, however each siRNA was used independently and at a concentration of 20 nM. All other reagent concentrations remained constant. Each assay was performed manually and the fluorescence was read with a FLUOstar Optima® plate reader (BMG Labtec Inc. Durham, NC) using excitation and emission wavelengths of 563 and 587 nm, respectively.

2.2.7 Statistical analysis

R^2 values were generated in Microsoft Excel by plotting individual survival scores from the duplicate screen against one another. All p-values were generated using a two-sided Student's t-test. Z-scores were only generated for confirmatory data where an average from 23-96 individual wells of data per assay (performed at least in triplicate) were measured,

allowing us an appropriate number of replicates to achieve robust statistical data. A Z-score is a dimensionless quantity representing a measurement of the number of standard deviations a sample is above or below the mean of a control. It is defined as:

$$z = \frac{x - \mu}{\sigma}$$

z = Z-score
x = the raw score to be standardized
μ= population mean
σ = standard deviation of the population

As such, Z-scores can be positive or negative depending on whether the sample is higher or lower than the mean of a control. For our results, we were interested in a negative Z-score as this showed that the survival of the experimental condition was lower than control (i.e. the condition was lethal). A sample with a Z-score of -3 or less is significantly different than control and is a threshold often used in synthetic lethal screens.

2.2.8 Cell proliferation assay with ALCL cell lines

Karpas 299, SUPM2 or Karpas 299 (SHP-$1^{+/+}$) cells were plated in 96-well format at a density of 5,000 cells/100 μL in complete RPMI. Increasing concentrations of the PNKP inhibitor A12B4C3 was added to each well in a constant volume of DMSO and left to incubate for 12-16 days. Eleven μL of 440 μM Alamar Blue was then added to each well and

left to incubate for 24-48 h after which fluorescence was determined as described above.

A pCI expression vector (Promega, Madison, WI) was used to transiently re-express SHP-1 in Karpas 299 cells (Hegazy et al, 2010). The Karpas 299 cells were grown in antibiotic free RPMI after which 10^7 cells were harvested per transfection in 500 µL total volume of antibiotic free RPMI. These cells were placed into a 4-mm electroporation cuvette (VWR, Radnor, PA) along with 10 µg of plasmid DNA. The cells were then electroporated using a BTX ECM 300 square electroporator (BTX Technologies Inc., Holliston, MA) at 225 V for three pulses of 8.5 ms. After electroporation, the cells were transferred to 20 mL of antibiotic-free RPMI and incubated for 24 h before experimentation.

2.2.9 Determination of mode of cell death

A549-Scramble or A549δPNKP cells were grown on coverslips in complete DMEM/F12 and were either transfected with ASN or SHP-1 siRNA. As a positive control for apoptosis the cell lines were treated with 100 µM 5-(p-bromobenzylidine)-α-isopropyl-4-oxo-2-thioxo-3-thiozolidineacetic acid (BH3I-1, Sigma-Aldrich, Oakville, ON), which is a known apoptosis inducer. The cells were grown under each condition for the indicated length of time before being subjected to a triple stain of Hoechst 33342, Ethidium Homodimer III and Annexin V-FITC as described by the kit manufacturer (Biotium, Hayward, CA).

2.2.10 Single-cell gel electrophoresis

A549-Scramble, A549δPNKP and A549 cells stably depleted of SHP-1 (A549δSHP-1 cells) were grown to confluence in 60-mm plates in complete DMEM/F12. The cells were irradiated with 5 Gy of γ-rays (^{60}Co Gammacell; Atomic Energy of Canada Limited, Ottawa, Canada) and incubated at 37°C for 0, 2, 6, and 24 h for neutral comet assays and 0, 10, 30, 60 or 120 min for the alkaline comet assay. Controls were also included in which cells were not irradiated to give the baseline level of DNA damage present in each cell line. Double and single-strand breaks were then determined by single-cell gel electrophoresis as previously described (Freschauf et al, 2010; Kumaravel et al, 2009).

2.2.11 γH2AX foci detection

To monitor the level of H2AX phosphorylation before and after γ-radiation, 1 x 10^5 cells (A549-Scramble or A549δSHP-1) were seeded on coverslips in 35-mm dishes with 2 mL DMEM/F12 without antibiotics and left overnight to adhere in a humidified incubator. The dishes were then treated with 5 Gy γ-radiation and left to repair for the indicated time points. Cells were then fixed to the coverslips at room temperature in PBS containing 4% paraformaldehyde for 20 min. The coverslips were rinsed with PBS one time and the cells were permeabilized in 0.5% Triton X-100 (Sigma-Aldrich) in PBS for 20 min at room temperature. The coverslips were then rinsed twice in PBS and incubated with anti-γH2AX primary antibody (Millipore, Billerica, MA) at a dilution of 1:1000 in PBS for 45 min

at 4^{o}C. The coverslips were then rinsed three times, once in 0.1% Triton X-100:PBS and twice in PBS, respectively, and incubated with Alexa Fluor 488 secondary antibody (Molecular Probes, Eugene, OR) at a dilution of 1:200 in PBS for 30 min at room temperature. The cells were again rinsed three times, once in 0.1% Triton X-100:PBS and twice in PBS, respectively, and mounted on slides with 1 mg/mL p-phenylenediamine and 1 µg/mL 4'6-diamidino-2-phenylindole (DAPI) in 90% glycerol in PBS. Phosphorylated H2AX foci were viewed with a LSM510 laser-scanning confocal microscope (Zeiss) and images were taken with a 20x objective lens using the same microscope settings for each slide. Fluorescence was normalized to background fluorescence and quantified using ImageJ (http://rsbweb.nih.gov/ij/). Error bars represent ± standard error of the mean.

2.2.12 Detection of reactive oxygen species (ROS)

The presence of hydroxyl radicals and peroxynitrite was detected using a commercial kit (Cell Technology, Mountain View, CA), which employs two dyes, aminophenyl fluorescein (APF) and hydroxyphenyl fluorescein (HPF), selective for the detection of these ROS. These dyes are normally non-fluorescent, however, when they encounter ROS, they exhibit fluorescence in a dose dependent manner. Cells were grown in 96-well format and transfected with either ASN or SHP-1 siRNA for 24 h prior to ROS detection. Cells were rinsed twice with modified Hanks balanced salt solution (HBSS) supplemented with 10 mM HEPES, 1 mM $MgCl_2$, 2

mM $CaCl_2$ and 2.7 mM glucose, after which APF or HPF, was diluted to 10 μM in the same modified HBSS and 100 mL applied to the cells for 45 min at 37°C in the dark. The plates were then read using a FLUOstar Optima® plate reader at an excitation wavelength of 488 nm and an emission wavelength of 515 nm. Fluorescence detection was then compared to controls to give the total increase in production of ROS under each condition.

2.2.13 Colony-forming assay

A549δSHP-1 and A549-Scramble cells were plated in the presence of increasing concentrations of A12B4C3 alone, or with or without the ROS scavenger WR1065. Cells were subjected to these conditions continuously for 10-14 days after which plates were stained with crystal violet and counted (Rasouli-Nia et al, 2004). Colonies containing fewer than 30 cells were omitted.

2.3 RESULTS

2.3.1 siRNA screen for the synthetic lethal partners of PNKP

To date, many PARP-based synthetic lethal and chemosensitization associations that have been studied involve partner proteins that function in a separate DNA repair pathway (Bryant et al, 2005; Farmer et al, 2005; Vilar et al, 2011; Williamson et al, 2010). We sought to discover synthetic lethal partnerships of PNKP, as an alternative to PARP, without necessarily limiting our search to partner proteins directly involved in DNA

repair. We performed an unbiased forward transfection screen using an extensive library of siRNAs targeting 6961 genes, in which a pool of four distinct siRNAs targets each gene. Two duplicate screens were performed; the first utilized A549 lung cancer cells stably depleted of PNKP (A549δPNKP), and the second A549 cells expressing a scrambled shRNA (A549-Scramble) under identical conditions. (The level of PNKP in the knockdown and control cells is shown in Supplemental Fig. A.1A). Cells were exposed to siRNA continuously for 72 h (allowing for at least two cell cycles to occur) at a concentration known to be effective at knocking down target proteins (data not shown). Cell survival was then determined by an Alamar Blue-based fluorescence assay (Schindler & Foley, 2010).

Cell survival scores after targeting each of the 6961 mRNAs were compared to an average internal plate control located on every plate screened, consisting of the average survival of 3 wells of the cells screened (A549δPNKP or A549-Scramble) transiently transfected with Allstars negative scrambled control siRNA (ASN) under identical screen conditions. Genes and their corresponding proteins were classified as potential hits for synthetic lethality with PNKP if the survival under the simultaneous knockdown condition was ≤33% when compared to the internal plate controls average. A comparison of the duplicate screens showed that an overwhelming majority of the siRNAs yielded reproducible phenotypes (Supplemental Fig. A.2) and a summary of the data derived from the mean values is outlined in Figure 2.1. Most of the proteins

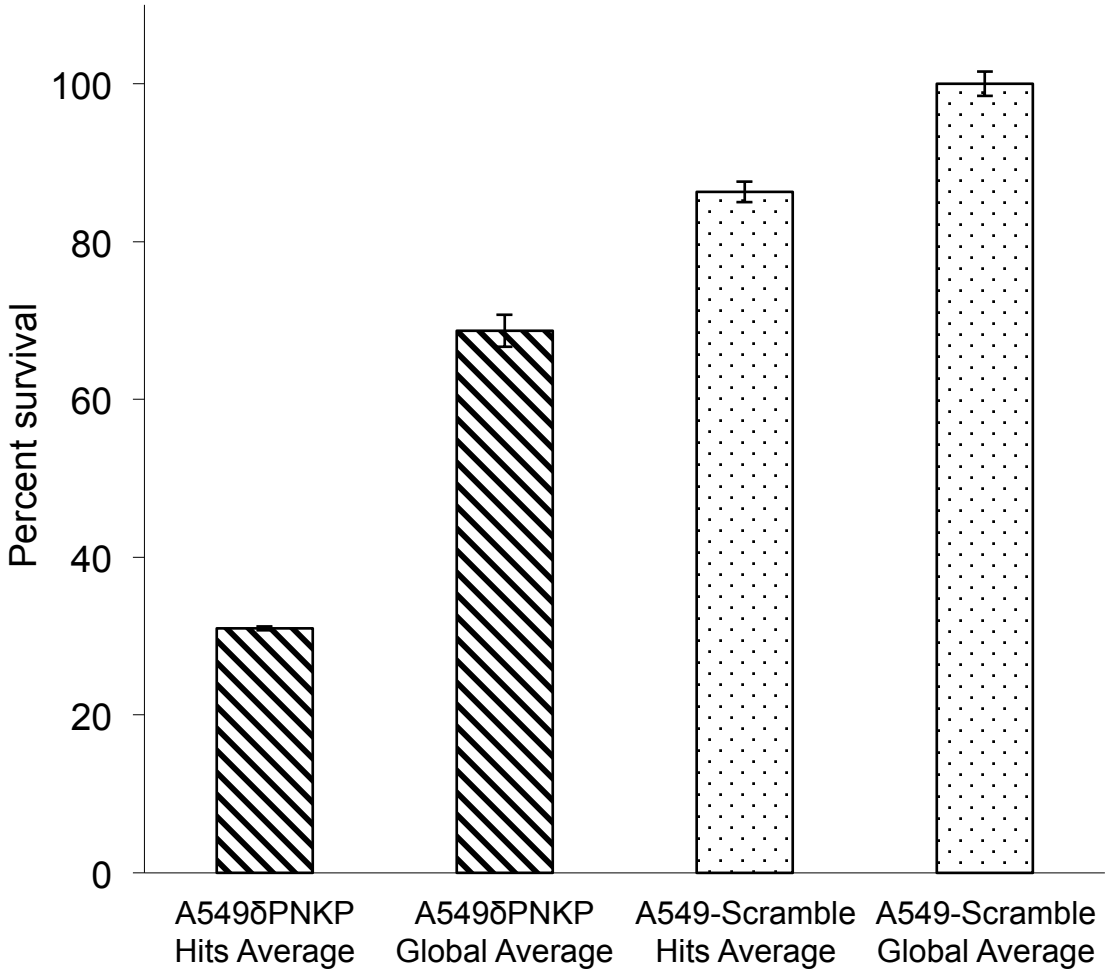
Percent survival
100
80
60
40
20
0
A549δPNKP Hits Average
A549δPNKP Global Average
A549-Scramble Hits Average
A549-Scramble Global Average

Figure 2.1. Overall survey of the screens for synthetic lethality with PNKP. The screens were performed using a forward transfection protocol with A549 cells stably depleted of PNKP (A549δPNKP) and cells stably expressing a scrambled siRNA (A549-Scramble). The first bar on the left represents the total mean cell survival values generated by the siRNAs targeting proteins deemed as potential synthetic lethal hits with PNKP designated on the basis of survival of an arbitrary cutoff of ≤33% compared to internal plate controls, which were normalized to 100% and represented by the bar on the far right. The second bar from the left represents the cell survival of the entire screen using A549δPNKP cells including the potential hits. The third bar from the left shows the mean survival of the A549-Scramble cells treated with the siRNAs identified as potential hits in the A549δPNKP screen. The difference between the first and third bars imply that most of the siRNAs causing lethality in A549δPNKP cells do not do so in the control A549-Scramble cells and thus require PNKP depletion to induce cytotoxicity.

identified as potential 'hits' in the screen were lethal only in combination with PNKP disruption and were not singularly lethal (for comparison SHP-1 data is graphically represented alongside two randomly selected proteins deemed "non-hits", Supplemental Fig. A.3).

A master list of potential synthetic lethal partners is shown in Supplemental Table A.1 (Supplemental Table A.2 shows the hits listed alphabetically). The positive hit rate was found to be 6.1% (425/6961) including 8 phosphatases, 97 kinases, 117 G-protein coupled receptors and 203 unclassified proteins. Of note, 14 tumour suppressors were identified as potentially synthetically lethal with PNKP (Table 2.1).

2.3.2 Confirmation of SHP-1 as a possible synthetic lethal partner of PNKP

Screening a large siRNA library is a valuable tool to identify potential synthetic lethal partners of PNKP, however, each hit must be experimentally confirmed by further analysis. One potential hit for synthetic lethality with PNKP identified in the screen was SHP-1, a protein tyrosine phosphatase that has been implicated as a tumour suppressor, functioning in the regulation of signal transduction pathways (Irandoust et al, 2009) to counter growth-promoting and oncogenic signals through its phosphatase activity (Wu et al, 2003).

To confirm the synthetic lethal relationship between PNKP and SHP-1, we repeated the analysis, but reduced the concentration of siRNA previously used in the screen from 56 to 20 nM and used each of the four

Table 2.1 Tumour suppressors identified as potentially synthetic lethal with PNKP by the siRNA screen

Gene ID	Gene Name	Survival with A549δPNKP[a]	Survival with A549-Scramble[a]
RASSF5	Ras association (Ral GDS/AF-6) domain family member 5	26%	77%
HTATIP2	HIV-1 Tat interactiveprotein 2, 30 kDa	29%	41%
EFNA1	ephrin-A1	30%	64%
CCNA1	cyclin A1	23%	52%
APEH	N-acylaminoacyl-peptide hydrolase	31%	74%
ING3	inhibitor of growth family, member 3	26%	88%
CSNK2A1	casein kinase 2, alpha 1 polypeptide	29%	46%
PRKCDBP	proteinkinase C, deltabindingprotein	27%	67%
CSNK2A2	casein kinase 2, alpha prime polypeptide	27%	59%
EXO1	exonuclease 1	23%	51%
SMG1	PI-3-kin SMG-1	27%	104%
SHP-1	Protein tyr phosphatase non-receptor type 6	28%	39%
PTEN	phosphatase and tensin homolog	31%	47%
DAPK1	death associated protein kinase 1	20%	82%

[a]These values were obtained with a relatively high concentration (56 nM) of siRNA for each target gene, which may explain the poor survival in A549-Scramble cells of some of the possible “hits”. All subsequent confirmatory experiments were conducted using 20 nM of siRNA to reduce toxicity in A549-Scramble cells.

originally pooled siRNAs separately in order to minimize the potential for off-target effects and limit toxicity in A549-Scramble cells transfected with the SHP-1 siRNA. When the distinct SHP-1 siRNAs were assayed, all four displayed selective killing of A549δPNKP cells and no or limited toxicity in control cells (Fig. 2.2A, siRNA #5 Z-factor = -12.3, $p < 0.001$; siRNA #10 Z-factor = -17.2, $p < 0.001$, siRNA #11 Z-factor = -6.88, $p < 0.001$, siRNA #6 Z-factor = -6.44, $p < 0.001$). Since all four siRNAs showed synthetic lethality with PNKP, as well as the capacity to deplete SHP-1 protein (Supplemental Fig. 2.1B), the effect was most likely attributable to the simultaneous depletion of PNKP and SHP-1, and not due to off-target effects. Furthermore, the lack of toxicity seen using ASN control siRNA with A549δPNKP cells indicated that non-specific activation of the RNAi pathway was not responsible for the observed lethality.

To further substantiate that a synthetic lethal partnership exists between SHP-1 and PNKP, we carried out a similar analysis with the MCF7 breast cancer cell line. We performed the cell proliferation assay using 20 nM of SHP-1 siRNA #5 with an MCF7 cell line stably depleted of PNKP (MCF7δPNKP). As seen with A549 cells, the combined disruption of both SHP-1 and PNKP was responsible for lethality, since the depletion of PNKP or SHP-1 individually was not lethal (Fig. 2.2B, Z-score = -3.4, $p < 0.001$), nor was the activation of RNAi machinery alone responsible for lethality (Fig. 2.2B). Similarly, in the reciprocal experiment, in which stable SHP-1 depleted A549 cells (A549δSHP-1) or A549-Scramble cells were transfected with siRNA targeting PNKP (Fig. 2.2C) or exposed to a small

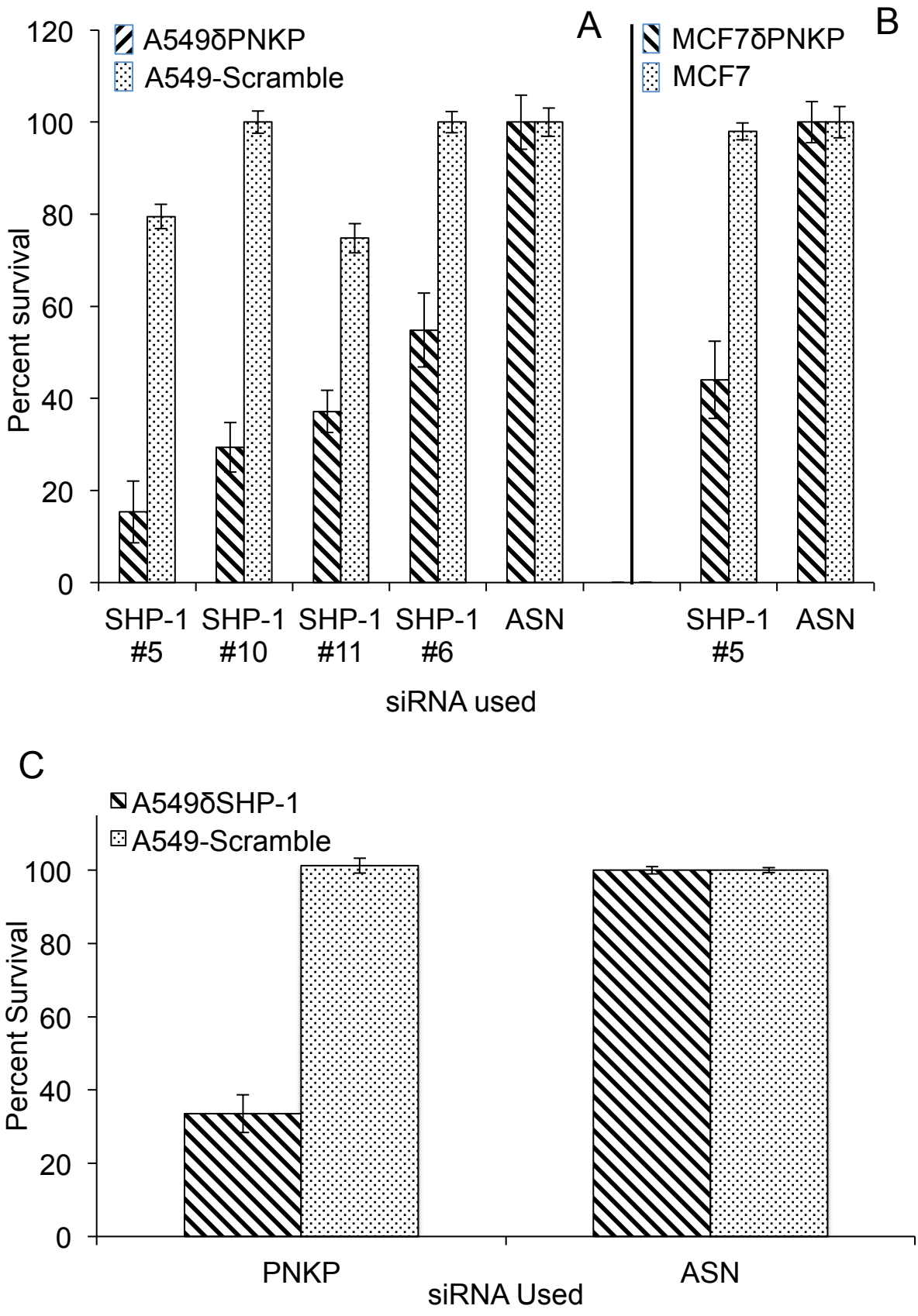
A
B
A549δPNKP
A549-Scramble
MCF7δPNKP
MCF7
Percent survival
120
100
80
60
40
20
0
SHP-1 #5
SHP-1 #10
SHP-1 #11
SHP-1 #6
ASN
SHP-1 #5
ASN
siRNA used
C
A549δSHP-1
A549-Scramble
Percent Survival
100
80
60
40
20
0
PNKP
ASN
siRNA Used

D

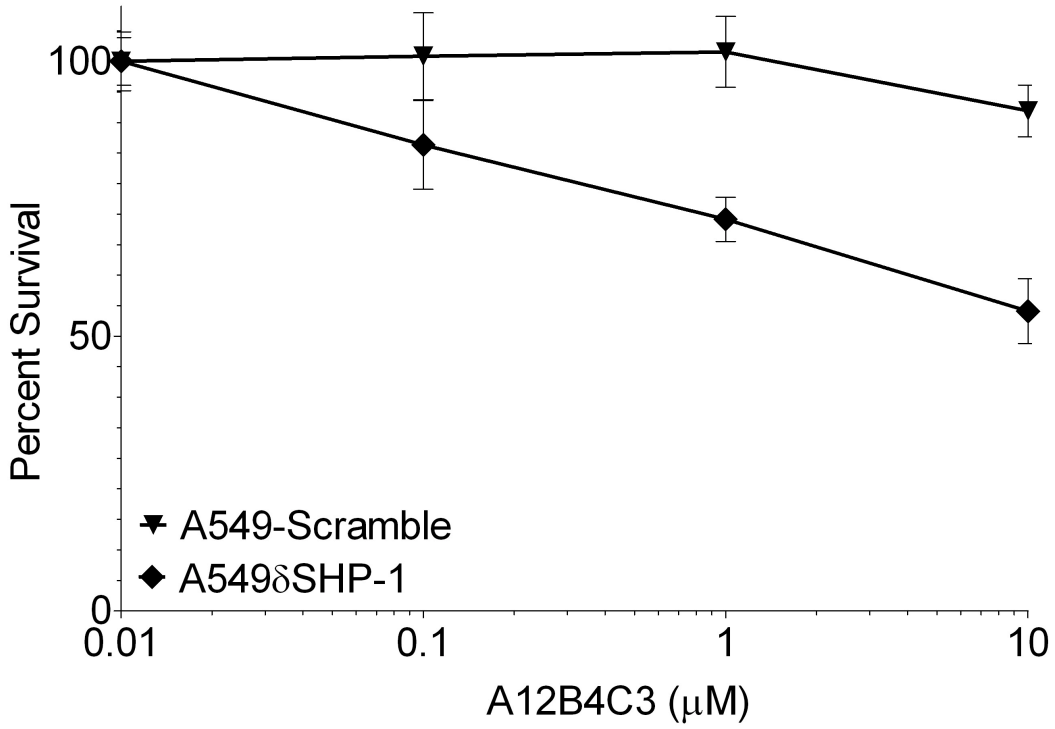
100
50
0
Percent Survival
A549-Scramble
A549δSHP-1
0.01
0.1
1
10
A12B4C3 (μM)

Figure 2.2. Confirmation of synthetic lethality between SHP-1 and PNKP. (A) Four distinct siRNAs (20 nM) targeting SHP-1 expression were used to transiently transfect both A549δPNKP and A549-Scramble cell lines. Error bars represent standard error (± S.E.) from at least three independent determinations. All SHP-1 siRNAs were lethal only when combined with PNKP disruption. Transient transfection with a control (Allstars negative, ASN) siRNA failed to elicit a cytotoxic response indicating that activation of the RNAi machinery was not responsible for cell killing. (B) Confirmation of the SHP-1/PNKP synthetic lethal relationship using MCF7 and MCF7δPNKP (MCF7 cells stably depleted of PNKP) cells. (C) Survival of A549δSHP-1 and A549-Scramble cells transiently transfected with an siRNA against PNKP. (D) Survival of A549δSHP-1 cells exposed to increasing concentration of the PNKP phosphatase inhibitor A12B4C3. Error bars represent standard error (± S.E.) from at least three independent determinations.

molecule inhibitor of PNKP phosphatase activity, A12B4C3 (Fig. 2.2D), lethality was only observed when both PNKP and SHP-1 were disrupted.

We also show that small molecule inhibition or siRNA-mediated knockdown of PARP1 is insufficient to cause a lethal effect in A549δSHP-1 cells (Supplemental Fig. A.4), indicating that PARP1 cannot substitute for PNKP in synthetic lethal relationships with SHP-1, and therefore for some tumours PNKP may serve as an alternative therapeutic target to PARP1.

2.3.3 Mode of cell death

To identify the mechanism by which cells undergo disrupted SHP-1/PNKP-mediated synthetic lethality, A549-Scramble and A549δPNKP cells were grown on coverslips and transiently transfected with ASN or SHP-1 siRNA. As a positive control, cells were treated with the apoptosis inducer BH3I-1. Cells were then simultaneously stained with Hoechst 33342, Ethidium Homodimer III and Annexin V-FITC. Hoechst 33342 stains the nuclei of healthy and unhealthy cells alike, while Ethidium Homodimer III identifies cells that are in late stage of apoptosis or are necrotic, and Annexin V identifies early apoptotic cells. Figure 2.3A shows there was a small population of apoptotic and necrotic cells following transfection of both cell lines with ASN. As expected, treatment with BH3I-1 induced a substantial increase in apoptosis in both cell lines (Fig. 2.3B). Co-disruption of SHP-1 and PNKP by transient transfection of SHP-1 siRNA into the PNKP-depleted cell line also caused a substantial increase in the proportion of apoptotic cells, with only a small increase in the

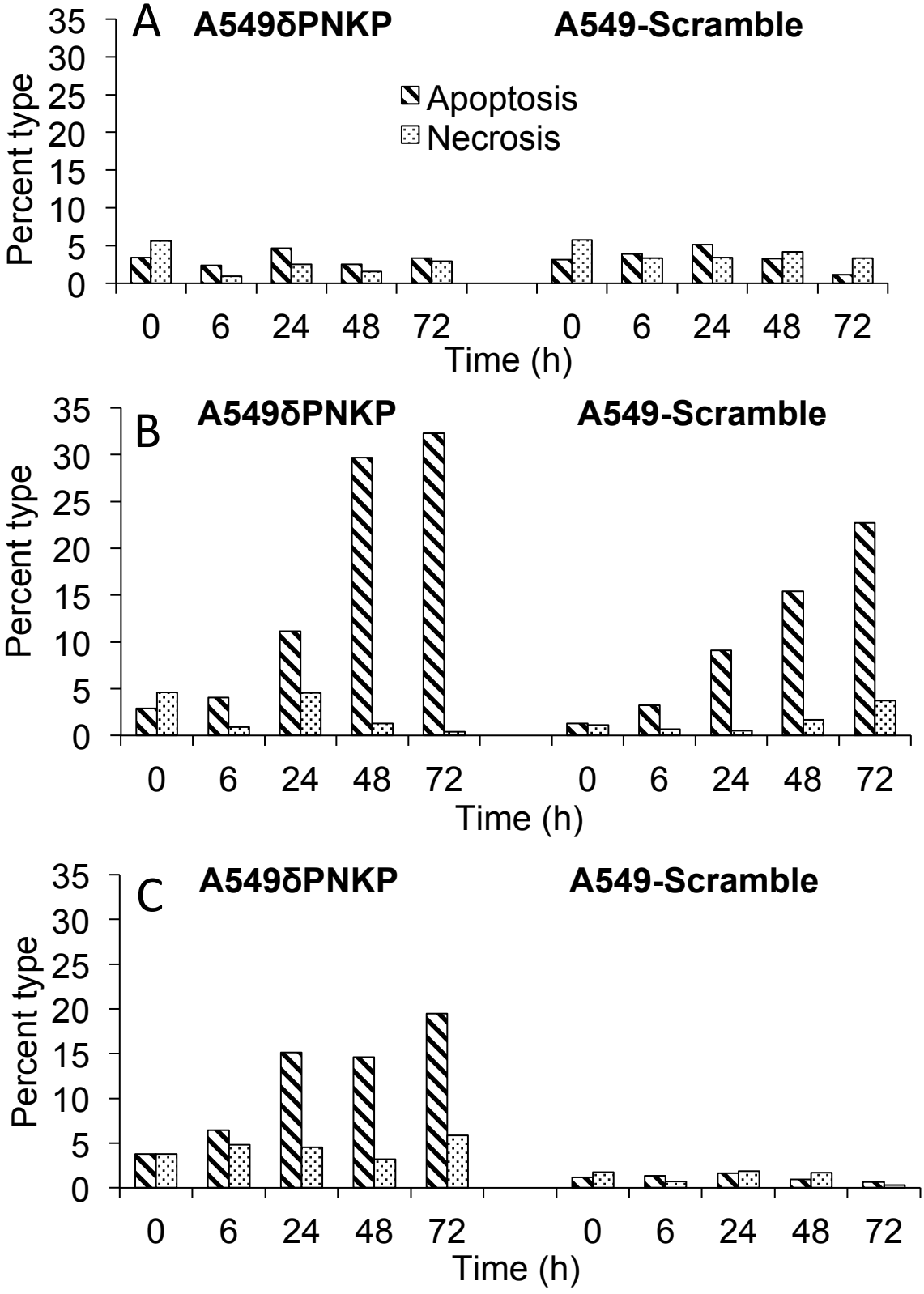
A
A549δPNKP
A549-Scramble
Apoptosis
Necrosis
Percent type
35
30
25
20
15
10
5
0
0 6 24 48 72 0 6 24 48 72
Time (h)
B
A549δPNKP
A549-Scramble
Percent type
35
30
25
20
15
10
5
0
0 6 24 48 72 0 6 24 48 72
Time (h)
C
A549δPNKP
A549-Scramble
Percent type
35
30
25
20
15
10
5
0
0 6 24 48 72 0 6 24 48 72
Time (h)

Figure 2.3. Mode of cell death of cells undergoing synthetic lethality due to the simultaneous disruption of SHP-1 and PNKP. (A) A549δPNKP and A549-Scramble cells were transiently transfected with ASN control siRNA and apoptosis and necrosis was determined over a 72-hour period as described in Materials and Methods at times after transfection. (B) Additional treatment of the ASN-transfected cells with the potent apoptosis inducer BH3I-1. (C) Induction of apoptosis and necrosis in A549δPNKP and A549-Scramble cells transiently transfected with SHP-1 siRNA.

necrotic population (Fig. 2.3C). In contrast, no induction of apoptosis was observed following transient transfection of SHP-1 siRNA in the cell line expressing scramble shRNA. Thus these data indicate that cells undergoing SHP-1/PNKP induced synthetic lethality do so by an apoptotic mechanism.

2.3.4 Survival of naturally occurring SHP-1 positive and negative cells in response to PNKP inhibition

The utility of synthetic lethality will lie in the capacity to translate potential associations into targeted therapy, possibly using inhibitors of one of the partners as a single agent. To investigate the feasibility of taking advantage of the newly identified partnership between SHP-1 and PNKP, we subjected two anaplastic large cell lymphoma cell lines, Karpas 299 (naturally SHP-$1^{-/-}$) and SUP-M2 (naturally SHP-$1^{+/+}$), to an increasing concentration of the small molecule inhibitor of PNKP DNA 3'-phosphatase activity, A12B4C3 (Freschauf et al, 2009), over a period of 12-16 days. The dose response curves (Fig. 2.4) indicate that at A12B4C3 doses ≥ 10 μM there was a marked decrease in survival of the SHP-$1^{-/-}$ cells, while the SHP-$1^{+/+}$ cells remained viable. To confirm the central role of SHP-1 in the observed response we expressed wild-type SHP-1 in Karpas 299 cells (western blot shown in Supplemental Fig. A.1C), and these cells displayed reduced sensitivity to A12B4C3.

2.3.5 Underlying mechanism of the PNKP/SHP-1 synthetic lethality

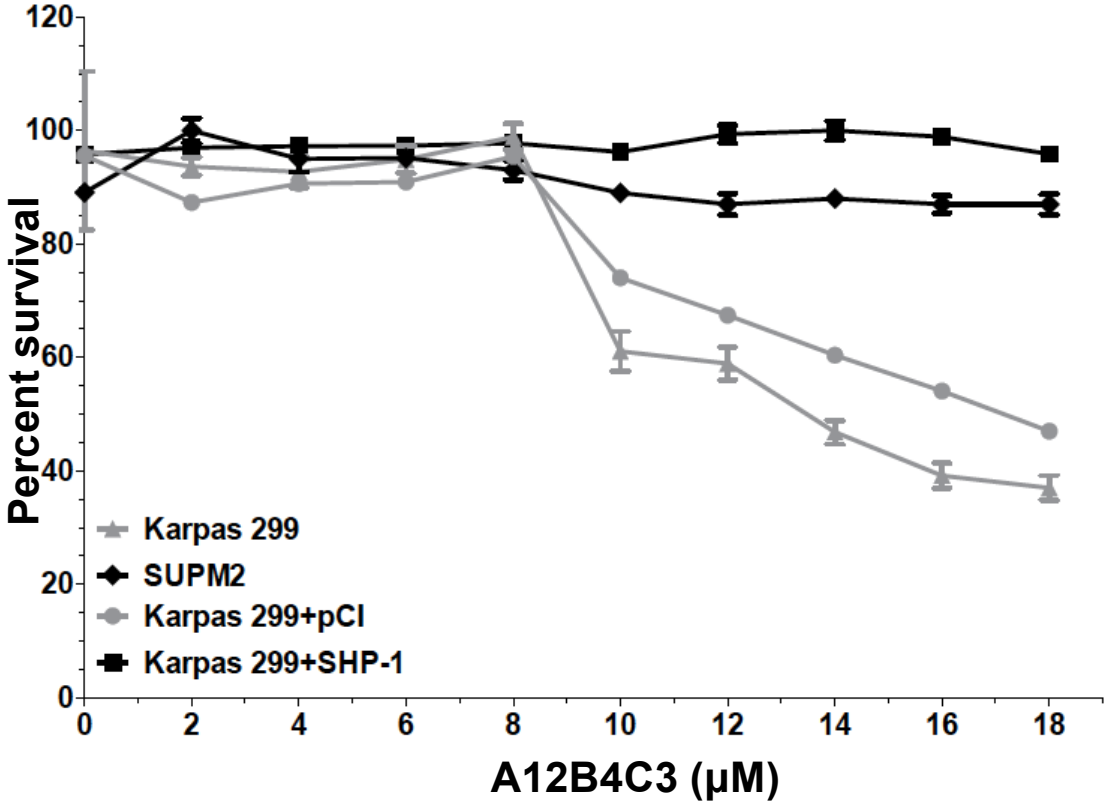

Figure 2.4. Survival of ALCL cells under PNKP inhibition. Karpas 299 (ALCL cells naturally lacking functional SHP-1), SUP-M2 cells (control ALCL cell line, which expresses normal levels of SHP-1), Karpas 299 cells reconstituted with SHP-1 (Karpas 299+SHP-1) and vector only controls (Karpas 299+pCI) were treated with an increasing concentrations of the PNKP inhibitor A12B4C3 for 12-16 days. Survival was measured using an Alamar Blue-based fluorescence assay. Error bars represent standard error (± S.E.) from at least three independent determinations.

The mechanism for synthetic lethality involving PARP1 and BRCA1 or 2 is considered to be an interplay between two DNA repair pathways (Bryant et al, 2005; Dedes et al, 2011; Farmer et al, 2005; Helleday, 2011), and thus to date, there has been considerable focus on the critical involvement of both proteins of a synthetic lethal partnership in DNA surveillance or repair (Amir et al, 2010; Bolderson et al, 2009; Chan & Bristow, 2010; Dedes et al, 2011; Gien & Mackay, 2010; Martin et al, 2010; Mendes-Pereira et al, 2009; Stefansson et al, 2009). SHP-1 is a protein tyrosine phosphatase known to negatively regulate receptor tyrosine kinase signaling (Irandoust et al, 2009; Kharitonenkov et al, 1997). There is no evidence to date to indicate that SHP-1 is involved in DNA repair. We therefore sought to determine if SHP-1 plays a major role in regulating DSB or SSB repair. Accordingly, A549-Scramble and A549δSHP-1 cells were irradiated and DSBR was followed by visualizing the formation of γH2AX foci as well as by single-cell gel electrophoresis (comet assay) under neutral conditions and SSBR by comet assay under alkaline conditions. A549-Scramble and A549δSHP-1 cells showed reasonably similar kinetics (Fig. 2.5A-C) for the formation and removal of γH2AX foci over the course of 24 h following irradiation, suggesting that loss of SHP-1 did not significantly affect the rate of repair of DSB, although a greater number of foci appeared to be generated in the first 15 minutes following irradiation of A549δSHP-1 cells. Interestingly, there was also a notable presence of γH2AX foci in the unirradiated A549δSHP-1 cells and a proportionately higher level of foci at each time point after irradiation,

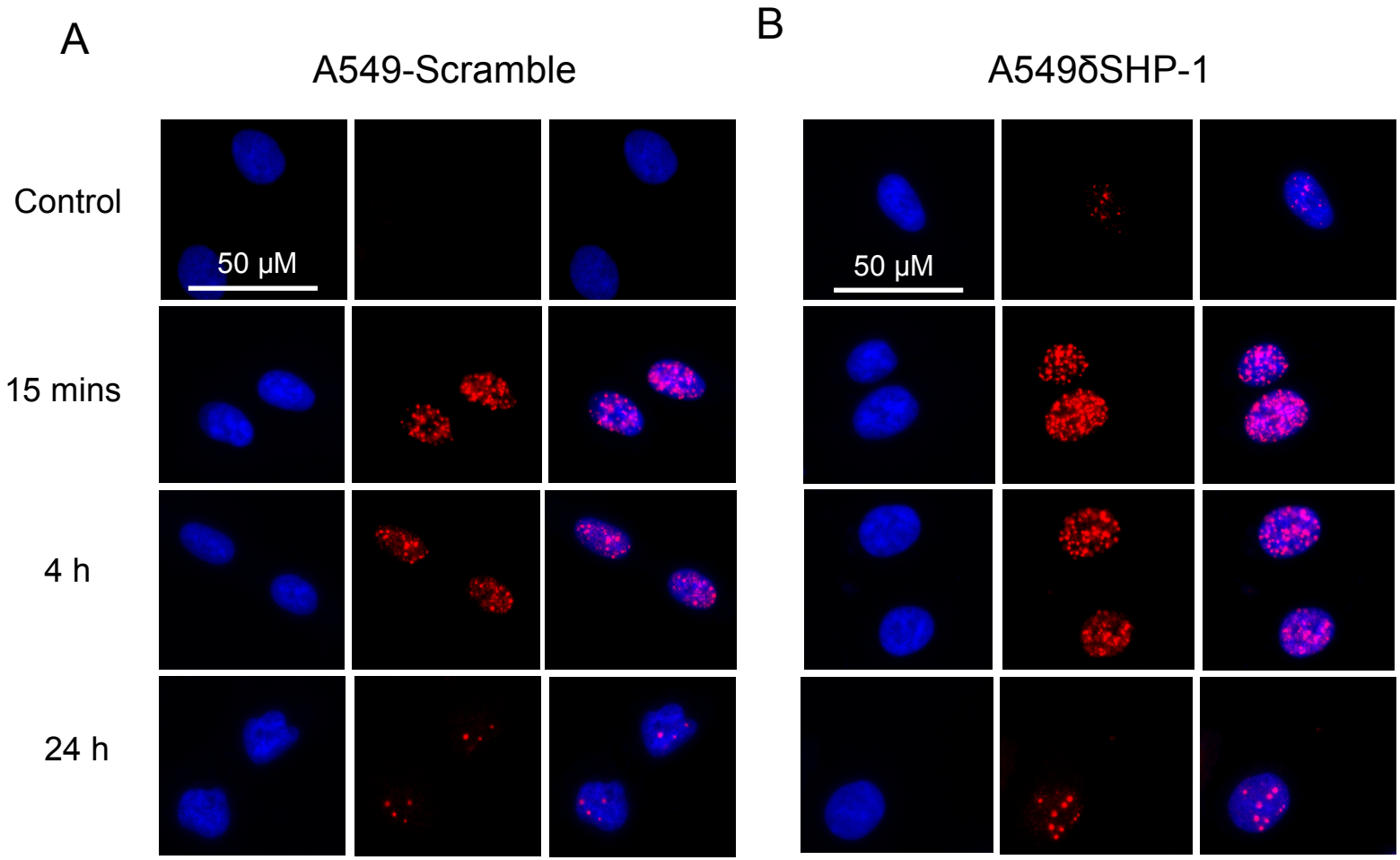
A
A549-Scramble
B
A549δSHP-1
Control
15 mins
4 h
24 h
50 μM
50 μM

C

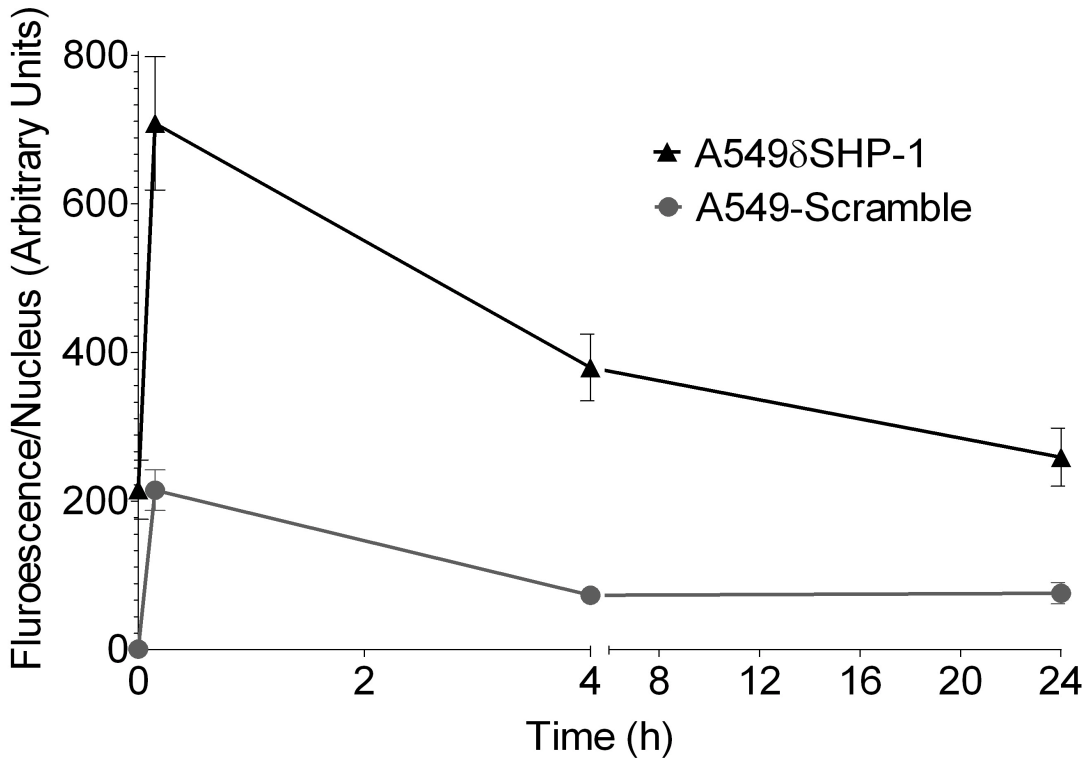
Fluroescence/Nucleus (Arbitrary Units)
800
600
400
200
0
0
2
4
8
12
16
20
24
Time (h)
A549δSHP-1
A549-Scramble

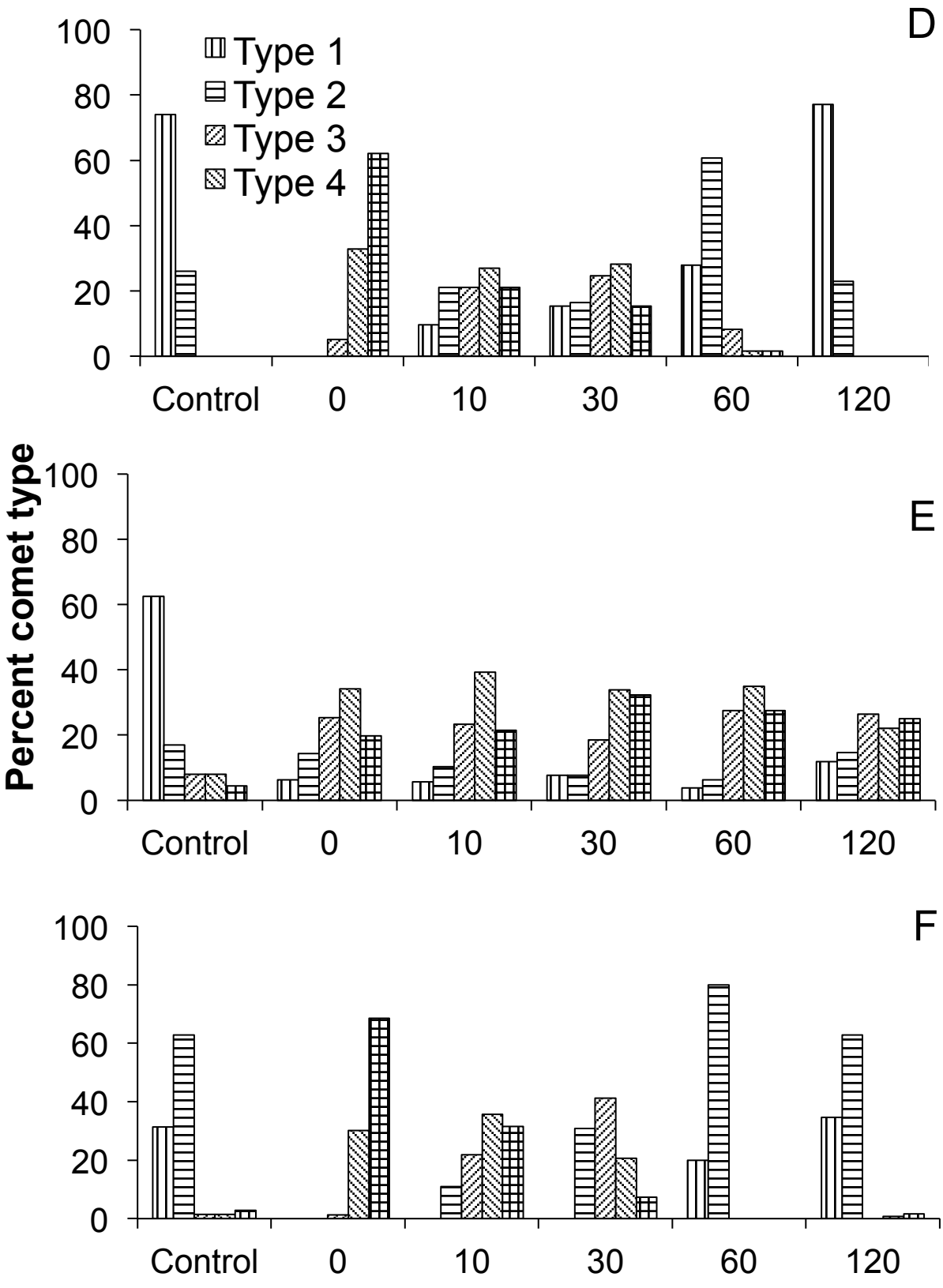
D
Type 1
Type 2
Type 3
Type 4
100
80
60
40
20
0
Control
0
10
30
60
120
Percent comet type
E
F

Figure 5. Influence of SHP-1 on DNA repair. Cells were plated 24 h in advance, after which they were subjected to γ-radiation (5 Gy). The repair of DSBs was monitored by γH2AX focus formation (A-C), and SSBs by the alkaline comet assay (D-F). (A) and (B) Typical staining of unirradiated and irradiated A549-Scramble and A549δSHP-1 cells, showing staining with nuclear stain DAPI (left-hand column) and γH2AX antibody (middle column), and overlay (right-hand column). (C) Quantification of the average integrated fluorescence intensity per nucleus due to phosphorylation of histone H2AX as a function of time after 5-Gy irradiation. (D-F) SSB repair in A549-Scramble cells, A549δPNKP cells showing the effect of a down-regulation of a well-characterized DNA strand break repair enzyme, and A549δSHP-1 cells (see Supplemental Fig. 5 for classification of comets with type 1 comets having the least damage and type 5 comets having the most damage).

including the 24 h time point when almost all foci had disappeared in the A549-Scramble cells. The results of the γH2AX assay were supported by the neutral comet assay (Supplemental Figs. A.5 and A.6). DSBR in irradiated A549-Scramble cells was almost complete by 24 h (Supplemental Fig. A.6A). In contrast, the loss of a recognized DNA repair enzyme such as PNKP (A549δPNKP cells) severely retarded the rate of repair (Supplemental Fig. A.6B), in agreement with previous observations (Freschauf et al, 2010). The A549δSHP-1 cells showed a similar rate of DSBR as A549-Scramble cells (Supplemental Fig. A.6C), again indicating that SHP-1 does not play a significant role in DSBR, but there was a noticeably elevated level of DSB present in the untreated A549δSHP-1 cells as evidenced by a large proportion of cells showing type 2 comets or above (Supplemental Fig. A.6C).

When A549-Scramble cells were subjected to the alkaline comet assay (Fig. 2.5D-F), we observed total repair of radiation-induced SSBs after 120 minutes (Fig. 2.5D) in marked contrast to DNA repair deficient A549δPNKP cells (Fig. 2.5E). SHP-1 knockdown cells showed a very similar response to radiation as A549-Scramble cells, indicating that SHP-1 is not significantly involved in the repair of SSBs (Fig. 2.5F), but, as with the DSB data, we observed a modestly higher level of SSBs in the unirradiated SHP-1 depleted cells than in the controls.

The results above render it unlikely that the primary cause of the synthetic lethal partnership between PNKP and SHP-1 is due to an interaction between two DNA repair pathways akin to PARP and the BRCA

proteins, and we therefore sought an alternative explanation. One clue provided by the repair assays was the higher level of strand breaks in the unirradiated SHP-1 depleted cells, which, together with reports in the literature regarding elevated levels of ROS in SHP-1 depleted cells (Krotz et al, 2005), led us to an alternative hypothesis that reduced SHP-1 expression leads to the generation of ROS-induced DNA strand-breaks, the repair of which are dependent on PNKP activity. To investigate this supposition, we examined the basal level of ROS (hydroxyl radicals and peroxynitrite together) produced in the wild-type and SHP-1 depleted cells that were used to establish the synthetic lethal partnership between PNKP and SHP-1. We found that when SHP-1 was depleted to approximately 15% of wild-type level, ~40% more ROS were produced in both A549 and MCF7-based cell lines (Figs. 2.6A and B).

To further corroborate a role for ROS in the synthetic lethal partnership between PNKP and SHP-1, we treated A549-Scramble and A549δSHP-1 cells with the PNKP inhibitor, A12B4C3, in the presence or absence of the ROS scavenger WR1065 (Dziegielewski et al, 2008; Walker et al, 2009) to determine if a reduction in cellular ROS concentration would rescue the lethal phenotype conferred to cells upon co-disruption of PNKP and SHP-1 (Fig. 2.7). (Doses of the two chemical reagents were chosen so as to avoid toxicity in the control A549-Scramble cells). In the absence of the ROS scavenger, treatment of the A549δSHP-1 cells with A12B4C3 resulted in ~30% cytotoxicity, which contrasts with the complete abrogation of cytotoxicity when A12B4C3 was co-administered

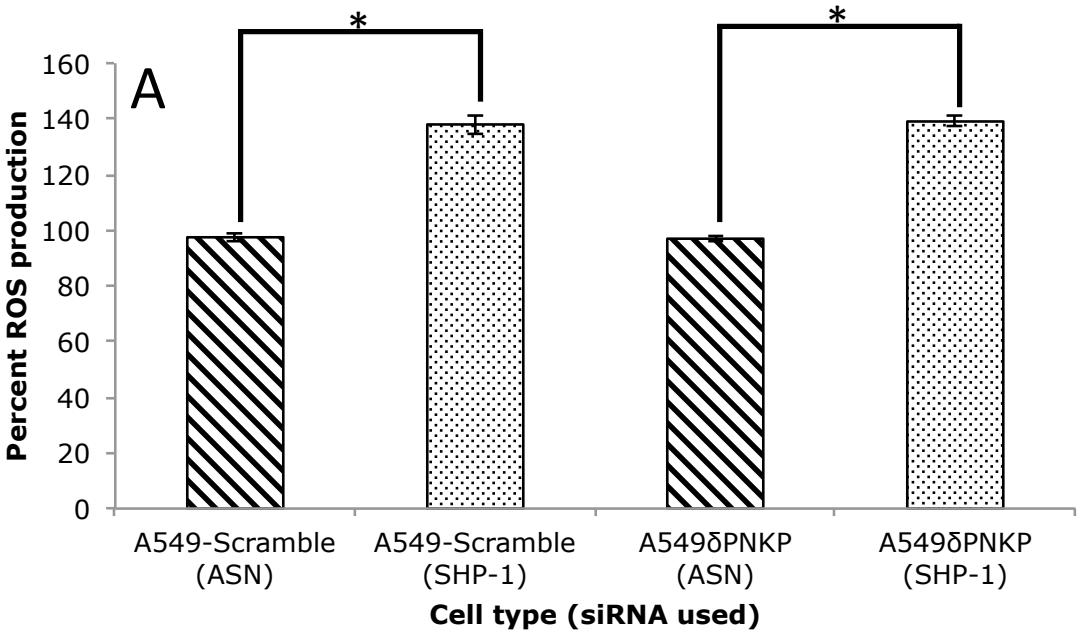
A
Percent ROS production
160
140
120
100
80
60
40
20
0
*
*
A549-Scramble (ASN)
A549-Scramble (SHP-1)
A549δPNKP (ASN)
A549δPNKP (SHP-1)
Cell type (siRNA used)

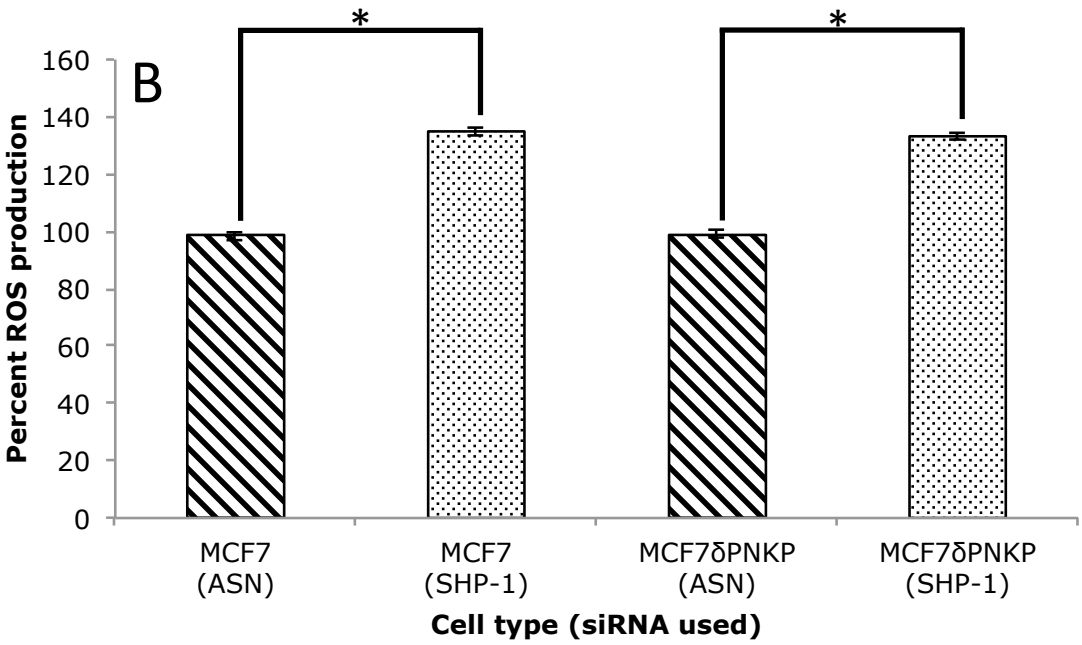
B
Percent ROS production
160
140
120
100
80
60
40
20
0
*
*
MCF7 (ASN)
MCF7 (SHP-1)
MCF7δPNKP (ASN)
MCF7δPNKP (SHP-1)
Cell type (siRNA used)

Figure 2.6. Depletion of SHP-1 causes an increase in production of reactive oxygen species. (A) Expression of SHP-1 was transiently knocked down using siRNA in A549-based cell lines and production of reactive oxygen species was measured as described in Materials and Methods. The cell lines are listed on top and the siRNA used is listed in parentheses below. Error bars represent standard deviation (± S.D.) from at least three independent determinations carried out in duplicate. (B) Data obtained with MCF7-based cell lines under identical conditions. All differences marked with an asterisk are statistically significant with $p < 0.01$.

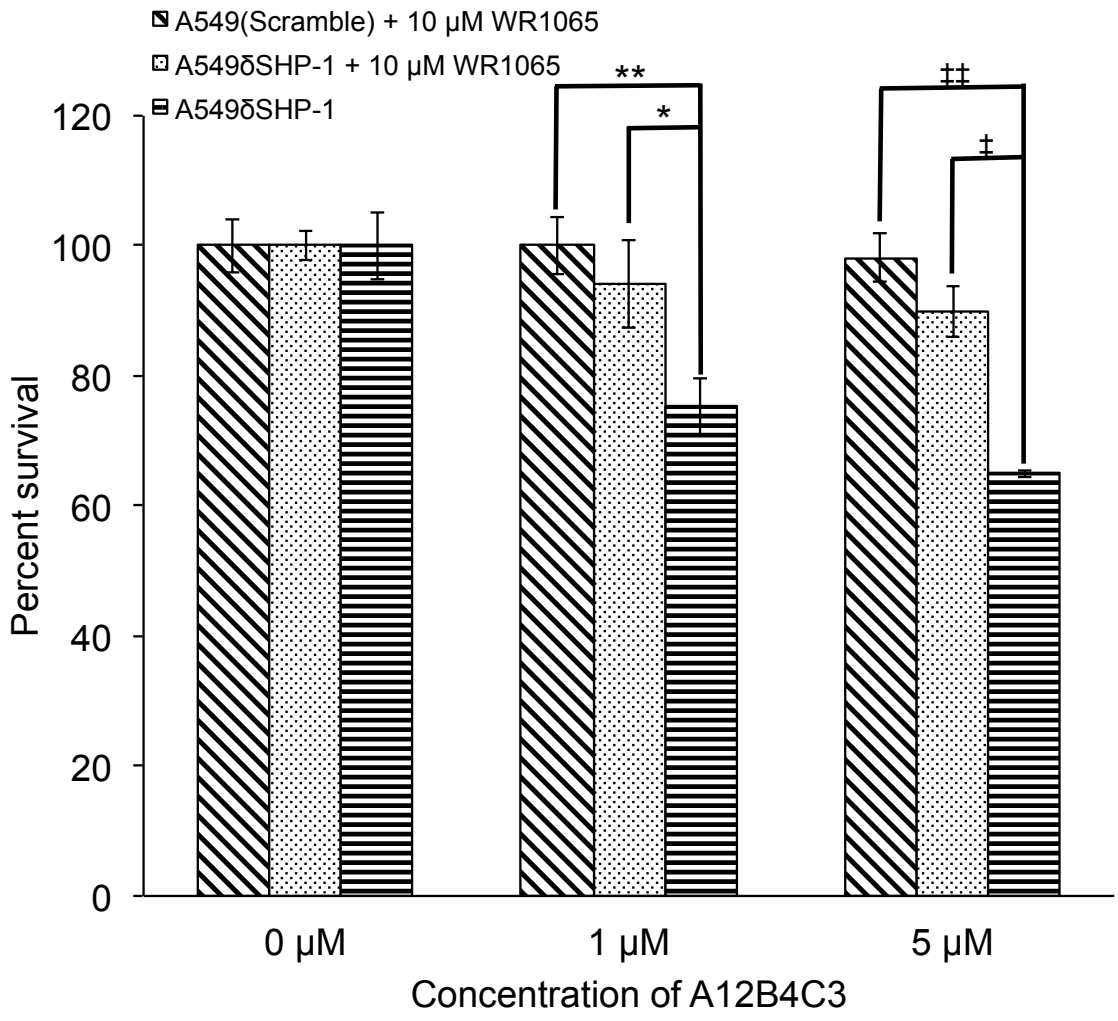

Figure 2.7. Rescue of lethal phenotype upon addition of ROS scavenger WR1065. A549δSHP-1 cells were subjected to A12B4C3 at 1 μM or 5 μM in the presence of absence of 10 μM of the ROS scavenger WR1065 in a colony-forming assay. A549-Scramble cells treated with 10 μM WR1065 showed no toxicity at the concentrations tested. All marked values are statistically significant at $p < 0.01$. Error bars represent standard error (± S.E.) from at least three independent determinations.

with WR1065, implicating a critical role for ROS in the PNKP/SHP-1 synthetic lethal partnership.

2.4 DISCUSSION

Synthetic lethality is a promising avenue for cancer therapy and even in its early development appears to be clinically effective (Audeh et al, 2010; Glendenning & Tutt). Our screen identified 425 possible synthetic lethal partners of PNKP, representing 6.1% of genes tested, which is typical for initial screens of this type (Azorsa et al, 2009; Colombi et al, 2011; Naik et al, 2009). Of these proteins, 14 are currently considered to be tumour suppressors, including PTEN and SHP-1. From the standpoint of potential therapeutic benefit in cancer treatment there is clearly considerable advantage to identifying partnerships of tumour suppressors. The participation of some tumour suppressors in synthetic lethal partnerships has been noted before. PTEN has a partnership with PARP (Mendes-Pereira et al, 2009), which has been attributed to reduced DSBR by homologous recombination (McEllin et al, 2010), while p53 has been shown to have synthetic lethal partnerships with the protein kinases SGK2 and PAK3 (Baldwin et al, 2010). Loss-of-function mutants are considered notoriously hard to treat, as protein function is difficult to re-establish pharmacologically and re-establishment of tumour suppressor activity is technically challenging. However, through the use of the concept of synthetic lethality, such mutant cells become targetable (Canaani, 2009; Chan & Giaccia, 2011). This is possible because in principle synthetic

lethality targets the tumour suppressor's lethal partner, thereby only affecting the naturally protein deficient cancer cells to cause the cytotoxic double disruption, effectively leaving normal cells unharmed. Side effects are therefore theorized to be minor, and in practice this can be seen. In the clinical trials using Olaparib in BRCA1- and BRCA2-mutated ovarian cancer, the only grade 3 toxicities observed were nausea (7%) and leukopenia (5%) (Underhill et al, 2010).

Of the tumour suppressors identified, we chose to further validate SHP-1 as it has been shown to be deficient or absent in a substantial number of human cancers (Irandoust et al, 2009; Kharitonenkov et al, 1997; Oka et al, 2001). Tissue microarray analysis of the SHP-1 status of 207 paraffin-embedded samples of a diverse assortment of malignant lymphomas and leukemias revealed that ≥90% of diffuse large cell lymphoma, follicle center lymphoma, Hodgkin's disease (HD), mantle cell lymphoma (MCL), peripheral T cell lymphoma (PL), adult T cell lymphoma/leukemia (ATLL) specimens and 100% of NK/T cell lymphoma specimens showed no detectable SHP-1 expression (Cariaga-Martinez et al, 2009; Delibrias et al, 1997; Oka et al, 2001). Similarly, SHP-1 was expressed at reduced or undetectable levels in 40 of 45 malignant prostate samples (Cariaga-Martinez et al, 2009). This raises the possibility that clinically effective inhibitors of PNKP or other synthetic lethal partners of SHP-1 may provide substantial benefit to patients with these particular cancers.

The mode of synthetic lethality-induced cell death is of clinical interest.

Cells undergoing necrosis lose membrane integrity early and release cytotoxic constituents that can damage neighboring cells, or induce an undesirable immune response (Krysko et al, 2006). However, apoptotic cells do not cause such an immune response. They are recognized by the host immune system and phagocytized by macrophages in a highly regulated process required for tissue homeostasis and immune regulation (Krysko et al, 2006). Therefore, apoptosis may be an advantageous mode of cell death for cells undergoing synthetic lethality (Baehrecke, 2002; deBakker et al, 2004; Krysko et al, 2006).

As the number of newly discovered synthetic lethal partnerships increases, it will be important to define their respective underlying biochemical mechanisms. To date, most attention has focused on partnerships between enzymes involved in DNA single- and double-strand break repair pathways. In our examination of DSBR (Fig. 2.5A-C), we observed a greater production of γH2AX foci over the first 15 min post-irradiation in the A549δSHP-1 cells than in the A549-Scramble cells. This could be interpreted as slower repair of DSB, but alternatively it could reflect a higher level of free radicals as discussed below. It is noticeable that, similar to the control cells, there was a marked decline in foci in the A549δSHP-1 cells by the 4-hour time point, indicative of efficient DSBR. This data coupled with our observation of efficient SSBR (Fig. 2.5D-F) led us to look for an alternative mechanism for SHP-1/PNKP synthetic lethality. It has been observed previously that SHP-1 depletion causes an increase in ROS production in HUVEC cells through its negative regulation of

NAD(P)H-oxidase–dependent superoxide production (Krotz et al, 2005). Furthermore, SHP-1, in common with many other protein-tyrosine phosphatases, is susceptible to oxidation of key cysteine residues in its catalytic domain by reactive oxygen species, including those generated by ionizing radiation (Barrett et al, 2005; Heneberg & Draber, 2005). Our data (Fig. 2.6) indicate that SHP-1 depletion in A549 and MCF7 cells also causes an increase in ROS production, which in turn results in elevated DNA strand cleavage (Fig. 2.5 and Supplemental Fig. A.6). (Radiation-induced inactivation of the residual SHP-1 present in the SHP-1 knockdown cells, and the resulting increase in ROS, could explain the higher production of γH2AX foci in these cells at 15 min post-irradiation). We inferred that, when coupled with PNKP-mediated disruption of DNA repair, increased ROS production causes a cytotoxic accumulation of DNA damage. The elimination of cytotoxicity conferred by treatment with the free radical scavenger WR1065 (Fig. 2.7) provided additional support for such a mechanism. Since PNKP acts on SSBs, as well as DSBs, an increase in unrepaired ROS-induced SSBs would lead to an increase in DSB formation during S-phase, potentially saturating DSB repair because these newly-formed DSBs would also require the action of PNKP at their termini. Our findings further extend the observation by Martin et al. (Martin et al, 2011), who showed that depletion of PINK1 causes an elevation of ROS and toxicity in a mismatch-repair deficient background. Importantly, this mechanism may apply to other yet to be identified synthetic lethal

partnerships between proteins involved in ROS regulation and oxidative DNA damage repair.

2.5 ACKNOWLEDGEMENTS

We thank Dr. Aghdass Rasouli-Nia for technical support and Dr. Sunita Ghosh for statistical support. Dr. Robert Ingham (Department of Medical Microbiology and Immunology, University of Alberta) for assistance with electroporation of Karpas cells.

2.6 FINANCIAL SUPPORT

This work was supported by the Canadian Institutes of Health Research (grant numbers MOP 15385*and* MOP 115069*to MW; MOP 77746 to EF). TRM is the recipient of graduate studentships from the Alberta Cancer Foundation and Alberta Innovates - Health Solutions. EF is a scholar of Alberta Innovates – Health Solutions and holds a Canada Research Chair in Innate Immunity.*

2.7 REFERENCES

Amir E, Seruga B, Serrano R, Ocana A (2010) Targeting DNA repair in breast cancer: a clinical and translational update. *Cancer Treat Rev* **36:** 557-565

Audeh MW, Carmichael J, Penson RT, Friedlander M, Powell B, Bell-McGuinn KM, Scott C, Weitzel JN, Oaknin A, Loman N, Lu K, Schmutzler RK, Matulonis U, Wickens M, Tutt A (2010) Oral poly(ADP-ribose) polymerase inhibitor olaparib in patients with BRCA1 or BRCA2 mutations and recurrent ovarian cancer: a proof-of-concept trial. *Lancet* **376:** 245-251

Azorsa DO, Gonzales IM, Basu GD, Choudhary A, Arora S, Bisanz KM, Kiefer JA, Henderson MC, Trent JM, Von Hoff DD, Mousses S (2009) Synthetic lethal RNAi screening identifies sensitizing targets for gemcitabine therapy in pancreatic cancer. *J Transl Med* **7:** 43

Baehrecke EH (2002) How death shapes life during development. *Nat Rev Mol Cell Biol* **3:** 779-787

Baldwin A, Grueneberg DA, Hellner K, Sawyer J, Grace M, Li W, Harlow E, Munger K (2010) Kinase requirements in human cells: V. Synthetic lethal interactions between p53 and the protein kinases SGK2 and PAK3. *Proc Natl Acad Sci U S A* **107:** 12463-12468

Barrett DM, Black SM, Todor H, Schmidt-Ullrich RK, Dawson KS, Mikkelsen RB (2005) Inhibition of protein-tyrosine phosphatases by mild oxidative stresses is dependent on S-nitrosylation. *J Biol Chem* **280:** 14453-14461

Bolderson E, Richard DJ, Zhou BB, Khanna KK (2009) Recent advances in cancer therapy targeting proteins involved in DNA double-strand break repair. *Clin Cancer Res* **15:** 6314-6320

Bryant HE, Schultz N, Thomas HD, Parker KM, Flower D, Lopez E, Kyle S, Meuth M, Curtin NJ, Helleday T (2005) Specific killing of BRCA2-deficient tumours with inhibitors of poly(ADP-ribose) polymerase. *Nature* **434:** 913-917

Canaani D (2009) Methodological approaches in application of synthetic lethality screening towards anticancer therapy. *Br J Cancer* **100:** 1213-1218

Cariaga-Martinez AE, Lorenzati MA, Riera MA, Cubilla MA, De La Rossa A, Giorgio EM, Tiscornia MM, Gimenez EM, Rojas ME, Chaneton BJ, Rodriguez DI, Zapata PD (2009) Tumoural prostate shows different expression pattern of somatostatin receptor 2 (SSTR2) and

phosphotyrosine phosphatase SHP-1 (PTPN6) according to tumour progression. *Adv Urol***:** 723831

Chan DA, Giaccia AJ (2011) Harnessing synthetic lethal interactions in anticancer drug discovery. *Nat Rev Drug Discov* **10:** 351-364

Chan N, Bristow RG (2010) "Contextual" synthetic lethality and/or loss of heterozygosity: tumour hypoxia and modification of DNA repair. *Clin Cancer Res* **16:** 4553-4560

Colombi M, Molle KD, Benjamin D, Rattenbacher-Kiser K, Schaefer C, Betz C, Thiemeyer A, Regenass U, Hall MN, Moroni C (2011) Genome-wide shRNA screen reveals increased mitochondrial dependence upon mTORC2 addiction. *Oncogene* **30:** 1551-1565

deBakker CD, Haney LB, Kinchen JM, Grimsley C, Lu M, Klingele D, Hsu PK, Chou BK, Cheng LC, Blangy A, Sondek J, Hengartner MO, Wu YC, Ravichandran KS (2004) Phagocytosis of apoptotic cells is regulated by a UNC-73/TRIO-MIG-2/RhoG signaling module and armadillo repeats of CED-12/ELMO. *Curr Biol* **14:** 2208-2216

Dedes KJ, Wilkerson PM, Wetterskog D, Weigelt B, Ashworth A, Reis-Filho JS (2011) Synthetic lethality of PARP inhibition in cancers lacking BRCA1 and BRCA2 mutations. *Cell Cycle* **10:** 1192-1199

Delibrias CC, Floettmann JE, Rowe M, Fearon DT (1997) Downregulated expression of SHP-1 in Burkitt lymphomas and germinal center B lymphocytes. *J Exp Med* **186:** 1575-1583

Dziegielewski J, Baulch JE, Goetz W, Coleman MC, Spitz DR, Murley JS, Grdina DJ, Morgan WF (2008) WR-1065, the active metabolite of amifostine, mitigates radiation-induced delayed genomic instability. *Free Radic Biol Med* **45:** 1674-1681

Evers B, Schut E, van der Burg E, Braumuller TM, Egan DA, Holstege H, Edser P, Adams DJ, Wade-Martins R, Bouwman P, Jonkers J (2010) A high-throughput pharmaceutical screen identifies compounds with specific toxicity against BRCA2-deficient tumours. *Clin Cancer Res* **16:** 99-108

Fanta M, Zhang H, Bernstein N, Glover M, Karimi-Busheri F, Weinfeld M (2001) Production, characterization, and epitope mapping of monoclonal antibodies against human polydeoxyribonucleotide kinase. *Hybridoma* **20:** 237-242

Farmer H, McCabe N, Lord CJ, Tutt AN, Johnson DA, Richardson TB, Santarosa M, Dillon KJ, Hickson I, Knights C, Martin NM, Jackson SP, Smith GC, Ashworth A (2005) Targeting the DNA repair defect in BRCA mutant cells as a therapeutic strategy. *Nature* **434:** 917-921

Fong PC, Boss DS, Yap TA, Tutt A, Wu P, Mergui-Roelvink M, Mortimer P, Swaisland H, Lau A, O'Connor MJ, Ashworth A, Carmichael J, Kaye SB, Schellens JH, de Bono JS (2009) Inhibition of poly(ADP-ribose) polymerase in tumours from BRCA mutation carriers. *N Engl J Med* **361:** 123-134

Freschauf GK, Karimi-Busheri F, Ulaczyk-Lesanko A, Mereniuk TR, Ahrens A, Koshy JM, Rasouli-Nia A, Pasarj P, Holmes CF, Rininsland F, Hall DG, Weinfeld M (2009) Identification of a small molecule inhibitor of the human DNA repair enzyme polynucleotide kinase/phosphatase. *Cancer Res* **69:** 7739-7746

Freschauf GK, Mani RS, Mereniuk TR, Fanta M, Virgen CA, Dianov GL, Grassot JM, Hall DG, Weinfeld M (2010) Mechanism of action of an imidopiperidine inhibitor of human polynucleotide kinase/phosphatase. *J Biol Chem* **285:** 2351-2360

Gien LT, Mackay HJ (2010) The Emerging Role of PARP Inhibitors in the Treatment of Epithelial Ovarian Cancer. *J Oncol* **2010:** 151750

Glendenning J, Tutt A PARP inhibitors--current status and the walk towards early breast cancer. *Breast* **20 Suppl 3:** S12-19

Hegazy SA, Wang P, Anand M, Ingham RJ, Gelebart P, Lai R (2010) The tyrosine 343 residue of nucleophosmin (NPM)-anaplastic lymphoma kinase (ALK) is important for its interaction with SHP1, a cytoplasmic tyrosine phosphatase with tumour suppressor functions. *J Biol Chem* **285:** 19813-19820

Helleday T (2011) The underlying mechanism for the PARP and BRCA synthetic lethality: Clearing up the misunderstandings. *Mol Oncol* **5:** 387-393

Heneberg P, Draber P (2005) Regulation of cys-based protein tyrosine phosphatases via reactive oxygen and nitrogen species in mast cells and basophils. *Curr Med Chem* **12:** 1859-1871

Iglehart JD, Silver DP (2009) Synthetic lethality--a new direction in cancer-drug development. *N Engl J Med* **361:** 189-191

Irandoust M, van den Berg TK, Kaspers GJ, Cloos J (2009) Role of tyrosine phosphatase inhibitors in cancer treatment with emphasis on SH2 domain-containing tyrosine phosphatases (SHPs). *Anticancer Agents Med Chem* **9:** 212-220

Kharitonenkov A, Chen Z, Sures I, Wang H, Schilling J, Ullrich A (1997) A family of proteins that inhibit signalling through tyrosine kinase receptors. *Nature* **386:** 181-186

Krotz F, Engelbrecht B, Buerkle MA, Bassermann F, Bridell H, Gloe T, Duyster J, Pohl U, Sohn HY (2005) The tyrosine phosphatase, SHP-1, is a negative regulator of endothelial superoxide formation. *J Am Coll Cardiol* **45:** 1700-1706

Krysko DV, D'Herde K, Vandenabeele P (2006) Clearance of apoptotic and necrotic cells and its immunological consequences. *Apoptosis* **11:** 1709-1726

Kumaravel TS, Vilhar B, Faux SP, Jha AN (2009) Comet Assay measurements: a perspective. *Cell Biol Toxicol* **25:** 53-64

Lindahl T, Nyberg B (1972) Rate of depurination of native deoxyribonucleic acid. *Biochemistry* **11:** 3610-3618

Lucchesi JC (1968) Synthetic lethality and semi-lethality among functionally related mutants of Drosophila melanfgaster. *Genetics* **59:** 37-44

Martin SA, Hewish M, Sims D, Lord CJ, Ashworth A (2011) Parallel high-throughput RNA interference screens identify PINK1 as a potential therapeutic target for the treatment of DNA mismatch repair-deficient cancers. *Cancer Res* **71:** 1836-1848

Martin SA, McCabe N, Mullarkey M, Cummins R, Burgess DJ, Nakabeppu Y, Oka S, Kay E, Lord CJ, Ashworth A (2010) DNA polymerases as potential therapeutic targets for cancers deficient in the DNA mismatch repair proteins MSH2 or MLH1. *Cancer Cell* **17:** 235-248

McEllin B, Camacho CV, Mukherjee B, Hahm B, Tomimatsu N, Bachoo RM, Burma S (2010) PTEN loss compromises homologous recombination repair in astrocytes: implications for glioblastoma therapy with temozolomide or poly(ADP-ribose) polymerase inhibitors. *Cancer Res* **70:** 5457-5464

Mendes-Pereira AM, Martin SA, Brough R, McCarthy A, Taylor JR, Kim JS, Waldman T, Lord CJ, Ashworth A (2009) Synthetic lethal targeting of PTEN mutant cells with PARP inhibitors. *EMBO Mol Med* **1:** 315-322

Naik S, Dothager RS, Marasa J, Lewis CL, Piwnica-Worms D (2009) Vascular Endothelial Growth Factor Receptor-1 Is Synthetic Lethal to Aberrant {beta}-Catenin Activation in Colon Cancer. *Clin Cancer Res* **15:** 7529-7537

Oka T, Yoshino T, Hayashi K, Ohara N, Nakanishi T, Yamaai Y, Hiraki A, Sogawa CA, Kondo E, Teramoto N, Takahashi K, Tsuchiyama J, Akagi T (2001) Reduction of hematopoietic cell-specific tyrosine phosphatase SHP-1 gene expression in natural killer cell lymphoma and various types of lymphomas/leukemias : combination analysis with cDNA expression array and tissue microarray. *Am J Pathol* **159:** 1495-1505

Pal SK, Mortimer J (2009) Triple-negative breast cancer: novel therapies and new directions. *Maturitas* **63:** 269-274

Rasouli-Nia A, Karimi-Busheri F, Weinfeld M (2004) Stable down-regulation of human polynucleotide kinase enhances spontaneous mutation frequency and sensitizes cells to genotoxic agents. *Proc Natl Acad Sci U S A* **101:** 6905-6910

Schindler A, Foley E (2010) A functional RNAi screen identifies hexokinase 1 as a modifier of type II apoptosis. *Cell Signal* **22:** 1330-1340

Stefansson OA, Jonasson JG, Johannsson OT, Olafsdottir K, Steinarsdottir M, Valgeirsdottir S, Eyfjord JE (2009) Genomic profiling of breast tumours in relation to BRCA abnormalities and phenotypes. *Breast Cancer Res* **11:** R47

Underhill C, Toulmonde M, Bonnefoi H (2010) A review of PARP inhibitors: from bench to bedside. *Ann Oncol*

Vilar E, Bartnik CM, Stenzel SL, Raskin L, Ahn J, Moreno V, Mukherjee B, Iniesta MD, Morgan MA, Rennert G, Gruber SB (2011) MRE11 deficiency increases sensitivity to poly(ADP-ribose) polymerase inhibition in microsatellite unstable colorectal cancers. *Cancer Res* **71:** 2632-2642

Walker DM, Kajon AE, Torres SM, Carter MM, McCash CL, Swenberg JA, Upton PB, Hardy AW, Olivero OA, Shearer GM, Poirier MC, Walker VE (2009) WR1065 mitigates AZT-ddI-induced mutagenesis and inhibits viral replication. *Environ Mol Mutagen* **50:** 460-472

Weinfeld M, Mani RS, Abdou I, Aceytuno RD, Glover JN (2011) Tidying up loose ends: the role of polynucleotide kinase/phosphatase in DNA strand break repair. *Trends Biochem Sci*

Williamson CT, Muzik H, Turhan AG, Zamo A, O'Connor MJ, Bebb DG, Lees-Miller SP (2010) ATM deficiency sensitizes mantle cell lymphoma cells to poly(ADP-ribose) polymerase-1 inhibitors. *Mol Cancer Ther* **9:** 347-357

Wu C, Sun M, Liu L, Zhou GW (2003) The function of the protein tyrosine phosphatase SHP-1 in cancer. *Gene* **306:** 1-12

Chapter 3: Synthetic lethal targeting of PTEN deficient cancers using selective disruption of polynucleotide kinase/phosphatase

Synthetic lethal targeting of PTEN-deficient cancers using selective disruption of polynucleotide kinase/phosphatase

[1]Todd R. Mereniuk, [2]Ana M. Mendes-Pereira, [3]Edan Foley, [2,4]Alan Ashworth, and [1]Michael Weinfeld

Affiliations of authors:
[1]Experimental Oncology, Department of Oncology, University of Alberta, Edmonton, AB, Canada T6G 1Z2
[2]The Breakthrough Breast Cancer Research Center, The Institute of Cancer Research, London, UK
[3]Department of Medical Microbiology and Immunology, University of Alberta, Edmonton, AB, Canada T6G 2S2
[4]CRUK Gene Function Laboratory, The Institute of Cancer Research, London, UK

Correspondence to: Michael Weinfeld
Cross Cancer Institute
University of Alberta
11560 University Ave
Edmonton, AB, Canada, T6G 1Z2
Tel: 780 432 8438
Fax: 780 432 8428
E-mail: michael.weinfeld@albertahealthservices.ca.

Running title: Synthetic lethal partnership between PNKP and PTEN

Total number of Figures in main text - 7

Key words: Synthetic lethality, polynucleotide kinase/phosphatase, PTEN, targeted therapy, synthetic sickness

3.1 INTRODUCTION

Synthetic lethality provides a means to target loss-of-function mutations commonly associated with the formation of neoplastic malignancies because it takes advantage of a cell's propensity to lose tumour suppressor function during its stepwise progression to cancer cell formation by targeting another protein not essential for cell survival. Co-disruption of both of these non-essential proteins, or the genes encoding them, in the same cell causes lethality, whereas each corresponding single disruption is compatible with survival (Brough et al, 2011a; Chan & Giaccia, 2011; Hartwell et al, 1997; Reinhardt et al, 2009). In this way it is possible to selectively kill only those cells in which both of these proteins are disrupted, i.e. cancer cells, while the effect on normal cells is considerably less detrimental. Therapeutic advantage can also be gained through the related concept of "synthetic sickness", in which co-disruption of the genes/proteins weakens severely weakens cells and increases their sensitivity to radiation or cytotoxic drugs (Chalmers et al, 2010; Kaelin, 2005; Martin et al, 2010).

To date, most of the focus on synthetic lethality has centered on the use of inhibitors of poly(ADP-ribose) polymerase (PARP) and cancers that have lost function of the breast cancer susceptibility loci (BRCA) tumour suppressors (Bryant & Helleday, 2006; Bryant et al, 2005; Comen & Robson, 2010; Farmer et al, 2005). However, increasing evidence shows that PARP inhibitors may benefit not only BRCA deficient cancers but also

those that display a phenotype as if BRCA was lost (BRCAness), such as triple-negative breast cancers (Comen & Robson, 2010). In fact, the PARP inhibitor BSI-201 is currently in phase III clinical trials as a combination treatment with carboplatin and gemcitabine, the preliminary results of which look very promising (Gartner et al, 2010). PARP inhibitors have since been shown to be relevant to the fight of cancers lacking non-classical DNA repair proteins such as the major tumour suppressor phosphatase and tensin homolog deleted on chromosome 10 (PTEN) (Mendes-Pereira et al, 2009). PTEN is lost in a broad spectrum of hereditary and sporadic human cancers, and is the second most lost tumour suppressor behind only p53 (Simpson & Parsons, 2001; Yin & Shen, 2008). It has many functions (reviewed in detail in (Simpson & Parsons, 2001)), but of particular importance to cancer are its functions in regulating cell growth and the cell cycle and its critical role in anti-apoptotic pathways.

We have recently broadened the scope of synthetic lethality to include polynucleotide kinase/phosphatase (PNKP) as another viable therapeutic target (Mereniuk et al, 2012). Like PARP, PNKP is an enzyme involved in the repair of DNA strand breaks. It possesses two activities, a 3'-DNA phosphatase and 5'-DNA kinase, which are required to restore the chemical composition of strand break termini to forms suitable for the subsequent action of DNA polymerases and ligases, i.e. 3'-hydroxyl and 5'-phosphate termini (Jilani et al, 1999; Karimi-Busheri et al, 1999). PNKP

participates in several repair pathways including base excision repair, single and double-strand break repair and the repair of strand breaks induced by topoisomerase I poisons (reviewed in (Allinson, 2010; Weinfeld et al, 2011)). Depletion of PNKP activity, either by shRNA or a small molecule inhibitor of its phosphatase activity, sensitizes cells to ionizing radiation and the topoisomerase I poison camptothecin (Rasouli-Nia et al, 2004). Importantly, loss of PNKP leads to an increase in spontaneous mutation frequency, indicating that the enzyme is required for the repair of endogenous DNA damage induced by reactive oxygen species (Rasouli-Nia et al, 2004).

To identify potential synthetic lethal partners of PNKP we previously performed an siRNA-library based screen of 6961 targets comprising the "druggable" genome and discussed our findings regarding the partnership with the tumour suppressor SHP-1 (Mereniuk et al, 2012). Among the other potential synthetic lethal partners of PNKP we identified *PTEN*. Here we report the validation of our initial findings confirming that indeed PNKP and PTEN act in a synthetic lethal partnership. We demonstrate that PNKP/PTEN synthetic lethality can be induced in a variety of cell lines representing different tumour sites, including a naturally PTEN-deficient prostate cancer cell line. We also show that loss of *PTEN* coupled with partial inhibition of PNKP significantly sensitizes cells to ionizing radiation. Our data suggest that the clinical usefulness of PNKP disruption may be extended to include $PTEN^{-/-}$ cancers.

3.2 MATERIAL AND METHODS

3.2.1 Cell Lines

A549 cells were purchased from the American Type Culture Collection (Manassas, VA). A549δPNKP (A549 cells stably depleted of PNKP using shRNA) and A549-SC (A549 cells stably expressing a scrambled shRNA) have been previously described (Mereniuk et al, 2012). The HCT116 human colon cancer parental cell line and its PTEN knockout variants and G418-resistant control (Lee et al, 2004) were generously provided by Dr. Todd Waldman (Georgetown University, Washington, DC). The PC3 human prostate cancer parental cell line and its variants were previously described (Mendes-Pereira et al, 2009).

Cell lines were cultured at 37°C and 5% CO_2 in a humidified incubator in a 1:1 mixture of Dulbecco's Modified Eagle's Medium and F12 (DMEM/F12) supplemented with 10% FBS, 50 U/mL penicillin, 50 µg/mL streptomycin, 2 mM L-glutamine, 0.1 mM non-essential amino acids and 1 mM sodium pyruvate. All culture supplements were purchased from Invitrogen (Carlsbad, CA).

3.2.2 Vectors and siRNA

pSUPER.neo vectors (Oligoengine, Seattle, WA) contained either an shRNA directed against nucleotides 1391-1410 of PNKP (Rasouli-Nia et al, 2004) to stably deplete PNKP in A549 cells or an shRNA to no known gene target (scrambled shRNA) to generate the control cell line A549-SC.

The pBABE.puro (Addgene, Cambridge, MA) vectors contained wild type RAD 51 cDNA or wild type or mutated PTEN cDNA used to generate the PC3 reconstituted cell lines: WT PTEN (full length, wild-type PTEN), p.K289E (PTEN mutant with reduced nuclear shuttling), p.R55fs*1 (truncation mutant normally found in PC3), p.C124S (a phosphatase inactive PTEN mutant) (Mendes-Pereira et al, 2009).

All siRNAs were purchased from Qiagen (Mississauga, ON) with the exception of PNKP siRNA, which was purchased from Ambion (Austin, TX).

3.2.3 Stable transfection

20,000 cells were plated and allowed to adhere overnight in a 24-well dish at 37°C and 5% CO_2. The transfection mixture was prepared from two separate solutions, the first containing 1 µg of plasmid DNA dissolved in 50 µL total of Opti-MEM (Invitrogen) and the second 3 µL of Lipofectamine2000 (Invitrogen) in 50 µL total Opti-MEM. The two solutions were incubated at room temperature for 5 min before combination, mixed and then held at room temperature for 20 min. The media from the pre-plated cells was removed and replaced with the transfection mixture, and the cells were incubated for 24 h at 37°C and 5% CO_2. The cells were then trypsinized and transferred into 6 x 100-mm plates in DMEM/F12 without antibiotics and incubated overnight at 37°C and 5% CO_2. The following day, media was removed and replaced with complete DMEM/F12 containing 500 µg/mL G418 for pSUPER.neo-based reconstituted cell lines or 5

μg/mL puromycin for pBABE.puro-based reconstituted cell lines. The pSUPER.neo-transformed cells were allowed to form single colonies and after 10-18 days the colonies were picked and clonally expanded prior to protein analysis. The pBABE.puro transformed cell lines were used as heterogeneous populations.

3.2.4 siRNA library screen

As previously described (Mereniuk et al, 2012), Qiagen's "druggable" genome siRNA library was first distributed into 89 x 96-well plates at a concentration of 1 μM, each well containing four separate siRNAs to the same mRNA target. Also added to each plate were three additional control wells (C12, D12 and E12) of AllStars Negative (ASN) scrambled siRNA (Qiagen). Then, utilizing a JANUS Automated Workstation (PerkinElmer, Waltham, MA), 4,000 A549δPNKP or A549-SC cells were seeded into each well of a 96-well plate in a final volume of 100 μL DMEM/F12 without penicillin/streptomycin and allowed to adhere overnight in a humidified incubator. The following day, transfection mixture was generated as described above (56 nM siRNA and a total of 0.23 μL Dharmafect transfection reagent 1 per well, (Dharmacon, Lafayette, CO). Media was aspirated from the plates containing cells, and 100 μL of the transfection mixture was added to each well and allowed to incubate for 72 h. After incubation, 10% v/v of 440 μM Alamar Blue (Sigma-Aldrich, Oakville, ON) was added to each well and the cells were incubated for 50-90 min, after

which the fluorescence in each well was determined using an EnVision 2104 Multilabel Reader (PerkinElmer) with an excitation wavelength of 563 nm and emission wavelength of 587 nm.

3.2.5 Transient transfection

4,000 cells were plated per well in a 96-well plate, and allowed 24 h to adhere in a humidified incubator at 37°C and 5% CO_2. All wells surrounding samples were filled with 100 µL distilled water to control for evaporation effects. 16 nM final concentration of siRNA was added to 50 µL total reaction volume in Opti-MEM (Invitrogen). At the same time as siRNA-Opti-MEM incubation, a 1:25 dilution of Dharmafect transfection reagent 1 in Opti-MEM was allowed to incubate at room temperature for 5 min, to provide a final volume of 0.12 µL of transfection reagent per well. Equal volumes of the two transfection solutions were then combined and held at room temperature for 20 min. The media was then removed from the cells and 100 µL of the transfection mixture was added per well and the plate was incubated at 37°C and 5% CO_2 for 72 h.

3.2.6 Protein analysis

Approximately 10^6 transiently transfected cells were washed twice with ice cold PBS, trypsinized, and collected by centrifugation at 600 *g* for 10 min at 4°C. The supernatant was aspirated and the cell pellet was resuspended in 200 µL of CHAPS buffer (0.5% CHAPS, 137 mM NaCl, 50

mM Tris-HCl pH 7.5, 1 mM EDTA) and rocked for 1 h at 4°C, after which cell debris was removed by centrifugation at 17,500 *g* for 20 min at 4°C. Determination of whole cell lysate concentration was then conducted using the Bradford Assay.

Western blots were carried out with 50 µg of whole cell lysate. Monoclonal primary antibodies were incubated 1:1000 in 5% milk in PBST overnight at 4°C (Cell Signaling, Beverly, MA). All secondary antibodies were incubated 1:5000 for 45 min at room temperature.

3.2.7 Cell proliferation and clonogenic survival assays

Cell proliferation assays were performed using the transient transfection technique described above, however, after incubation with siRNA for 72 h, 10% v/v of 440 µM Alamar Blue was added to each well and the cells were incubated for 50-90 min, after which the fluorescence in each well was determined using an EnVision 2104 Multilabel Reader with an excitation wavelength of 563 nm and emission wavelength of 587 nm. HCT116 based cell lines were subjected to a 10.7% v/v 440 µM Alamar Blue solution per well for the same times indicated.

The effect on survival of simultaneous disruption of two proteins was conducted using a clonogenic survival assay. To allow cells time to adhere to the plates, cells were seeded in 60-mm dishes 24 h in advance. Cells were treated with the PNKP inhibitor A12B4C3 ((Freschauf et al, 2009; Freschauf et al, 2010), kindly provided by Dr. Dennis Hall, University of

Alberta) for 9-14 consecutive days at 0 μM, 0.1 μM, 1 μM, and 10 μM final concentration, where 100 cells were plated for the 0 μM, 0.1 μM and 1 μM concentration groups and 300 cells in the 10 μM concentration group. Colonies were then stained with a crystal violet stain containing 20% methanol for one hour, after which the plates were washed in warm water and left to dry overnight. Colonies of 50+ cells were then counted using an automated colony counter (Oxford Optronix, Oxford, UK).

To determine the radiation response, cells were treated with 0, 1, 2, 4, 6, or 8 Gy γ-radiation (^{60}Co Gammacell; Atomic Energy of Canada Limited, Ottawa, Canada) under continuous PNKP inhibition using 2 mM A12B4C3.

3.2.8 Statistical analysis

All p-values were generated using a two-sided Student's t-test. Z-scores were generated from an average from 24-96 individual wells of data per assay (performed at least in triplicate), allowing us an appropriate number of replicates to achieve robust statistical data. A Z-score is a dimensionless quantity representing a measurement of the number of standard deviations a sample is above or below the mean of a control. It is defined as:

$$z = \frac{x - \mu}{\sigma}$$

z = Z-score
x = the raw score to be standardized

μ= population mean
σ = standard deviation of the population

As such, Z-scores can be positive or negative depending on whether the sample is higher or lower than the mean of a control. For our results, we were interested in a negative Z-score as this showed that the survival of the experimental condition was lower than control (i.e. the condition was lethal). A sample with a Z-score of -3 or less is significantly different than control as it falls at least three standard deviations less than the average of the control.

3.2.9 Determination of mode of cell death

A549-SC or A549δPNKP cells were grown on coverslips in complete DMEM/F12 and were transfected with ASN or PTEN siRNA. As a positive control, the cells were treated with 100 μM 5-(p-bromobenzylidine)-α-isopropyl-4-oxo-2-thioxo-3-thiozolidineacetic acid (BH3I-1, Sigma-Aldrich, Oakville, ON), which is a known to induce apoptosis. The cells were triple-stained after the indicated length of time with Hoechst 33342, Ethidium Homodimer III and Annexin V-FITC as previously described (Mereniuk et al, 2012).

3.3 RESULTS

3.3.1 Confirming PTEN as a possible synthetic lethal partner of PNKP

To date, most proteins shown to have synthetic lethal associations

involve PARP and partner proteins functioning in a separate DNA repair pathway (Bryant & Helleday, 2006; Bryant et al, 2005; Farmer et al, 2005). We sought to discover synthetic lethal partnerships of PNKP, as an alternative to PARP, without necessarily limiting our search to partner proteins directly involved in DNA repair. We performed a forward transfection screen with an extensive library of siRNAs targeting 6961 genes using pooled samples of four distinct siRNAs targeting each gene. The screen was performed in duplicate using A549 lung cancer cells stably depleted of PNKP (A549δPNKP) and again using cells expressing a scrambled shRNA (A549-SC) under identical conditions. Cells were exposed to siRNA transfection complexes continuously for 72 h allowing for at least two cell cycles to occur at a concentration known to be effective at knocking down target proteins. Cell survival was then determined by an Alamar Blue-based reduction assay (Schindler & Foley, 2010).

Cell survival scores after targeting each of the 6961 mRNAs were compared to controls located on the same plate and when the duplicate screens were compared to each other, they were shown to be highly reproducible. Amongst the potential synthetic lethal partners of PNKP was the major tumour suppressor PTEN. Figure 3.1A shows the difference between five selected tumour suppressors compared to two proteins shown to be not lethal when co-disrupted with PNKP.

To confirm the synthetic lethal relationship between PNKP and PTEN, we repeated the transfections, but reduced the concentration of siRNA

previously used in the screen by 3.5-fold, which still showed synthetic lethality in PNKP knockdown cells yet were non-lethal to A549-SC control cells (Fig. 3.1B). We then sought to use each of the four originally pooled siRNAs separately in order to further minimize the potential for off-target effects (Fig. 3.2A). When the distinct siRNAs directed against PTEN were assayed, two displayed selective killing of A549δPNKP cells and no toxicity in control cells, siRNA #6 Z-factor = -9.0, $p < 0.001$; siRNA #8 Z-factor = -9.1, $p < 0.001$). Since more than one siRNA showed synthetic lethality with PNKP, the effect was most likely attributable to the double knockdown of PNKP and PTEN and not due to off-target effects. Activation of the RNAi pathway using AllStars negative control siRNA (ASN) is also not responsible for the lethality seen, indicating this is a true synthetic lethal partnership. The greater cytotoxicity seen with the PTEN/PNKP double knockdown using PTEN #6 siRNA is higher than when using PTEN #8 siRNA probably reflected the efficiency of the two siRNAs to knockdown PTEN expression (Fig. 3.2C). This would imply a dose response effect that may have implications regarding natural levels of active PTEN found in tumours.

To further substantiate that a synthetic lethal partnership exists between PTEN and PNKP, we carried out a similar analysis with the MCF7 breast cancer cell line and #6 siRNA. As seen with A549 cells, the combined disruption of both PTEN and PNKP was responsible for lethality,

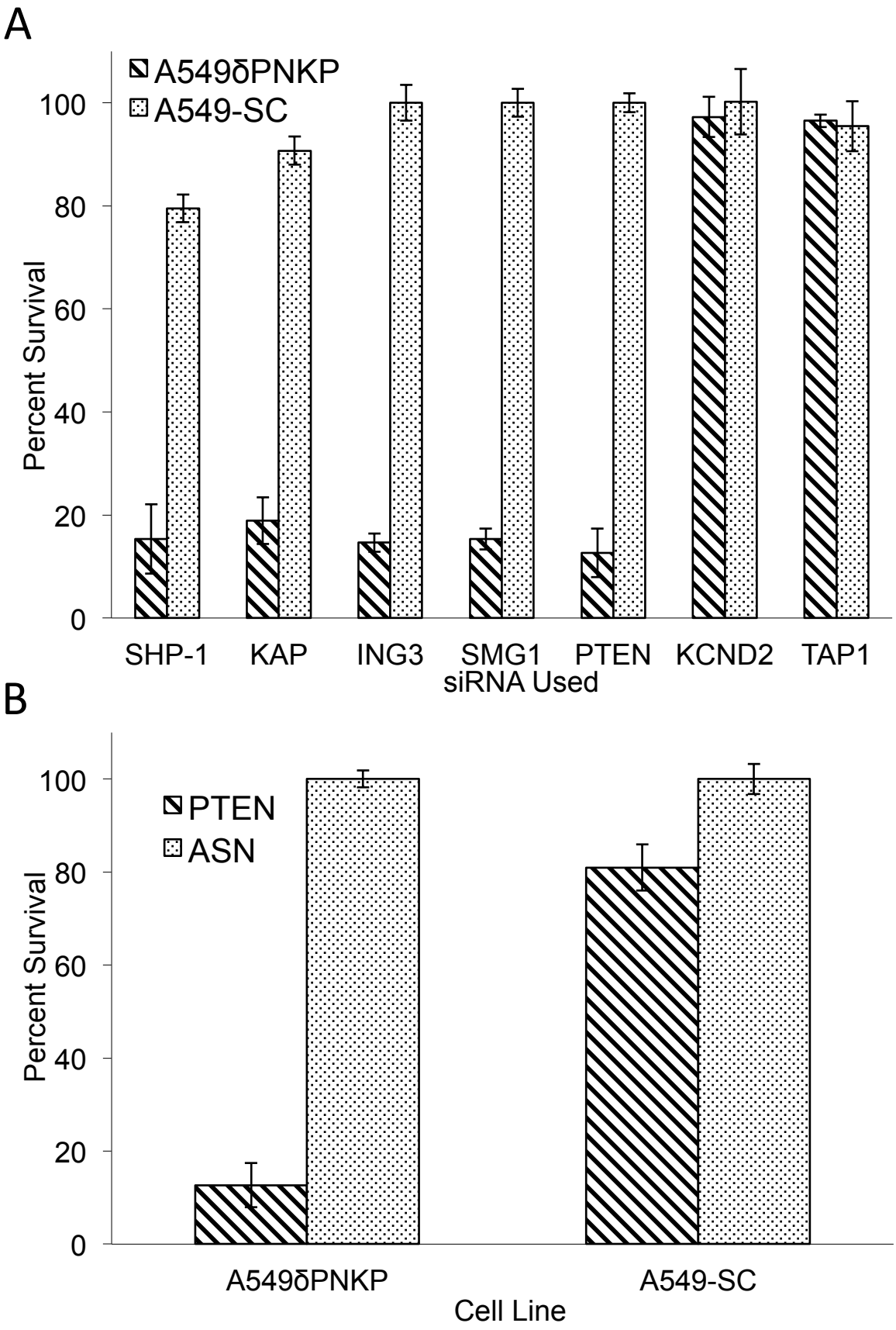
A
A549δPNKP
A549-SC
Percent Survival
0
20
40
60
80
100
SHP-1
KAP
ING3
SMG1
PTEN
KCND2
TAP1
siRNA Used
B
PTEN
ASN
Percent Survival
0
20
40
60
80
100
A549δPNKP
A549-SC
Cell Line

Figure 3.1. Five tumour suppressors potentially synthetic lethal with PNKP identified through screening. 56 nM of 6961 pooled siRNAs (four distinct siRNAs per pool) were used to screen two cell lines; A549δPNKP (A549 stably depleted of PNKP) and A549-SC (A549 stably expressing a scrambled shRNA) in duplicate. Fourteen known or implicated tumour suppressor genes were identified, of which five are shown here. Only when PNKP is co-disrupted with its potential synthetic lethal partner is lethality seen. Two randomly selected genes (*KCND2 and TAP1*) are shown to identify the difference between potential hits and non-hits. (B) Further confirmation of PTEN-PNKP synthetic lethality. ASN = AllStars Negative scrambled control siRNA. To help control for the off-target effects of siRNA in our confirmation experiments a reduced concentration of siRNA was used. Specifically, 16 nM of siRNA (3.5-fold less than the concentrations employed for screening) was used to transiently transfect A549δPNKP and A549-SC cells. This graph shows that in the three cell lines, A549δPNKP, A549-SC and A549 parental control cells, only when PTEN is knocked down in combination with PNKP do we see lethality (Z-factor = -9.01, $p < 0.001$). The loss of PTEN alone is not lethal, nor is the activation of the siRNA machinery responsible for the effects seen. Error bars represent standard error (± S.E.) from at least three independent determinations.

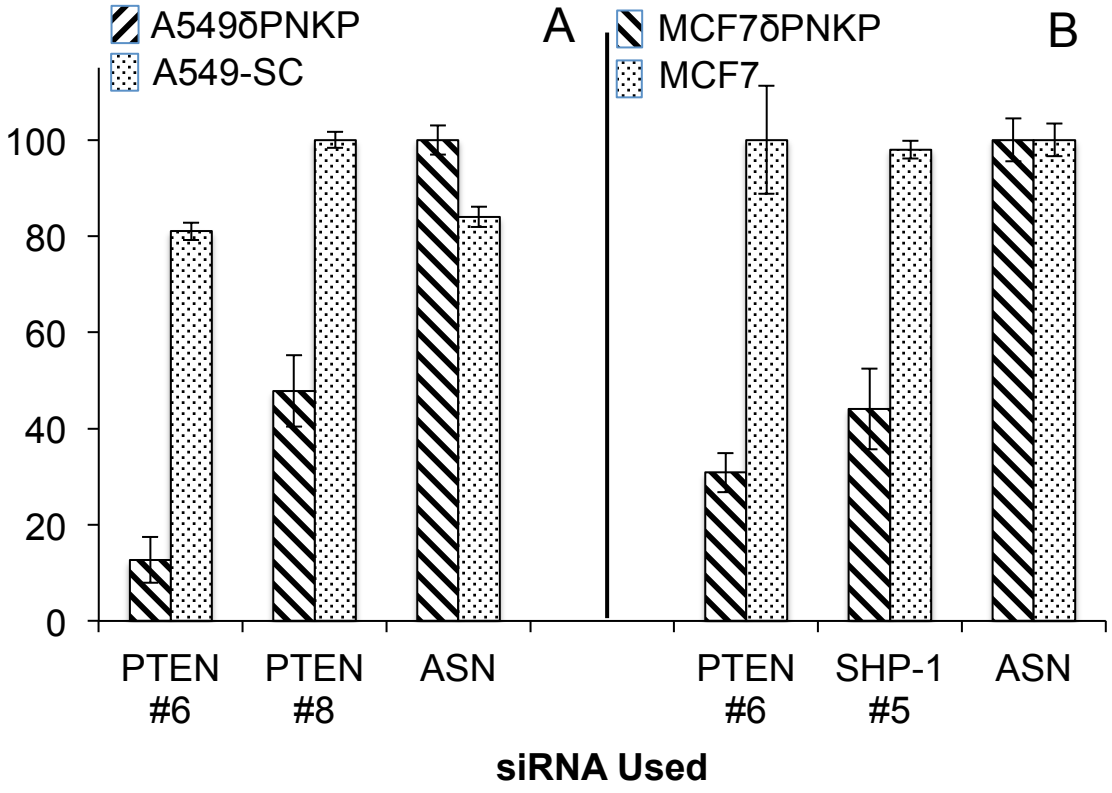
A549δPNKP
A549-SC
A
MCF7δPNKP
MCF7
B
100
80
60
40
20
0
PTEN #6
PTEN #8
ASN
PTEN #6
SHP-1 #5
ASN
siRNA Used

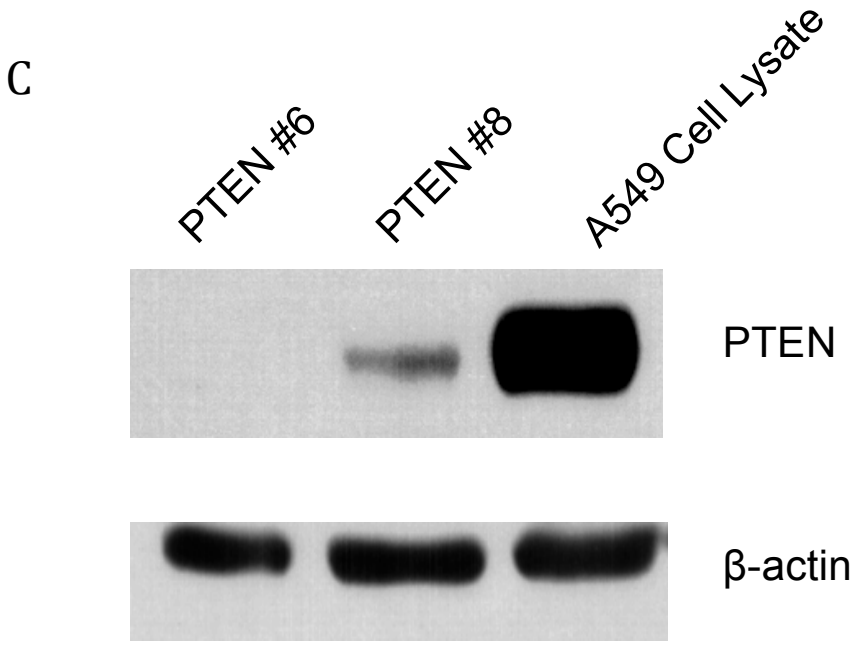
C
PTEN #6
PTEN #8
A549 Cell Lysate
PTEN
β-actin

Figure 3.2. (A) Utilization of independent siRNAs targeting PTEN. The four siRNAs that were pooled for screening purposes were tested independently to assess their effectiveness at killing A549δPNKP cells. The likelihood that the effects seen are due to off-target effects is lessened if multiple siRNAs produce similar results. Two of the four siRNAs caused lethality in combination with PNKP disruption, of which PTEN #6 siRNA displayed greater cytotoxicity than PTEN #8 siRNA (PTEN #6 Z-factor = -9.01, $p < 0.001$, PTEN #8 Z-factor = -9.06, $p < 0.001$). (B) To test whether the PTEN/PNKP synthetic lethal relationship holds true across cancer types, wild type MCF7 breast cancer cells were transiently transfected with PTEN #6 siRNA alongside MCF7 cells stably depleted of PNKP (MCF7δPNKP). (C) Western blot of A549 cells transiently transfected with PTEN #6 and PTEN #8 siRNAs. The data suggest that the disparity in survival seen with PTEN #6 and PTEN #8 siRNAs when combined with PNKP disruption is probably due to the lower effectiveness of PTEN #8 siRNA at knocking down PTEN expression than PTEN #6 siRNA. Error bars represent standard error (± S.E.) from at least three independent determinations.

since the depletion of PNKP or PTEN individually was not lethal (Fig. 3.2B, Z-score for PTEN = -8.0, $p < 0.001$, Z-score for SHP-1 = -3.4, $p < 0.001$), nor is the activation of RNAi machinery responsible for lethality. These findings imply that a true synthetic lethal relationship exists between PTEN and PNKP.

Finally, isogenically matched HCT116 parental, Neo124 vector only ($PTEN^{+/+}$) and $PTEN^{-/-}$ (#22 and #35) cells (Lee et al, 2004) were subjected to increasing concentrations of the PNKP phosphatase inhibitor A12B4C3 (Freschauf et al, 2009). Figure 3.3 clearly shows that loss of PTEN sensitized the cells to A12B4C3 and the importance of the DNA 3'-phosphatase activity of PNKP to the synthetic lethal process.

3.3.2 Mode of cell death

To identify how cells in which PTEN and PNKP are simultaneously die, A549-SC and A549δPNKP cells were grown on glass coverslips and transiently transfected with either PTEN or ASN siRNA. As a positive control, the known apoptosis inducer, BH3I-1 was added to the medium at a concentration of 100 μM. After the indicated lengths of time, cells were triple stained with Hoechst 33342, Ethidium Homodimer III and Annexin V-FITC. Using this triple stain, we were able to distinguish between those cells that are undergoing apoptosis, necrosis or neither (Mereniuk et al, 2012). Figure 3.4A shows that there exists a small population of both

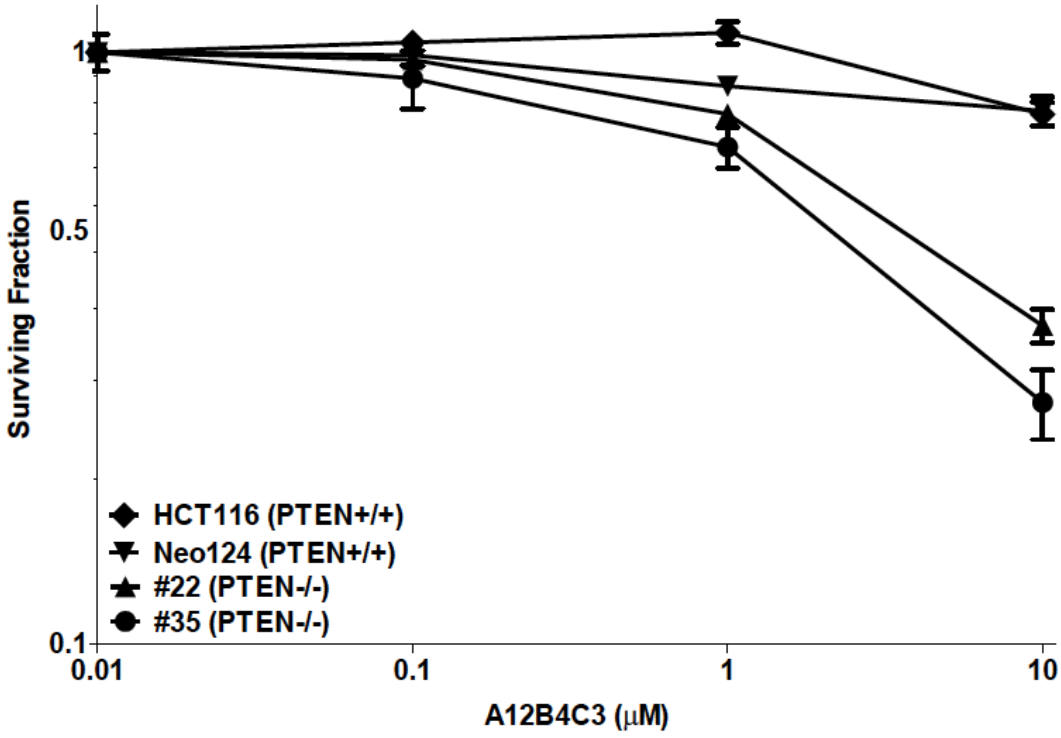
Surviving Fraction
1
0.5
0.1
0.01
0.1
1
10
A12B4C3 (μM)
HCT116 (PTEN+/+)
Neo124 (PTEN+/+)
#22 (PTEN-/-)
#35 (PTEN-/-)

Figure 3.3. Colony-forming assay testing the survival of PTEN negative cells. Isogenically matched $PTEN^{+/+}$ cells (HCT116 parental and Neo124 vector control cells) and two $PTEN^{-/-}$ HCT116 strains #22 (A) and #35 (B) were subjected to increasing concentrations of the PNKP inhibitor A12B4C3 and survival was assessed by the colony forming assay. Only PTEN negative cells were selectively sensitive to treatment with A12B4C3. Error bars represent standard error (± S.E.) from at least three independent determinations, each experiment was done in triplicate for a minimum of nine total assessed plates.

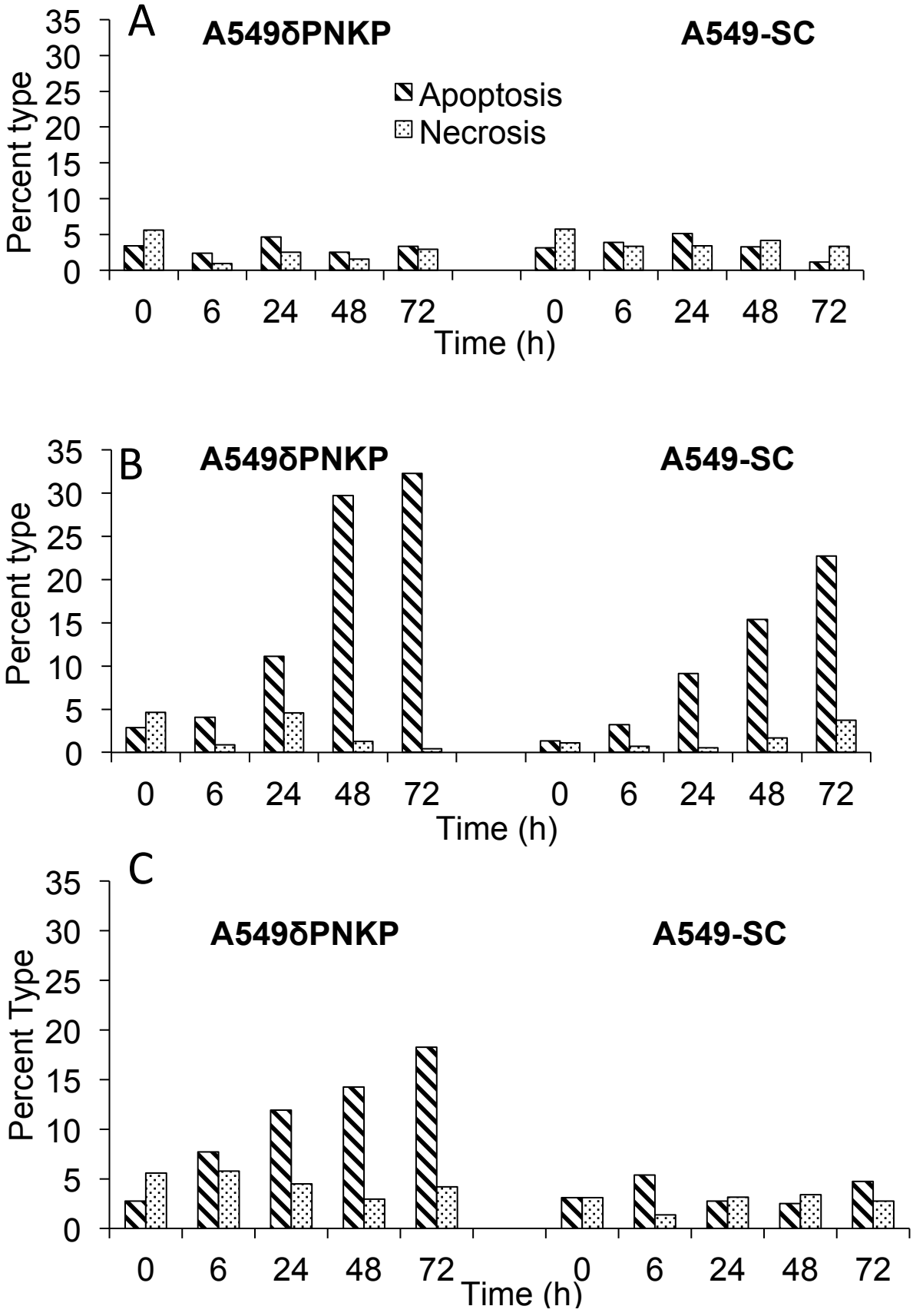
A
A549δPNKP
A549-SC
Apoptosis
Necrosis
Percent type
35
30
25
20
15
10
5
0
0 6 24 48 72 0 6 24 48 72
Time (h)
B
A549δPNKP
A549-SC
Percent type
35
30
25
20
15
10
5
0
0 6 24 48 72 0 6 24 48 72
Time (h)
C
A549δPNKP
A549-SC
Percent Type
35
30
25
20
15
10
5
0
0 6 24 48 72 0 6 24 48 72
Time (h)

Figure 3.4. Determination of the mode of cell death of cells undergoing synthetic lethality due to the concurrent ablation of PTEN and PNKP function. (A) A549δPNKP and A549-SC cells were transiently transfected with scrambled control ASN siRNA and the proportion of apoptotic versus necrotic cells was determined at times post-transfection as described in the Materials and Methods section. (B) ASN-treated cells were additionally treated with the apoptosis inducer BH3I-1. (C) Measurement of apoptotic and necrotic cells at the indicated time points post-PTEN siRNA transient transfection.

apoptotic and necrotic cells present at every time point, however, treatment of cells with BH3I-1 dramatically increased the proportion of apoptotic cells relative to necrotic cells beginning at 24 h post-treatment in both A549-SC and A549δPNKP (Fig. 3.4B). Similarly, when both PTEN and PNKP are disrupted in the same cell, there is a substantial increase in apoptosis (Fig. 3.4C). Conversely, when PTEN is knocked down in A549-SC cells, there is no increase in the proportion of either apoptotic or necrotic cells. Therefore, cells that are both PTEN and PNKP dysfunctional undergo cell death through apoptotic mechanisms, similar to cells in which both SHP-1 and PNKP are doubly disrupted (Mereniuk et al, 2012).

3.3.3 Survival of naturally occurring PTEN negative cells in response to PNKP inhibition

The utility of synthetic lethality will lie in the capacity to translate potential associations into targeted therapy, possibly using inhibitors of one of the partners as a single agent. To investigate the feasibility of taking advantage of the newly identified partnership between PTEN and PNKP, we subjected the prostate cancer cell line, PC3 (naturally $PTEN^{-/-}$) to increasing concentrations of the PNKP inhibitor A12B4C3 (Freschauf et al, 2009) over a period of 12-16 days. The dose response curve (Fig. 3.5A) indicates that at A12B4C3 concentrations ≥ 10 μM there was a marked decrease in survival of the PC3 parental cell line. We then made use of

A

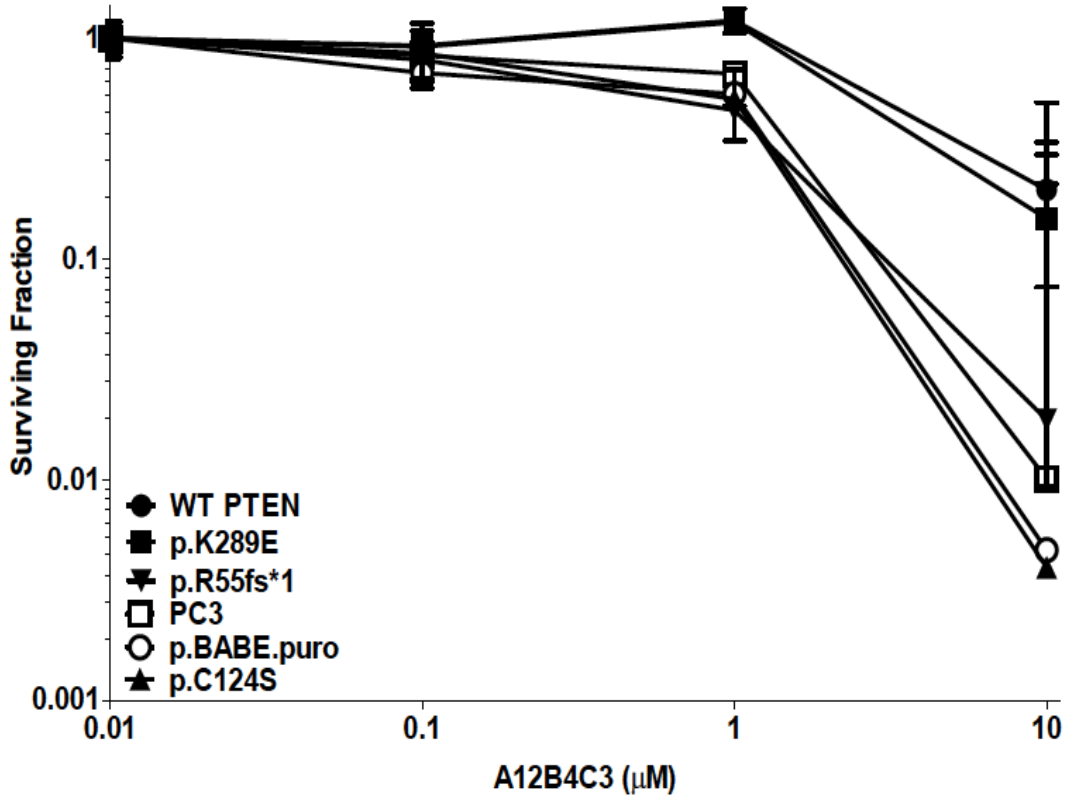
Surviving Fraction
1
0.1
0.01
0.001
0.01
0.1
1
10
A12B4C3 (μM)
WT PTEN
p.K289E
p.R55fs*1
PC3
p.BABE.puro
p.C124S

B

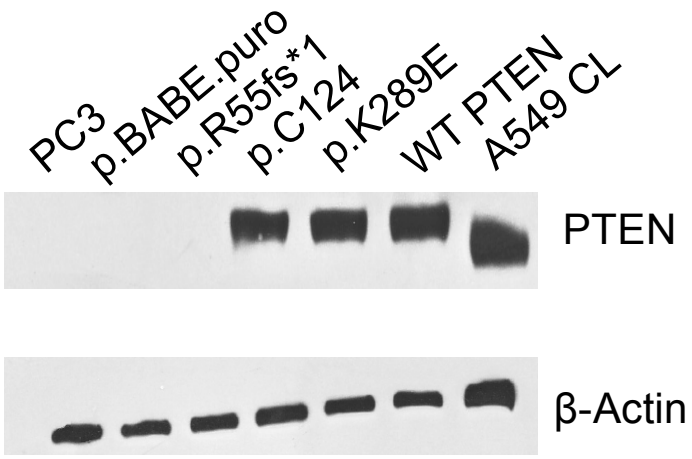
PC3
p.BABE.puro
p.R55fs*1
p.C124
p.K289E
WT PTEN
A549 CL
PTEN
β-Actin

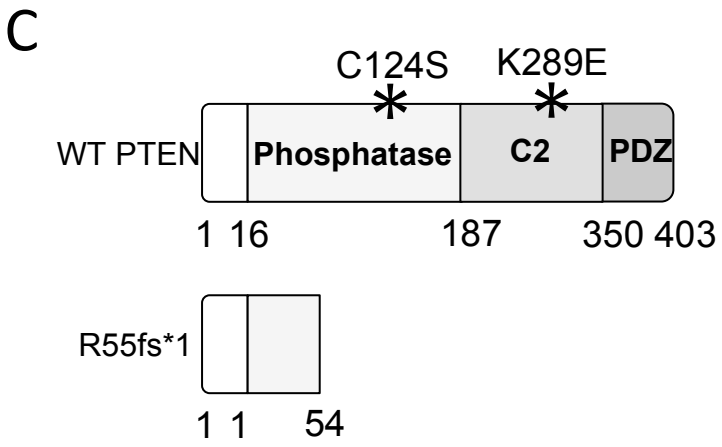
C
C124S
K289E
WT PTEN
Phosphatase
C2
PDZ
1 16
187
350 403
R55fs*1
1 1
54

Figure 3.5. Identification of the critical function of PTEN for survival under PNKP disruption. (A) PC3 cells (naturally occurring $PTEN^{-/-}$ prostate cancer cells) were transfected with expression vectors encoding various forms of PTEN: p.BABE.puro – vector only; WT PTEN – full length, wild-type PTEN cDNA; p.K289E – PTEN mutant with reduced nuclear shuttling cDNA; p.R55fs*1 – truncation mutant normally found in PC3 cDNA; p.C124S – phosphatase inactive PTEN mutant cDNA. Survival under PNKP inhibition was restored only when wild-type PTEN and phosphatase active but cytoplasmically-trapped PTEN was re-expressed in PC3 cells. All other plasmids did not rescue lethality. Error bars represent standard error (± S.E.) from at least three independent determinations, each experiment was done in triplicate for a minimum of nine total assessed plates. (B) Western blots showing the PTEN-null cell line PC3 transfected with vector only, PTEN truncation mutant, or the different forms of full length PTEN. (C) Graphical representation of the various forms of PTEN used to reconstitute PC3 cells. Also shown is the truncation mutation of PTEN normally found in PC3 cells (R55fs*1) and the location of the other mutations in PTEN, whether it was in the phosphatase domain (as is the case of C124S) or the structural domain involved in targeting proteins to cell membranes (C2, in the case of K289E). The final domain (PDZ) is a structural domain commonly found in signaling proteins, but was not mutated in these experiments.

ectopic expression of various wild type and mutant PTEN- bearing vectors to further analyze the role of key components of PTEN in this phenomenon (Figs. 3.5B and C). As anticipated, expression of the empty vector, p.BABE.puro, and a vector coding for the *PTEN* deletion-frameshift mutation found in PC3 cells, p.R55fs*1, did not alter the result seen with the parental PC3 cells. Similarly, ectopic expression of the catalytically inactive mutant of *PTEN*, coding for the C124S altered protein, also failed to elicit an increase in the survival of A12B4C3 treated cells. In contrast, PC3 cells reconstituted with either wild type PTEN (WT) protein or the phosphatase proficient but cytoplasmically trapped PTEN modified protein, K289E, restored resistance to PNKP-inhibition. Finally, because of a potential association between PTEN and Rad51 (McEllin et al, 2010; Mendes-Pereira et al, 2009; Mukherjee & Karmakar, 2012; Shen et al, 2007), we examined PC3 cells ectopically expressing *RAD51* cDNA, but found no increase in survival in response to treatment with A12B4C3 (Fig. 3.6A, western blot showing ectopic expression of RAD51 protein in PC3 is shown in Fig. 3.6B). From these data we infer that the critical function of PTEN lies in its phosphatase activity and its localization in the cytoplasm.

Taken together, our results with a naturally PTEN-deficient tumour cell line suggest that it may be possible to exploit the synthetic lethal relationship between PNKP and PTEN in the clinical management of $PTEN^{-/-}$ cancers.

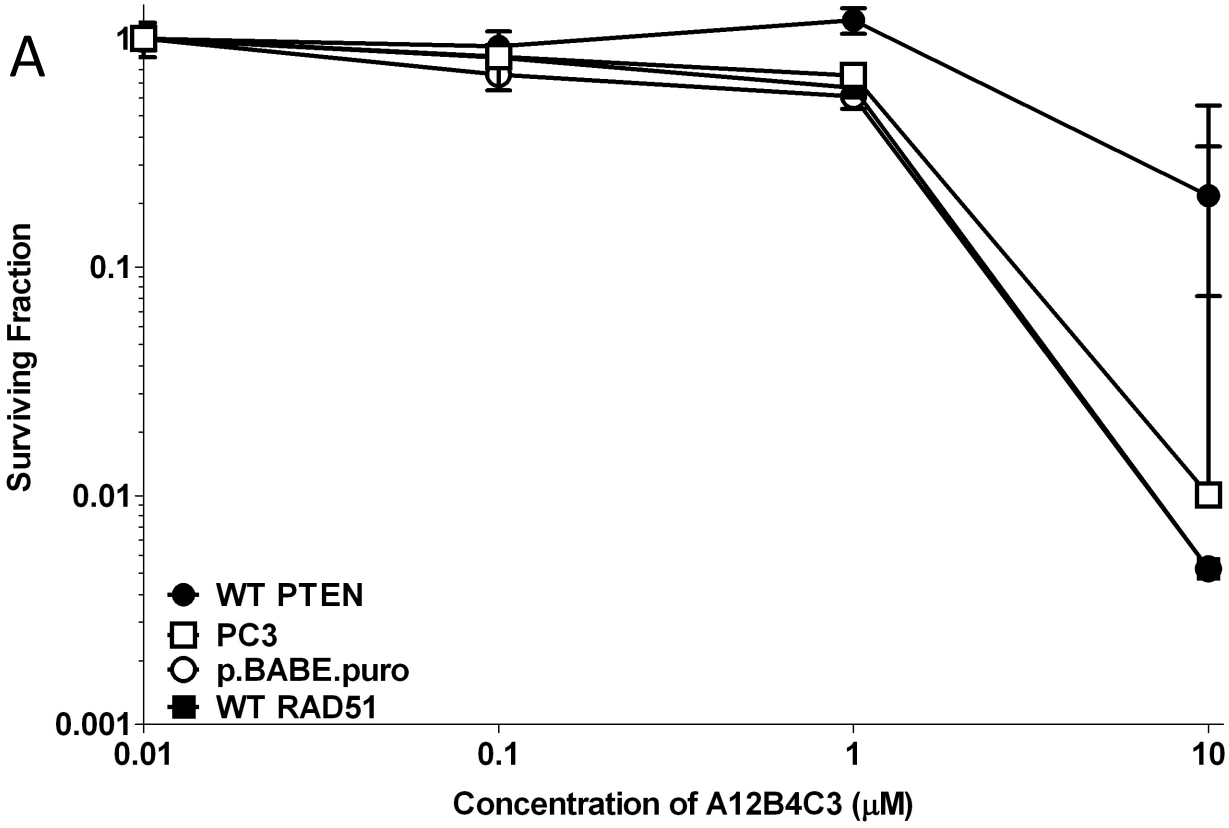
A
Surviving Fraction
1
0.1
0.01
0.001
0.01
0.1
1
10
Concentration of A12B4C3 (μM)
WT PTEN
PC3
p.BABE.puro
WT RAD51

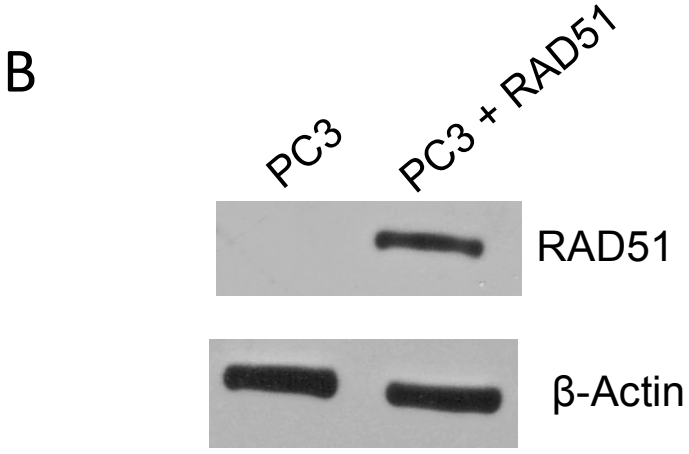
B
PC3
PC3 + RAD51
RAD51
β-Actin

Figure 3.6. Ectopic expression of RAD51 protein does not rescue synthetic lethality seen between PTEN and PNKP. PC3 cells were transfected with a vector expressing full length, wild-type RAD51 cDNA (WT RAD51). Increased expression of this homologous recombination protein did not negate synthetic lethality between PTEN and PNKP. Error bars represent standard error (± S.E.) from at least three independent determinations, each experiment was done in triplicate for a minimum of nine total assessed plates. (B) Western blot depicting the level of RAD51 expression in PC3 cells.

3.3.4 Radiosensitization by combined disruption of PNKP and PTEN

We have previously observed that depletion or inhibition of PNKP sensitizes cells to ionizing radiation (Freschauf et al, 2009; Rasouli-Nia et al, 2004). We therefore subjected the control and two PTEN$^{-/-}$ HCT116 cell lines to additional testing to determine if disruption of PNKP in PTEN negative cells would hypersensitize these cells to ionizing radiation (Fig. 3.7). Cells were incubated with a non-toxic concentration (2 μM) of A12B4C3 (or just the DMSO vehicle) for 24 h prior to irradiation with doses up to 8 Gy and then maintained in the presence of the PNKP inhibitor until colonies were counted. As expected A12B4C3 sensitized the control PTEN$^{+/+}$ HCT116 cells to radiation in a similar manner to that previously seen with A549 cells (Freschauf et al, 2009). We also observed that the PTEN$^{-/-}$ cell lines were modestly radiosensitive in comparison to the control cell line in accordance with published data (Lee et al, 2004). However, when PTEN and PNKP were simultaneously disrupted, there was a significant enhancement of radiosensitization.

3.4 DISCUSSION

We have confirmed a synthetic lethal relationship between PTEN and the DNA repair protein PNKP following our initial screen (Mereniuk et al, 2012). PTEN is the second most frequently compromised tumour suppressor. The gene is located on chromosome 10q23, and its down

A

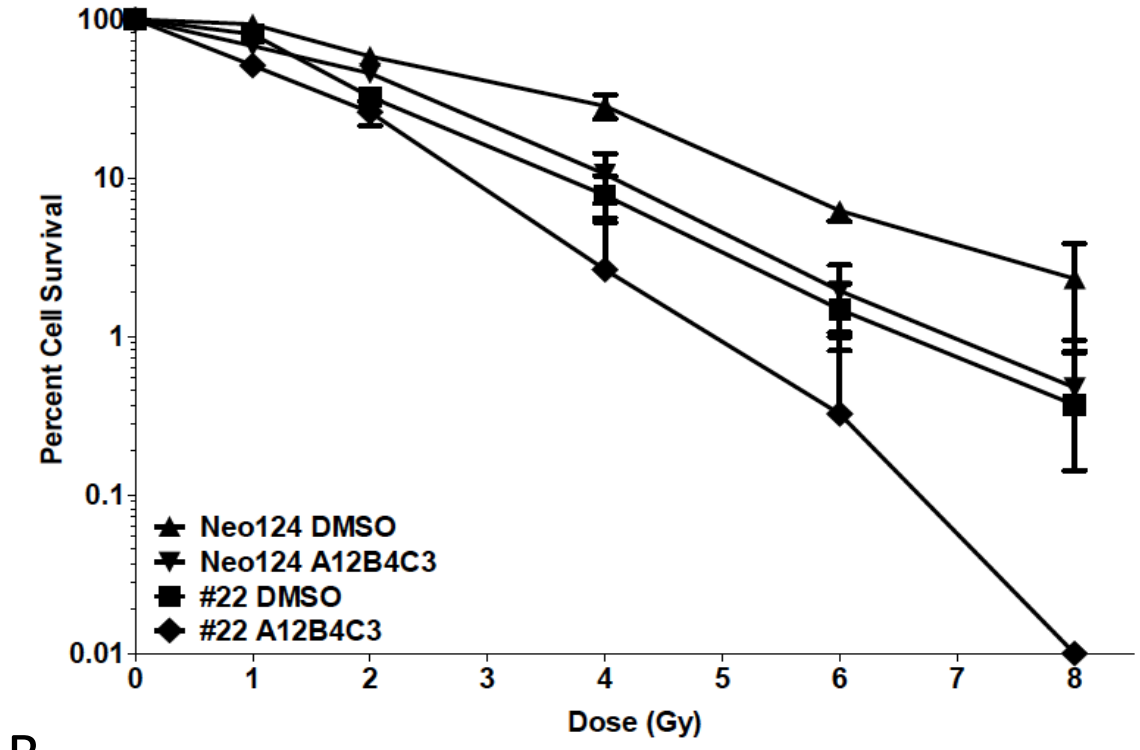
100
10
1
0.1
0.01
Percent Cell Survival
0
1
2
3
4
5
6
7
8
Dose (Gy)
Neo124 DMSO
Neo124 A12B4C3
#22 DMSO
#22 A12B4C3

B

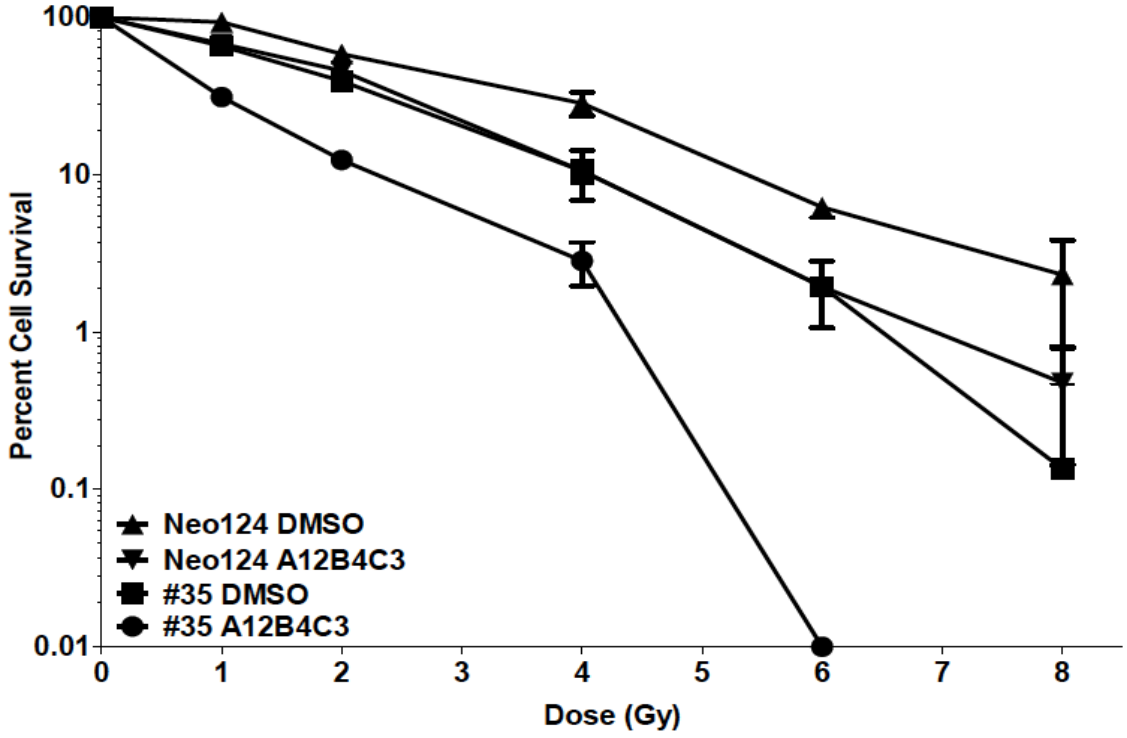
100
10
1
0.1
0.01
Percent Cell Survival
0
1
2
3
4
5
6
7
8
Dose (Gy)
Neo124 DMSO
Neo124 A12B4C3
#35 DMSO
#35 A12B4C3

Figure 3.7. Utilization of synthetic sickness as a possible therapeutic paradigm. (A) Vector only control HCT116 cells (Neo124), and HCT116 PTEN knockout strains #22 (A) and #35 (B) were grown in the presence of the PNKP inhibitor A12B4C3 (2 μM) or DMSO vehicle for 24 h and then subjected to increasing doses of γ-radiation and further incubated in the presence of A12B4C3. Survival was measured using the colony-forming assay. Inhibition of PNKP and loss of PTEN alone modestly sensitized the cells to radiation, but a more marked radiosensitization was observed when the PTEN knockout cells were irradiated and further incubated in the presence of A12B4C3. Error bars represent standard error (± S.E.) from at least three independent determinations, each experiment was done in triplicate for a minimum of nine total assessed plates.

(Simpson & Parsons, 2001; Yin & Shen, 2008). Specifically, PTEN mutations occur most frequently in four cancer types: glioblastoma, regulation or complete loss is implicated in the development and/or progression of many sporadic human cancers endometrial, melanoma and prostate at 28.8%, 34.6%, 12.1% and 11.8% respectively (Yin & Shen, 2008). PTEN-deficient tumours thus represent an excellent target for synthetic lethal approaches to treatment. Other synthetic lethal partners of PTEN have been discovered including PARP (Mendes-Pereira et al, 2009), and more recently the TTK protein tyrosine kinase (Brough et al, 2011b). Interestingly, TTK was also identified in our initial screen of synthetic lethal partners of PNKP (Mereniuk et al, 2012).

PTEN plays a critical role as an antagonist of the phosphoinositide 3-kinase (PI3K) pathway in the cytoplasm through its lipid phosphatase function by dephosphorylating the 3 position of the second messenger phosphatidylinositol 3,4,5-triphosphate (PIP3) to form inactive phosphatidylinositol 4,5-bisphosphate (PIP2), thereby suppressing downstream signaling events, including those involving phosphoinositide-dependent kinase-1 (PDK1) and the serine/threonine kinase Akt (Carracedo et al, 2011; Mounir et al, 2009; Myers et al, 1997; Raftopoulou et al, 2004; Tamura et al, 1998; Wong et al, 2010; Zhang & Yu, 2010). When PTEN is deficient, there is an accumulation of PIP3, which activates downstream signaling molecules such as the Akt and mTOR complex 1. In addition to its cytoplasmic roles, PTEN also localizes to the nucleus in a

cell cycle dependent manner with higher levels seen in G0/G1 (Ginn-Pease & Eng, 2003). In the nucleus, the protein phosphatase activity of PTEN regulates MAPK phosphorylation and cyclin D1 (Weng et al, 2002; Weng et al, 2001) and progression of the cell cycle. Several studies have also linked PTEN to genomic stability and homologous recombination primarily via expression of *RAD51* (McEllin et al, 2010; Mendes-Pereira et al, 2009; Mukherjee & Karmakar, 2012; Shen et al, 2007), although this is an issue of some debate (Fraser et al, 2012; Hunt et al, 2012).

The synthetic lethality manifested by the treatment of PTEN-deficient tumour cells with PARP inhibitors has been ascribed to a reduction in RAD51 levels and homologous recombination coupled with incomplete single-strand break repair (Mendes-Pereira et al, 2009). In contrast, the synthetic lethality we observed between PTEN and PNKP could not be alleviated by ectopic expression of *RAD51* (Fig. 3.6A). Furthermore, unlike the response to PARP inhibition, resistance to PNKP inhibition was restored by expression of the phosphatase active and cytoplasmically-restricted PTEN K289E protein, but not the catalytically inactive C124S protein that can enter the nucleus. Therefore, the function of PTEN that is critical for survival under PNKP disruption most likely lies in its cytoplasmic function as a lipid phosphatase in signal transduction pathways. These clear differences between the responses to RAD51 and PTEN isoforms indicate that distinct mechanisms underlie the synthetic lethal pathways

between PTEN and PARP and between PTEN and PNKP despite the fact that both PARP and PNKP play significant roles in DNA strand break repair.

From a clinical standpoint the use of a repair protein inhibitor in a synthetic sickness approach offers two advantages - either augmenting cell killing for a given dose of the primary genotoxic anticancer agent, or allowing the use of a lower dose of the primary agent to achieve the same level of cancer cell killing but reducing the likelihood of normal tissue damage. The potential of such an approach was shown by the significant increase in radiosensitization afforded by co-treatment with the PNKP inhibitor. This provides a possible therapeutic modality in which PTEN negative tumours would first be sensitized by inhibition of PNKP and then targeted by focused radiation. Since PNKP disruption is well tolerated by PTEN proficient cells (i.e. normal cells), there would be little damage to normal tissues, and thus side effects should be minimized.

3.5 REFERENCES

Allinson SL (2010) DNA end-processing enzyme polynucleotide kinase as a potential target in the treatment of cancer. *Future Oncol* **6:** 1031-1042

Brough R, Frankum JR, Costa-Cabral S, Lord CJ, Ashworth A (2011a) Searching for synthetic lethality in cancer. *Curr Opin Genet Dev* **21:** 34-41

Brough R, Frankum JR, Sims D, Mackay A, Mendes-Pereira AM, Bajrami I, Costa-Cabral S, Rafiq R, Ahmad AS, Cerone MA, Natrajan R, Sharpe R, Shiu KK, Wetterskog D, Dedes KJ, Lambros MB, Rawjee T, Linardopoulos S, Reis-Filho JS, Turner NC, Lord CJ, Ashworth A (2011b) Functional Viability Profiles of Breast Cancer. *Cancer Discov* **1:** 260-273

Bryant HE, Helleday T (2006) Inhibition of poly (ADP-ribose) polymerase activates ATM which is required for subsequent homologous recombination repair. *Nucleic Acids Res* **34:** 1685-1691

Bryant HE, Schultz N, Thomas HD, Parker KM, Flower D, Lopez E, Kyle S, Meuth M, Curtin NJ, Helleday T (2005) Specific killing of BRCA2-deficient tumours with inhibitors of poly(ADP-ribose) polymerase. *Nature* **434:** 913-917

Carracedo A, Alimonti A, Pandolfi PP (2011) PTEN level in tumour suppression: how much is too little? *Cancer Res* **71:** 629-633

Chalmers AJ, Lakshman M, Chan N, Bristow RG (2010) Poly(ADP-ribose) polymerase inhibition as a model for synthetic lethality in developing radiation oncology targets. *Semin Radiat Oncol* **20:** 274-281

Chan DA, Giaccia AJ (2011) Harnessing synthetic lethal interactions in anticancer drug discovery. *Nat Rev Drug Discov* **10:** 351-364

Comen EA, Robson M (2010) Poly(ADP-ribose) polymerase inhibitors in triple-negative breast cancer. *Cancer J* **16:** 48-52

Farmer H, McCabe N, Lord CJ, Tutt AN, Johnson DA, Richardson TB, Santarosa M, Dillon KJ, Hickson I, Knights C, Martin NM, Jackson SP, Smith GC, Ashworth A (2005) Targeting the DNA repair defect in BRCA mutant cells as a therapeutic strategy. *Nature* **434:** 917-921

Fraser M, Zhao H, Luoto KR, Lundin C, Coackley C, Chan N, Joshua AM, Bismar TA, Evans A, Helleday T, Bristow RG (2012) PTEN deletion in prostate cancer cells does not associate with loss of RAD51 function:

implications for radiotherapy and chemotherapy. *Clin Cancer Res* **18:** 1015-1027

Freschauf GK, Karimi-Busheri F, Ulaczyk-Lesanko A, Mereniuk TR, Ahrens A, Koshy JM, Rasouli-Nia A, Pasarj P, Holmes CF, Rininsland F, Hall DG, Weinfeld M (2009) Identification of a small molecule inhibitor of the human DNA repair enzyme polynucleotide kinase/phosphatase. *Cancer Res* **69:** 7739-7746

Freschauf GK, Mani RS, Mereniuk TR, Fanta M, Virgen CA, Dianov GL, Grassot JM, Hall DG, Weinfeld M (2010) Mechanism of action of an imidopiperidine inhibitor of human polynucleotide kinase/phosphatase. *J Biol Chem* **285:** 2351-2360

Gartner EM, Burger AM, Lorusso PM (2010) Poly(adp-ribose) polymerase inhibitors: a novel drug class with a promising future. *Cancer J* **16:** 83-90

Ginn-Pease ME, Eng C (2003) Increased nuclear phosphatase and tensin homologue deleted on chromosome 10 is associated with G0-G1 in MCF-7 cells. *Cancer Res* **63:** 282-286

Hartwell LH, Szankasi P, Roberts CJ, Murray AW, Friend SH (1997) Integrating genetic approaches into the discovery of anticancer drugs. *Science* **278:** 1064-1068

Hunt CR, Gupta A, Horikoshi N, Pandita TK (2012) Does PTEN loss impair DNA double-strand break repair by homologous recombination? *Clin Cancer Res* **18:** 920-922

Jilani A, Ramotar D, Slack C, Ong C, Yang XM, Scherer SW, Lasko DD (1999) Molecular cloning of the human gene, PNKP, encoding a polynucleotide kinase 3'-phosphatase and evidence for its role in repair of DNA strand breaks caused by oxidative damage. *J Biol Chem* **274:** 24176-24186

Kaelin WG, Jr. (2005) The concept of synthetic lethality in the context of anticancer therapy. *Nat Rev Cancer* **5:** 689-698

Karimi-Busheri F, Daly G, Robins P, Canas B, Pappin DJ, Sgouros J, Miller GG, Fakhrai H, Davis EM, Le Beau MM, Weinfeld M (1999) Molecular characterization of a human DNA kinase. *J Biol Chem* **274:** 24187-24194

Lee C, Kim JS, Waldman T (2004) PTEN gene targeting reveals a radiation-induced size checkpoint in human cancer cells. *Cancer Res* **64:** 6906-6914

Martin SA, McCabe N, Mullarkey M, Cummins R, Burgess DJ, Nakabeppu Y, Oka S, Kay E, Lord CJ, Ashworth A (2010) DNA polymerases as potential therapeutic targets for cancers deficient in the DNA mismatch repair proteins MSH2 or MLH1. *Cancer Cell* **17:** 235-248

McEllin B, Camacho CV, Mukherjee B, Hahm B, Tomimatsu N, Bachoo RM, Burma S (2010) PTEN loss compromises homologous recombination repair in astrocytes: implications for glioblastoma therapy with temozolomide or poly(ADP-ribose) polymerase inhibitors. *Cancer Res* **70:** 5457-5464

Mendes-Pereira AM, Martin SA, Brough R, McCarthy A, Taylor JR, Kim JS, Waldman T, Lord CJ, Ashworth A (2009) Synthetic lethal targeting of PTEN mutant cells with PARP inhibitors. *EMBO Mol Med* **1:** 315-322

Mereniuk TR, Maranchuk RA, Schindler A, Penner JC, Freschauf GK, Hegazy SA, Lai R, Foley E, Weinfeld M (2012) Genetic screening for synthetic lethal partners of polynucleotide kinase/phosphatase: potential for targeting SHP-1 depleted cancers. *Cancer Research* **Submitted**

Mounir Z, Krishnamoorthy JL, Robertson GP, Scheuner D, Kaufman RJ, Georgescu MM, Koromilas AE (2009) Tumour suppression by PTEN requires the activation of the PKR-eIF2alpha phosphorylation pathway. *Sci Signal* **2:** ra85

Mukherjee A, Karmakar P (2012) Attenuation of PTEN perturbs genomic stability via activation of Akt and down-regulation of Rad51 in human embryonic kidney cells. *Mol Carcinog*

Myers MP, Stolarov JP, Eng C, Li J, Wang SI, Wigler MH, Parsons R, Tonks NK (1997) P-TEN, the tumour suppressor from human chromosome 10q23, is a dual-specificity phosphatase. *Proc Natl Acad Sci U S A* **94:** 9052-9057

Raftopoulou M, Etienne-Manneville S, Self A, Nicholls S, Hall A (2004) Regulation of cell migration by the C2 domain of the tumour suppressor PTEN. *Science* **303:** 1179-1181

Rasouli-Nia A, Karimi-Busheri F, Weinfeld M (2004) Stable down-regulation of human polynucleotide kinase enhances spontaneous mutation frequency and sensitizes cells to genotoxic agents. *Proc Natl Acad Sci U S A* **101:** 6905-6910

Reinhardt HC, Jiang H, Hemann MT, Yaffe MB (2009) Exploiting synthetic lethal interactions for targeted cancer therapy. *Cell Cycle* **8:** 3112-3119

Schindler A, Foley E (2010) A functional RNAi screen identifies hexokinase 1 as a modifier of type II apoptosis. *Cell Signal* **22:** 1330-1340

Shen WH, Balajee AS, Wang J, Wu H, Eng C, Pandolfi PP, Yin Y (2007) Essential role for nuclear PTEN in maintaining chromosomal integrity. *Cell* **128:** 157-170

Simpson L, Parsons R (2001) PTEN: life as a tumour suppressor. *Exp Cell Res* **264:** 29-41

Tamura M, Gu J, Matsumoto K, Aota S, Parsons R, Yamada KM (1998) Inhibition of cell migration, spreading, and focal adhesions by tumour suppressor PTEN. *Science* **280:** 1614-1617

Weinfeld M, Mani RS, Abdou I, Aceytuno RD, Glover JN (2011) Tidying up loose ends: the role of polynucleotide kinase/phosphatase in DNA strand break repair. *Trends Biochem Sci*

Weng LP, Brown JL, Baker KM, Ostrowski MC, Eng C (2002) PTEN blocks insulin-mediated ETS-2 phosphorylation through MAP kinase, independently of the phosphoinositide 3-kinase pathway. *Hum Mol Genet* **11:** 1687-1696

Weng LP, Brown JL, Eng C (2001) PTEN coordinates G(1) arrest by down-regulating cyclin D1 via its protein phosphatase activity and up-regulating p27 via its lipid phosphatase activity in a breast cancer model. *Hum Mol Genet* **10:** 599-604

Wong KK, Engelman JA, Cantley LC (2010) Targeting the PI3K signaling pathway in cancer. *Curr Opin Genet Dev* **20:** 87-90

Yin Y, Shen WH (2008) PTEN: a new guardian of the genome. *Oncogene* **27:** 5443-5453

Zhang S, Yu D (2010) PI(3)king apart PTEN's role in cancer. *Clin Cancer Res* **16:** 4325-4330

Chapter 4: Polynucleotide kinase/phosphatase's function in double-strand break repair is important for synthetic lethal relationships

4.1 INTRODUCTION

Synthetic lethality has quickly become one of the most heavily investigated new therapeutic modalities due to its potential as a patient and cancer specific treatment (Aggarwal & Brosh, 2009; Canaani, 2009; Iglehart & Silver, 2009). Synthetic lethality is a condition in which the disruption of two or more non-essential genes/proteins in the same cell causes cell death, yet cells harbouring mutations in only one of these genes remain viable (Dobzhansky, 1946; Lucchesi, 1968). This is a particularly valuable phenomenon in cancer therapy as only the cancer cells contain mutations to a key gene, such as a tumour suppressor gene, so that disruption of a synthetic lethal partner will be toxic to these cells, whereas, normal tissues will only be singularly disrupted and thus remain viable.

To date, most synthetic lethal partnerships have been shown to occur between combinations of DNA repair genes (Bryant et al, 2005; Farmer et al, 2005). Most of the attention has been specifically focused on the partnerships between poly(ADP-ribose) polymerase 1 (PARP1), a single-strand break repair (SSBR) protein, and proteins involved in double-strand break repair (DSBR) (Liang et al, 2009; O'Connor et al, 2007; Williamson et al). For example, in 2005, the Ashworth and Helleday groups published back-to-back papers outlining a synthetic lethal association between PARP1 and the BRCA proteins, which are involved in the homologous recombination (HR) DSBR pathway (Bryant et al, 2005;

Farmer et al, 2005). This generated considerable excitement as it allowed specific targeting of cancer cells containing BRCA mutations while leaving normal cells ($BRCA^{+/+}$ and $BRCA^{+/-}$) unaffected. Since normal tissues are spared, adverse side effects typically associated with cancer therapy should be greatly reduced. This treatment paradigm has already entered clinical trials, for example the PARP1 inhibitor BSI-201 is currently in Phase III trials for patients with ER-, PR- and Her2- (or triple-) negative metastatic breast cancer (2009; Gartner et al, 2010; Pal & Mortimer, 2009), and shows great promise. Furthermore, the success of another PARP1 inhibitor, Olaparib (Dungey et al, 2009; Evers et al, 2010; Fong et al, 2009; O'Brien & Stokoe, 2009; Pal & Mortimer, 2009; Stefansson et al, 2009; Venkitaraman, 2009; Williamson et al; Zander et al), in the treatment of breast and ovarian cancers relied heavily on the synthetically lethal partnership between PARP1 and the BRCA proteins.

One of the interesting facets of synthetic lethality is that it occurs in the absence of exogenous DNA damaging agents and relies on the fact that the DNA of every human cell is subjected to continuous endogenous damage throughout our lives (Lindahl & Nyberg, 1972), primarily from attack by free-radicals produced by normal cellular metabolism (Breimer, 1991; Frenkel, 1992). It has been estimated that greater than 10,000 SSBs and approximately 10 DSBs are formed per cell per day. Normal tissues are equipped to deal with this attack on DNA through the use of SSBR and the two major DSBR pathways, HR and nonhomologous end-joining

(NHEJ). Even when SSBR is disrupted, the two remaining DSBR pathways are capable of handling the increase in the formation of DSBs in healthy cells. However, in cancers harbouring mutations in HR, the cells are not equipped to handle this increase in DSB formation and this forms the basis for the most commonly ascribed mechanism for synthetic lethality seen when both PARP and BRCA are disrupted in the same cells.

Briefly, cancer cells (DSBR-deficient) are treated with PARP inhibitors, preventing repair of naturally occurring SSBs. When these cells enter S-phase, the unrepaired SSBs are converted to DSBs due to replication fork collapse (Bolderson et al, 2009; O'Connor et al, 2007). Since the patient's normal cells ($BRCA^{+/-}$) still retain both HR and NHEJ function, they can repair this increase in DSBs and the cell remains unharmed (Bolderson et al, 2009; O'Connor et al, 2007). However, in the DSBR deficient cancer cells ($BRCA^{-/-}$) the inhibition of SSBR and subsequent increase in DSB formation is enough to saturate NHEJ, thereby allowing DSBs to evade repair. The result is the cytotoxic accumulation of DSBs in cancer cells, which eventually leads to specific cancer cell death.

Endogenous reactive oxygen species (ROS) can attack DNA in several ways including attack of the phosphodiester backbone itself to generate SSBs, attack of bases to cause base damage or the generation of apurinic/apyrimidinic (AP) sites (Parsons et al, 2005c; Rass et al, 2007). According to the current model of the base excision repair (BER) pathway,

damaged bases are excised by a DNA glycosylase at the N-glycosyl bond between the base and the deoxyribose sugar to form AP sites (Allinson et al, 2004; Das et al, 2006; Trivedi et al, 2008). The DNA backbone itself at the AP site is then cleaved by either an AP endonuclease to form 3' hydroxyl (3'OH) termini and 5' deoxyribose phosphate (5'dRP) termini, or by an AP lyase to form a 3' unsaturated aldehydic end group and a 5' phosphate (5'P) end group (Allinson et al, 2004; Caldecott, 2007; Caldecott, 2008; Das et al, 2006; Trivedi et al, 2008). The resulting SSB is then recognized by PARP, which catalyzes the formation of negatively charged poly(ADP-ribose) (PAR) residues upon itself, and serves as a flag for the recruitment of the scaffold protein, X-ray cross complementing protein 1 (XRCC1), an end-processing enzyme such as polynucleotide kinase/phosphatase (PNKP) or APTX, and DNA ligase III (Lig3), in a heterotrimeric complex to the strand break (Parsons et al, 2005b; Woodhouse & Dianov, 2008; Woodhouse et al, 2008). This complex is followed closely by DNA polymerase β (Polβ) (Caldecott, 2007; Caldecott et al, 1995; Dianov et al, 2003). The end-processing enzyme repairs any damaged DNA termini to the elongation and ligation competent 3' hydroxyl (3'OH) and 5'P groups (Bernstein et al, 2005; Caldecott, 2003; Date et al, 2004; Gueven et al, 2004; Mani et al, 2001; Moreira et al, 2001; Rasouli-Nia et al, 2004). Polβ then inserts missing nucleotides, and Lig3 seals the nick (Masaoka et al, 2009; Parsons et al, 2005a). The end-result is error-free repair of DNA (Friedberg, 2006).

Interestingly, PNKP also has function in DSBR, more specifically in NHEJ. NHEJ is an iterative DSBR pathway, which operates throughout the cell cycle, however, it is particularly important in G_0, G_1 and early S-phase when homology directed repair is not available (Hartlerode & Scully, 2009; Pastwa & Blasiak, 2003). Once a DSB is introduced into the DNA, the first step of NHEJ is the binding of the Ku70/Ku80 heterodimer to the broken DNA termini. These proteins act as scaffold proteins upon which the NHEJ repair complex is formed (Hartlerode & Scully, 2009; Iliakis, 2009; Pastwa & Blasiak, 2003). Next, the Ku70/Ku80 heterodimer moves inward along the DNA approximately 10 base pairs allowing space for the binding of DNA-dependent protein kinase catalytic subunit (DNA-PK_{cs}) on the DNA ends (Yoo & Dynan, 1999). DNA-PK_{cs} acts as a DNA end-bridging protein, keeping the two DNA ends in close proximity (Chen et al, 2000; DeFazio et al, 2002). DNA-PK_{cs} also becomes activated upon binding to the Ku70/80 heterodimer, activating its serine/threonine activity allowing phosphorylation of many substrates *in vivo*, including: itself, Ku70, Ku80, XRCC4, Cernunnos/XRCC4-like factor (XLF), Artemis and DNA ligase IV (Lig4) (Hartlerode & Scully, 2009; Yaneva et al, 1997). Regulatory phosphorylation on DNA-PK_{cs} and Artemis (Chan et al, 2002; Chen et al, 2005; Ma et al, 2005) activates the endonuclease function of Artemis allowing the formation of blunt, or near-blunt ended DNA ends, which is necessary for the final resolution of the DSB (Goodarzi et al, 2006). PNKP can then act on the damaged DNA termini to achieve elongation and

ligation competent 5'P and 3'OH groups, if necessary (Lieber, 2010). Finally, XRCC4 in complex with Lig4 can ligate the DNA together, resulting in error prone DNA repair as Artemis resects the DNA to achieve (near)-blunt ended DNA (Audebert et al, 2006; Ma et al, 2005; Yannone et al, 2008).

In 2008, Turner *et al.* found a synthetic lethal relationship between PNKP and PARP, providing the first evidence to our knowledge of synthetic lethality as it relates to DNA repair but not involving the BRCA proteins (Turner et al, 2008). This led us to attempt to identify whether PNKP can substitute for PARP in synthetic lethal associations relevant to cancer research and eventually led to us showing that there are other possible explanations for synthetic lethal relationships between proteins aside from the cytotoxic accumulation of DSBs through inhibition of both SSBR and DSBR (Mereniuk et al, 2012a). For example, the synthetic lethal partnership between PNKP and SHP-1 depends on the increase in ROS production through disruption of SHP-1 functioning and subsequent prevention of DNA repair through the interference of PNKP activity (Mereniuk et al, 2012a). Furthermore, we have also shown that the synthetic lethal relationship between PTEN and PNKP depends on the cytoplasmic, phosphatase function of PTEN, likely in the PI3K/Akt pathway where it plays a key role in the regulation of cell growth, the cell cycle and the apoptotic pathway (Cantley & Neel, 1999; Mendes-Pereira et al, 2009; Mereniuk et al, 2012b; Simpson & Parsons, 2001; Yin & Shen, 2008).

These results show that synthetic lethal relationships exist between proteins not directly involved in DNA repair, and that PNKP may be a valuable therapeutic target for clinical investigation into synthetic lethality.

Given the ability to target PNKP through small molecule inhibition (Freschauf et al, 2009), and our previous findings involving PNKP in synthetic lethal associations (Mereniuk et al, 2012a; Mereniuk et al, 2012b), we sought to determine the exact function of PNKP in synthetic lethal relationships. We address our hypothesis by using cells with key SSBR proteins inactivated and testing these cells using small molecule chemical inhibitors and siRNA techniques for synthetically lethal partnerships. We wish to pinpoint whether it is PNKP's role in SSBR or DSBR that is important for lethality, as well as determining which, if any, catalytic function of the bifunctional DNA repair protein PNKP is critical.

4.2 MATERIALS AND METHODS

4.2.1 Cell Lines

A549 (human lung carcinoma cells) were obtained from the American Type Culture Collection (Manassas, VA). The A549 cell line stably depleted of PNKP (A549δPNKP) was generated and cultured as described previously (Rasouli-Nia et al, 2004). A549 cells stably expressing a scrambled shRNA to no known gene target (A549-Scramble) were generated and cultured as described previously (Mereniuk et al, 2012a). A549 cells expressing a dominant negative to DNA Polymerase β

(PolβDN) and A549 vector only controls (A549-LZ) were obtained as a gift from Dr. Conchita Vens. M059J and M095K cell lines, which were generated from the same human glioblastoma and are deficient and not deficient in DNA-PK_{cs} activity, respectively, were obtained as a gift from Dr. Joan Turner (University of Alberta, Edmonton, AB). The Chinese hamster ovary cell line EM9 and its XRCC1-complemented variant H9T3-7-1 (Thompson et al, 1990) were obtained as a gift from Dr. Larry Thompson (Lawrence Livermore National Laboratory, Livermore, CA). All the cell lines were cultured at 37°C and 5% CO_2 in a humidified incubator in a 1:1 mixture of Dulbecco's Modified Eagle's Medium and F12 (DMEM/F12) supplemented with 10% fetal bovine serum (FBS), penicillin (50 U/mL), streptomycin (50 µg/mL), L-glutamine (2 mM), non-essential amino acids (0.1 mM) and sodium pyruvate (1 mM). All culture supplements were purchased from Invitrogen (Carlsbad, CA).

4.2.2 Inhibitors

PNKP inhibitor (A12B4C3) was generated as described previously (Freschauf et al, 2009), and was diluted to a stock concentration of 1 mM in DMSO. DPQ (3,4-Dihydro-5[4-(1-piperindinyl)butoxy]-1(2H)-isoquinoline) was purchased from Calbiochem and diluted to a stock concentration of 1 mM in DMSO.

4.2.3 RNAi

pSUPER.neo vectors expressing shRNA targeting PNKP or no known gene target (scrambled shRNA) were purchased from OligoEngine (Seattle, WA) and were stably transfected into A549 cells as described previously (Mereniuk et al, 2012a; Rasouli-Nia et al, 2004). AllStars Negative, PARP, and DNA Polβ siRNAs were purchased from Qiagen (Mississauga, ON), and PNKP siRNA was purchased from Ambion (Invitrogen) and were diluted to a 20 μM stock solution in TE buffer.

4.2.4 Stable transfection

20,000 A549 cells were plated overnight in a 24-well dish at 37°C and 5% CO_2. 1 μg of plasmid DNA was then incubated in 50 μL total of Opti-MEM at the same time as 3 μL of Lipofectamine2000 was incubated in 50 μL total Opti-MEM at room temperature for 5 min. The plasmid DNA solution was then combined with the Lipofectamine2000 solution and incubated at room temperature for 20 min. The media from the pre-plated A549 cells was then removed and the transfection complexes were added and the cells incubated for 24 h at 37°C and 5% CO_2. The next day, the cells were trypsinized and transferred into 5 x 100-mm plates in DMEM/F12 without antibiotics and incubated overnight at 37°C and 5% CO_2. The following day, the media was removed and replaced with DMEM/F12 containing 650 μg/mL G418. Single-clone colonies, which were allowed to form over 10-18 days, were then picked and seeded into 24-well

plates. Cells populations were allowed to expand until there were enough cells to make cell lysate as described above.

4.2.5 Transient transfections

2500-4000 cells were plated per well in a 96-well plate, and allowed 24 h to adhere in a humidified incubator at 37°C and 5% CO_2. All wells surrounding samples were filled with 100 µL ddH_20 to guard against evaporation effects. 20 nM final concentration of siRNA was added to Opti-MEM at the same time as 1:25 dilution of Dharmafect Transfection 1 or Lipofectamine2000 and maintained at room temperature for 5 min. The two solutions were then combined and transfection complexes were allowed to form at room temperature for 20 min. The media was then removed from the cells and 100 µL of the transfection complexes was added per well and the plate was incubated at 37°C and 5% CO_2 for 72 h. Cells were then expanded and either used to make whole cell lysate for Western blots, or used in the proliferation assay as described below.

4.2.6 Proliferation Assay

2500-3500 cells were plated per well in a 96-well dish with all wells surrounding samples filled with 100 µL ddH_20 and kept in a humidified incubator at 37°C and 5% CO_2 for 24 h. Drugs were added to the cells in DMEM/F12 and siRNA complexes were added to cells in DMEM/F12 without penicillin and streptomycin. The cells were then incubated in the

presence of the drug or siRNA for a total of 72 h at 37°C and 5% CO_2. After incubation, 10% v/v of 440 µM Alamar Blue (Sigma-Aldrich, Oakville, ON) was added to each well and the cells were incubated for 50-90 min, after which the fluorescence in each well was determined using an EnVision 2104 Multilabel Reader (PerkinElmer) with an excitation wavelength of 563 nm and emission wavelength of 587 nm.

4.2.7 Colony Forming Assay

The effect on cell survival of simultaneous inhibition of two DNA repair proteins was measured using the clonogenic survival assay. To allow attachment, cells were seeded on a 60-mm dish 24 hours before addition of drug or siRNA. Cells were seeded at different densities to achieve 100-1000 colonies per plate after treatment. Drug or siRNA were then added to the plates, which were then returned to the incubator for 9-14 days. Colonies were then stained with crystal violet and counted using an automated Colcount colony counter (Oxford Optronix, Oxford, UK).

4.2.8 Western Blotting

Approximately 8 x 10^5 cells were washed twice with ice cold PBS and resuspended in CHAPS buffer (0.5% CHAPS, 137 mM NaCl, 50 mM Tris-HCl pH 7.5, and 1 mM EDTA). Cells were then rocked for 1 h at 4°C, after which cell debris was spun down at 600 *g* for 20 minutes at 4°C. Determination of whole cell lysate protein concentration was then

performed using the Bradford Assay. 50 µg of protein was added to 1 x sample buffer and boiled for 5 min. Samples were then separated by 10% SDS-PAGE (200V for 50 minutes at room temperature) and transferred to a nitrocellulose membrane by wet transfer (100V for 1 hour at 4°C). Membranes were then blocked in 5% PBSMT for 1 h at room temperature. Monoclonal primary antibodies were incubated with the membrane at a 1:2500 dilution in 5% PBSMT overnight at 4°C. Polyclonal primary antibodies were incubated at a 1:5000 dilution in 5% PBSMT overnight at 4°C. Membranes then underwent 5 x 10 min washes in PBST before being incubated with the appropriate HRP-conjugated secondary antibody at a 1:5000 dilution in 5% PBSMT for 30 min at room temperature. Membranes were then washed 6 x 5 min in PBST and incubated with 2 mL total of Lumi-Light Western Blotting substrate (Roche, Mississauga, ON) for 5 min before autoradiography.

4.3 RESULTS

4.3.1 Synthetic lethality status between PNKP and proteins involved in SSBR

We have previously found that PNKP may be an effective alternative to PARP1 in deriving potentially therapeutic synthetic lethal partnerships (Mereniuk et al, 2012a; Mereniuk et al, 2012b). We sought to identify the important repair function of PNKP in these synthetic lethal relationships initially by investigating the synthetic lethal status of PNKP

with other SSBR proteins. We performed cell proliferation assays in which cells were continuously exposed to inhibitors or siRNA for 72 h, which allowed for at least two cell cycles to occur. After each treatment was completed, cell survival was determined by an Alamar Blue-based fluorescence assay (Schindler & Foley, 2010). We found that when shRNA-mediated PNKP-depleted A549 human lung carcinoma (A549δPNKP) cells were treated with the PARP inhibitor (3,4-Dihydro-5[4-(1-piperindinyl)butoxy]-1(2H)-isoquinoline) (DPQ) (Mizuguchi et al, 2011) (Fig. 4.1), there was a dose-dependent increase in lethality in agreement with previous data (Turner et al, 2008). Conversely, when the same concentrations of PARP1 inhibitor were applied to A549 cells expressing a scrambled shRNA (A549-Scramble), no such increase in lethality was observed. This indicated the sensitivity of these cells to DPQ was dependent on PNKP depletion and not the activation of the RNAi machinery. This immediately suggested that the important role of PNKP in synthetic lethal relationships lies in its participation in DSBR. If the SSBR functions of PNKP were important for synthetic lethality, co-disruption with PARP would show no effect as the two major DNA repair pathways remain active (NHEJ and HR), and would be able to compensate for the increase in DSB formation. If this were true, however, disruption of other critical SSBR proteins should be synthetic lethal when PNKP activity is silenced.

To test this hypothesis, we selected another SSBR protein, XRCC1, to determine if it has a synthetic lethal partnership with PNKP. The

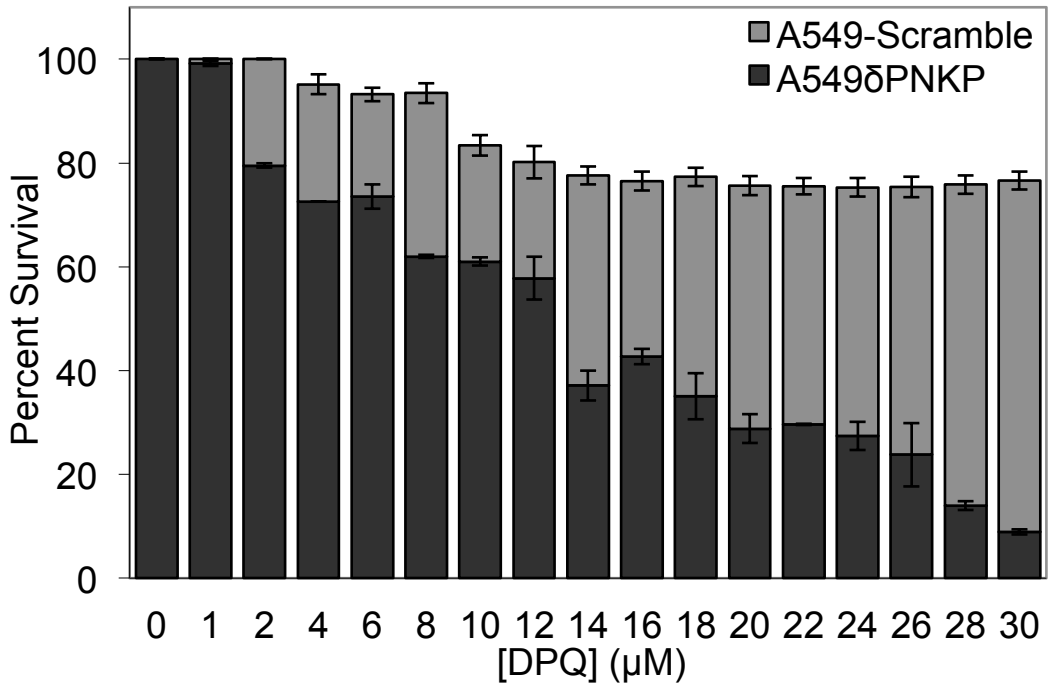

Figure 4.1. Synthetic lethality between DNA SSBR proteins PARP and PNKP. The proliferation assay was performed using cells stably depleted of PNKP (A549δPNKP) and cells stably expressing a scrambled shRNA (A549-Scramble). The darker bars represent the mean survival of A549δPNKP cells when treated with increasing concentrations of DPQ. The lighter bars denote the average survival of A549-Scramble control cells when treated with the same concentrations of DPQ. Significant cytotoxicity is observed only when both PNKP and PARP are co-disrupted, indicating that this is a true synthetic lethal relationship. Error bars represent standard error (±S.E.) from at least three independent experiments.

XRCC1-deficient EM9 Chinese hamster ovary cell line and its XRCC1-complemented derivative H9T3-7-1 were subjected to increasing concentrations of both PARP and PNKP inhibitors (Freschauf et al, 2009; Mizuguchi et al, 2011) (Figs. 4.2A and 4.2B, respectively). We found that increasing the concentration of DPQ elicited no corresponding increase in lethality. Counter to our expectations, we also observed no significant lethality following treatment with A12B4C3 in either the XRCC1 positive or negative cells. One possible explanation for the failure of the PNKP inhibitor to induce a toxic response in EM9 cells may lie in the observation that XRCC1 is dispensable for SSBR in human cells. XRCC1-deficient human cells can still undergo repair of SSBs, albeit at a retarded rate compared to XRCC1-proficient cells, so long as cell cycle checkpoints remain intact (Brem & Hall, 2005).

We therefore tested if another key SSBR protein, Polβ, possesses a synthetic lethal partnership with PNKP. We obtained a Polβ-dominant negative (PolβDN) variant of the A549 cell line, in which the DNA binding domain of Polβ, but not its catalytic domain, is over-expressed (Vens et al, 2002). When this cell line and its vector-only control (A549-LZ) were exposed to increasing concentrations of A12B4C3, we discovered that Polβ and PNKP do indeed show a synthetic lethal relationship (Fig. 4.3A). In line with this finding we were unable to generate a variant of the PolβDN cell line in which PNKP is stably knocked down by shRNA (data not shown). However, since the A549 PolβDN cell line employs a dominant

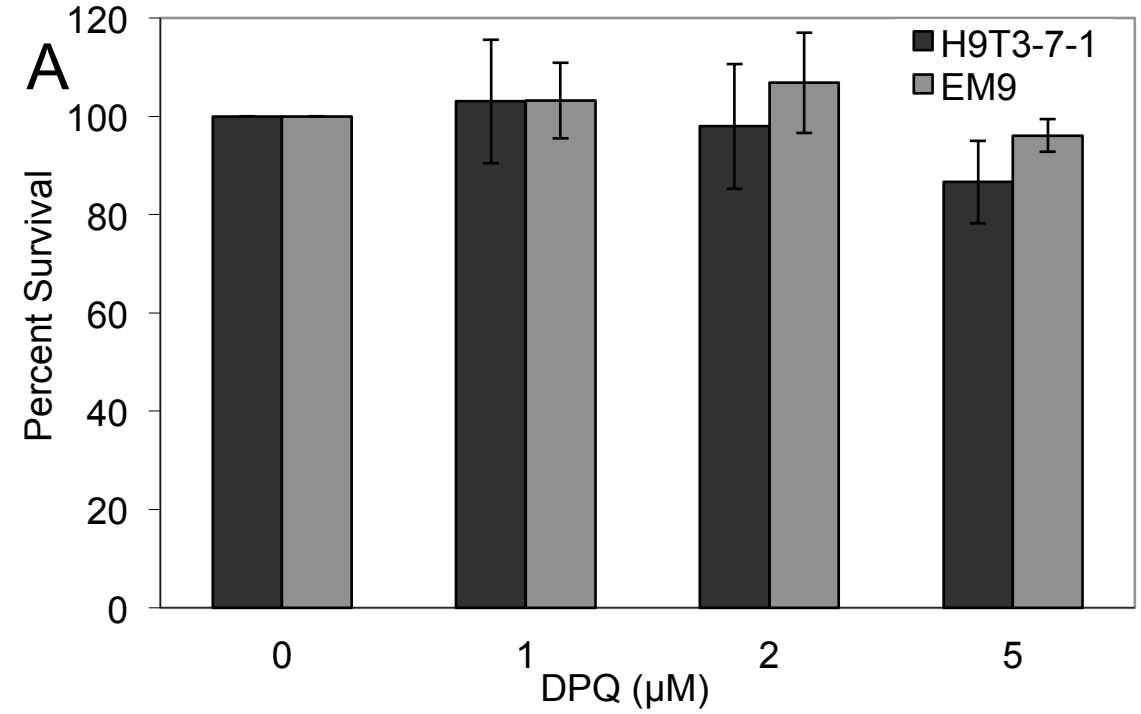
A
120
100
80
60
40
20
0
Percent Survival
H9T3-7-1
EM9
0
1
2
5
DPQ (μM)

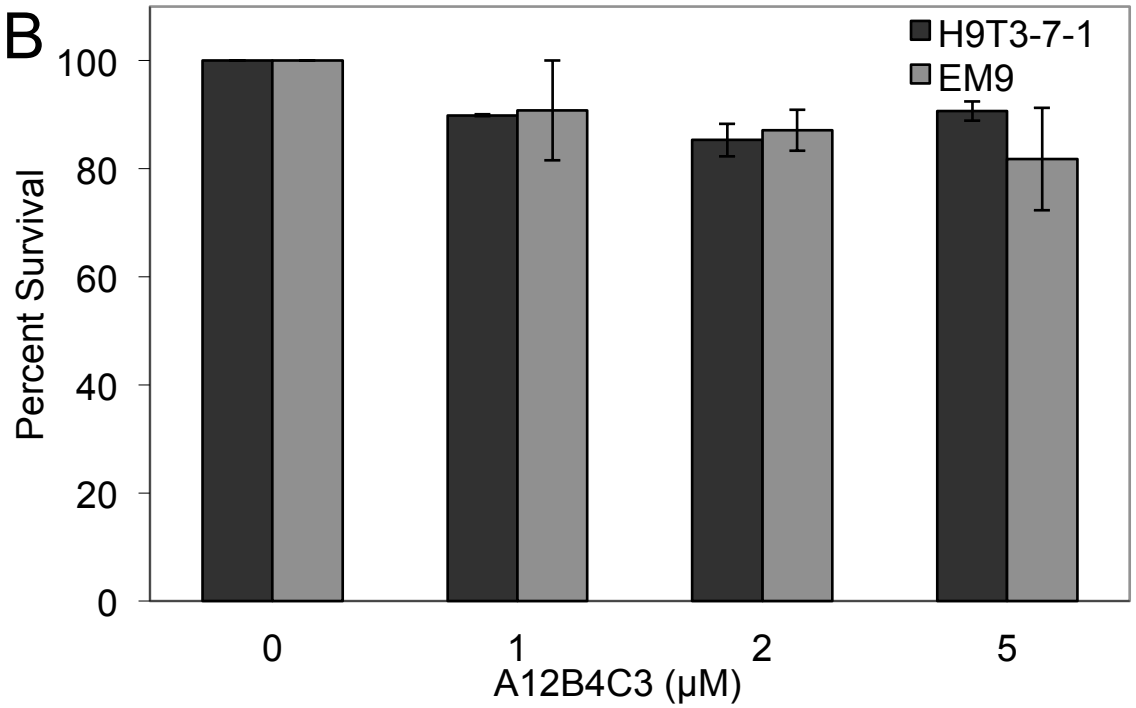
B
100
80
60
40
20
0
Percent Survival
H9T3-7-1
EM9
0
1
2
5
A12B4C3 (μM)

Figure 4.2. XRCC1-deficient hamster cells are resistant to inhibition of PARP1 and PNKP. (A) EM9 cells (lacking XRCC1) and H9T3-7-1 cells (EM9 cells expressing XRCC1) were treated with increasing concentrations of DPQ. At the concentrations tested the PARP1 inhibitor elicited little toxicity and there was no difference between the two cell lines. (B) A similar response was observed following treatment of the two cell lines with the PNKP inhibitor A12B4C3, implying that there is not a synthetic lethal association between XRCC1 and PNKP. Error bars represent standard error (±S.E.) from at least three independent experiments.

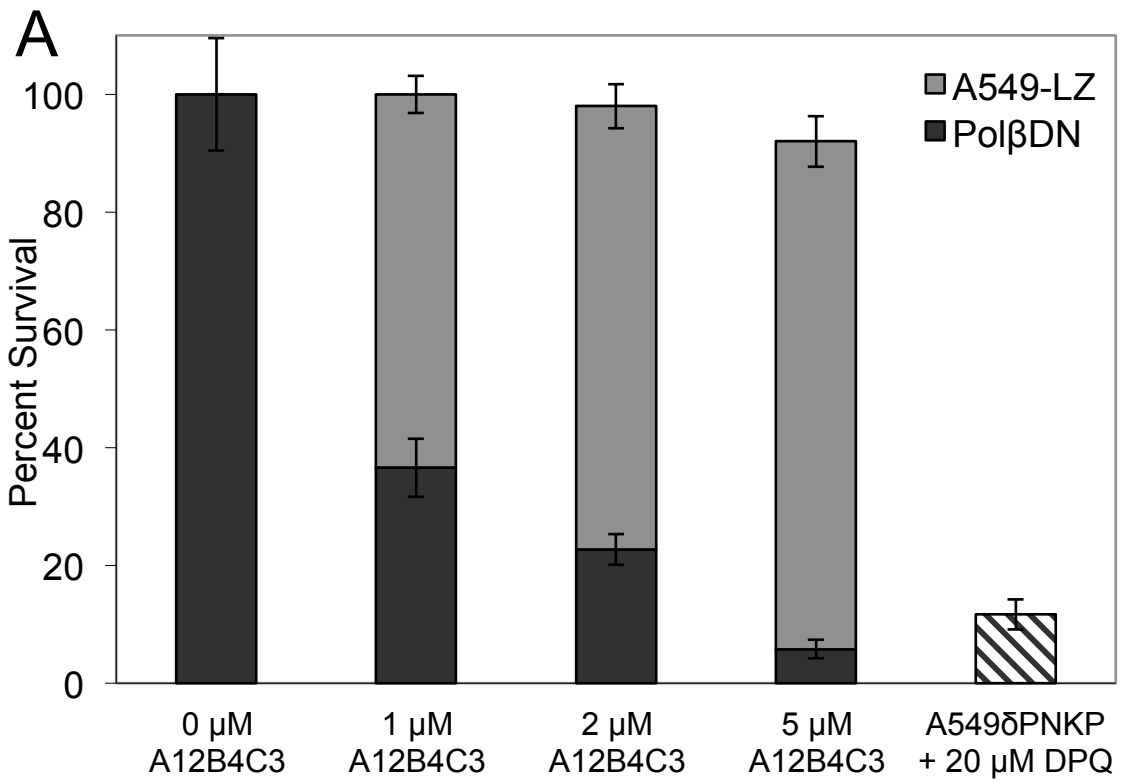
A
Percent Survival
100
80
60
40
20
0
A549-LZ
PolβDN
0 μM A12B4C3
1 μM A12B4C3
2 μM A12B4C3
5 μM A12B4C3
A549δPNKP + 20 μM DPQ

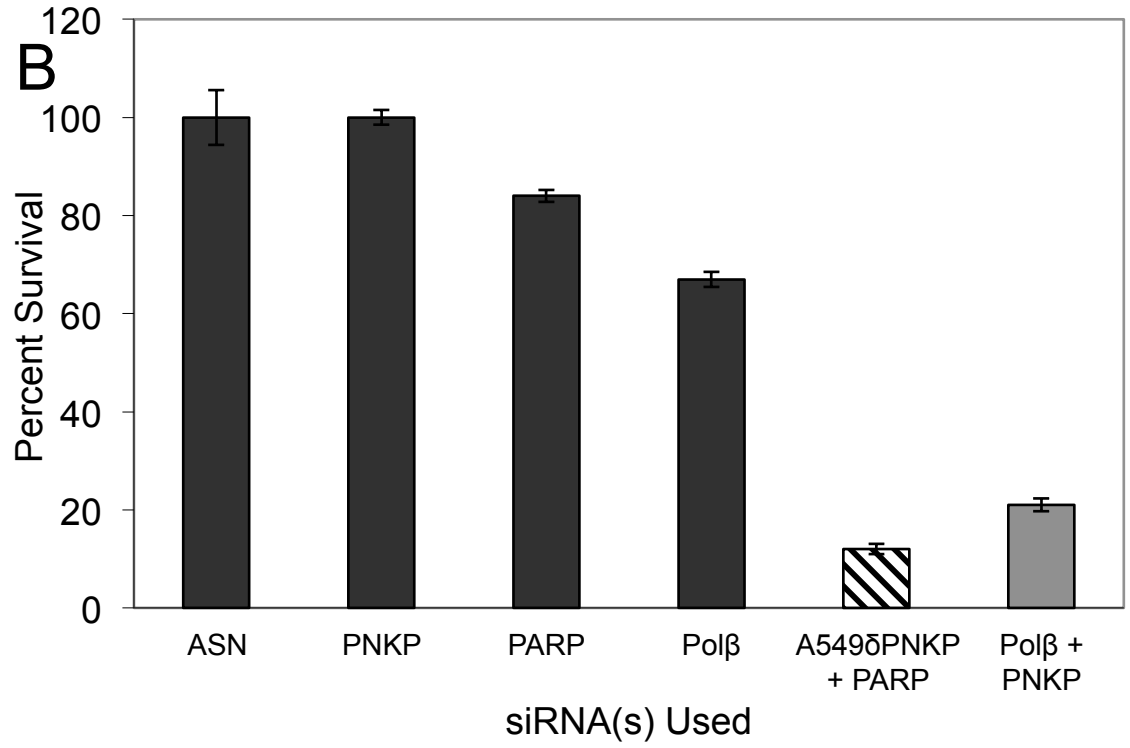
B
Percent Survival
120
100
80
60
40
20
0
ASN
PNKP
PARP
Polβ
A549δPNKP + PARP
Polβ + PNKP
siRNA(s) Used

Figure 4.3. Synthetic lethality between PNKP and DNA polymerase β. (A) A proliferation assay was performed using an A549-based cell line expressing a dominant negative form of Polβ (PolβDN) and a vector control cell line (A549-LZ). The darker bars show the survival of PolβDN cells in response to PNKP inhibition by A12B4C3 whereas the lighter bars show the survival of the vector control cells under the same conditions. For a comparison the known synthetic lethal combination of PNKP and PARP is shown on the far right with a striped bar. Error bars represent standard error (±S.E.) from at least three independent experiments. The results indicate a synthetic lethal relationship between PNKP and Polβ. (B) To verify the PNKP/Polβ synthetic lethal relationship we performed another proliferation assay involving co-transfection with siRNAs to both PNKP and Polβ. The dark bars represent the control transfections as well as the single protein knockdowns. The striped bar represents the known synthetic lethal association between PNKP and PARP, shown for comparison. The lighter bar on the far right shows the double knockdown of both PNKP and Polβ. Error bars represent standard error (±S.E.) from at least three independent experiments.

negative approach, it is possible that blocking access of other key DNA repair proteins to the strand break by the Polb fragment produces a different result to simply reducing the cellular level of Polb. To address this issue, we tested a double siRNA-mediated knockdown of PNKP and Polβ in A549 parental cells. Cells were continuously treated with the siRNA complexes in a forward transfection protocol for 72 h, after which an Alamar Blue-based reduction assay (Schindler & Foley, 2010) was performed to quantify cell survival. Synthetic lethality between Polβ and PNKP is still seen (Fig. 4.3B), suggesting that the removal of Polβ catalytic activity or of the protein itself is essential for lethality under PNKP disruption. Prevention of access to DNA damage by other DNA repair proteins by the dominant negative fragment of Polβ does not seem to be the cause of lethality under PNKP disruption, implying that it is a true synthetic lethal association that exists between Polβ and PNKP. This finding also provides evidence to support our hypothesis that PNKP's function in DSBR is important in synthetic lethal partnerships.

4.3.2 Non-lethality upon co-disruption of DNA-PK$_{cs}$ and PNKP

The function of PNKP in DSBR is more specifically attributed to NHEJ. NHEJ is an error-prone DSBR pathway active throughout the cell cycle that opts to link highly cytotoxic broken chromosomes together, rather than waiting until late-S/G2 phase when HR can take place, resulting in the possible deletion of several nucleotides at site of the strand

breaks (Chan et al, 2002; Chen et al, 2000; DeFazio et al, 2002; Hartlerode & Scully, 2009; Lieber, 2010; Pastwa & Blasiak, 2003). Since our data pointed to a DSBR roll for PNKP in synthetic lethality, it was important to see if PNKP holds synthetic lethal relationships with major proteins involved in NHEJ. To investigate this, we tested the sensitivity of M059J (DNA-$PK_{cs}^{-/-}$) glioblastoma cells to A12B4C3 and observed that inhibition of PNKP in M059J cells did not have a toxic effect (Fig. 4.4A). This also agrees with previous data in which a stable PNKP knockdown was established in M059J cells (Karimi-Busheri et al, 2007). This would be expected if PNKP's function in NHEJ is critical for synthetic lethality, since knocking out both PNKP and DNA-PK_{cs} would lead to the disruption of the same DNA repair pathway. Alternatively, it is possible that double knockout of SSBR and NHEJ is not lethal in general, and that HR can compensate for the increase in DSB production in the absence of these two repair pathways. To examine whether this is true or not, we tested the response of M059J and M059K (isolated from the same glioblastoma as M059J but DNA-$PK_{cs}^{+/+}$) cells to PARP inhibition. In this way we would be simultaneously knocking out both SSBR and NHEJ, leaving only HR functional. We found that HR alone could not compensate for this increase in DSBs and the cells eventually accumulated a cytotoxic level of DSBs (Fig. 4.4B).

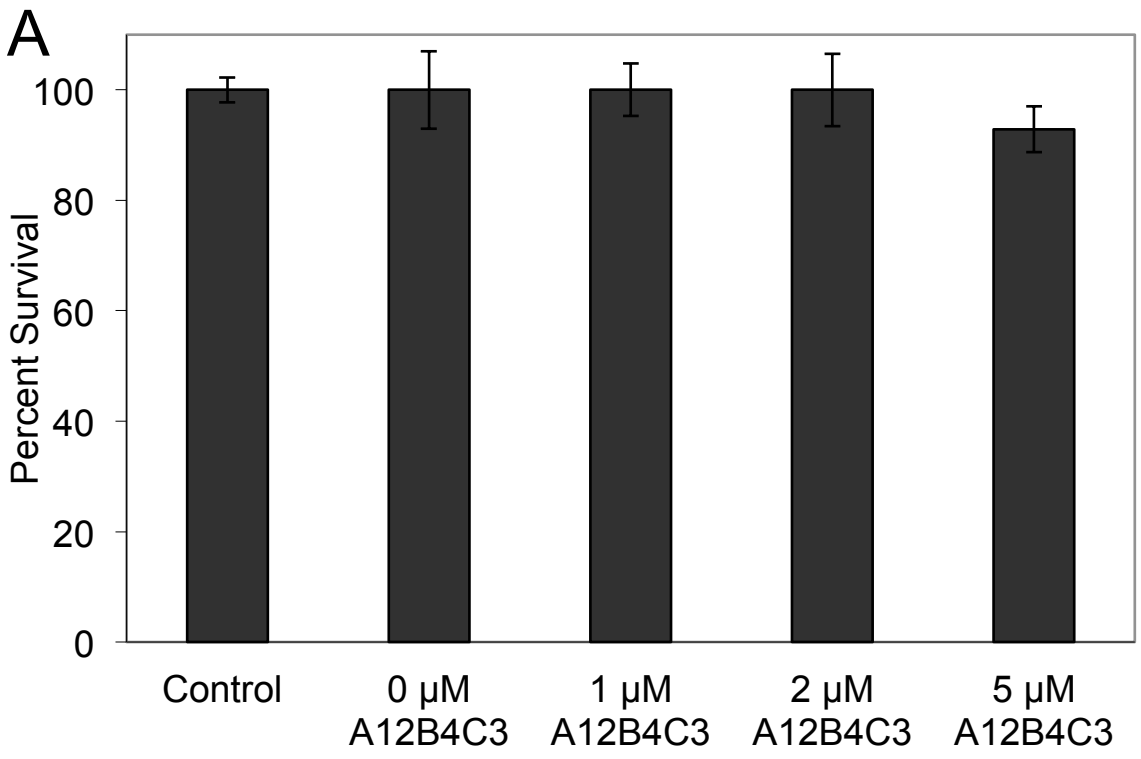
A
Percent Survival
100
80
60
40
20
0
Control
0 μM A12B4C3
1 μM A12B4C3
2 μM A12B4C3
5 μM A12B4C3

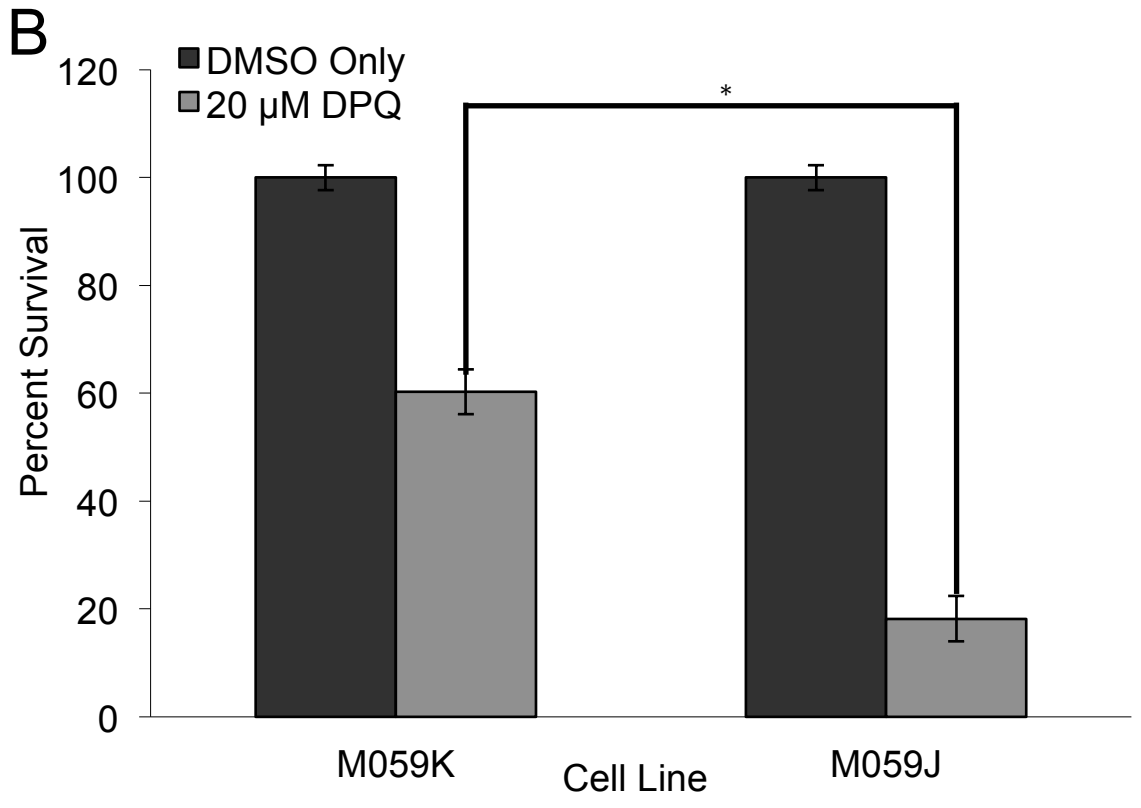
B
DMSO Only
20 μM DPQ
*
Percent Survival
120
100
80
60
40
20
0
M059K
M059J
Cell Line

Figure 4.4. Co-disruption of PNKP and DNA-PK_{cs} is not lethal. (A) M059J (DNA-$PK_{cs}^{-/-}$) cells were tested to determine their synthetic lethal status with PNKP. Increasing concentrations of A12B4C3 showed that there is not a synthetic lethal partnership between PNKP and DNA-PK_{cs}. (B) To investigate if co-disruption of SSBR and NHEJ is cytotoxic M059J and M059K cells (DNA-$PK_{cs}^{-/-}$ and DNA-$PK_{cs}^{+/+}$, respectively) were subjected to PARP1 inhibition. Even though the M059K cells displayed some sensitivity to 20 μM DPQ, there was a greater than 3-fold difference in survival in comparison to M059J cells (* denotes $p < 0.01$). This indicates that lethality does occur when SSBR and NHEJ are compromised and provides evidence for the notion that PNKP's function in NHEJ is important in synthetic lethal associations. Error bars represent standard error (±S.E.) from at least three independent experiments.

4.3.4 Isolating the specific function of PNKP that is critical for synthetic lethality

PNKP is a bifunctional DNA repair protein, possessing both 3'-phosphatase and 5'-kinase functions (Dobson & Allinson, 2006; Freschauf et al, 2009; Rasouli-Nia et al, 2004). We were keen to determine the contribution of loss of either of these catalytic functions of PNKP towards synthetic lethality. A12B4C3 is a specific PNKP phosphatase inhibitor (Freschauf et al, 2009), however, we wished to discover if the kinase function of PNKP was equally important to synthetic lethal relationships, or if it is simply the phosphatase function of PNKP that was critical. We stably transfected A549δPNKP cells with RNAi-resistant, mutant forms of *PNKP* and tested their survival in response to the PARP1 inhibitor DPQ. Figure 4.5A shows that DPQ concentrations used during these experiments are only mildly toxic to A549 cells. When A549δPNKP were stably transfected with vectors expressing a kinase-proficient but phosphatase-dead (D171A and D173A), or a phosphatase-proficient but kinase-dead (K378A) form of PNKP, using site-directed mutagenesis of RNAi-resistant, full-length PNKP (Tahbaz et al, 2012), rescue of the lethal phenotype under PARP inhibition was partially rescued (Figs. 4.5B and 4.5C, respectively). Furthermore, stable transfection of an RNAi-resistant full length but both kinase- and phosphatase-dead PNKP shows no increase in survival (Fig. 4.5D). The survival of cells ectopically expressing either singly-functioning PNKP at 10 μM DPQ is statistically different when both catalytic functions of PNKP are

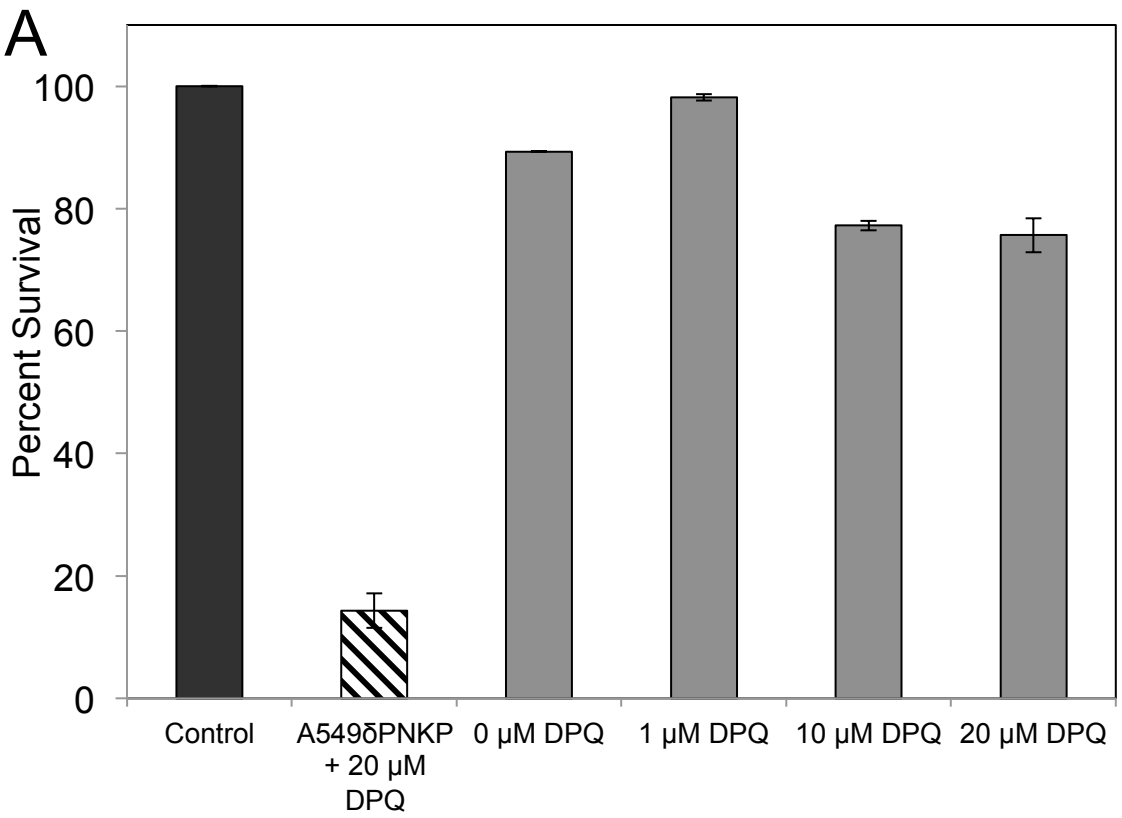
A
Percent Survival
100
80
60
40
20
0
Control
A549δPNKP + 20 μM DPQ
0 μM DPQ
1 μM DPQ
10 μM DPQ
20 μM DPQ

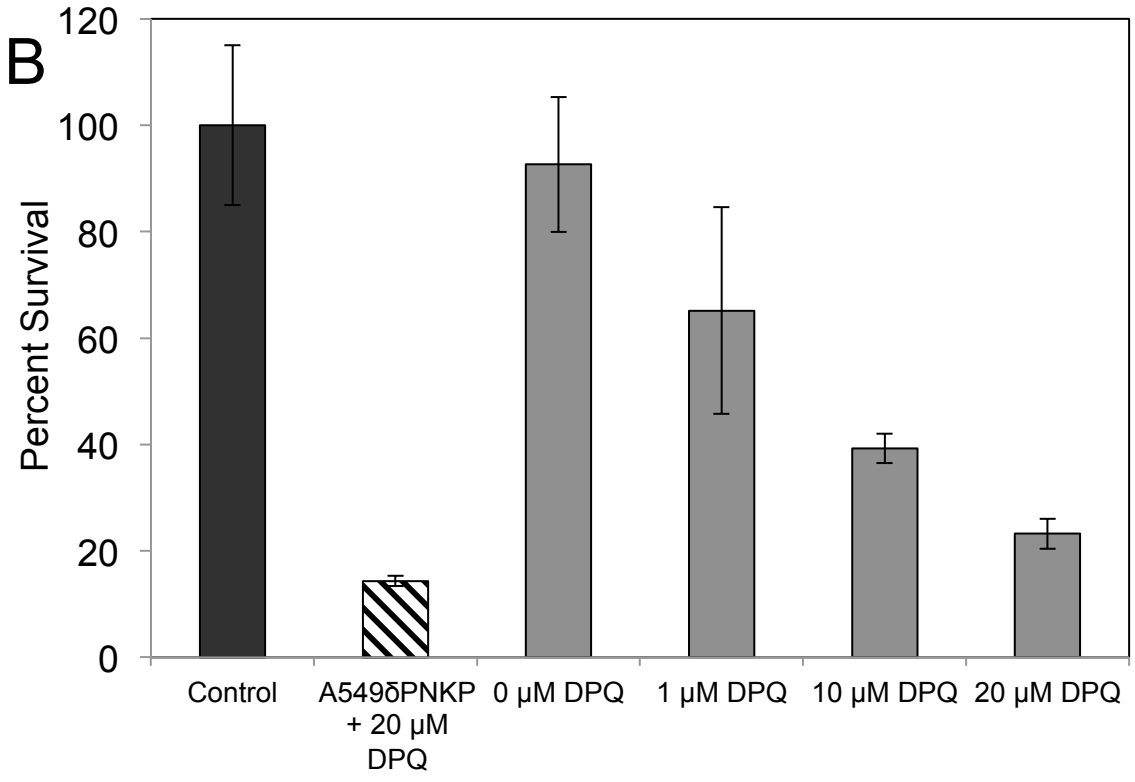
B
Percent Survival
120
100
80
60
40
20
0
Control
A549δPNKP + 20 μM DPQ
0 μM DPQ
1 μM DPQ
10 μM DPQ
20 μM DPQ

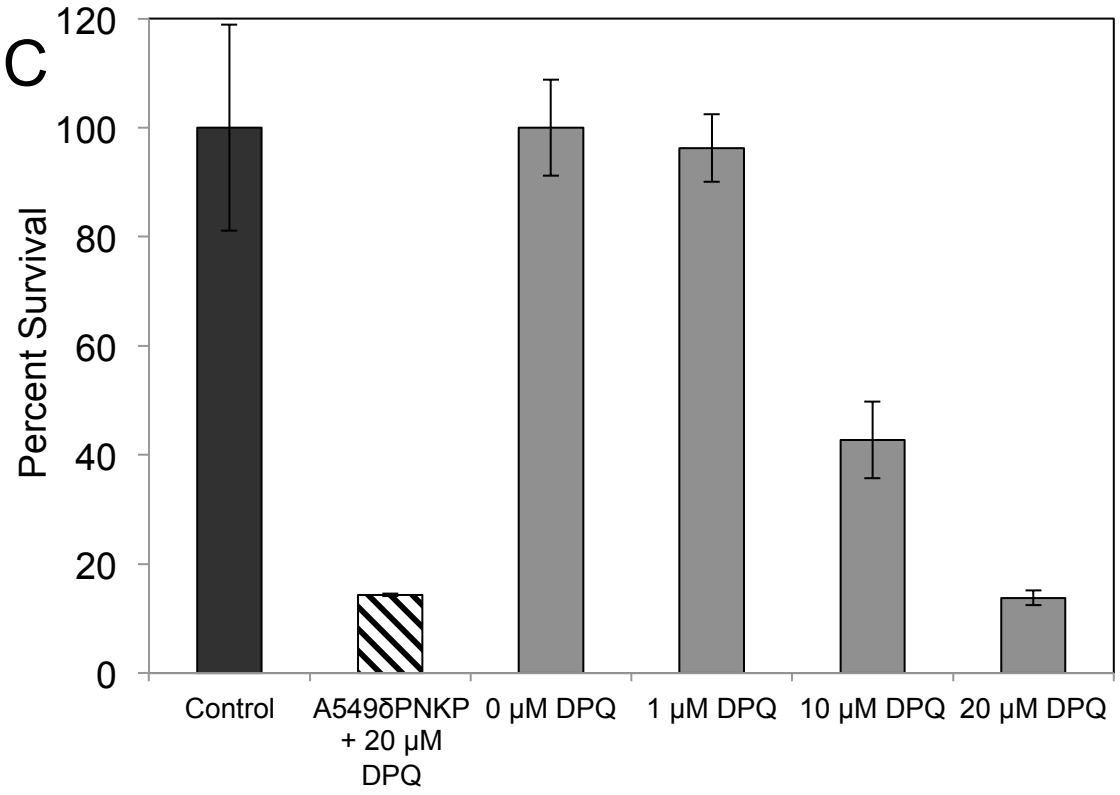
C
120
100
80
60
40
20
0
Percent Survival
Control
A549δPNKP + 20 μM DPQ
0 μM DPQ
1 μM DPQ
10 μM DPQ
20 μM DPQ

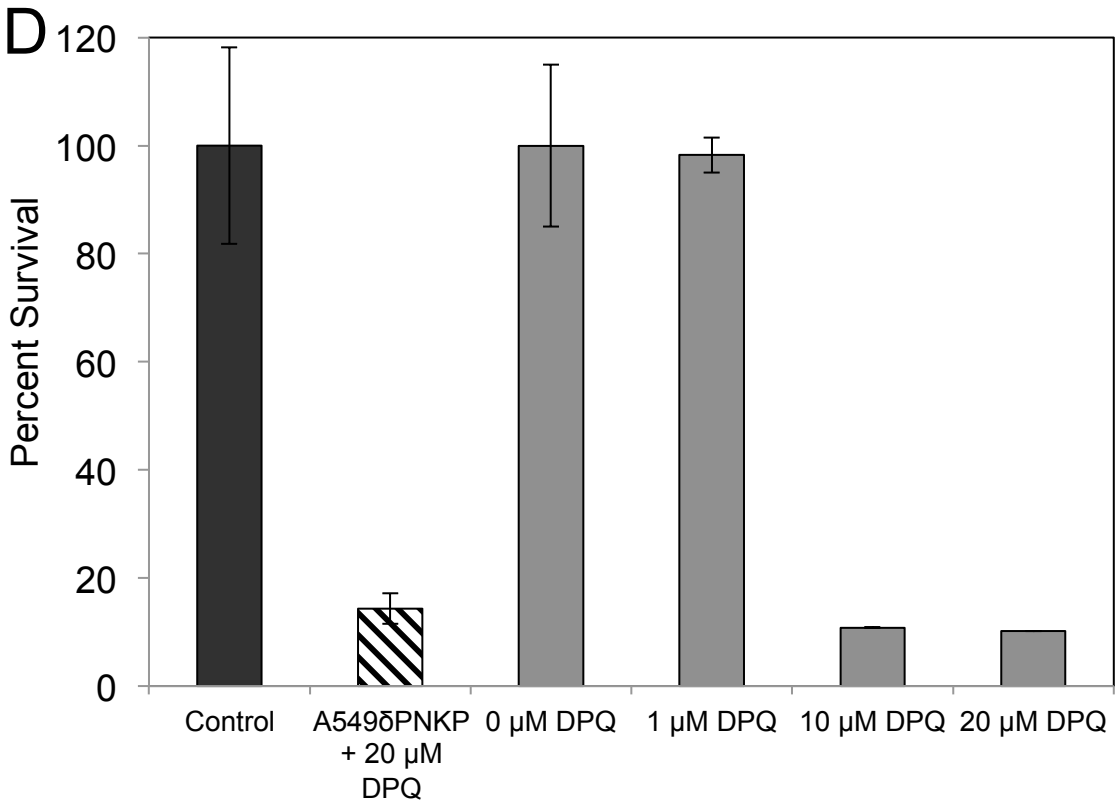
D
120
100
80
60
40
20
0
Percent Survival
Control
A549δPNKP + 20 μM DPQ
0 μM DPQ
1 μM DPQ
10 μM DPQ
20 μM DPQ

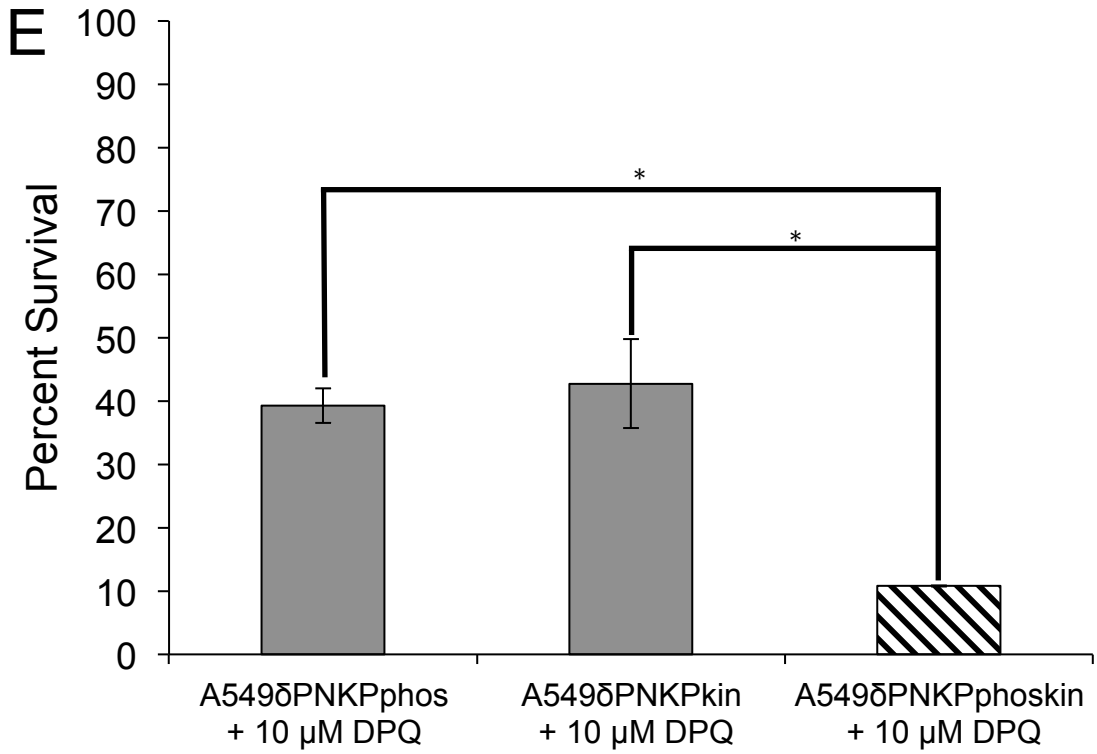
Percent Survival
100
90
80
70
60
50
40
30
20
10
0
*
*
A549δPNKPphos
+ 10 μM DPQ
A549δPNKPkin
+ 10 μM DPQ
A549δPNKPphoskin
+ 10 μM DPQ

Figure 4.5. Loss of PNKP enzymatic function in synthetic lethal relationships. (A) A549 parental cells were treated with increasing concentrations of DPQ to determine toxicity. (B) A549δPNKP cells transiently transfected with an RNAi-insenstive, kinase proficient but phosphatase-dead form of PNKP (A549δPNKPphos) treated with the same concentrations of DPQ. (C) A549δPNKP cells transiently transfected with an RNAi-insensitive, phosphatase proficient but kinase-dead form of PNKP subjected to PARP inhibition. (D) A549δPNKP cells transiently transfected with an RNAi-insensitive but both phosphatase-dead and kinase-dead form of PNKP treated with DPQ. (E) At 10 μM DPQ there is a significant increase in survival of the single mutant forms of PNKP compared to the double mutant PNKP (* denotes $p < 0.01$). These results indicate that loss of either the phosphatase or kinase activities of PNKP can contribute to synthetic lethality with PARP and that the physical presence of PNKP is not enough to rescue lethality under PARP inhibition. Error bars represent standard error (±S.E.) from at least three independent experiments.

disrupted (Fig. 4.5E, $p < 0.01$). This indicates that both the kinase and phosphatase functions of PNKP are important for the survival of cells under synthetic lethal conditions, and the presence of the PNKP protein itself is insufficient for rescue.

4.4 DISCUSSION

Synthetic lethality is a promising avenue for cancer research and therapy, and even in the short time since its utilization in the clinic, it has been shown to be effective (O'Brien & Stokoe, 2009; Pal & Mortimer, 2009). Synthetic lethality provides a means to selectively target cancer cells for death yet simultaneously leave normal cells unharmed because only cancer cells lose critical protein function during the course of neoplastic transformation whereas normal tissues do not. Thus one of the great potential benefits of the development of synthetic lethal treatments is their relatively benign consequences in terms of side effects. This lack of serious adverse side effects can be seen in the clinical trials of the PARP inhibitor Olaparib on BRCA1- and BRCA2-mutated ovarian cancer. To date, the only grade 3 toxicities observed were nausea (7%) and leukopenia (5%) (Fong et al, 2009; Gartner et al, 2010; Underhill et al, 2010).

Clearly, not all cancers will be susceptible to PARP1 inhibitors and there is thus a great need to identify additional synthetic lethal relationships. We have previously found that PNKP may be a clinically valuable therapeutic target in synthetic lethal treatment paradigms, potentially

benefiting many cancer sufferers. We previously identified 425 genes/proteins that are potentially synthetic lethal with PNKP (Mereniuk et al, 2012a), including SHP-1 and PTEN. Here we sought to pinpoint the function(s) of PNKP that when diminished is (are) responsible for synthetic lethality afforded by these partnerships. We found that PNKP shares a synthetic lethal relationship with both PARP and Polβ (Figs. 4.1 and 4.3, respectively), suggesting that it is PNKP's role in DSBR that is critical to protect against synthetic lethality. PNKP's function in DSBR relates to the NHEJ pathway where it dephosphorylates 3'-phosphate and phosphorylates 5'-hydroxyl groups found at DSBs to generate elongation and ligation competent 3'-hydroxyl and 5'-phosphate groups (Freschauf et al, 2009; Rasouli-Nia et al, 2004). If this is correct, then co-disruption of PNKP with a major NHEJ protein should not be lethal as it would simply disrupt one, albeit important, DNA repair pathway. This was seen in practice when we found that PNKP does not hold a synthetic lethal association with DNA-PK_{cs}, a critical NHEJ protein. We further ruled out the possibility that co-disruption of both the SSBR and NHEJ pathways does not necessarily lead to a lethal phenotype, by showing that DPQ-mediated inhibition of PARP1 is toxic to cells lacking NHEJ function (Fig. 4.4). These results support the hypothesis that PNKP's role in NHEJ is the important function for synthetic lethal associations. One possible explanation for this is that perhaps another DNA end-processing enzyme, such as APTX, can substitute for PNKP at SSBs, but not at DSBs. In this

example, SSBs harbouring PNKP-treatable ends

PNKP is a dual functioning DNA repair enzyme, with both kinase and phosphatase activities. We observed that when either the kinase or phosphatase functions are reconstituted in PNKP-depleted cells partial rescue of the lethal phenotype under DPQ treatment was obtained (Fig. 4.5). No rescue was observed when the vector expressing the RNAi-insensitive, but kinase and phosphatase-dead form of PNKP was stably transfected into these cells (Fig. 4.5D). This indicates that both the 3'-phosphatase and the 5'-kinase functions are almost equally important for cell survival under otherwise synthetic lethal conditions.

The data described in this chapter may be of clinical interest. First, PARP inhibitors may be effective against cancers with mutations in NHEJ, such as Artemis-deficient lymphomas (Moshous et al, 2003), and therefore not confined to tumours with HR deficiencies. Secondly, drugs targeting either the kinase or phosphatase function alone, such as A12B4C3, should be effective to an extent, but ideally a drug affecting both functional domains of PNKP, such as one that disrupts the three-dimensional folding of PNKP, should be more beneficial. Additionally, treatment using si- or shRNA directed towards PNKP would also be effective at treating such cancers, as this type of therapy would deplete the protein itself, preventing both functions of PNKP in the cell.

4.5 REFERENCES

Aggarwal M, Brosh RM, Jr. (2009) Hitting the bull's eye: novel directed cancer therapy through helicase-targeted synthetic lethality. *J Cell Biochem* **106:** 758-763

Allinson SL, Sleeth KM, Matthewman GE, Dianov GL (2004) Orchestration of base excision repair by controlling the rates of enzymatic activities. *DNA Repair (Amst)* **3:** 23-31

Audebert M, Salles B, Weinfeld M, Calsou P (2006) Involvement of polynucleotide kinase in a poly(ADP-ribose) polymerase-1-dependent DNA double-strand breaks rejoining pathway. *J Mol Biol* **356:** 257-265

Bernstein NK, Williams RS, Rakovszky ML, Cui D, Green R, Karimi-Busheri F, Mani RS, Galicia S, Koch CA, Cass CE, Durocher D, Weinfeld M, Glover JN (2005) The molecular architecture of the mammalian DNA repair enzyme, polynucleotide kinase. *Mol Cell* **17:** 657-670

BiPar Sciences presents interim phase 2 results for PARP inhibitor BSI-201 at San Antonio Breast Cancer Symposium. (2009) *Cancer Biol Ther* **8:** 2-3

Bolderson E, Richard DJ, Zhou BB, Khanna KK (2009) Recent advances in cancer therapy targeting proteins involved in DNA double-strand break repair. *Clin Cancer Res* **15:** 6314-6320

Breimer LH (1991) Repair of DNA damage induced by reactive oxygen species. *Free Radic Res Commun* **14:** 159-171

Brem R, Hall J (2005) XRCC1 is required for DNA single-strand break repair in human cells. *Nucleic Acids Res* **33:** 2512-2520

Bryant HE, Schultz N, Thomas HD, Parker KM, Flower D, Lopez E, Kyle S, Meuth M, Curtin NJ, Helleday T (2005) Specific killing of BRCA2-deficient tumours with inhibitors of poly(ADP-ribose) polymerase. *Nature* **434:** 913-917

Caldecott KW (2003) DNA single-strand break repair and spinocerebellar ataxia. *Cell* **112:** 7-10

Caldecott KW (2007) Mammalian single-strand break repair: mechanisms and links with chromatin. *DNA Repair (Amst)* **6:** 443-453

Caldecott KW (2008) Single-strand break repair and genetic disease. *Nat Rev Genet* **9:** 619-631

Caldecott KW, Tucker JD, Stanker LH, Thompson LH (1995) Characterization of the XRCC1-DNA ligase III complex in vitro and its absence from mutant hamster cells. *Nucleic Acids Res* **23:** 4836-4843

Canaani D (2009) Methodological approaches in application of synthetic lethality screening towards anticancer therapy. *Br J Cancer* **100:** 1213-1218

Cantley LC, Neel BG (1999) New insights into tumour suppression: PTEN suppresses tumour formation by restraining the phosphoinositide 3-kinase/AKT pathway. *Proc Natl Acad Sci U S A* **96:** 4240-4245

Chan DW, Chen BP, Prithivirajsingh S, Kurimasa A, Story MD, Qin J, Chen DJ (2002) Autophosphorylation of the DNA-dependent protein kinase catalytic subunit is required for rejoining of DNA double-strand breaks. *Genes Dev* **16:** 2333-2338

Chen BP, Chan DW, Kobayashi J, Burma S, Asaithamby A, Morotomi-Yano K, Botvinick E, Qin J, Chen DJ (2005) Cell cycle dependence of DNA-dependent protein kinase phosphorylation in response to DNA double strand breaks. *J Biol Chem* **280:** 14709-14715

Chen L, Trujillo K, Sung P, Tomkinson AE (2000) Interactions of the DNA ligase IV-XRCC4 complex with DNA ends and the DNA-dependent protein kinase. *J Biol Chem* **275:** 26196-26205

Das A, Wiederhold L, Leppard JB, Kedar P, Prasad R, Wang H, Boldogh I, Karimi-Busheri F, Weinfeld M, Tomkinson AE, Wilson SH, Mitra S, Hazra TK (2006) NEIL2-initiated, APE-independent repair of oxidized bases in DNA: Evidence for a repair complex in human cells. *DNA Repair (Amst)* **5:** 1439-1448

Date H, Igarashi S, Sano Y, Takahashi T, Takano H, Tsuji S, Nishizawa M, Onodera O (2004) The FHA domain of aprataxin interacts with the C-terminal region of XRCC1. *Biochem Biophys Res Commun* **325:** 1279-1285

DeFazio LG, Stansel RM, Griffith JD, Chu G (2002) Synapsis of DNA ends by DNA-dependent protein kinase. *EMBO J* **21:** 3192-3200

Dianov GL, Sleeth KM, Dianova, II, Allinson SL (2003) Repair of abasic sites in DNA. *Mutat Res* **531:** 157-163

Dobson CJ, Allinson SL (2006) The phosphatase activity of mammalian polynucleotide kinase takes precedence over its kinase activity in repair of single strand breaks. *Nucleic Acids Res* **34:** 2230-2237

Dobzhansky T (1946) Genetics of Natural Populations. Xiii. Recombination and Variability in Populations of Drosophila Pseudoobscura. *Genetics* **31:** 269-290

Dungey FA, Caldecott KW, Chalmers AJ (2009) Enhanced radiosensitization of human glioma cells by combining inhibition of poly(ADP-ribose) polymerase with inhibition of heat shock protein 90. *Mol Cancer Ther* **8:** 2243-2254

Evers B, Schut E, van der Burg E, Braumuller TM, Egan DA, Holstege H, Edser P, Adams DJ, Wade-Martins R, Bouwman P, Jonkers J (2010) A high-throughput pharmaceutical screen identifies compounds with specific toxicity against BRCA2-deficient tumours. *Clin Cancer Res* **16:** 99-108

Farmer H, McCabe N, Lord CJ, Tutt AN, Johnson DA, Richardson TB, Santarosa M, Dillon KJ, Hickson I, Knights C, Martin NM, Jackson SP, Smith GC, Ashworth A (2005) Targeting the DNA repair defect in BRCA mutant cells as a therapeutic strategy. *Nature* **434:** 917-921

Fong PC, Boss DS, Yap TA, Tutt A, Wu P, Mergui-Roelvink M, Mortimer P, Swaisland H, Lau A, O'Connor MJ, Ashworth A, Carmichael J, Kaye SB, Schellens JH, de Bono JS (2009) Inhibition of poly(ADP-ribose) polymerase in tumours from BRCA mutation carriers. *N Engl J Med* **361:** 123-134

Frenkel K (1992) Carcinogen-mediated oxidant formation and oxidative DNA damage. *Pharmacol Ther* **53:** 127-166

Freschauf GK, Karimi-Busheri F, Ulaczyk-Lesanko A, Mereniuk TR, Ahrens A, Koshy JM, Rasouli-Nia A, Pasarj P, Holmes CF, Rininsland F, Hall DG, Weinfeld M (2009) Identification of a small molecule inhibitor of the human DNA repair enzyme polynucleotide kinase/phosphatase. *Cancer Res* **69:** 7739-7746

Friedberg EC (2006) *DNA repair and mutagenesis*, 2nd edn. Washington, D.C.: ASM Press.

Gartner EM, Burger AM, Lorusso PM (2010) Poly(adp-ribose) polymerase inhibitors: a novel drug class with a promising future. *Cancer J* **16:** 83-90

Goodarzi AA, Yu Y, Riballo E, Douglas P, Walker SA, Ye R, Harer C, Marchetti C, Morrice N, Jeggo PA, Lees-Miller SP (2006) DNA-PK

autophosphorylation facilitates Artemis endonuclease activity. *EMBO J* **25:** 3880-3889

Gueven N, Becherel OJ, Kijas AW, Chen P, Howe O, Rudolph JH, Gatti R, Date H, Onodera O, Taucher-Scholz G, Lavin MF (2004) Aprataxin, a novel protein that protects against genotoxic stress. *Hum Mol Genet* **13:** 1081-1093

Hartlerode AJ, Scully R (2009) Mechanisms of double-strand break repair in somatic mammalian cells. *Biochem J* **423:** 157-168

Iglehart JD, Silver DP (2009) Synthetic lethality--a new direction in cancer-drug development. *N Engl J Med* **361:** 189-191

Iliakis G (2009) Backup pathways of NHEJ in cells of higher eukaryotes: cell cycle dependence. *Radiother Oncol* **92:** 310-315

Karimi-Busheri F, Rasouli-Nia A, Allalunis-Turner J, Weinfeld M (2007) Human polynucleotide kinase participates in repair of DNA double-strand breaks by nonhomologous end joining but not homologous recombination. *Cancer Res* **67:** 6619-6625

Liang Y, Lin SY, Brunicardi FC, Goss J, Li K (2009) DNA damage response pathways in tumour suppression and cancer treatment. *World J Surg* **33:** 661-666

Lieber MR (2010) The Mechanism of Double-Strand DNA Break Repair by the Nonhomologous DNA End-Joining Pathway. *Annu Rev Biochem*

Lindahl T, Nyberg B (1972) Rate of depurination of native deoxyribonucleic acid. *Biochemistry* **11:** 3610-3618

Lucchesi JC (1968) Synthetic lethality and semi-lethality among functionally related mutants of Drosophila melanfgaster. *Genetics* **59:** 37-44

Ma Y, Pannicke U, Lu H, Niewolik D, Schwarz K, Lieber MR (2005) The DNA-dependent protein kinase catalytic subunit phosphorylation sites in human Artemis. *J Biol Chem* **280:** 33839-33846

Mani RS, Karimi-Busheri F, Cass CE, Weinfeld M (2001) Physical properties of human polynucleotide kinase: hydrodynamic and spectroscopic studies. *Biochemistry* **40:** 12967-12973

Masaoka A, Horton JK, Beard WA, Wilson SH (2009) DNA polymerase beta and PARP activities in base excision repair in living cells. *DNA Repair (Amst)* **8:** 1290-1299

Mendes-Pereira AM, Martin SA, Brough R, McCarthy A, Taylor JR, Kim JS, Waldman T, Lord CJ, Ashworth A (2009) Synthetic lethal targeting of PTEN mutant cells with PARP inhibitors. *EMBO Mol Med* **1:** 315-322

Mereniuk TR, Maranchuk RA, Schindler A, Penner JC, Freschauf GK, Hegazy SA, Lai R, Foley E, Weinfeld M (2012a) Genetic screening for synthetic lethal partners of polynucleotide kinase/phosphatase: potential for targeting SHP-1 depleted cancers. *(Submitted)*

Mereniuk TR, Mendes-Pereira AM, Foley E, Ashworth A, Weinfeld M (2012b) Synthetic lethal targeting of PTEN-deficient cancers using selective disruption of polynucleotide kinase/phosphatase.

Mizuguchi H, Terao T, Kitai M, Ikeda M, Yoshimura Y, Das AK, Kitamura Y, Takeda N, Fukui H (2011) Involvement of protein kinase Cdelta/extracellular signal-regulated kinase/poly(ADP-ribose) polymerase-1 (PARP-1) signaling pathway in histamine-induced up-regulation of histamine H1 receptor gene expression in HeLa cells. *J Biol Chem* **286:** 30542-30551

Moreira MC, Barbot C, Tachi N, Kozuka N, Uchida E, Gibson T, Mendonca P, Costa M, Barros J, Yanagisawa T, Watanabe M, Ikeda Y, Aoki M, Nagata T, Coutinho P, Sequeiros J, Koenig M (2001) The gene mutated in ataxia-ocular apraxia 1 encodes the new HIT/Zn-finger protein aprataxin. *Nat Genet* **29:** 189-193

Moshous D, Pannetier C, Chasseval Rd R, Deist Fl F, Cavazzana-Calvo M, Romana S, Macintyre E, Canioni D, Brousse N, Fischer A, Casanova JL, Villartay JP (2003) Partial T and B lymphocyte immunodeficiency and predisposition to lymphoma in patients with hypomorphic mutations in Artemis. *J Clin Invest* **111:** 381-387

O'Brien T, Stokoe D (2009) Converting cancer mutations into therapeutic opportunities. *EMBO Mol Med* **1:** 297-299

O'Connor MJ, Martin NM, Smith GC (2007) Targeted cancer therapies based on the inhibition of DNA strand break repair. *Oncogene* **26:** 7816-7824

Pal SK, Mortimer J (2009) Triple-negative breast cancer: novel therapies and new directions. *Maturitas* **63:** 269-274

Parsons JL, Dianova, II, Allinson SL, Dianov GL (2005a) DNA polymerase beta promotes recruitment of DNA ligase III alpha-XRCC1 to sites of base excision repair. *Biochemistry* **44:** 10613-10619

Parsons JL, Dianova, II, Allinson SL, Dianov GL (2005b) Poly(ADP-ribose) polymerase-1 protects excessive DNA strand breaks from deterioration during repair in human cell extracts. *FEBS J* **272:** 2012-2021

Parsons JL, Dianova, II, Boswell E, Weinfeld M, Dianov GL (2005c) End-damage-specific proteins facilitate recruitment or stability of X-ray cross-complementing protein 1 at the sites of DNA single-strand break repair. *FEBS J* **272:** 5753-5763

Pastwa E, Blasiak J (2003) Non-homologous DNA end joining. *Acta Biochim Pol* **50:** 891-908

Rasouli-Nia A, Karimi-Busheri F, Weinfeld M (2004) Stable down-regulation of human polynucleotide kinase enhances spontaneous mutation frequency and sensitizes cells to genotoxic agents. *Proc Natl Acad Sci U S A* **101:** 6905-6910

Rass U, Ahel I, West SC (2007) Actions of aprataxin in multiple DNA repair pathways. *J Biol Chem* **282:** 9469-9474

Schindler A, Foley E (2010) A functional RNAi screen identifies hexokinase 1 as a modifier of type II apoptosis. *Cell Signal* **22:** 1330-1340

Simpson L, Parsons R (2001) PTEN: life as a tumour suppressor. *Exp Cell Res* **264:** 29-41

Stefansson OA, Jonasson JG, Johannsson OT, Olafsdottir K, Steinarsdottir M, Valgeirsdottir S, Eyfjord JE (2009) Genomic profiling of breast tumours in relation to BRCA abnormalities and phenotypes. *Breast Cancer Res* **11:** R47

Tahbaz N, Subedi S, Weinfeld M (2012) Role of polynucleotide kinase/phosphatase in mitochondrial DNA repair. *Nucleic Acids Res* **40:** 3484-3495

Thompson LH, Brookman KW, Jones NJ, Allen SA, Carrano AV (1990) Molecular cloning of the human XRCC1 gene, which corrects defective DNA strand break repair and sister chromatid exchange. *Mol Cell Biol* **10:** 6160-6171

Trivedi RN, Wang XH, Jelezcova E, Goellner EM, Tang JB, Sobol RW (2008) Human methyl purine DNA glycosylase and DNA polymerase beta

expression collectively predict sensitivity to temozolomide. *Mol Pharmacol* **74:** 505-516

Turner NC, Lord CJ, Iorns E, Brough R, Swift S, Elliott R, Rayter S, Tutt AN, Ashworth A (2008) A synthetic lethal siRNA screen identifying genes mediating sensitivity to a PARP inhibitor. *EMBO J* **27:** 1368-1377

Underhill C, Toulmonde M, Bonnefoi H (2010) A review of PARP inhibitors: from bench to bedside. *Ann Oncol*

Venkitaraman AR (2009) Targeting the molecular defect in BRCA-deficient tumours for cancer therapy. *Cancer Cell* **16:** 89-90

Vens C, Dahmen-Mooren E, Verwijs-Janssen M, Blyweert W, Graversen L, Bartelink H, Begg AC (2002) The role of DNA polymerase beta in determining sensitivity to ionizing radiation in human tumour cells. *Nucleic Acids Res* **30:** 2995-3004

Williamson CT, Muzik H, Turhan AG, Zamo A, O'Connor MJ, Bebb DG, Lees-Miller SP ATM deficiency sensitizes mantle cell lymphoma cells to poly(ADP-ribose) polymerase-1 inhibitors. *Mol Cancer Ther* **9:** 347-357

Woodhouse BC, Dianov GL (2008) Poly ADP-ribose polymerase-1: an international molecule of mystery. *DNA Repair (Amst)* **7:** 1077-1086

Woodhouse BC, Dianova, II, Parsons JL, Dianov GL (2008) Poly(ADP-ribose) polymerase-1 modulates DNA repair capacity and prevents formation of DNA double strand breaks. *DNA Repair (Amst)* **7:** 932-940

Yaneva M, Kowalewski T, Lieber MR (1997) Interaction of DNA-dependent protein kinase with DNA and with Ku: biochemical and atomic-force microscopy studies. *EMBO J* **16:** 5098-5112

Yannone SM, Khan IS, Zhou RZ, Zhou T, Valerie K, Povirk LF (2008) Coordinate 5' and 3' endonucleolytic trimming of terminally blocked blunt DNA double-strand break ends by Artemis nuclease and DNA-dependent protein kinase. *Nucleic Acids Res* **36:** 3354-3365

Yin Y, Shen WH (2008) PTEN: a new guardian of the genome. *Oncogene* **27:** 5443-5453

Yoo S, Dynan WS (1999) Geometry of a complex formed by double strand break repair proteins at a single DNA end: recruitment of DNA-PKcs induces inward translocation of Ku protein. *Nucleic Acids Res* **27:** 4679-4686

Zander SA, Kersbergen A, van der Burg E, de Water N, van Tellingen O, Gunnarsdottir S, Jaspers JE, Pajic M, Nygren AO, Jonkers J, Borst P, Rottenberg S Sensitivity and acquired resistance of BRCA1;p53-deficient mouse mammary tumours to the topoisomerase I inhibitor topotecan. *Cancer Res* **70:** 1700-1710

Chapter 5: Discussion

5.1 DISCUSSION

5.1.1 Treatment of loss-of-function cancers using a synthetic lethal or synthetic sickness approach

The vast majority of cancer-related mutations, i.e. ~80%, involve the loss of function of tumour suppressors. We have therefore focused our attention on the identification of tumour suppressors as potential synthetic lethal partners with PNKP. Using our arbitrary cut-off criteria of ≤33% survival of the doubly disrupted cells versus control transfected cells, we identified 14 currently known tumour suppressors as possibly synthetic lethal with PNKP. However, this does not include other proteins identified in the screen that have yet to be characterized as tumour suppressors.

When we probed for more information on these 14 proteins, we found that one protein in particular, the protein tyrosine phosphatase SHP-1, was of particular interest because it had been shown to be lost in a diverse assortment of malignant lymphomas and leukemias. Work by other groups revealed that ≥90% of diffuse large cell lymphoma, follicle center lymphoma, Hodgkin's disease (HD), mantle cell lymphoma (MCL), peripheral T cell lymphoma (PL), adult T cell lymphoma/leukemia (ATLL) specimens and 100% of NK/T cell lymphoma specimens showed no detectable SHP-1 expression (Cariaga-Martinez et al, 2009; Delibrias et al, 1997; Oka et al, 2001). Furthermore, SHP-1 was also shown to be expressed at diminished or undetectable levels in 40 of 45 malignant prostate samples (Cariaga-Martinez et al, 2009).

Using a synthetic lethal approach, a single agent therapy designed to target and disrupt PNKP function may benefit these cancer sufferers. Since only the cancer cells have lost SHP-1 function, they will be susceptible to PNKP disruption and spontaneously undergo apoptosis, leaving normal cells unscathed by the treatment. Through the establishment and subsequent testing of stable cell lines lacking PNKP protein and/or function, we have determined that PNKP disruption is well tolerated by healthy cells. Coupled with the fact that in principle synthetic lethal treatments do not require combination with other modalities, such as chemotherapy or radiotherapy, to see an effect, this suggests that agents targeting PNKP function in synthetic lethal treatment paradigms may produce little to no serious side effects (Freschauf et al, 2009; Freschauf et al, 2010; O'Brien & Stokoe, 2009; Rasouli-Nia et al, 2004; Weinfeld et al, 2011). Due to the potential that synthetic lethal treatment holds, many partnerships are currently being investigated, most focusing on combinations using PARP inhibitors and a list of these drugs is presented in Table 5.1.

SHP-1 was just one of the 14 known tumour suppressors identified through screening. Another tumour suppressor, PTEN, was also implicated. This protein, which is lost in a large number of sporadic cancers, has been shown to be the second most disrupted tumour suppressor in cancers behind only p53. We also verified that PTEN holds a synthetic lethal relationship with PNKP and that no exogenous DNA damaging agents are

Table 5.1 Clinical trials using PARP inhibitors as a combination therapy

PARP Inhibitor	Combination Agent	Type	Administration (PARP inhibitor)	Phase	Status
ABT-888	Cycolphosphamide	Advanced solid tumours, lymphomas	PO	I	Ongoing
ABT-888	Topotecan	Advanced solid tumours, lymphomas	PO	I	Complete
ABT-888	Temozolomide	Prostate (metastatic castration resistant and up to 2 failed non-hormonal systemic therapies)	PO	I	Ongoing
ABT-888	Temozolomide	Leukemia	PO	I	Recruiting
ABT-888	Liposomal Doxorubicin	Breast, fallopian tube, ovarian, peritoneal cavity	PO	I	Not yet open
ABT-888	Carboplatin	Advanced solid tumours	PO	I	Recruiting
ABT-888	Temozolomide	Medulloblastoma, pontine glioma, ependymoma, astrycytoma, primitive neuroectodermal tumours	PO	I	Ongoing
ABT-888	Temozolomide	Non-hematologic, metastataic melanoma, breast, ovarian, primary peritoneal, fallopian tube, hepatocellular	PO	I	Complete
ABT-888	Cyclophosphamide	Ovarian, primary peritoneal, serous carcinoma, triple-negative breast, fallopian tube	PO	II	Ongoing
ABT-888	Carboplatin and Paclitaxel	Hepatic, renal, advanced solid tumours	PO	I	Withdrawn
ABT-888	Radiation	Breast	PO	I	Not yet open
ABT-888	Temozolomide	Breast, metastatic breast (BRCA1/2 mutated)	PO	II	Ongoing
ABT-888	Temozolomide	Colorectal	PO	II	Recruiting
ABT-888	Topotecan	Ovarian, primary peritoneal, solid tumours	PO	I/II	Recruiting
ABT-888	Bevacizumab and/or Carboplatin and/or Paclitaxel	Fallopian tube, ovarian, peritoneal	PO	I	Recruiting
ABT-888	Bortezomib and Dexamethasone	Relapsed refractory myeloma	PO	I	Recruiting
ABT-888	Bendamustine and Rituximab	Lymphoma, multiple myeloma, plasma cell, small intestine, solid tumours	PO	I/II	Recruiting
ABT-888	Bortezomib	Multiple myeloma	PO	I	Recruiting
ABT-888	5-fluorouracil, oxaliplatin and	Metastatic pancreatic	PO	I/II	Recruiting

	leucovorin				
ABT-888	Cisplatin and Vinorelabine Tartrate	ER-negative, BRCA1/2 mutated breast/ovarian, male breast, PR-negative, recurrent breast, stage IIIC/IV breast, triple-negative breast	PO	I	Recruiting
ABT-888	Temozolomide	Metastatic melanoma	PO	II	Ongoing
ABT-888	Topotecan	Chronic myelopriliferative disorders, leukemia, myelodysplastic syndromes	PO	I	Recruiting
ABT-888	Mytomycin C	Solid tumours (homologous recombination repair deficient)	PO	I	Recruiting
ABT-888	Radiation	Nervous system, brain	PO	I	Recruiting
ABT-888	Carboplatin and Dinaciclib	Advanced solid tumours (BRCA1/2 mutated)	PO	I	Recruiting
ABT-888	Low-dose, fractionated radiation	Advanced solid tumours with peritoneal carcinomatosis	PO	I	Recruiting
ABT-888	Capecitabine and Oxaliplatin	Breast and ovarian (BRCA1/2 mutated), colorectal, gastric, pancreatic, solid tumours	PO	I	Suspended
ABT-888	Carboplatin and Paclitaxel	Lung	PO	I/II	Recruiting
ABT-888	Cisplatin and Gemcitabine	Bladder, extrahepatic bile duct, gall bladder, liver, lung, pancreatic, renal pelvis, ureter	PO	I	Recruiting
ABT-888	Filgrastim, Pegfilgrastim and Topotecan	Cervical	PO	II	Recruiting
ABT-888	Neratinib, AMG386, ANG479 + Metformin	Breast	PO	II	Recruiting
ABT-888	CS7017	Advanced solid, lymphoma, multiple myeloma	PO	I	Recruiting
BSI-201	Gemcitabine and Carboplatin	Breast	IV	III	Ongoing
BSI-201	Gemcitabine and Carboplatin	Triple-negative breast	IV	II	Recruiting
BSI-201	Temozolomide	Malignant glioma (newly diagnosed)	IV	I/II	Recruiting
BSI-201	Irinotecan	Triple-negative breast, brain metastases	IV	II	Recruiting
BSI-201	Gemcitabine and Carboplatin	Squamous cell lung	IV	III	Recruiting

BSI-201	Carboplatin and/or Paclitaxel	Uterine carcinosarcoma	IV	II	Ongoing
BSI-201	Gemcitabine and Carboplatin	Breast	IV	II	Complete
BSI-201	Topotecan	Advanced solid tumours	IV	I	Complete
BSI-201	Temozolomide	Advanced solid tumours	IV	I	Complete
BSI-201	Gemcitabine	Advanced solid tumours	IV	I	Complete
BSI-201	Carboplatin and/or Paclitaxel	Advanced solid tumours	IV	I	Complete
BSI-201	Radiation	Brain metastases	IV	I	Not yet open
BSI-201	Gemcitabine and Carboplatin	Metastatic breast	IV	II	Ongoing
BSI-201	Gemcitabine and/or Carboplatin and/or Paclitaxel and/or Liposomal Doxorubicin	Advanced solid tumours	IV	I	Recruiting
BSI-201	Paclitaxel	Breast	IV	II	Ongoing
BSI-201	Irinotecan	Advanced solid tumours	IV	I/II	Complete
BSI-201	Gemcitabine and/or Cisplatin	Non-small cell lung cancer (stage IV)	IV	II	Complete
BSI-201	Gemcitabine and Carboplatin	Advanced solid tumours	IV	I	Ongoing
CEP-9722	Gemcitabine and Cisplatin	Advanced solid tumours, mantle cell lymphoma	PO	I	Recruiting
E7016	Temozolomide	Advanced solid tumours	PO	I	Ongoing
Olaparib	Dacarbazine	Advanced solid tumours	PO	I	Complete
Olaparib	Topotecan	Advanced solid tumours	PO	I	Complete
Olaparib	Gemcitabine	Pancreatic	PO	I	Ongoing
Olaparib	Cisplatin and Gemcitabine	Solid tumours (unresectable or metastatic)	PO	I	Complete
Olaparib	Bevacizumab	Advanced solid tumours	PO	I	Complete
Olaparib	Gemcitabine	Advanced solid tumours	PO	I	Ongoing
Olaparib	Carboplatin	Breast (BRCA1/2 mutated)	PO	I	Recruiting
Olaparib	Carboplatin	Ovarian (BRCA1/2 mutated)	PO	I	Recruiting
Olaparib	Liposomal Doxorubicin	Ovarian (BRCA1/2 mutated)	PO	II	Ongoing
Olaparib	Carboplatin and/or Paclitaxel	Triple-negative breast	PO	I	Ongoing
Olaparib	Carboplatin and/or Paclitaxel	Ovarian	PO	II	Ongoing
Olaparib	Paclitaxel	Gastric	PO	II	Ongoing
Olaparib	Carboplatin	Mixed muellerian, cervical, ovarian, breast, primary peritoneal, fallopian tube,	PO	I	Recruiting

		endometrial, carcinosarcoma			
Olaparib	Temozolomide	Brain, central nervous system tumours	PO	I	Recruiting
Olaparib	Cediranib	Ovarian, primary peritoneal, fallopian tube	PO	I/II	Recruiting
Olaparib	Irinotecan, Cisplatin and Mytomycin C	Pancreatic	PO	I/II	Recruiting
Olaparib	Radiation (50 Gy in 25 fractions)	Oesophagus	PO	I	Not yet open
Olaparib	Gefitinib	Non-small cell lung	PO	I/II	Recruiting
Olaparib	Cisplatin and Radiation	Squamous cell carcinoma	PO	I	Not yet open
Rucaparib	Cisplatin	Breast	IV	II	Recruiting
Rucaparib	Carboplatin	Advanced solid tumours	IV	I	Recruiting

required to induce apoptosis in cancer cells. However, we have also shown that an alternative approach using synthetic lethal interactions may be possible, a regimen termed synthetic sickness. In this approach, we hypersensitize PTEN-deficient cells using a systemic PNKP inhibitor at a concentration lower than is required to see significant synthetic lethality. This initial step will cause some cancerous cells to undergo apoptosis, however, we can drastically increase the amount of cell killing by subjecting the cells to γ-radiation or a topoisomerase I poison. In this way, we should still be able to retain selective death of cancer cells, yet increase the effectiveness of the treatment. Again, since healthy cells withstand PNKP disruption well, side effects associated with treatment are predicted to be minor. Another important advantage of regimens based on synthetic sickness lies in the possibility of reducing the dosage of chemotherapeutic drugs or radiation to achieve the same level of tumour control, which of course will reduce the deleterious side effects of the drugs or radiation. This is one likely reason why there are more clinical trials involving synthetic lethal interactions using combination therapies (Table 5.1) than those relying solely on single agent therapies (Table 5.2).

Furthermore, we have also discovered that both functions of PNKP are important to synthetic lethality. Disruption of either the phosphatase or kinase function of PNKP alone does sensitize cells to treatments targeting synthetic lethal partners, however the double knockout is significantly more sensitive to such treatments (Fig. 4.5). This information may be clinically valuable as those chemical inhibitors would be maximally beneficial if both of PNKP's

Table 5.2. Clinical trials using PARP inhibitors as single agents

PARP Inhibitor	Type	Administration (PARP inhibitor)	Phase	Status
ABT-888	Refractory solid tumours; lymphoid	PO	I	Complete
ABT-888	Multiple myeloma	PO	I	Recruiting
ABT-888	Ovarian	PO	I/II	Recruiting
ABT-888	Colorectal	PO	I	Recruiting
ABT-888	Fallopian tube, ovarian, primary peritoneal (BRCA1/2 mutated)	PO	II	Not yet open
AZD2461	Refractory solid tumours	PO	I	Ongoing
BMN763	Advanced or recurrent solid tumours	PO	I	Recruiting
BMN763	Acute myeloid leukemia, myelodysplastic syndrome, chronic lymphocytic leukemia, mantle cell lymphoma	PO	I	Recruiting
BSI-201	BRCA1/2 associated (epithelial ovarian, fallopian, or primary peritoneal)	IV	II	Complete
BSI-201	Ovarian	IV	II	Ongoing
BSI-201	Advanced solid tumours	IV	I	Complete
CEP-9722	Advanced solid tumours	PO	I/II	Complete
MK-4827	Advanced solid tumours, BRCA1/2 Mutated	PO	I	Terminated
MK-4827	Mantle-cell lymphoma	PO	II	Withdrawn
Olaparib	Advanced solid tumours (BRCA1/2 Mutated)	PO	I	Recruiting
Olaparib	Advanced breast (BRCA1/2 mutated)	PO	II	Complete
Olaparib	Advanced ovarian (BRCA1/2 mutated)	PO	II	Complete
Olaparib	Colorectal	PO	II	Ongoing
Olaparib	Ovarian, breast, prostate, pancreatic, advanced solid tumours	PO	II	Ongoing
Olaparib	Advanced metatstatic solid tumours (refractory to standard treatments)	PO	I	Complete
Rucaparib	Advanced breast or ovarian (BRCA1/2 Mutated)	IV	I/II	Recruiting

catalytic functions could be selectively silenced, such as drugs that disrupt the three-dimensional folding of PNKP. Additionally, treatment of cancers lacking a synthetic lethal partner of PNKP with an si- or shRNA would be beneficial as this type of treatment depletes the protein itself, preventing both functions of PNKP in the cell.

5.1.2 Using synthetic lethality for gain-of-function mutant cancers

Synthetic lethal approaches are not limited solely to treatment of loss-of-function mutations. It has been shown that it may also be possible to target some gain-of-function mutations using synthetic lethal treatment regimens. To date, most of the effort into treatment of cancers harbouring oncogenic mutations has involved selective silencing of the oncogene itself (summarized in Table 5.3). However, some groups have shown that certain cancers have become reliant on proteins separate from the oncogenic driver mutation in what has come to be known as 'non-oncogene addiction' (Figure 5.1) (Solimini et al, 2007). For example, cells with an oncogenic overexpression of the KRAS protein have become dependent on the serine/threonine protein kinase STK33 (Scholl et al, 2009). In cells expressing mutated KRAS, STK33 was shown to promote cell viability through the suppression of mitochondrial apoptosis through the S6K1-induced inactivation of the death-promoting factor, BAD. This dependence on STK33, however, was not seen in normal, non-KRAS-mutated cells. Targeted disruption of STK33 will therefore selectively kill

Table 5.3 Oncogenic targets of directed cancer therapies

Targeted Oncogene	Cancer Caused	Clinical Agent
HER-2	Breast	Trastuzumab (combination)
BCR/ABL	CML	Imatinib (monotherapy)
C-KIT	Gastrointestinal stromal	Imatinib (monotherapy)
EGFR	NSCLC	Gefitinib, Erlotinib (monotherapy)
EGFR	Head and neck, colorectal	Cetuximab (combination)
EGFR	Pancreas	Erlotinib (combination)
VEGF	Breast, colorectal, kidney	Bevacizumab (combination)
VEGFR, RAF	Kidney	Sorafenib (monotherapy)

*adapted from (Weinstein, 2002).

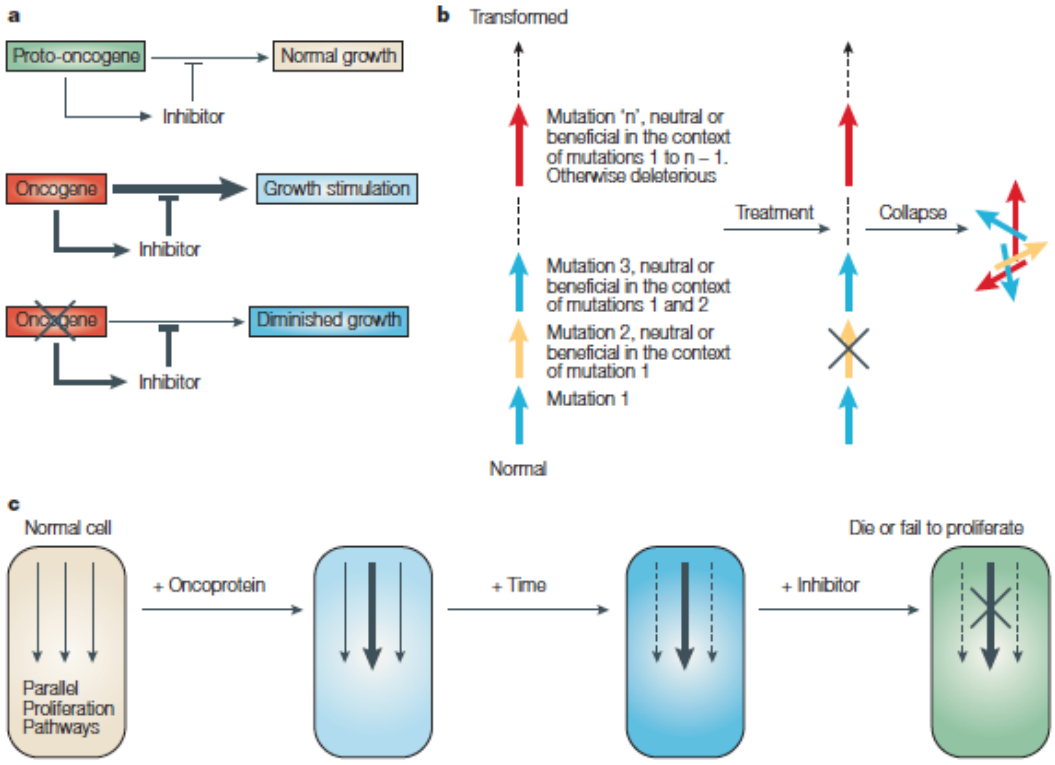

Figure 4 | **Models of oncogene addiction. a** | Many oncogenes paradoxically induce pro-mitogenic signals as well as anti-mitogenic (or pro-apoptotic) signals. Growth stimulation results from oncogene activation presumably because the former is dominant to the latter. However, acute inactivation of the oncogene might cause growth cessation or death if the anti-mitogenic/pro-apoptotic signals decay more slowly than the mitogenic signals (for example, because of differences in mRNA and protein half-life). Adapted from REF. 53. **b** | Oncogene dependency due to gene–gene interactions. Cancer cells accumulate mutations (arrows) over time that cumulatively lead to a transformed phenotype. Selection favours acquisition of mutations that are neutral or beneficial (adaptive) in the context of the mutations that preceded them. However, some of these changes might be deleterious (red arrow) were it not for the changes that preceded them. If true, correcting early genetic changes (yellow arrow) will unmask these deleterious effects. In this model, cancer cells behave like a molecular 'house of cards'. **c** | Activation (indicated by bold arrow) of an oncogenic pathway diminishes selection pressure to maintain collateral signalling pathways. Silencing of these collateral pathways over time, because of genetic or epigenetic changes, leads to oncogene dependency. Adapted from REF. 57.

Figure 5.1. Models of oncogene addiction (Kaelin, 2005).

only cancer cells as only these cells have become reliant on STK33, while normal cells would remain unharmed by treatment. In other words, cells with over-active KRAS are critically dependent on STK33 function for survival and therefore reveals STK33 as a potential therapeutic target for patients with cancers expressing mutant KRAS alleles.

KRAS mutated cancers are not the only cancers showing non-oncogene addiction, other synthetic lethal partners of oncogenic proteins have been uncovered and are listed below in Table 5.4. This suggests the investigation of synthetic lethal interactions into oncogene-expressing cancers will also be important for the development of tailor-made cancer therapies and further illustrates the importance of the identification of synthetic lethal partnerships to the future of cancer research.

5.1.3 Future directions

Approximately 80% of cancers harbour a loss of tumour suppressor function. In the past, loss-of-function mutations were hard to treat as protein function is difficult to re-establish pharmacologically and reconstitution of tumour suppressor protein is technically challenging. However, through use of the concept of synthetic lethality, these mutations become targetable. This is possible because the loss-of-function mutation itself is not targeted; it is the synthetic lethal partner of said protein. In this fashion, only those cells that are doubly disrupted, i.e.; cancer cells, will be affected, thus leaving normal cells unharmed. We have identified many proteins potentially synthetic lethal with PNKP through large-scale, siRNA

Table 5.4 Oncogenic mutations and the possible synthetic lethal treatment targets

Oncogene	Potential Target
KRAS	STK33 (Scholl et al, 2009)
KRAS	TBK1 (Barbie et al, 2009)
MYC	CDK1 (Goga et al, 2007)
N-Myc	CDK2 (Molenaar et al, 2009)
VHL	mTOR (Thomas et al, 2006)
FA proteins	ATM (Kennedy et al, 2007)
pVHL	MET (Pennacchietti et al, 2003)
pVHL	CDK6 (Hara et al, 2006)
pVHL	MEK1 (Hayashi et al, 2005)
KRAS	PLK1 (Luo et al, 2009)
Ras	PKCδ (Zhu et al, 2010)

library-based screening, including 14 tumour suppressors. We have selected two of these proteins for further testing (SHP-1 and PTEN), and there is therefore a need to validate the synthetic lethal status of the remaining proteins. Further investigation into these tumour suppressors may allow many more cancer subtypes to be targeted, potentially benefiting many more cancer sufferers.

To date, most of the investigation into synthetic lethality has been in relation to effects seen in combination with PARP. We have not limited our investigation into synthetic lethality to proteins involved directly in DNA repair. One interesting result of this is that there seemed to be an inordinate number of G-protein coupled receptors (GPCRs) possibly showing synthetic lethality with PNKP. These seven-pass transmembrane proteins are well-characterized proteins involved in signal transduction pathways in eukaryotes. These proteins bind a vast array of ligands and are also the target of approximately 40% of all medicinal drugs (Overington et al, 2006; Rask-Andersen et al, 2011). The potential druggability of these proteins presents an attractive target for the development of chemotherapeutics designed for use in conjunction with a targeted disruption of PNKP. An investigation into why GPCRs are particularly sensitive to PNKP disruption is required and may provide information into the mechanisms or requirements for synthetic lethal conditions in general.

We have also found that synthetic lethality may not be the only possible beneficial treatment stemming from the investigation into synthetic lethal partnerships. It is likely that for some tumours a ‘synthetic sickness’

approach may provide greater efficacy than simply depending on synthetic lethality through a single protein inhibitor. We have shown that when cells are hypersensitized through the co-disruption of PNKP and PTEN, administration of γ-radiation provided a significant increase in total cell killing than just the double disruption of PNKP and PTEN. Therefore, when experiments are performed to confirm the partnerships originally identified in the initial screen, it would be beneficial to examine the potential for capitalizing on synthetic sickness as well as synthetic lethality.

Knowledge of cancer genetic and protein status is essential for the utilization of synthetic lethal techniques in a clinical setting. Simply knowing that two genes/proteins are synthetic lethal in combination is not sufficient for an effective, patient specific treatment if tumour suppressor activity of the patient's cancer itself is not known. Fortunately the cost of genome sequencing is falling fast, and continues to decline everyday. For example, in July 2001, the cost of performing a genome-wide sequence was roughly $100,000,000. As of October 2011, the cost of the same genome sequence was roughly $30,000. With the continued development of next-generation sequencing technology and competition between sequencing companies such as Complete Genomics and deCODE Genetics, the goal of a '$1,000 genome' is possible in the foreseeable future (Wong et al, 2011). We can utilize this technology to provide information regarding the specific somatic mutations that lead to the development of a particular patient's cancer. Once key mutations are discovered, such as loss of certain tumour suppressor function or gain of function in oncogenes, we

could consult the master list of synthetic lethal partnerships, find the lethal association with the identified tumour suppressor or oncogene and administer the treatment accordingly. Given that the average cost of a year's worth of Imatinib, one of the first small molecules designed to specifically target a cancer-specific mutation by selectively inhibiting the oncogenic BCR-ABL gene fusion and used in the treatment of chronic mylogenous leukemia and gastrointestinal stromal tumours, is between $32,000 and $71,000, the additional cost of running genome sequencing to gather information on appropriate treatment paradigms seems inconsequential given the potential for immediate effectiveness (Hislop et al, 2011). Furthermore, identification of potential patient specific treatments using synthetic lethal approaches could also offer a cost reduction to healthcare as only treatments based on scientific evidence will be administered, and gone will be the days when often ineffective broad spectrum, non-specific chemotherapeutic agents targeting only highly proliferative cells are administered to most cancer patients. The benefits of synthetic lethal technologies (i.e. patient specific, cost saving in the long term for healthcare, fewer side effects, no/less additional treatments such as radiotherapy or combination chemotherapy needed) far outweigh potential drawbacks (i.e. greater expense in the short term). There is thus a great need to expand the repertoire of known synthetic lethal combinations in human cells.

One other area that needs to be investigated further is the identification of potent and specific inhibitors to synthetic lethal partner

proteins, highlighted by the use of PARP1 inhibitors in BRCA-mutated cells. Once identified, the synthetic lethal partner needs to be disrupted in some fashion, and this is where development of small molecule inhibitors will flourish. However, some proteins will not be targetable using small molecule inhibitors due to certain aspects of the proteins themselves. For example, most small molecule inhibitors target a protein's active site (e.g. PARP1 inhibitors Olaparib and BSI-201). It may therefore be impossible to target catalytically inactive proteins using small molecule inhibitors. In this instance, one could target the partner protein using siRNA technology. The systemic delivery of siRNA is receiving increasing attention. For example, through the use of lipid-, polymer- and nanoparticle-based delivery vehicles, the stability, bioavailability and target specificity of siRNAs systemically administered has increased exponentially (Ifediba & Moore, 2012). However, delivery into solid tumours remains a challenge (Rahman et al, 2012). It is therefore critical that the development of effective siRNA delivery tools be investigated to maximize the benefit of treatment based on synthetic lethality.

Furthermore, as our ability to target delivery vehicles specifically to cancer cells improves, so too would our treatment options. For example, if such a vehicle were to be generated, a new treatment paradigm emerges where both pairs of a synthetic lethal partnership can be selectively targeted (e.g. A12B4C3 for PNKP inhibition coupled with an siRNA towards SHP-1) to cancer cells using the same vehicle. Thus the need to rely on cancer specific mutations for treatment options decreases.

5.1.4 Conclusions

We have found 425 potential synthetic lethal partners of PNKP, including 14 known tumour suppressors. This value does not include those proteins in the remaining 411 'hits' that are tumour suppressors, yet are currently awaiting identification, implying the clinical benefit of PNKP-based treatment paradigms holds great potential beyond what is stated here. Of these 14 tumour suppressors, we chose to further investigate two, SHP-1 and PTEN, as these proteins have been shown to be lost is a substantial number of sporadic cancers.

We found that disruption of SHP-1 function allows an accumulation of ROS in cells, the resulting DNA damage from which PNKP-deficient cells cannot repair. There is thus an increase in the level of DNA damage in these cells until the accumulation of damage ultimately becomes cytotoxic and the cells undergo apoptosis.

Apoptosis is the preferred method of cell death, as opposed to necrosis. Necrotic cells release cytotoxic cell constituents that have a damaging effect on neighbouring cells, or induce an immune response. Apoptotic cells do not cause such a response, and instead apoptotic cells are phagocytized by macrophages in a highly regulated process. Therefore, SHP-1 and PTEN deficient cancers are ideal candidates for treatment targeting PNKP function as damage to neighbouring tissues will be minimized. Interestingly, cells that are PNKP/PTEN doubly dysfunctional also undergo apoptosis, and the critical function of PTEN lies

in its cytoplasmic phosphatase activity, most likely in signal transduction pathways.

We were then keen to discover the precise function and repair capacity of PNKP responsible for synthetic lethality. We found that it is PNKP's function in NHEJ that is critical for lethality and that both catalytic functions of PNKP, i.e. 3' phosphatase and 5' kinase, are important for synthetic lethality. However, when both activities are targeted simultaneously, there is a significant increase in cell killing during treatment.

Ideally, every human synthetic lethal association will eventually be determined. With this information we will be better able to effectively treat patients on an individual basis. For example, a patient may come to the clinic to have their cancer assayed. After determining which proteins are deficient in that patients particular cancer, we could consult the master list of synthetic lethal associations and assign a personalized treatment regimen specific to their cancer. This will provide a substantial reduction in the cost of cancer therapy as a whole as ineffective treatment paradigms will not be given, potentially saving millions of taxpayer dollars.

5.2 REFERENCES

Barbie DA, Tamayo P, Boehm JS, Kim SY, Moody SE, Dunn IF, Schinzel AC, Sandy P, Meylan E, Scholl C, Frohling S, Chan EM, Sos ML, Michel K, Mermel C, Silver SJ, Weir BA, Reiling JH, Sheng Q, Gupta PB, Wadlow RC, Le H, Hoersch S, Wittner BS, Ramaswamy S, Livingston DM, Sabatini DM, Meyerson M, Thomas RK, Lander ES, Mesirov JP, Root DE, Gilliland DG, Jacks T, Hahn WC (2009) Systematic RNA interference reveals that oncogenic KRAS-driven cancers require TBK1. *Nature***462:** 108-112

Cariaga-Martinez AE, Lorenzati MA, Riera MA, Cubilla MA, De La Rossa A, Giorgio EM, Tiscornia MM, Gimenez EM, Rojas ME, Chaneton BJ, Rodriguez DI, Zapata PD (2009) Tumoural prostate shows different expression pattern of somatostatin receptor 2 (SSTR2) and phosphotyrosine phosphatase SHP-1 (PTPN6) according to tumour progression. *Adv Urol***:** 723831

Delibrias CC, Floettmann JE, Rowe M, Fearon DT (1997) Downregulated expression of SHP-1 in Burkitt lymphomas and germinal center B lymphocytes. *J Exp Med***186:** 1575-1583

Freschauf GK, Karimi-Busheri F, Ulaczyk-Lesanko A, Mereniuk TR, Ahrens A, Koshy JM, Rasouli-Nia A, Pasarj P, Holmes CF, Rininsland F, Hall DG, Weinfeld M (2009) Identification of a small molecule inhibitor of

the human DNA repair enzyme polynucleotide kinase/phosphatase. *Cancer Res***69:** 7739-7746

Freschauf GK, Mani RS, Mereniuk TR, Fanta M, Virgen CA, Dianov GL, Grassot JM, Hall DG, Weinfeld M (2010) Mechanism of action of an imidopiperidine inhibitor of human polynucleotide kinase/phosphatase. *J Biol Chem***285:** 2351-2360

Goga A, Yang D, Tward AD, Morgan DO, Bishop JM (2007) Inhibition of CDK1 as a potential therapy for tumours over-expressing MYC. *Nat Med***13:** 820-827

Hara S, Nakashiro K, Klosek SK, Ishikawa T, Shintani S, Hamakawa H (2006) Hypoxia enhances c-Met/HGF receptor expression and signaling by activating HIF-1alpha in human salivary gland cancer cells. *Oral Oncol***42:** 593-598

Hayashi M, Sakata M, Takeda T, Tahara M, Yamamoto T, Okamoto Y, Minekawa R, Isobe A, Ohmichi M, Tasaka K, Murata Y (2005) Up-regulation of c-met protooncogene product expression through hypoxia-inducible factor-1alpha is involved in trophoblast invasion under low-oxygen tension. *Endocrinology***146:** 4682-4689

Hislop J, Quayyum Z, Elders A, Fraser C, Jenkinson D, Mowatt G, Sharma P, Vale L, Petty R (2011) Clinical effectiveness and cost-effectiveness of imatinib dose escalation for the treatment of unresectable and/or metastatic gastrointestinal stromal tumours that have progressed on treatment at a dose of 400 mg/day: a systematic review and economic evaluation. *Health Technol Assess***15:** 1-178

Ifediba MA, Moore A (2012) In vivo imaging of the systemic delivery of small interfering RNA. *Wiley Interdiscip Rev Nanomed Nanobiotechnol*

Kaelin WG, Jr. (2005) The concept of synthetic lethality in the context of anticancer therapy. *Nat Rev Cancer***5:** 689-698

Kennedy RD, Chen CC, Stuckert P, Archila EM, De la Vega MA, Moreau LA, Shimamura A, D'Andrea AD (2007) Fanconi anemia pathway-deficient tumour cells are hypersensitive to inhibition of ataxia telangiectasia mutated. *J Clin Invest***117:** 1440-1449

Luo J, Emanuele MJ, Li D, Creighton CJ, Schlabach MR, Westbrook TF, Wong KK, Elledge SJ (2009) A genome-wide RNAi screen identifies multiple synthetic lethal interactions with the Ras oncogene. *Cell***137:** 835-848

Molenaar JJ, Ebus ME, Geerts D, Koster J, Lamers F, Valentijn LJ, Westerhout EM, Versteeg R, Caron HN (2009) Inactivation of CDK2 is synthetically lethal to MYCN over-expressing cancer cells. *Proc Natl Acad Sci U S A***106:** 12968-12973

O'Brien T, Stokoe D (2009) Converting cancer mutations into therapeutic opportunities. *EMBO Mol Med***1:** 297-299

Oka T, Yoshino T, Hayashi K, Ohara N, Nakanishi T, Yamaai Y, Hiraki A, Sogawa CA, Kondo E, Teramoto N, Takahashi K, Tsuchiyama J, Akagi T (2001) Reduction of hematopoietic cell-specific tyrosine phosphatase SHP-1 gene expression in natural killer cell lymphoma and various types of lymphomas/leukemias : combination analysis with cDNA expression array and tissue microarray. *Am J Pathol***159:** 1495-1505

Overington JP, Al-Lazikani B, Hopkins AL (2006) How many drug targets are there? *Nat Rev Drug Discov***5:** 993-996

Pennacchietti S, Michieli P, Galluzzo M, Mazzone M, Giordano S, Comoglio PM (2003) Hypoxia promotes invasive growth by transcriptional activation of the met protooncogene. *Cancer Cell***3:** 347-361

Rahman MA, Amin AR, Wang X, Zuckerman JE, Choi CH, Zhou B, Wang D, Nannapaneni S, Koenig L, Chen Z, Chen ZG, Yen Y, Davis ME, Shin

DM (2012) Systemic delivery of siRNA nanoparticles targeting RRM2 suppresses head and neck tumour growth. *J Control Release*

Rask-Andersen M, Almen MS, Schioth HB (2011) Trends in the exploitation of novel drug targets. *Nat Rev Drug Discov***10:** 579-590

Rasouli-Nia A, Karimi-Busheri F, Weinfeld M (2004) Stable down-regulation of human polynucleotide kinase enhances spontaneous mutation frequency and sensitizes cells to genotoxic agents. *Proc Natl Acad Sci U S A***101:** 6905-6910

Scholl C, Frohling S, Dunn IF, Schinzel AC, Barbie DA, Kim SY, Silver SJ, Tamayo P, Wadlow RC, Ramaswamy S, Dohner K, Bullinger L, Sandy P, Boehm JS, Root DE, Jacks T, Hahn WC, Gilliland DG (2009) Synthetic lethal interaction between oncogenic KRAS dependency and STK33 suppression in human cancer cells. *Cell***137:** 821-834

Solimini NL, Luo J, Elledge SJ (2007) Non-oncogene addiction and the stress phenotype of cancer cells. *Cell* **130:** 986-988

Thomas GV, Tran C, Mellinghoff IK, Welsbie DS, Chan E, Fueger B, Czernin J, Sawyers CL (2006) Hypoxia-inducible factor determines sensitivity to inhibitors of mTOR in kidney cancer. *Nat Med* **12:** 122-127

Weinfeld M, Mani RS, Abdou I, Aceytuno RD, Glover JN (2011) Tidying up loose ends: the role of polynucleotide kinase/phosphatase in DNA strand break repair. *Trends Biochem Sci*

Weinstein IB (2002) Cancer. Addiction to oncogenes--the Achilles heal of cancer. *Science* **297:** 63-64

Wong KM, Hudson TJ, McPherson JD (2011) Unraveling the genetics of cancer: genome sequencing and beyond. *Annu Rev Genomics Hum Genet* **12:** 407-430

Zhu T, Chen L, Du W, Tsuji T, Chen C (2010) Synthetic Lethality Induced by Loss of PKC delta and Mutated Ras. *Genes Cancer* **1:** 142-151

Appendix A: Supplementary material and analysis from Chapter 2

Genetic screening for synthetic lethal partners of polynucleotide kinase/phosphatase: potential for targeting SHP-1 depleted cancers

[1]Todd R. Mereniuk, [2]Robert A. Maranchuk, [2]Anja Schindler, [1]Jonathan C. Penner, [1]Gary K. Freschauf, [3]Samar Hegazy, [3]Raymond Lai, [2]Edan Foley, and [1]Michael Weinfeld

Affiliations of authors:
[1]Experimental Oncology, Department of Oncology, University of Alberta, Edmonton, AB, Canada T6G 1Z2
[2]Department of Medical Microbiology and Immunology, University of Alberta, Edmonton, AB, Canada T6G 2S2
[3]Department of Laboratory Medicine and Pathology, University of Alberta, Edmonton, AB, Canada T6G 1Z2

Correspondence to: Michael Weinfeld
Cross Cancer Institute
University of Alberta
11560 University Ave
Edmonton, AB, Canada, T6G 1Z2
Tel: 780 432 8438
Fax: 780 432 8428
E-mail: michael.weinfeld@albertahealthservices.ca.

Running title: PNKP/SHP-1 synthetic lethality, Supplemental Material

Key words: Synthetic lethality, genetic screen, reactive oxygen species, polynucleotide kinase/phosphatase, SHP-1

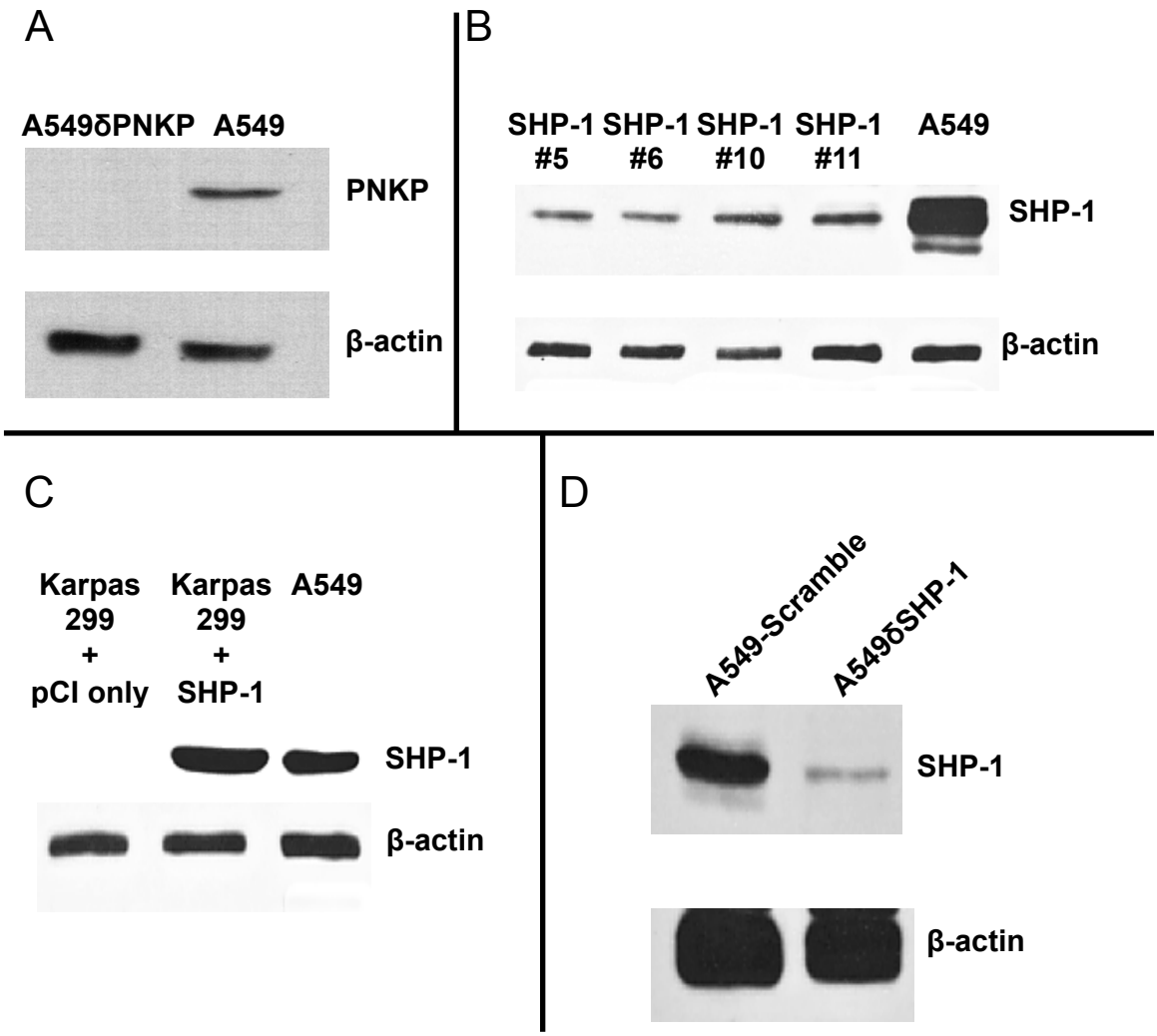

Supplemental Figure A.1. Western blots of key proteins used during experimentation. (A) Stable knockdown of PNKP in A549δPNKP compared to A549-Scramble control lysate. (B) Transient knockdown of SHP-1 in A549 using four distinct siRNAs targeting SHP-1 mRNA. (C) Re-expression of SHP-1 in Karpas 299 cells alongside the vector only control (Karpas+pCI) and a positive control (A549). (D) Level of SHP-1 protein remaining in the stable A549δSHP-1 cell line.

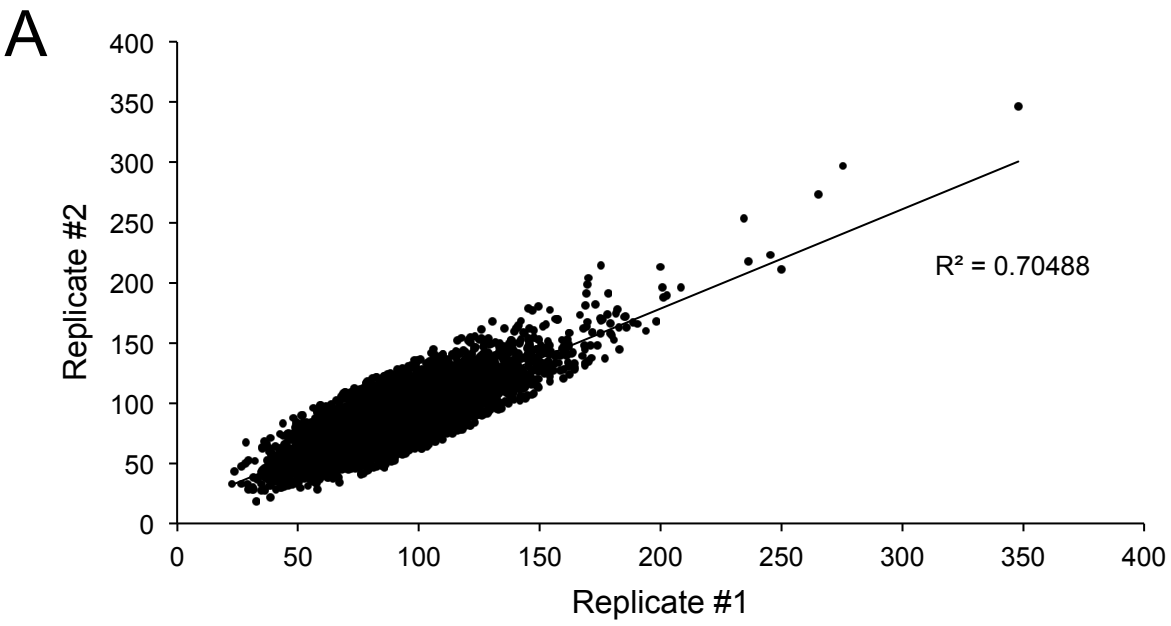
A
Replicate #2
Replicate #1
R² = 0.70488
0
50
100
150
200
250
300
350
400

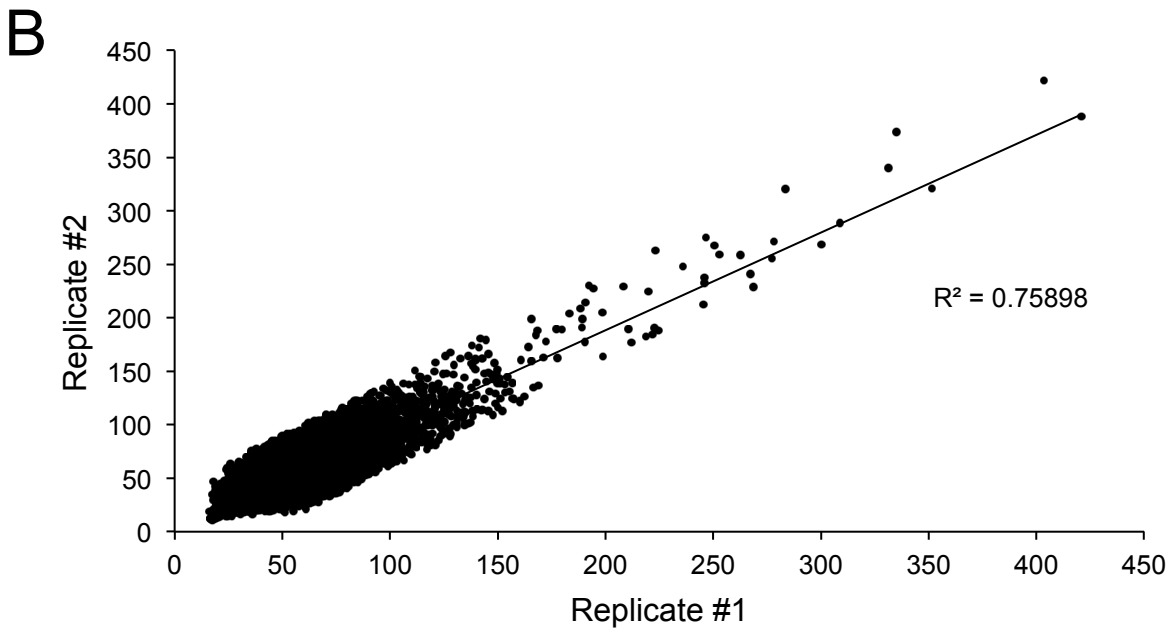
B
Replicate #2
Replicate #1
R² = 0.75898
0
50
100
150
200
250
300
350
400
450

Supplemental Figure A.2. Comparative analysis of the entire druggable genome siRNA screen. Cell viability values from all the plates in the screen were normalized and plotted against their respective replicates. In both the screen using (A) A549-Scramble cells and (B) A549δPNKP cells, the duplicates were shown to have good reproducibility with R^2 values of 0.705 and 0.759, respectively.

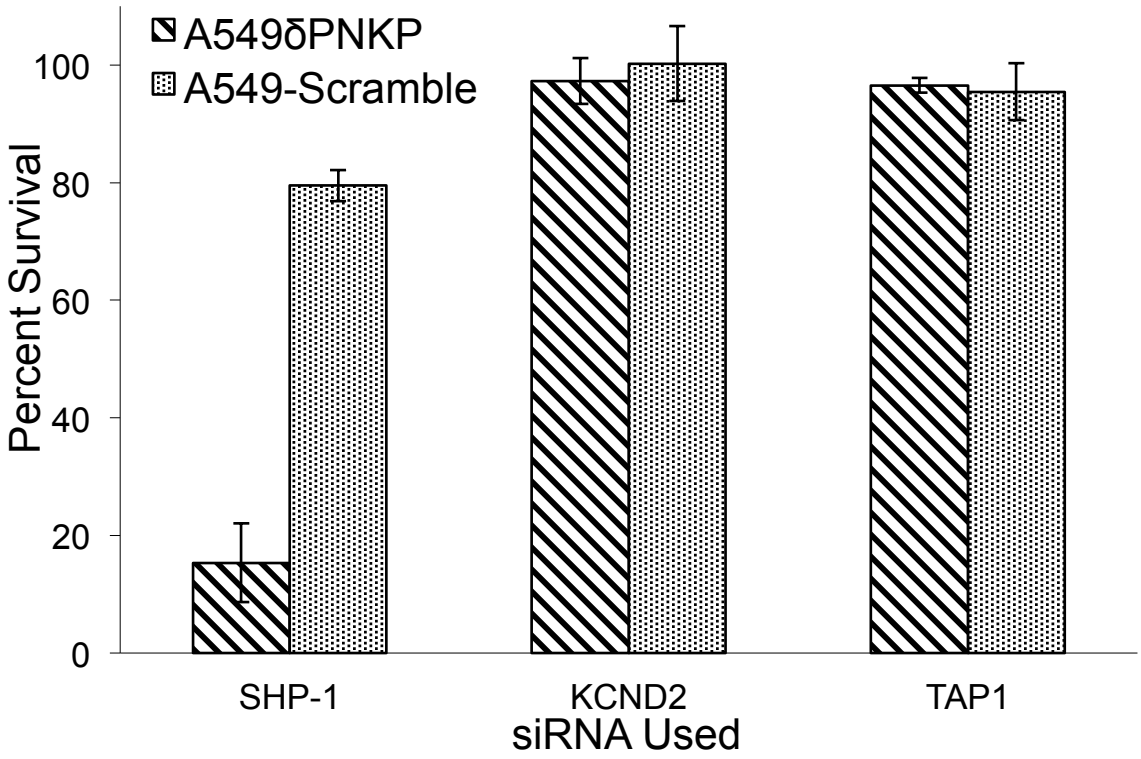

Supplemental Figure A.3. Survival of SHP-1 and PNKP co-disrupted cells compared to randomly selected “non-hits”. There was a large difference in survival between those that were deemed hits when compared to those that were labeled “non-hits”. Error bars represent standard error (± S.E.) from at least three independent determinations for the SHP-1 values. Error bars for the KCND2 and TAP1 values represent standard error (± S.E.) taken from the raw data from the duplicate screens.

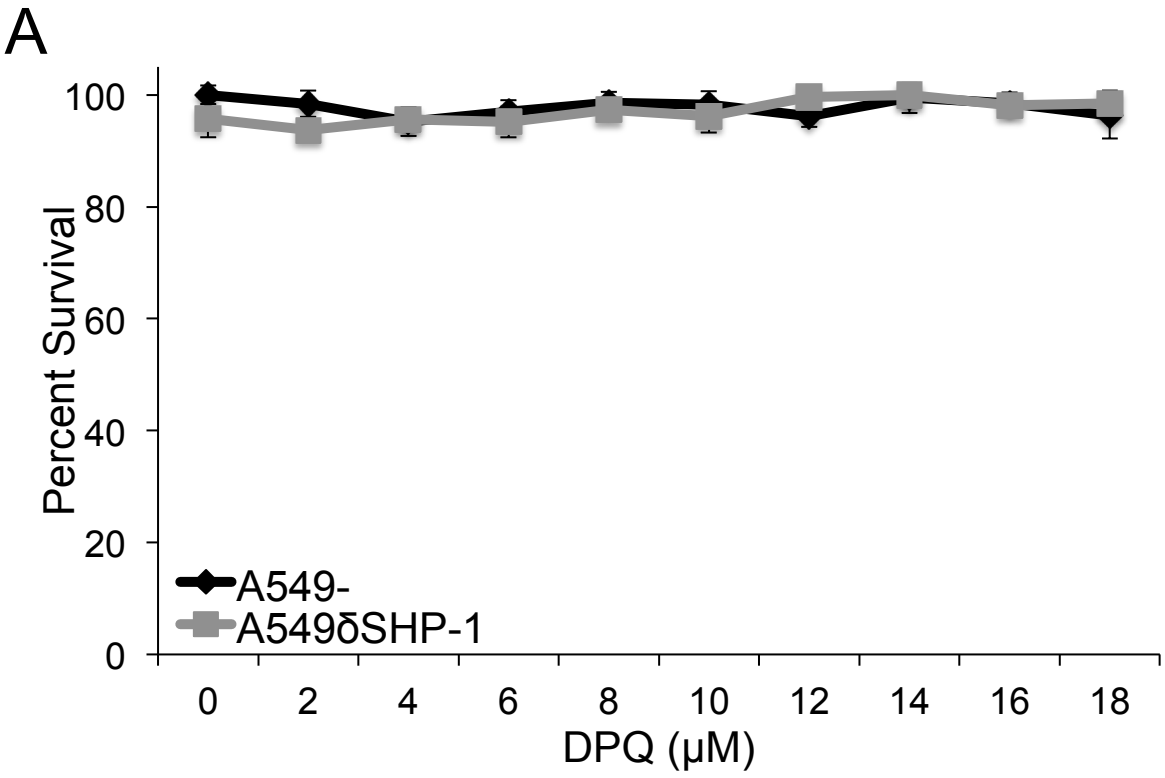
A
100
80
60
40
20
0
Percent Survival
A549-
A549δSHP-1
0
2
4
6
8
10
12
14
16
18
DPQ (μM)

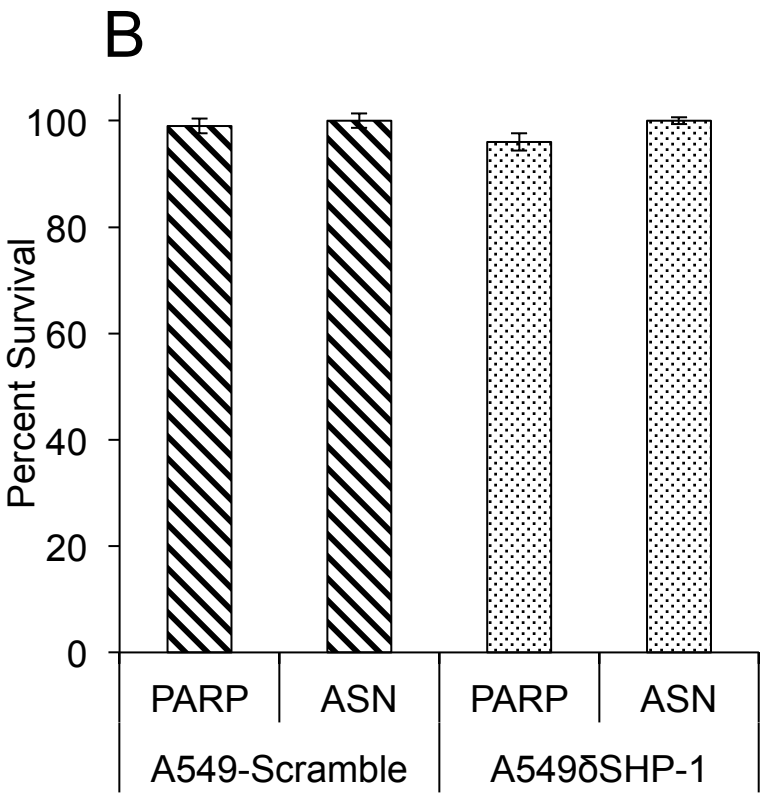
B
100
80
60
40
20
0
Percent Survival
PARP
ASN
PARP
ASN
A549-Scramble
A549δSHP-1

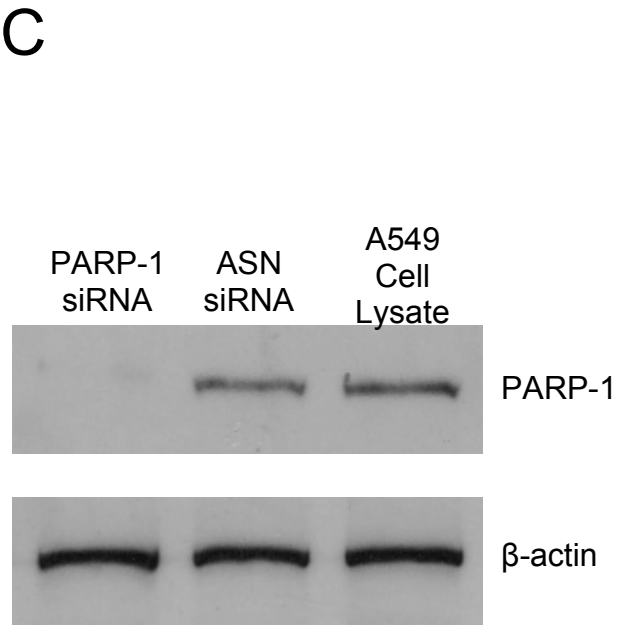
C
PARP-1 siRNA
ASN siRNA
A549 Cell Lysate
PARP-1
β-actin

Supplemental Figure A.4. Lack of synthetic lethality between PARP and SHP-1. A549-Scramble and A549δSHP-1 cells were treated with (A) the PARP-1 inhibitor DPQ or (B) PARP-1 or ASN siRNA. (C) Shows the western of the PARP-1 siRNA knockdown.

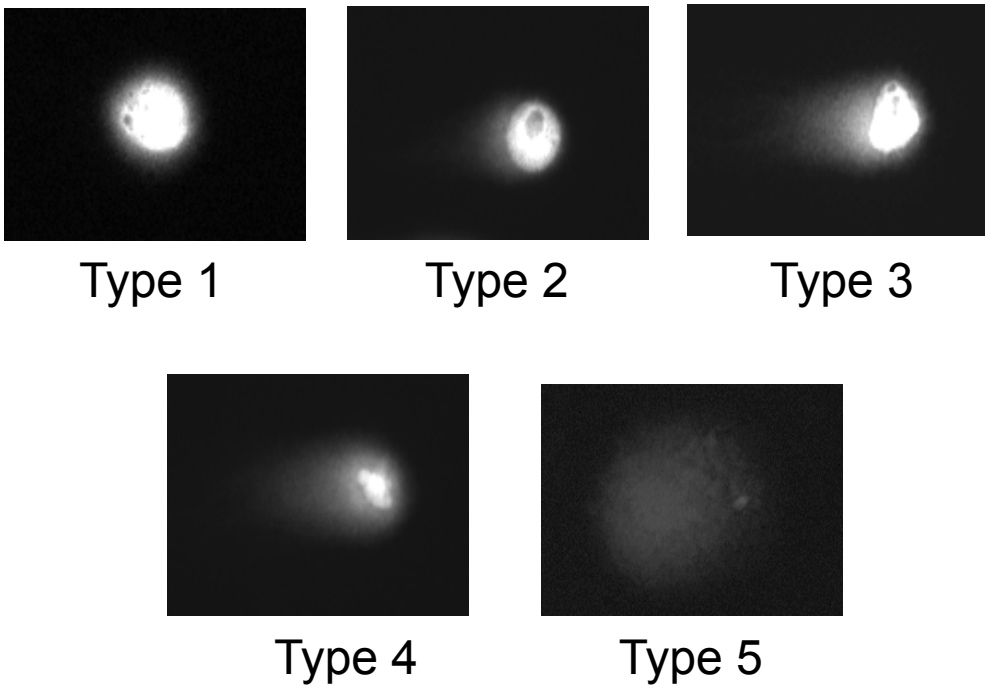

Supplemental Figure A.5. Characteristics of typical comets scored. The tail of the comets indicates the level of DNA damage present in these cells beginning with type 1 comets that showed no DNA damage, progressing to type 5 comets, which showed the most DNA damage (Kumaravel et al, 2009).

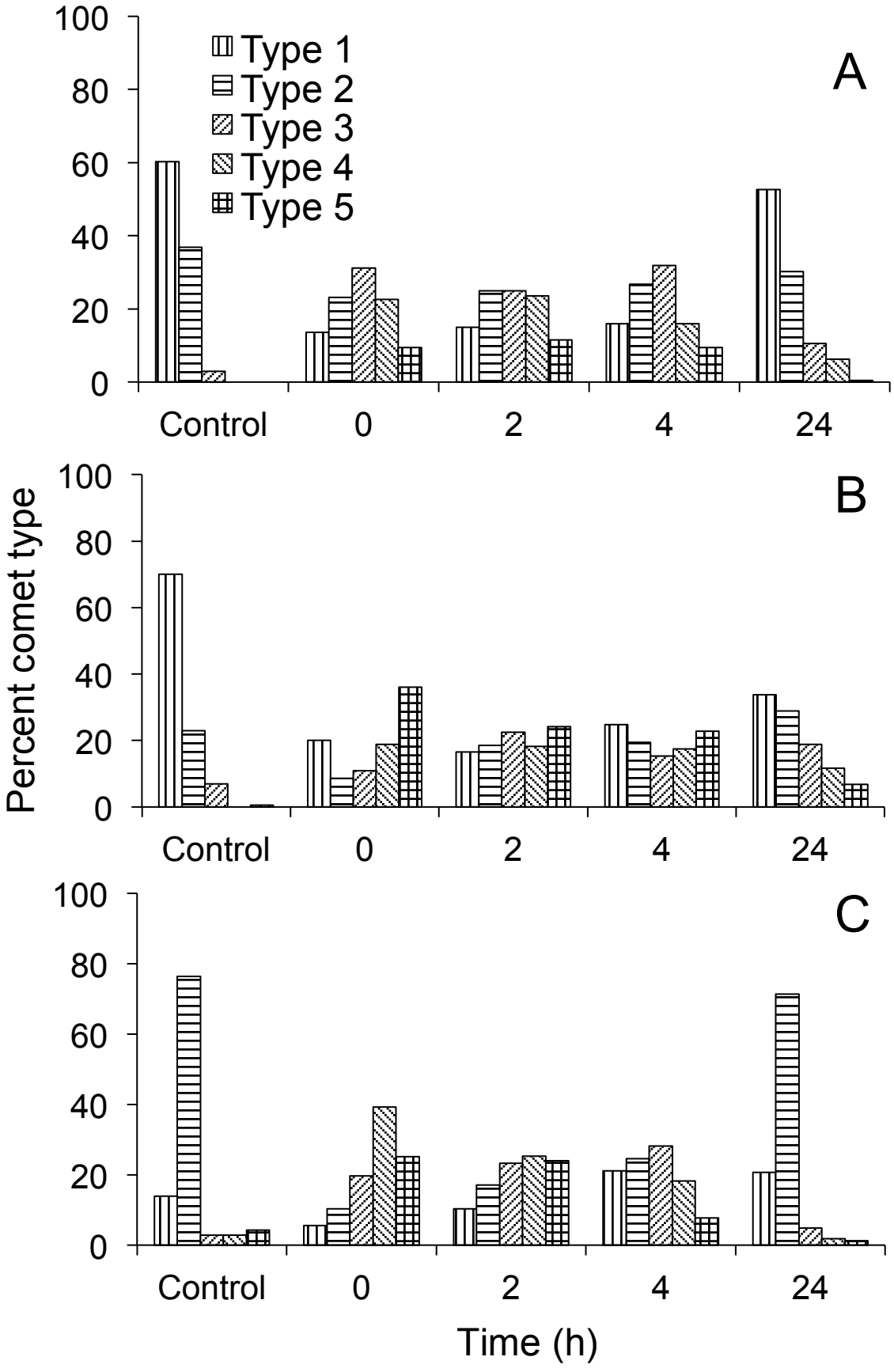
Type 1
Type 2
Type 3
Type 4
Type 5
A
B
C
Percent comet type
100
80
60
40
20
0
Control
0
2
4
24
Time (h)

Supplemental Figure A.6. Influence of SHP-1 on DNA DSBR. Cells were plated 24 h in advance, after which they were subjected to γ-radiation (5 Gy). The repair of DSBs at different times after irradiation was monitored by single-cell gel electrophoresis (comet assay) under neutral conditions (A-C) (see Supplemental Fig. A.5 for classification of comets). (A) DSBs in A549-Scramble cells were almost completely repaired by 24 h. (B) A549δPNKP cells showed severely retarded repair of DSBs. (C) DSB repair in A549δSHP-1 cells showed similar kinetics to control A549-Scramble cells, but there appeared to be a higher basal level of DSBs in unirradiated A549δSHP-1 cells

Supplemental Table A.1: List of potential synthetic lethal partners of PNKP identified through screening ordered according to placement on Druggable Genome plate

Plate ID	Position	% Survival	% Control	Gene Name	Gene Description
Dg1	A4	22	91	USP8	ubiquitin specific peptidase 8
Dg1	B10	28	59	CHRNG	cholinergic receptor nicotinic gamma
Dg1	C4	30	73	FNDC3B	fibronectin type 3
Dg1	C6	24	51	TICAM1	toll-like receptor adaptor molecule 1
Dg1	C8	31	63	KIAA0317	KIAA0317
Dg1	C10	26	64	ABCE1	ATP-binding cassette,subfamily E, member1
Dg1	D3	26	77	RASSF5	Ras association (Ral GDS/AF-6)
Dg1	D6	28	47	ALOX5	arachidonate 5-lipoxygenase
Dg1	D9	28	52	AFM	afamin
Dg1	D11	28	58	CFLAR	CASP8 and FADD like apoptosis regulator
Dg1	E2	29	87	CD79A	CD79a molecule, immunoglobulin-associated
Dg1	E10	26	70	TRIP6	thyroid hormone receptor interactor 6
Dg1	F10	30	72	APTX	aprataxin
Plate ID	**Position**	**% Survival**	**% Control**	**Gene Name**	**Gene Description**
Dg2	A10	31	56	USP45	ubiquitin specific peptidase 45
Dg2	B3	30	70	SIM1	single-minded homolog 1
Dg2	B8	25	45	C2orf28	chr. 2 open reading frame 28
Dg2	B9	30	70	APP	amyloid beta (A4) precursor protein
Dg2	C3	28	63	GNRH1	gonadotropin-releasing hormone 1
Dg2	C7	31	50	AIP	aryl hydrocarbon receptor interacting protein
Dg2	C8	30	71	IL11RA	interleukin 11 receptor alpha

Dg2	D3	29	80	SLC5A5	solute carrier family 5(sodium iodide symporter)
Dg2	D4	29	75	RNF141	ring finger protein 141
Dg2	D5	31	62	MTA1	metastasis associated 1
Dg2	E2	29	82	GYPC	glycophorin C (Gerbich blood group)
Dg2	E3	28	75	SHH	sonic hedgehog homolog
Dg2	E10	31	45	KIAA0999	KIAA0999
Dg2	F2	28	93	WNT1	wingless-type MMTV integration site family 1
Dg2	G4	30	66	AMIGO2	adhesion molecule with Ig-like domain 2
Dg2	G7	21	29	COPB2	coatomer protein complex subunit beta 2
Plate ID	**Position**	**% Survival**	**% Control**	**Gene Name**	**Gene Description**
Dg3	F3	28	69	ITGB6	integrin beta 6
Dg3	G4	30	67	RAD23B	RAD23 homolog B
Plate ID	**Position**	**Survival**	**% Control**	**Gene Name**	**Gene Description**
Dg4	B4	30	50	RHBDF1	rhomboid 5 homolog 1
Dg4	B10	25	53	SLC25A17	solute carrier family 25
Dg4	C3	22	52	SCH8A	sodium channel voltage gated type 8 alpha
Dg4	C5	22	49	LBR	lamin B receptor
Dg4	C6	23	49	UQCRH	ubiquinol-cytochrome c reductase hinge protein
Dg4	C7	29	41	HTATIP2	HIV-1 Tat interactive protein 2, 30 kDa
Dg4	C8	27	35	CD8B	CD8b molecule
Dg4	D2	27	41	STEAP4	STEAP family member 4
Dg4	D4	28	39	TAF10	TAF10 pol II TATA box binding (TBP)
Dg4	D5	23	40	GNS	glucosamine (N-actelyt)-6-sulfate
Dg4	E3	24	37	UHRF2	ubiquitin-like with PHD and ring finger domain 2
Dg4	E5	23	48	WIPF2	WAS/WASL interacting protein family member 2
Dg4	E9	25	59	AIPL1	aryl hydrocarbon receptor interacting protein 1

Dg4	F3	27	58	SMPD1	sphingomyelin phosphodiesterase 1
Dg4	F5	23	52	CCL22	chemokine (C-C motif) ligand 22
Dg4	F9	24	67	TRERF1	transcriptional regulating factor 1
Dg4	F10	22	53	KCNT1	potassium channel subfamily T member 1
Dg4	G3	23	68	HR	hairless homolog
Dg4	G4	24	74	GUCA1B	guanylate cyclase activator 1 B (retina)
Dg4	G5	23	57	CD80	CD80
Dg4	G7	26	67	EIF2C4	eukaryotic translation initiation factor 2C,4
Dg4	H3	26	74	PCMTD2	protein-L-isoaspartate (D-aspartate)
Dg4	H5	28	78	UBC	ubiquitin
Plate ID	**Position**	**% Survival**	**% Control**	**Gene Name**	**Gene Description**
Dg5	A5	32	61	PSMD2	proteasome (prosome, macropain) 26S
Plate ID	**Position**	**% Survival**	**% Control**	**Gene Name**	**Gene Description**
Dg6	C3	30	89	MEFV	mediterranean fever
Dg6	C4	30	77	ABCB5	ATP binding cassette, subfamily B (MDR/TAP)
Dg6	C7	30	64	EFNA1	ephrin-A1
Dg6	D6	30	77	KLK15	Kallikrein-related peptidase 15
Dg6	D9	30	89	FRAG1	FGF receptor activating protein 1
Dg6	F5	27	89	RBM24	RNA binding motif protein 24
Plate ID	**Position**	**% Survival**	**% Control**	**Gene Name**	**Gene Description**
Dg7	D6	29	86	RGS12	regulator of G-protein signaling 12
Plate ID	**Position**	**% Survival**	**% Control**	**Gene Name**	**Gene Description**

Dg8					
Plate ID	**Position**	**% Survival**	**% Control**	**Gene Name**	**Gene Description**
Dg9	A5	28	41	CKAP5	cytoskeleton associated protein 5
Dg9	C3	23	51	EXO1	exonuclease 1
Dg9	C4	29	55	ECE1	endothelin converting enzyme 1
Dg9	C6	29	55	DAK	dihydroxyacetone kinase 2 homolog
Dg9	C8	26	53	BCAM	basal cell adhesion molecule
Dg9	D5	23	52	CCNA1	cyclin A1
Dg9	D9	18	30	KIF11	kinesin family member 11
Dg9	E3	27	74	CPA5	carboxypeptidase A5
Dg9	E4	30	67	MGC52282	hypothecial locus MGC52282
Dg9	E9	29	66	ABCC13	ATP binding cassette subfamily C (CFTR/MRP)
Dg9	F5	24	83	KCNQ1	potassium voltage gated channel, KQT like 1
Dg9	F7	28	58	IFNW1	interferon omega 1
Dg9	G3	26	61	SDCBP	syndecan binding
Dg9	G8	24	62	STAT2	signal transducer and activator of transc. 2
Plate ID	**Position**	**% Survival**	**% Control**	**Gene Name**	**Gene Description**
Dg10	B3	28	63	CCHC	CCHC-type zinc finger nucleic acid binding
Dg10	B5	25	97	TREX1	three prime repair exonuclease 1
Dg10	B6	25	75	GNA15	guanine nucleotide binding protein alpha 15
Dg10	B10	30	69	GTPBP4	GTP binding protein 4
Dg10	C3	27	63	MASP2	mannan-binding lectin serine peptidase 2
Dg10	C4	22	48	PSMD14	proteasome 26S subunit non-ATPase 14
Dg10	D5	26	40	BMP3	bone morphogenetic protein 3
Dg10	D6	29	70	ZNF280A	zinc finger protein 280A

Dg10	D7	22	60	IL17A	interleukin 17A
Dg10	E6	27	72	CAPN3	calpain 3 (p94)
Dg10	E8	29	66	IRF2BP1	interferon regulatory factor 2 binding protein 1
Dg10	E10	25	60	GRIA4	glutamate receptor ionotrophic AMPA4
Dg10	F5	29	52	HSD17B3	hydroxysteroid (17-beta) dehydrogenase 3
Dg10	F6	26	68	CYP3A5	cytochrome P450 family 3 subfamily A poly. 5
Dg10	F8	29	54	ALDH7A1	aldehyde dehydrogenase 7 family mamber A1
Dg10	F9	28	61	TRIM65	tripartite motif-containing 65
Plate ID	**Position**	**% Survival**	**% Control**	**Gene Name**	**Gene Description**
Dg11	D8	31	43	FAM173B	family with seq. similarity 173 member B
Plate ID	**Position**	**% Survival**	**% Control**	**Gene Name**	**Gene Description**
Dg12					
Plate ID	**Position**	**% Survival**	**% Control**	**Gene Name**	**Gene Description**
Dg13	C3	28	61	IL16	interleukin 16
Dg13	C4	30	85	BPIL2	bactericidal/permeability-increasing protein-like2
Dg13	F10	30	74	SMUG1	single-strand-selctective uracil-DNA glycosylase1
Dg13	H3	28	69	CLEC4A	C-type lectin domain family 4 member A
Plate ID	**Position**	**% Survival**	**% Control**	**Gene Name**	**Gene Description**
Dg14	C2	31	70	EIF3C	eukaryotic translation initiation factor 3 subunit C
Dg14	F5	22	50	RPLP2	ribosomal protein large P2
Plate	**Position**	**%**	**%**	**Gene Name**	**Gene Description**

ID		Survival	Control		
Dg15	B2	26	116	HERPUD1	homocysteine-inducible ER stress inducible
Dg15	B9	29	31	DHRS1	dehydrogenase/reductase (SDR family) 1
Plate ID	**Position**	**% Survival**	**% Control**	**Gene Name**	**Gene Description**
Dg16	B6	30	61	WTAP	wilms tumour 1 associated protein
Dg16	F8	24	45	MBL2	mannose-binding lectin 2, soluble
Plate ID	**Position**	**% Survival**	**% Control**	**Gene Name**	**Gene Description**
Dg17	D4	30	115	HSD17B13	hydroxysteroid (17-beta) dehydrogenase 13
Plate ID	**Position**	**% Survival**	**% Control**	**Gene Name**	**Gene Description**
Dg18	C6	28	87	SPRYD5	SPRY domain containing 5
Plate ID	**Position**	**% Survival**	**% Control**	**Gene Name**	**Gene Description**
Dg19	C5	28	81	IL31RA	interleukin 31 receptor A
Dg19	D3	25	49	RBM8A	RNA binding motif protein 8A
Dg19	H4	28	76	MKRN2	makorin ring finger protein 2
Plate ID	**Position**	**% Survival**	**% Control**	**Gene Name**	**Gene Description**
Dg20	C3	24	90	ITSN2	intersectin 2
Plate ID	**Position**	**% Survival**	**% Control**	**Gene Name**	**Gene Description**
Dg21					

Plate ID	**Position**	**% Survival**	**% Control**	**Gene Name**	**Gene Description**
Dg22	C3	30	153	IGSF10	immunoglobulin superfamily member 10
Dg22	D10	29	93	C2orf42	chr. 2 open reading frame 42
Dg22	F6	19	58	EIF4A3	eukaryotic translation initiation factor 4A isoform3
Dg22	F7	24	81	DUSP27	dual specificity phosphatase 27
Dg22	G5	22	101	MRGPRD	MAS-related GPR member D
Dg22	G6	25	99	CYP2S1	cytochrome P450 family 2 sub S poly 1
Dg22	G10	27	65	KCNK17	potassium channel sub K member 17
Dg22	H3	30	105	F13A1	coagulation factor XIII A1 poly.
Dg22	H5	25	147	BTC	betacellulin
Plate ID	**Position**	**% Survival**	**% Control**	**Gene Name**	**Gene Description**
Plate ID	**Position**	**% Survival**	**% Control**	**Gene Name**	**Gene Description**
Dg24	B3	28	234	SERPINA12	serpin pepidase inhibitor clade A
Dg24	B5	25	139	MARCH2	membrane-associated ring finger (C3HC4) 2
Dg24	B6	30	153	GGH	gamma glutamyl hydrolase
Dg24	C5	24	129	JUP	hunction plakoglobin
Dg24	D5	17	73	RPL36	ribosomal protein L36
Dg24	H2	24	151	SPRYD5	SPRY domain conatining 5
Plate ID	**Position**	**% Survival**	**% Control**	**Gene Name**	**Gene Description**
Dg25	B7	28	118	DLAT	dihyrdolipoamide S-acetyltransferase
Dg25	C3	27	132	CYLD	cylindromastosis (turban tumour syndrome)
Dg25	E6	31	98	USP51	ubiquitin specific peptidase 51

Dg25	F2	25	56	SLC39A6	solute carrier family 39
Plate ID	**Position**	**% Survival**	**% Control**	**Gene Name**	**Gene Description**
Dg26	B3	29	83	CD4	CD4 molecule
Dg26	E5	25	40	ADAR	adenosine deaminase RNA specific
Dg26	F3	29	67	CD160	CD160 molecule
Dg26	G8	25	54	KCNJ12	potassium inwardly-rectifying channel subJ 12
Plate ID	**Position**	**% Survival**	**% Control**	**Gene Name**	**Gene Description**
Dg27	C10	28	62	RPSA	ribosomal protein SA
Dg27	D7	27	97	APOC3	apolipoprotein C-III
Dg27	F2	28	93	GNA12	guanine nucleotide binding protein alpha 12
Dg27	F9	27	42	CCT4	chaperonin containing TCP1 subunit 4 delta
Plate ID	**Position**	**% Survival**	**% Control**	**Gene Name**	**Gene Description**
Dg28					
Plate ID	**Position**	**% Survival**	**% Control**	**Gene Name**	**Gene Description**
Dg29					
Plate ID	**Position**	**% Survival**	**% Control**	**Gene Name**	**Gene Description**
Dg30					
Plate ID	**Position**	**% Survival**	**% Control**	**Gene Name**	**Gene Description**
Dg31					

Plate ID	**Position**	**% Survival**	**% Control**	**Gene Name**	**Gene Description**
Dg32					
Plate ID	**Position**	**% Survival**	**% Control**	**Gene Name**	**Gene Description**
Dg33	F7	33	53	ITGB4	integrin beta 4
Dg33	G3	26	55	PCSK2	proproetin convertase subtillisin/kexin type 2
Plate ID	**Position**	**% Survival**	**% Control**	**Gene Name**	**Gene Description**
Dg34					
Plate ID	**Position**	**% Survival**	**% Control**	**Gene Name**	**Gene Description**
Dg35					
Plate ID	**Position**	**% Survival**	**% Control**	**Gene Name**	**Gene Description**
Dg36	B2	27	86	BCL2L13	BCL2-like 13 (apoptosis facilitator)
Dg36	B3	18	88	PGGT1B	protein geranylgeranyltransferase type I beta
Dg36	C5	29	75	KCNJ11	potassium inwardly-rectifying channel sub J
Plate ID	**Position**	**% Survival**	**% Control**	**Gene Name**	**Gene Description**
Dg37	B3	25	112	NR1D2	nuclear receptor sub 1 group D member 2
Dg37	B10	27	84	MDM2	Mdm2 p53 binding protein homolog
Dg37	H3	22	53	KIF3A	kinesin family member 3A
Plate	**Position**	**%**	**%**	**Gene Name**	**Gene Description**

ID		Survival	Control		
Dg38	B2	32	69	TOB1	transducer of ERBB2, 1
Dg38	G6	27	83	TDG	thymine-DNA glycosylase
Dg38	H5	26	66	PLAT	plasminogen activator tissue
Plate ID	**Position**	**% Survival**	**% Control**	**Gene Name**	**Gene Description**
Dg39	B8	26	63	CR1L	complemenet componenet (3b/4b) receptor
Dg39	F4	24	52	TGFB1	transforming growth factor beta 1
Plate ID	**Position**	**% Survival**	**% Control**	**Gene Name**	**Gene Description**
Dg40	A9	24	44	CACNG4	calcium channel voltage gated gamma 4
Dg40	B10	29	51	C12orf72	chr. 12 open reading frame 72
Dg40	D5	31	74	APEH	N-acylaminacyl-peptide hydrolase
Dg40	D10	30	68	POU3F4	POU class 3 homeobox 4
Dg40	G8	28	47	BCL2L14	BCL2-like 14 (apoptosis facilitator)
Plate ID	**Position**	**% Survival**	**% Control**	**Gene Name**	**Gene Description**
Dg41	C10	29	59	GALNS	galactosamine (N-acetyl)-6-sulfate sulfatase
Plate ID	**Position**	**% Survival**	**% Control**	**Gene Name**	**Gene Description**
Dg42					
Plate ID	**Position**	**% Survival**	**% Control**	**Gene Name**	**Gene Description**
Dg43					

Plate ID	Position	% Survival	% Control	Gene Name	Gene Description
Dg44	B4	31	104	CXADR	coxsackie virus and adenovirus receptor
Dg44	B7	30	121	C1orf112	chr. 1 open reading frame 112
Dg44	G10	29	53	ZNF335	zinc finger protein 335
Plate ID	**Position**	**% Survival**	**% Control**	**Gene Name**	**Gene Description**
Dg45					
Plate ID	**Position**	**% Survival**	**% Control**	**Gene Name**	**Gene Description**
Dg46					
Plate ID	**Position**	**% Survival**	**% Control**	**Gene Name**	**Gene Description**
Dg47					
Plate ID	**Position**	**% Survival**	**% Control**	**Gene Name**	**Gene Description**
Dg48					
Plate ID	**Position**	**% Survival**	**% Control**	**Gene Name**	**Gene Description**
Plate ID	**Position**	**% Survival**	**% Control**	**Gene Name**	**Gene Description**
Dg50					
Plate ID	**Position**	**% Survival**	**% Control**	**Gene Name**	**Gene Description**

Plate ID	**Position**	**% Survival**	**% Control**	**Gene Name**	**Gene Description**
Dg52	B8	25	90	XPOT	exportin tRNA (nuclear export receptor tRNA)
Dg52	C8	24	52	RGPD5	RANBP2-like and GRIP domain conatining 5
Dg52	D8	33	54	RAB41	RAB41 member RAS oncogene family
Dg52	D11	32	65	GZMH	granzyme H(cathepsin G-like 2 protein h-CCPX)
Plate ID	**Position**	**% Survival**	**% Control**	**Gene Name**	**Gene Description**
Dg53	C8	28	60	USP44	ubiquitin specific peptidase 44
Plate ID	**Position**	**% Survival**	**% Control**	**Gene Name**	**Gene Description**
Dg54					
Plate ID	**Position**	**% Survival**	**% Control**	**Gene Name**	**Gene Description**
Dg55	C2	29	98	TNFSF12	tumour necrosis factor superfamily member 12
Dg55	C10	29	48	ELK1	ELK1 member of ETS oncogene family
Dg55	E4	25	81	HEXB	hexosaminidase B (beta poly)
Dg55	E5	29	64	PRKCSH	protein kinase C substrate 80K-H
Dg55	E7	25	66	NR2F1	nuclear receptor sub 2 group F member 1
Dg55	E8	32	60	Unidentified ORF	Unidentified ORF
Dg55	E9	33	80	CD300LB	CD300 molecule-like family member D
Dg55	F7	32	62	PH-4	hypoxia-inducible factor prolyl 4-hydroxylase
Dg55	G8	30	54	JMJD2A	jumonji domain containing 2A
Plate	**Position**	**%**	**%**	**Gene Name**	**Gene Description**

ID		Survival	Control		
Dg56	C4	26	105	CLCN3	chloride channel 3
Dg56	C8	32	86	HSP90B1	heat shock proetin 90kDa beta (Grp94) 1
Dg56	D10	29	93	MTMR1	myotubularin related protein 1
Plate ID	**Position**	**% Survival**	**% Control**	**Gene Name**	**Gene Description**
Plate ID	**Position**	**% Survival**	**% Control**	**Gene Name**	**Gene Description**
Dg58					
Plate ID	**Position**	**% Survival**	**% Control**	**Gene Name**	**Gene Description**
Dg59	B7	25	97	FOLR3	folate receptor 3 (gamma)
Dg59	B8	29	111	RAB7B	RAB7B member RAS oncogene family
Dg59	C10	28	79	UPF1	UPF1 regulator of nonsense transcripts homolog
Plate ID	**Position**	**% Survival**	**% Control**	**Gene Name**	**Gene Description**
Dg60					
Plate ID	**Position**	**% Survival**	**% Control**	**Gene Name**	**Gene Description**
Dg61	D8	31	65	CENPE	centromere protein E, 312 kDa
Plate ID	**Position**	**% Survival**	**% Control**	**Gene Name**	**Gene Description**
Dg62					
Plate	**Position**	**%**	**%**	**Gene Name**	**Gene Description**

ID		Survival	Control		
Dg63					
Plate ID	**Position**	**% Survival**	**% Control**	**Gene Name**	**Gene Description**
Dg 64					
Plate ID	**Position**	**% Survival**	**% Control**	**Gene Name**	**Gene Description**
Dg65					
Plate ID	**Position**	**% Survival**	**% Control**	**Gene Name**	**Gene Description**
Dg66	B4	25	51	RPL4	ribosomal protein L4
Dg66	B5	31	120	TXNL1	thioredoxin-like 1
Plate ID	**Position**	**% Survival**	**% Control**	**Gene Name**	**Gene Description**
Dg67	B5	26	88	ING3	inhibitor of growth family member 3
Dg67	D4	32	78	TPX2	TPX2 microtubule-associated homolog
Dg67	D5	32	67	MMP8	matrix metallopeptidase 8
Plate ID	**Position**	**% Survival**	**% Control**	**Gene Name**	**Gene Description**
Dg68	B2	32	79	KDELR3	KDEL(Lys-Asp-Glu-Leu) ER protein retention rec 3
Dg68	C7	32	111	PNMT	phenylethanolamine N-methyltransferase
Plate ID	**Position**	**% Survival**	**% Control**	**Gene Name**	**Gene Description**
Dg69	C4	27	39	RPS27A	ribosomal protein S27a

Plate ID	Position	% Survival	% Control	Gene Name	Gene Description
Dg70	B4	31	105	KLK4	kallikrein-related peptidase 4
Dg70	B5	31	83	SNX6	sorting nexin 6
Dg70	B7	32	67	THRA	thyroid hormone receptor alpha
Dg70	B9	24	117	Unidentified ORF	Unidentified ORF
Dg70	C8	29	128	Unidentified ORF	Unidentified ORF
Dg70	C9	28	125	Unidentified ORF	Unidentified ORF
Dg70	D7	32	65	TXNDC3	thioredoxin domain containing 3 (spermatozoa)
Dg70	D8	28	115	Unidentified ORF	Unidentified ORF
Dg70	D9	24	115	Unidentified ORF	Unidentified ORF
Dg70	D10	31	125	Unidentified ORF	Unidentified ORF
Dg70	D11	25	109	Unidentified ORF	Unidentified ORF
Dg70	E8	30	110	Unidentified ORF	Unidentified ORF
Dg70	E9	27	120	Unidentified ORF	Unidentified ORF
Dg70	F8	30	101	Unidentified ORF	Unidentified ORF
Dg70	F10	24	99	Unidentified ORF	Unidentified ORF
Dg70	G5	32	40	C8orf79	chr. 8 open reading frame 79

Plate ID	Position	% Survival	% Control	Gene Name	Gene Description
Gp1	B8	25	90	OR56B1	olfactory receptor family 56 sub B member 1
Gp1	B10	30	95	LGR5	leucine-rich repeat-conatining GPR 5
Gp1	C9	28	102	GPR172B	G-proetin coupled receptor 172B
Gp1	D7	29	72	GHRHR	growth hormone releasing hormone receptor
Gp1	E4	31	55	MC2R	melanocortin 2 receptor
Plate ID	**Position**	**% Survival**	**% Control**	**Gene Name**	**Gene Description**
Gp2	C11	23	42	FPR2	formyl peptide receptor 2
Gp2	D10	25	59	NMUR2	neuromedin U recetor 2
Gp2	E6	28	67	GPR61	G-protein coupled receptor 61
Plate ID	**Position**	**% Survival**	**% Control**	**Gene Name**	**Gene Description**
Gp3	B10	28	103	GPR44	G-protein coupled receptor 44
Gp3	C4	30	87	AVPR1A	arginine vasopressin receptor 1A
Plate ID	**Position**	**% Survival**	**% Control**	**Gene Name**	**Gene Description**
Gp4	A2	22	75	GHSR	growth hormone secretagogue receptor
Gp4	A4	29	68	GALR3	galanin receptor 3
Gp4	A5	30	66	FAM62A	family with seq similarity 62(C2 domain) A
Gp4	A6	31	76	GALR2	galanin receptor 2
Gp4	A8	30	90	CASR	calcium-sensing receptor
Gp4	B2	29	84	NPR3	natriuretic peptide receptor C/guanylate cyclase C
Gp4	B3	28	90	MC5R	melanocortin 5 receptor
Gp4	B4	31	96	TAAR1	trace amine associated receptor 1
Gp4	B5	28	103	GPR32	G-protein coupled receptor 32

Gp4	B10	22	106	GPR12	G-protein coupled receptor 12
Gp4	C3	23	67	CELSR1	cadherin, EGF LAG seven-pass G-type receptor 1
Gp4	C4	28	63	MAS1	MAS1 oncogene
Gp4	C5	28	68	OR5P3	olfactory receptor family 5 sub P member 3
Gp4	C6	27	63	NTSR1	neurotensin receptor 1
Gp4	C7	30	97	ADORA2A	adenosine A2a receptor
Gp4	C9	28	86	CHRM4	cholinergic receptor muscarinic 4
Gp4	C10	25	50	ADRB3	adrenergic beta-3 receptor
Gp4	C11	28	62	TAS2R43	taste receptor type 2 member 43
Gp4	D2	22	66	OR8G5	olfactory receptor family 8 sub G member 5
Gp4	D3	29	67	ADRA1B	adrenergic alpha-1B-receptor
Gp4	D4	26	76	GPR158	G-protein coupled receptor 158
Gp4	D5	25	76	CCR2	chemokine (C-C motif) receptor 2
Gp4	D6	29	71	MAS1L	MAS1 oncogene-like
Gp4	D7	25	66	TAAR9	trace amine associated receptor 9
Gp4	D8	29	85	LOC727811	similar to chemokine (C-C motif) receptor -like 2
Gp4	D10	29	61	SSTR3	somatostatin receptor 3
Gp4	E2	25	72	TAS2R16	taste receptor type 2 member 16
Gp4	E6	24	71	P2RY10	purinergic receptor P2Y G-protein coupled 10
Gp4	E8	21	64	MCHR1	melanin-concentrating hormone receptor 1
Gp4	E9	25	64	TAS2R60	taste receptor type 2 member 60
Gp4	E10	29	64	GPR6	G-protein coupled receptor 6
Gp4	F3	28	74	OPN5	opsin 5
Gp4	F4	25	66	BAI2	brain specific angiogenesis inhibitors 2
Gp4	F5	25	64	ADORA3	adenosine A3 receptor
Gp4	F6	20	49	TAS2R38	taste receptor type 2 member 38
Gp4	F8	27	93	GPR108	G-protein coupled receptor 108
Gp4	G2	28	72	NPFFR2	neuropeptide FF receptor 2
Gp4	G4	22	66	GPR50	G-protein coupled receptor 50

Gp4	G5	25	76	ADORA3	adenosine A3 receptor
Gp4	G8	21	72	OPN1MW	opsin 1 (cone pigments) medium-wave sensitive
Gp4	G9	26	79	CYSLTR1	cysteinyl leukotriene receptor 1
Gp4	H4	29	76	CCR10	chemokine (C-C motif) receptor 10
Plate ID	**Position**	**% Survival**	**% Control**	**Gene Name**	**Gene Description**
Gp5	B2	29	143	GPR109A	G-protein coupled receptor 109A
Gp5	B10	24	125	F2RL1	coagulation factor II (thrombin) receptor-like 1
Gp5	C6	29	82	GPR52	G-protein coupled receptor 52
Gp5	D8	31	81	GPR183	G-protein coupled receptor 183
Gp5	E2	24	73	GPR112	G-protein coupled receptor 112
Gp5	E8	26	65	OR1D2	olfactory receptor family 1 sub D member 2
Gp5	F7	19	54	GPR39	G-protein coupled receptor 39
Plate ID	**Position**	**% Survival**	**% Control**	**Gene Name**	**Gene Description**
Gp6	A2	26	69	OXER1	oxoeicosanoid (OXE) receptor 1
Gp6	B4	27	89	GPR142	G-protein coupled receptor 142
Gp6	B5	28	94	NPY1R	neuropeptide Y receptor Y1
Gp6	B7	29	68	GPR133	G-protein coupled receptor 133
Gp6	B11	30	102	OR6C2	olfactory receptor family 6
Gp6	C4	28	74	TFRC	transferrin receptor (p90, CD71)
Gp6	D6	24	78	SMO	smoothened homolog
Gp6	G10	30	79	CD200R1	CD200 receptor 1
Gp6	H3	31	99	OR51E2	olfactory receptor family 51 sub E member 2
Plate	**Position**	**%**	**%**	**Gene Name**	**Gene Description**

ID		Survival	Control		
Gp7	A8	19	133	OR52H1	olfactory receptor family 52 sub H member 1
Gp7	A9	21	124	APLNR	apelin receptor
Gp7	A10	20	126	GABBR1	gamma-aminobutyric acid (GABA) B receptor 1
Gp7	A11	21	141	GPRC6A	G-protein coupled family C grp 6 member A
Gp7	B6	20	81	GPR115	G protein coupled receptor 115
Gp7	B7	16	102	P2RY8	purinergic receptor P2Y G protein coupled 8
Gp7	B8	16	111	OR56B1	olfactory receptor family 56 sub B member 1
Gp7	B9	16	120	TAAR2	trace amine associated receptor 2
Gp7	B10	15	120	LGR5	leucine-rich repeat-containing GPCR 5
Gp7	B11	16	128	OR2D2	olfactory receptor family 2 sub D member 2
Gp7	C4	21	72	ADRA1D	adrenergic alpha 1D receptor
Gp7	C5	21	41	GPR174	G protein coupled receptor 174
Gp7	C6	17	93	RRH	retinal pigment epithelium-derived rhodopsin
Gp7	C7	16	86	CSAR1	complement component 5a receptor 1
Gp7	C8	17	82	CHRM2	cholinergic receptor muscarinic 2
Gp7	C9	15	93	GPR172B	G protein coupled receptor 172B
Gp7	C10	15	101	OR10H5	olfactory receptor family 10 sub H member 5
Gp7	C11	16	104	TAS2R5	taste receptor type 2 member 5
Gp7	D6	16	71	VN1R1	vomeronasal 1 receptor 1
Gp7	D7	16	74	GHRHR	growth hormone releasing hormone receptor
Gp7	D8	15	80	OR10H2	olfactory receptor family 10 sub H member 2
Gp7	D9	14	86	GPR83	G protein coupled receptor 83
Gp7	D10	14	81	OR56B4	olfactory receptor family 56 sub B member 4
Gp7	D11	17	98	PTGER1	prostaglandin E receptor 1 (subtype EP1) 42 kDa
Gp7	E3	25	71	TAS2R9	taste receptor type 2 member 9
Gp7	E7	16	79	TRIB3	tribbles homolog 3
Gp7	E8	16	78	GPR81	G protein coupled receptor 81

Gp7	E9	16	80	OPN3	opsin 3
Gp7	E10	17	89	GPR132	G protein coupled receptor 132
Gp7	E11	17	91	EDNRA	endothelin receptor type A
Gp7	F4	26	55	MRGPRX2	MAS related GPR member X2
Gp7	F5	21	50	CCBP2	chemokine binding protein 2
Gp7	F6	14	74	HRH1	histamine receptor H1
Gp7	F7	14	76	GPR179	G protein coupled receptor 179
Gp7	F8	15	82	S1PR2	sphingosine-1-phosphate receptor 2
Gp7	F9	16	77	OR2H1	olfactory receptor family 2 sub H member 1
Gp7	F10	15	83	ADRA2A	adrenergic alpha 2A receptor
Gp7	F11	17	87	OR1C1	olfactory receptor family 10 sub H member 2
Gp7	G6	17	82	P2RY1	purinergic receptor P2Y G protein coupled 1
Gp7	G7	16	88	HTR1D	5-hydroxytryptamine (serotonin) receptor 10
Gp7	G8	18	92	P2RY12	purinergic receptor P2Y G protein coupled 12
Gp7	G9	16	87	GIPR	gastric inhibitory polypeptiode receptor
Gp7	G10	16	88	ADRA2B	adrenergic alpha 2B receptor
Gp7	G11	17	98	GPR98	G protein coupled receptor 98
Gp7	H6	20	88	GPR107	G protein coupled receptor 107
Gp7	H7	21	84	TRHR	thyrotropin-releasing hormone receptor
Gp7	H8	20	97	PROKR1	prokineticin receptor 1
Gp7	H10	23	106	OR8B8	olfactory receptor family 8 sub B member 8
Gp7	H11	19	105	GRM1	glutamate receptor metabotropic 1
Plate ID	**Position**	**% Survival**	**% Control**	**Gene Name**	**Gene Description**
Kin1	B4	28	60	WEE1	Wee 1 homolog
Kin1	B7	30	61	PKMYT1	protein kinase, membrane associated tyr/thr I
Kin1	B9	29	57	TWF1	twinfilin, actin-binding protein homolog 1

Kin1	D5	22	26	MAST2	microtubule associated serine/threonine kinase 2
Kin1	F11	28	68	RPS6KA2	ribosomal protein S6 kinase, 90kDa poly 2
Kin1	G2	31	66	RIPK1	receptor (TNFRSF) interacting ser/thr kinase 1
Plate ID	**Position**	**% Survival**	**% Control**	**Gene Name**	**Gene Description**
Kin2	C2	23	84	CALM3	calmodulin 3 (phosphorylase kinase delta)
Kin2	C6	23	64	SKP2	S-phase kinase-associated protein 2 (p45)
Kin2	D2	29	46	CSNK2A1	casein kinase 2 alpha 1 polypeptide
Kin2	D5	26	56	MET	met proto-oncogene(hepatocyte GFR)
Kin2	E4	27	67	PRKCDBP	protein kinase C delta binding protein
Kin2	F9	31	86	IRAK4	interleukin-1 receptor associated kinase 4
Plate ID	**Position**	**% Survival**	**% Control**	**Gene Name**	**Gene Description**
Kin3					
Plate ID	**Position**	**% Survival**	**% Control**	**Gene Name**	**Gene Description**
Kin4	B2	20	28	PLK1	polo-like kinase 1
Kin4	B3	26	40	HK1	hexokinase 1
Kin4	B4	31	58	TYK2	tyrosine kinase 2
Kin4	B8	23	35	DYRK3	dual-specificity tyrosine-(Y)-phos reg kinase 3
Kin4	C2	28	63	PANK1	pantothenate kinase 1
Kin4	C5	24	42	PCTK3	PCTAIRE protein kinase 3
Kin4	C9	29	50	AK7	adenylate kinase 7

Kin4	D2	27	57	STRADB	STE20-related kinase adaptor beta
Kin4	D6	27	38	CAMK2B	calcium/calmodulin-dependent protein kin II beta
Kin4	D8	22	41	CIB3	calcium and integrin binding family member 3
Kin4	E4	30	48	PFKFB1	6-phosphofructo-2-kinase/fructose-2,6-biphos 1
Kin4	E8	31	53	PHKB	phosphorylase kinase beta
Kin4	F6	26	60	CINP	cyclin-dependent kinase 2-interacting protein
Kin4	F11	29	47	DYRK4	dual-specificity tyrosine-(Y)-phos reg kinase 4
Kin4	G6	26	56	TBK1	TANK binding kinase 1
Kin4	H3	25	55	DGKB	diacylglycerol kinase beta 90 kDa
Plate ID	**Position**	**% Survival**	**% Control**	**Gene Name**	**Gene Description**
Kin5	B3	23	58	PIK3R3	phosphoinositide-3-kinase reg subunit 3
Kin5	B4	30	62	GSK3A	glycogen synthase kinase 3 alpha
Kin5	B5	20	57	CDC2	cell division cycle 2, G1 to S and G2 to M
Kin5	B7	25	70	MAP4K3	mitogen-activated protein kin kin kin kin 3
Kin5	C3	27	66	MAP2K5	mitogen-activated protein kin kin 5
Kin5	C4	30	60	PKN3	protein kinase N3
Kin5	C7	30	37	DYRK1B	dual-specificity tyr-(Y)-phos reg kin 1B
Kin5	C9	29	51	NME5	non-metastatic cells 5
Kin5	D3	26	56	VRK3	vaccinia related kinase 3
Kin5	D5	27	59	CSNK2A2	casein kinase 2 alpha prime poly.
Kin5	D6	30	52	ROS1	c-ros oncogene 1 receptor tyr kinase
Kin5	D8	30	59	TRAF3IP3	TRAF3 interacting protein 3
Kin5	D9	29	65	NEK5	NIMA (never in mitosis gene a) related kinase 5
Kin5	D10	28	66	SRPK2	SFRS protein kinase 2
Kin5	E3	30	63	MARK4	MAO/microtubule affinity-reg kinase 4
Kin5	F2	23	64	PRKD2	protein kinase D2

Kin5	F5	29	55	ETNK2	ethanolamine kinase 2
Plate ID	**Position**	**% Survival**	**% Control**	**Gene Name**	**Gene Description**
Kin6	D4	24	51	AURKB	aurora kinase B
Plate ID	**Position**	**% Survival**	**% Control**	**Gene Name**	**Gene Description**
Kin7	A2	30	62	CDK5R2	cyclin dependent kin 5 reg subunit 2 (p39)
Kin7	B3	27	90	OXSR1	oxidative stress responsive 1
Kin7	B4	28	74	ALPK3	alpha-kinase 3
Kin7	B5	23	94	STK24	ser/thr kin 24 (STE20 homolog)
Kin7	B6	28	99	DGKQ	diacylglycerol kinase theta 110kDa
Kin7	B7	27	102	VRK1	vaccinia related kinase 1
Kin7	B8	29	76	ADCK2	aarF domain containing kinase 2
Kin7	C2	25	57	ZMYND8	zinc finger, MYND type containing 8
Kin7	C3	26	78	SPRYD3	SPRY domain containing 3
Kin7	C5	29	30	PKIG	protein kinase (cAMP-dep,catalytic) inh. Gamma
Kin7	D2	25	93	SGK1	serum/glucocorticoid regulated kinase 1
Kin7	D3	28	77	BAIAP2L1	BAI1-associated protein 2-like 1
Kin7	D4	28	54	MAP3K7IP1	mitogen-activated protein kin kin kin 7 int 1
Kin7	D5	28	79	CERKL	ceramide kinase like
Kin7	E2	24	70	PDXK	pyridoxal (vitamin B6) kinase
Kin7	E3	26	73	CDK10	cyclin dependent kin 10
Kin7	E4	20	82	DAPK1	death associated protein kinase 1
Kin7	E5	23	68	GUCY2C	guanylate cyclase 2
Kin7	E6	30	68	STK32B	ser/thr kinase 32B
Kin7	F3	25	83	WNK4	WNK lysine deficient protein kinase 4

Kin7	F4	22	68	NME6	non-metastatic cells 6
Kin7	F5	27	51	UCKL1	uridine-cytidine kinase 1-like-1
Kin7	G2	25	88	MAPKAPK3	mitogen activated protein kin act pro kin 3
Kin7	G3	22	77	PICK1	protein int with PRKCA1
Kin7	G5	27	104	SMG1	PI-3-kin SMG-1
Kin7	G8	28	52	ERBB3	v-erb-b2 viral oncogene homolog 3
Plate ID	**Position**	**% Survival**	**% Control**	**Gene Name**	**Gene Description**
Kin8	B3	23	86	PAK7	p21 (Cdc42/Ras) activated kinase 7
Kin8	B4	28	75	BLK	B lymphoid tyrosine kinase
Kin8	B5	30	53	FGFR1	fibroblast growth factor receptor 1
Kin8	B6	26	81	BMPR1A	bone morphogenetic protein receptor type IA
Kin8	B8	29	76	AKAP8	A kinase (PRKA) anchor protein 8
Kin8	B9	26	54	MYLK4	myosin light chain kinase family member 4
Kin8	C7	28	61	TTK	TTK protein kinase
Kin8	D2	26	79	R10K2	R10 kinase 2
Kin8	E2	29	58	MKNK1	MAP kinase inter. Ser/thr kin 1
Kin8	E8	27	56	SLK	STE20-like kinase
Kin8	F3	24	81	PIK3C2B	phosphoinositide-3-kin class 2 beta poly
Kin8	F5	27	65	PACSIN3	protein kin C and casein kin substrate neurons 3
Kin8	G6	28	61	SPEG	SPEG complex locus
Plate ID	**Position**	**% Survival**	**% Control**	**Gene Name**	**Gene Description**
Kin9	B6	28	74	SNF1LIK	SNF1-like kinase
Kin9	D4	29	58	STK33	serine/threonine kinase 33
Kin9	E2	28	79	PFKP	phosphofructokinase platelet
Kin9	E7	29	87	STK16	serine/threonine kinase 16

Kin9	F2	29	74	ITK	IL 2-inducible T-cell kinase
Kin9	F5	30	86	TYR03	TYR03 protein tyrosine kinase
Kin9	G2	30	76	MAG13	membrane associated guanylate kinase 3
Kin9	G4	30	70	ULK4	unc-51-like kinase 4
Kin9	G11	19	114	EPHA10	EPH receptor A10
Kin9	H3	23	75	CAMK1D	calcium/calmodulin dep. Protein kin ID
Kin9	H5	30	82	CKB	creatine kinase brain
Kin9	H11	23	172	SCYL3	SCY1-like 3
Plate ID	**Position**	**% Survival**	**% Control**	**Gene Name**	**Gene Description**
PhP1	C6	32	63	PPP1R3F	protein phosphatase 1 reg (inhibitor) subunit F
PhP1	D6	21	67	PPP2R5C	protein phosphatase 2, reg subunit B' gamma
PhP1	D7	31	59	PPP1R15A	protein phosphatase 1, reg (inhibitor) sub 15A
PhP1	E7	24	68	SGPP1	sphingosine-1-phosphate phosphatase 1
PhP1	G7	23	49	PPP2R3B	protein phosphatase 2 (formerly 2A) reg sub B"
Plate ID	**Position**	**% Survival**	**% Control**	**Gene Name**	**Gene Description**
PhP2	C3	28	39	PTPN6	protein tyr phosphatase non-receptor type 6
PhP2	F2	33	59	PTPRF	protein tyr phosphatase receptor type F
PhP2	F11	31	47	PTEN	phosphatase and tensin homolog

Supplemental Table A.2. List of potential synthetic lethal partners of PNKP identified through screening ordered alphabetically

Gene Name	A549δPNKP	A549-Scramble
ABCB5	30	77
ABCC13	29	66
ABCE1	26	64
ADAR	25	40
ADCK2	29	76
ADORA2A	30	97
ADORA3	25	64
ADORA3	25	76
ADRA1B	29	67
ADRA1D	21	72
ADRA2A	15	83
ADRA2B	16	88
ADRB3	25	50
AFM	28	52
AIP	31	50
AIPL1	25	59
AK7	29	50
AKAP8	29	76
ALDH7A1	29	54
ALOX5	28	47
ALPK3	28	74
AMIGO2	30	66
APEH	31	74
APLNR	21	124
APOC3	27	97
APP	30	70
APTX	30	72
AURKB	24	51
AVPR1A	30	87
BAI2	25	66
BAIAP2L1	28	77
BCAM	26	53
BCL2L13	27	86
BCL2L14	28	47
BLK	28	75
BMP3	26	40

BMPR1A	26	81
BPIL2	30	85
BTC	25	147
C12orf72	29	51
C1orf112	30	121
C2orf28	25	45
C2orf42	29	93
C8orf79	32	40
CACNG4	24	44
CALM3	23	84
CAMK1D	23	75
CAMK2B	27	38
CAPN3	27	72
CASR	30	90
CCBP2	21	50
CCHC	28	63
CCL22	23	52
CCNA1	23	52
CCR10	29	76
CCR2	25	76
CCT4	27	42
CD160	29	67
CD200R1	30	79
CD300LB	33	80
CD4	29	83
CD79A	29	87
CD80	23	57
CD8B	27	35
CDC2	20	57
CDK10	26	73
CDK5R2	30	62
CELSR1	23	67
CENPE	31	65
CERKL	28	79
CFLAR	28	58
CHRM2	17	82
CHRM4	28	86
CHRNG	28	59
CIB3	22	41
CINP	26	60
CKAP5	28	41

CKB	30	82
CLCN3	26	105
CLEC4A	28	69
COPB2	21	29
CPA5	27	74
CR1L	26	63
CSAR1	16	86
CSNK2A1	29	46
CSNK2A2	27	59
CXADR	31	104
CYLD	27	132
CYP2S1	25	99
CYP3A5	26	68
CYSLTR1	26	79
DAK	29	55
DAPK1	20	82
DGKB	25	55
DGKQ	28	99
DHRS1	29	31
DLAT	28	118
DUSP27	24	81
DYRK1B	30	37
DYRK3	23	35
DYRK4	29	47
ECE1	29	55
EDNRA	17	91
EFNA1	30	64
EIF2C4	26	67
EIF3C	31	70
EIF4A3	19	58
ELK1	29	48
EPHA10	19	114
ERBB3	28	52
ETNK2	29	55
EXO1	23	51
F13A1	30	105
F2RL1	24	125
FAM173B	31	43
FAM62A	30	66
FGFR1	30	53
FNDC3B	30	73

FOLR3	25	97
FPR2	23	42
FRAG1	30	89
GABBR1	20	126
GALNS	29	59
GALR2	31	76
GALR3	29	68
GGH	30	153
GHRHR	29	72
GHRHR	16	74
GHSR	22	75
GIPR	16	87
GNA12	28	93
GNA15	25	75
GNRH1	28	63
GNS	23	40
GPR107	20	88
GPR108	27	93
GPR109A	29	143
GPR112	24	73
GPR115	20	81
GPR12	22	106
GPR132	17	89
GPR133	29	68
GPR142	27	89
GPR158	26	76
GPR172B	28	102
GPR172B	15	93
GPR174	21	41
GPR179	14	76
GPR183	31	81
GPR32	28	103
GPR39	19	54
GPR44	28	103
GPR50	22	66
GPR52	29	82
GPR6	29	64
GPR61	28	67
GPR81	16	78
GPR83	14	86
GPR98	17	98

GPRC6A	21	141
GRIA4	25	60
GRM1	19	105
GSK3A	30	62
GTPBP4	30	69
GUCA1B	24	74
GUCY2C	23	68
GYPC	29	82
GZMH	32	65
HERPUD1	26	116
HEXB	25	81
HK1	26	40
HR	23	68
HRH1	14	74
HSD17B13	30	115
HSD17B3	29	52
HSP90B1	32	86
HTATIP2	29	41
HTR1D	16	88
IFNW1	28	58
IGSF10	30	153
IL11RA	30	71
IL16	28	61
IL17A	22	60
IL31RA	28	81
ING3	26	88
IRAK4	31	86
IRF2BP1	29	66
ITGB4	33	53
ITGB6	28	69
ITK	29	74
ITSN2	24	90
JMJD2A	30	54
JUP	24	129
KCNJ11	29	75
KCNJ12	25	54
KCNK17	27	65
KCNQ1	24	83
KCNT1	22	53
KDELR3	32	79
KIAA0317	31	63

KIAA0999	31	45
KIF11	18	30
KIF3A	22	53
KLK15	30	77
KLK4	31	105
LBR	22	49
LGR5	30	95
LGR5	15	120
LOC727811	29	85
MAG13	30	76
MAP2K5	27	66
MAP3K7IP1	28	54
MAP4K3	25	70
MAPKAPK3	25	88
MARCH2	25	139
MARK4	30	63
MAS1	28	63
MAS1L	29	71
MASP2	27	63
MAST2	22	26
MBL2	24	45
MC2R	31	55
MC5R	28	90
MCHR1	21	64
MDM2	27	84
MEFV	30	89
MET	26	56
MGC52282	30	67
MKNK1	29	58
MKRN2	28	76
MMP8	32	67
MRGPRD	22	101
MRGPRX2	26	55
MTA1	31	62
MTMR1	29	93
MYLK4	26	54
NEK5	29	65
NME5	29	51
NME6	22	68
NMUR2	25	59
NPFFR2	28	72

NPR3	29	84
NPY1R	28	94
NR1D2	25	112
NR2F1	25	66
NTSR1	27	63
OPN1MW	21	72
OPN3	16	80
OPN5	28	74
OR10H2	15	80
OR10H5	15	101
OR1C1	17	87
OR1D2	26	65
OR2D2	16	128
OR2H1	16	77
OR51E2	31	99
OR52H1	19	133
OR56B1	25	90
OR56B1	16	111
OR56B4	14	81
OR5P3	28	68
OR6C2	30	102
OR8B8	23	106
OR8G5	22	66
OXER1	26	69
OXSR1	27	90
P2RY1	17	82
P2RY10	24	71
P2RY12	18	92
P2RY8	16	102
PACSIN3	27	65
PAK7	23	86
PANK1	28	63
PCMTD2	26	74
PCSK2	26	55
PCTK3	24	42
PDXK	24	70
PFKFB1	30	48
PFKP	28	79
PGGT1B	18	88
PH-4	32	62
PHKB	31	53

PICK1	22	77
PIK3C2B	24	81
PIK3R3	23	58
PKIG	29	30
PKMYT1	30	61
PKN3	30	60
PLAT	26	66
PLK1	20	28
PNMT	32	111
POU3F4	30	68
PPP1R15A	31	59
PPP1R3F	32	63
PPP2R3B	23	49
PPP2R5C	21	67
PRKCDBP	27	67
PRKCSH	29	64
PRKD2	23	64
PROKR1	20	97
PSMD14	22	48
PSMD2	32	61
PTEN	31	47
PTGER1	17	98
PTPN6	28	39
PTPRF	33	59
R10K2	26	79
RAB41	33	54
RAB7B	29	111
RAD23B	30	67
RASSF5	26	77
RBM24	27	89
RBM8A	25	49
RGPD5	24	52
RGS12	29	86
RHBDF1	30	50
RIPK1	31	66
RNF141	29	75
ROS1	30	52
RPL36	17	73
RPL4	25	51
RPLP2	22	50
RPS27A	27	39

RPS6KA2	28	68
RPSA	28	62
RRH	17	93
S1PR2	15	82
SCH8A	22	52
SCYL3	23	172
SDCBP	26	61
SERPINA12	28	234
SGK1	25	93
SGPP1	24	68
SHH	28	75
SIM1	30	70
SKP2	23	64
SLC25A17	25	53
SLC39A6	25	56
SLC5A5	29	80
SLK	27	56
SMG1	27	104
SMO	24	78
SMPD1	27	58
SMUG1	30	74
SNF1LIK	28	74
SNX6	31	83
SPEG	28	61
SPRYD3	26	78
SPRYD5	28	87
SPRYD5	24	151
SRPK2	28	66
SSTR3	29	61
STAT2	24	62
STEAP4	27	41
STK16	29	87
STK24	23	94
STK32B	30	68
STK33	29	58
STRADB	27	57
TAAR1	31	96
TAAR2	16	120
TAAR9	25	66
TAF10	28	39
TAS2R16	25	72

TAS2R38	20	49
TAS2R43	28	62
TAS2R5	16	104
TAS2R60	25	64
TAS2R9	25	71
TBK1	26	56
TDG	27	83
TFRC	28	74
TGFB1	24	52
THRA	32	67
TICAM1	24	51
TNFSF12	29	98
TOB1	32	69
TPX2	32	78
TRAF3IP3	30	59
TRERF1	24	67
TREX1	25	97
TRHR	21	84
TRIB3	16	79
TRIM65	28	61
TRIP6	26	70
TTK	28	61
TWF1	29	57
TXNDC3	32	65
TXNL1	31	120
TYK2	31	58
TYR03	30	86
UBC	28	78
UCKL1	27	51
UHRF2	24	37
ULK4	30	70
UPF1	28	79
UQCRH	23	49
USP44	28	60
USP45	31	56
USP51	31	98
USP8	22	91
VN1R1	16	71
VRK1	27	102
VRK3	26	56
WEE1	28	60

WIPF2	23	48
WNK4	25	83
WNT1	28	93
WTAP	30	61
XPOT	25	90
ZMYND8	25	57
ZNF280A	29	70
ZNF335	29	53
Unidentified ORF	32	60
Unidentified ORF	24	117
Unidentified ORF	29	128
Unidentified ORF	28	125
Unidentified ORF	28	115
Unidentified ORF	24	115
Unidentified ORF	31	125
Unidentified ORF	25	109
Unidentified ORF	30	110
Unidentified ORF	27	120
Unidentified ORF	30	101
Unidentified ORF	24	99

Appendix B: Material and methods

B.1 Materials and methods

B.1.1 Cells

A549 (human lung carcinoma) and MCF7 (human breast adenocarcinoma) cell lines were obtained from the American Type Culture Collection (Manassas, VA). A549 parental, A549 stable protein knockdown, A549δPNKP with stable re-expression of various isoforms of PNKP, A549-Scramble control and MCF7δPNKP cell lines were generated as described in the "Stable Transfection" section. EM9 and H9T3-7-1 (EM9-XRCC1$^{+/+}$) (chinese hamster ovary) cells were obtained as a gift from Dr. Kerry Brookman. A549 expressing a dominant negative to DNA Polymerase β (PolβDN) and A549 vector only controls (A549-LZ) were obtained as a gift from Dr. Conchita Vens. M059J and M095K cell lines generated from the same glioblastoma, which are deficient and not deficient in DNA-PK activity, respectively, were obtained as a gift from Dr. Joan Turner. #22 (HCT116 PTEN$^{-/-}$), #35 (HCT116 PTEN$^{-/-}$), Neo124 (vector only control of HCT116, PTEN$^{+/+}$), HCT116 (PTEN$^{+/+}$) were obtained as a gift from the lab of Dr. Robert G. Bristow (University of Toronto). PC3 cells were obtained as a gift from Dr. Alan Ashworth (The Institute of Cancer Research, London, UK).

All cell lines described above and their transfected derivatives were cultured at 37°C and 5% CO_2 in a humidified incubator in a 1:1 mixture of Dulbecco's Modified Eagle's Medium and F12 (DMEM/F12) supplemented with 10% fetal bovine serum (FBS), L-glutamine (2 mM), non-essential amino acids (0.1 mM) and sodium pyruvate (1 mM). All culture

supplements were purchased from Invitrogen (Carlsbad, CA). For comet assays and apoptosis/necrosis detection penicillin (50 U/mL) and streptomycin (50 µg/mL) were added to the DMEM/F12 (complete DMEM/F12).

Karpas 299 and SUPM2 cells (obtained as a gift from Dr. M. Kadin, Boston, MA) were cultured in RPMI-1640 medium (Sigma-Aldrich, Oakville, ON) supplemented with 10% FBS, 0.3 g/L L-glutamine and 2 g/L $NaHCO_3$.

B.1.2 Plasmids for stable transfections

A549δPNKP, A549δSHP-1, A549-Scramble and MCF7δPNKP cell lines were generated by stable transfection of pSUPER.neo constructs (Oligoengine, Seattle, WA) into A549 or MCF7. An shRNA directed against nucleotides 1391-1410 of PNKP (Rasouli-Nia et al, 2004) was used to stably deplete PNKP in A549 and MCF7 cells (A549δPNKP and MCF7δPNKP, respectively), and another shRNA expression vector targeting nucleotides 1313-1333 of SHP-1 was used to generate A549δSHP-1 cells (Mereniuk et al, 2012). A control cell line was also generated in which an shRNA to no known gene target (a scrambled shRNA, pSUPER.neo.Mamm-X, Oligoengine) was expressed in A549 cells (A549-Scramble).

Using targeted mutation of PNKP cDNA using the following primers generated RNAi-resistant PNKP plasmids:

RNAi-resistant PNKP (mutating shRNA targeting sequence):

Forward 5' – CAACCGGTTTCGAGAAATGACCGATTCCTCTC ATATCCCCG-3'

Reverse 5' – CGGGGATATGAGAGGAATCGGTCATTTCTCGAAACCGGTTG-3'

Phosphatase active, kinase negative (K378A):

Forward – 5'-GGGATTCCCTGGGGCCGGGGCCTCCACCTTTCTCAAGAAGC-3'

Reverse – 5'-GGGATTCCCTGGGGCCGGGGCCTCCACCTTTCTCAAGAAGC-3'

Phosphatase negative, kinase active (D171A and D173A):

Forward – 5'-AAGGTGGCTGGCTTTAATCTGAACGGGACGCTCATCACC-3'

Reverse – 5'-GGTGATGAGCGTCCCGTTCAGATTAAAGCCAGCCACCTT-3'

Phosphatase negative and kinase negative PNKP was generated stepwise by first generating the RNAi-resistant PNKP, then mutation to generate kinase inactive PNKP, and finally mutation to generate both the kinase and phosphatase inactive PNKP.

The pBABE.puro vectors contained wildtype or mutated PTEN, as well as the one containing wildtype RAD51, were used to make the PC3 reconstituted cell lines; WT PTEN, p.K289E, p.R55fs*1, WT RAD51, p.BABE.puro and p.C124S.

WT PTEN –full length, wild-type PTEN cDNA

p.K289E – PTEN mutant with reduced nuclear shuttling cDNA

p.R55fs*1 – truncation mutant normally found in PC3 cDNA

WT RAD51 – full length, wild-type RAD51 cDNA

p.BABE.puro – vector only

p.C124S – phosphatase inactive PTEN mutant cDNA

*These plasmids were obtained as a gift from Dr. Alan Ashworth (Mendes-Pereira et al, 2009). The stable transfection protocol is described below.

B.1.3 Stable transfections

Approximately 20,000 cells were plated and allowed to adhere overnight in a 24-well dish at 37°C and 5% CO_2. The transfection mixture was prepared from two separate solutions, the first containing 1 µg of plasmid DNA dissolved in 50 µL total of Opti-MEM (Invitrogen), and the second 3 µL of Lipofectamine2000 (Invitrogen) in 50 µL total Opti-MEM. The two solutions were incubated at room temperature for 5 min before combination, mixed and then held at room temperature for 20 min. The media from the pre-plated cells was removed and the transfection mixture was added and the cells were incubated for 24 h at 37°C and 5% CO_2. The cells were then trypsinized and replated into 6 x 100-mm plates in DMEM/F12 without antibiotics and incubated overnight at 37°C and 5% CO_2. The following day, media was removed and replaced with complete DMEM/F12 containing 500 µg/mL G418 or 7 µg/mL puromycin. After single-clone colonies were formed (10-18 days) the colonies were picked and expanded prior to protein analysis.

B.1.4 Transient transfections

Approximately 4,000 cells were plated per well in a 96-well plate, and allowed 24 h to adhere in a humidified incubator at 37°C and 5% CO_2. All wells surrounding samples were filled with 100 µL distilled water to control for evaporation effects. For protocol optimization and initial verification of selected hits, 56 nM final concentration of siRNA was added to 50 µL total reaction volume in Opti-MEM (Invitrogen). At the same time as siRNA-Opti-MEM incubation, a 1:25 dilution of Dharmafect Transfection Reagent 1 (Dharmacon, Lafayette, CO) in Opti-MEM was allowed to incubate at room temperature for 5 min, to provide a final volume of 0.23 µL of transfection reagent per well. The two transfection solutions were then combined and held at room temperature for 20 min. The media was then removed from the cells and 100 µL of the transfection mixture was added per well and the plate was incubated at 37°C and 5% CO_2 for 72 h. For confirmatory and subsequent transient transfections, the above protocol was followed, however a final concentration of 16-20 nM of siRNA was used.

B.1.5 siRNA and shRNA Sequences

B.1.5.1 siRNA:

Protein	Target Sequence	Company	Catalog Number
ASN	Proprietary	Qiagen	SI1027281
PARP1	CCGAGAAATCTCTTACCTCAA	Qiagen	SI02662989
PNKP	CGGGAAGTCCACCTTTCTCAA	Ambion	4390817
PNKP #1	CACGTGTGAGACAGCCCTGAA	Qiagen	SI00095866
PNKP #2	CACGTGAACAGGGACACGCTA	Qiagen	SI00095893
PNKP #3	CAAGCTGGTGATCTTCACCAA	Qiagen	SI00095900
PNKP #4	CGGGAAGTCCACCTTTCTCAA	Qiagen	SI00095907
POLB #2	CCGGAGCGAATGAGGCCTGTA	Qiagen	SI00041398
POLB #5	CAAGATATTGTACTAAATGAA	Qiagen	SI02629228
POLB #7	TACGAGTTCATCCATCAATTT	Qiagen	SI2663605
POLB #8	CAGGTTGATACCCAAAGATCA	Qiagen	SI03072524
PTEN #3	ACGGGAAGACAAGTTCATGTA	Qiagen	SI00006909
PTEN #4	TCGGCTTCTCCTGAAAGGGAA	Qiagen	SI00006916
PTEN #6	AAGGCGTATACAGGAACAATA	Qiagen	SI00301504
PTEN #8	ATCGATAGCATTTGCAGTATA	Qiagen	SI03048178
SHP-1 #5	CCGGAACAAATGCGTCCCATA	Qiagen	SI2658726
SHP-1 #6	TAGGCCCTGATGAGAACGCTA	Qiagen	SI02658733
SHP-1 #10	CCGAGTGTTGGAACTGAACAA	Qiagen	SI04436831
SHP-1 #11	CAAGGAGGATGTGTATGAGAA	Qiagen	SI04950407

B.1.5.2 shRNA:

Target mRNA	Target Sequence	Company	Catalog Number
Scramble	Proprietary	OligoEngine	VEC-cntl-0002
PNKP	GATCCCAGAGATGACGGACTCCTCTTTCAAGAGAAGAGGAGTCCGTCATCTCTTTTTTA	OligoEngine	VEC-PBS-0004
SHP-1	GATCCCCCCGGAACAAATGCGTCCCATATTCAAGAGATATGGGACGCATTTGTTCCGGTTTTTA	OligoEngine	VEC-PBS-0004

B.1.6 Antibodies:

Antibody	Source	Poly-/Monoclonal	Company	Catalog Number
PARP-1	Mouse	Monoclonal	Abcam	ab18376
Polβ	Mouse	Monoclonal	Abcam	ab3181
Polβ	Mouse	Polyclonal	Abcam	ab2856
XRCC1	Mouse	Monoclonal	Abcam	ab1838
PARP-1	Rabbit	Polyclonal	Alexis Biochemicals	ALX-210-302
PTEN	Rabbit	Monoclonal	Cell Signaling Technology	9552
PTEN (138G6)	Rabbit	Monoclonal	Cell Signaling Technology	9559
PTEN (D4.3)	Rabbit	Monoclonal	Cell Signaling Technology	9188
SHP-1	Rabbit	Monoclonal	Cell Signaling Technology	3759
PNKP (122)	Rabbit	Polyclonal	Generated in-lab	
PNKP (H101)	Mouse	Monoclonal	Generated in-lab	
γH2AX	Mouse	Monoclonal	Millipore	05-636
XRCC1	Rabbit	Polyclonal	Santa Cruz Biotechnology Inc.	sc-11429

B.1.7 Commonly Used Buffer Recipes

- **DMEM/F12 Medium**
  - 0.6 g $NaHOC_3$ (or 8mL of 7.5% w/v solution)
  - 5 mL L-Glutamine (10x)
  - 5 mL MEM Non-Essential Amino Acids (10x)
  - 5 mL Sodium Pyruvate (10x)
  - 5 mL Penicillin and Streptomycin (10x)
  - 50 mL Fetal Calf Serum (FBS)

- **Freezing Medium:**
  - 95% DMEM/F12
  - 5% DMSO

- **SDS-PAGE (10% Resolving Gel)**
  - 2.5 mL 40% Acrylamide/Bis
  - 2.5 mL 1.5 M Tris-HCl, pH 8.8
  - 100 µL 10% SDS
  - 4.9 mL ddH_20
  - 5 µL TEMED
  - 50 µL 10% Ammonium Persulfate

- **SDS-PAGE (4% Stacking Gel)**
  - 250 µL 40% Acrylamide/Bis
  - 630 µL 0.5 M Tris-HCl, pH 6.8
  - 25 µL 10% SDS
  - 1.6 mL ddH_20
  - 2.5 µL TEMED
  - 15 µL 10% Ammonium Persulfate

- **1x Sample Buffer:**
  - 50 µL β-mercaptoethanol
  - 950 µL Lamelli Buffer

- **LB Broth:**
  - 10 g Bacto-Tryptone
  - 10 g NaCl
  - 5 g Bacto-Yeast Extract
  - 950 mL ddH_20
  - Raise pH to 7.00 with 1 tablet of NaOH

- **LB Broth from Pre-made Powder:**
  - 25 g of LB powder
  - 1 L of ddH_20
- **LB + Antibiotic Plates:**
  - 5 g NaCl

- 5 g Tryptone
- 5 g Yeast Extract
- 10 g Agar
- 500 mL ddH_20
- 1:1000 Antibiotics
- pH to 7.4

- **CHAPS Buffer:**
  - 0.5% CHAPS
  - 137 mM NaCl
  - 50 mM Tris-HCl pH 7.5
  - 1mM EDTA

- **10x PBS Buffer**
  - 10.9 g Na_2HPO_4
  - 3.2 g KH_2PO_4
  - 90 g NaCl
  - 1 L ddH_20
  - pH to 7.2 with NaOH

- **Crystal Violet Stain**
  - 2 g crystal violet powder
  - 125 mL glacial acetic acid
  - 375 mL methanol

- **Resazurin (Alamar Blue)**
  - 0.1 g Alamar Blue powder
  - 1 L ddH_20

B.1.8 Protein analysis

Approximately 10^7 stably or transiently transfected cells were washed twice with ice cold PBS, trypsinized, and spun down at 600 *g* for 10 min at 4°C. The supernatant was aspirated and the cell pellet was resuspended in 200 µL of CHAPS buffer (0.5% CHAPS, 137 mM NaCl, 50 mMTris-HCl, pH 7.5, and 1 mM EDTA) and rocked for 1 h at 4°C, after which cell debris was spun down at 17,500 *g* for 20 min at 4°C. Determination of whole cell lysate concentration was then conducted using the Bradford Assay (Bio-Rad, Hercules, CA).

Western blots were conducted using 50 µg of whole cell lysate. Monoclonal antibodies were incubated at a concentration of 1:1000 in 5% PBSMT (PBS with 5% w/v skim milk) overnight at 4°C. Polyclonal primary antibodies were incubated (1:4000 dilution) in 5% PBSMT for 1 h at room temperature (SantaCruz Biotechnology, Santa Cruz, CA). All secondary antibodies were incubated (1:5000 dilution) for 45 min at room temperature (Jackson ImmunoResearch Laboratories, Inc. West Grove, PA).

B.1.9 siRNA library screen

Qiagen's "Druggable" genome siRNA library is comprised of four sub-classifications: phosphatases, kinases, G-protein coupled receptors and uncategorized proteins consisting of 205, 696, 490 and 5570 mRNA targets, respectively. The library was first distributed into 89 x 96-well plates at a total siRNA concentration of 1 μM, each well containing a pool of four separate siRNAs to the same mRNA target. Also added to the plates were three additional control wells (C12, D12 and E12) of AllStars Negative (ASN) scrambled siRNA (Qiagen). Then, utilizing a JANUS Automated Workstation (PerkinElmer, Waltham, MA), 4,000 A549δPNKP or A549-Scramble cells were seeded into each well of a 96-well plate in a final volume of 100 μL DMEM/F12 without penicillin/streptomycin and allowed to adhere overnight in a humidified incubator. The following day, transfection mixture was generated as described above (56 nM siRNA and a total of 0.23 μL Dharmafect transfection reagent 1 per well), media was aspirated from the plates containing cells, and 100 μL of the mixture was added to each well and allowed to incubate for 72 h. Then 10% v/v of 440 μM Alamar Blue (Sigma-Aldrich, Oakville, ON) was added to each well and the cells were incubated for 50-90 min after which the fluorescence in each well was determined using an EnVision 2104 Multilabel Reader (PerkinElmer) with an excitation wavelength of 563 nm and emission wavelength of 587 nm (Schindler & Foley, 2010). Each screen was performed in duplicate.

Transient transfections of siRNAs for synthetic lethal partners were

used for confirmatory assays, however each siRNA was used independently and at a concentration of 20 nM. All other reagent concentrations remained constant. Each assay was performed manually and the fluorescence was read with a FLUOstar Optima® plate reader (BMG Labtec Inc. Durham, NC) using excitation and emission wavelengths of 563 and 587 nm, respectively.

B.1.10 Statistical analysis

R^2 values were generated in Microsoft Excel by plotting individual survival scores from the duplicate screen against one another. All p-values were generated using a two-sided Student's t-test. Z-scores were only generated for confirmatory data where an average from 23-96 individual wells of data per assay (performed at least in triplicate) were measured, allowing us an appropriate number of replicates to achieve robust statistical data. A Z-score is a dimensionless quantity representing a measurement of the number of standard deviations a sample is above or below the mean of a control. It is defined as:

$$z = \frac{x - \mu}{\sigma}$$

z = Z-score
x = the raw score to be standardized
μ = population mean
σ = standard deviation of the population

As such, Z-scores can be positive or negative depending on whether the sample is higher or lower than the mean of a control. For our results, we were interested in a negative Z-score as this showed that the survival of the experimental condition was lower than control (i.e. the condition was lethal). A sample with a Z-score of -3 or less is significantly different than control and is a threshold often used in synthetic lethal screens.

B.1.11 Cell proliferation assay with ALCL cell lines

Karpas 299, SUPM2 or Karpas 299 (SHP-$1^{+/+}$) cells were plated in 96-well format at a density of 5,000 cells/100 µL in complete RPMI. Increasing concentrations of the PNKP inhibitor A12B4C3 was added to each well in a constant volume of DMSO and left to incubate for 12-16 days. Eleven µL of 440 µM Alamar Blue was then added to each well and left to incubate for 24-48 h after which fluorescence was determined as described above.

A pCI expression vector (Promega, Madison, WI) was used to transiently re-express SHP-1 in Karpas 299 cells (Hegazy et al, 2010). The Karpas 299 cells were grown in antibiotic free RPMI after which 10^7 cells were harvested per transfection in 500 µL total volume of antibiotic free RPMI. These cells were placed into a 4-mm electroporation cuvette (VWR, Radnor, PA) along with 10 µg of plasmid DNA. The cells were then electroporated using a BTX ECM 300 square electroporator (BTX Technologies Inc., Holliston, MA) at 225 V for three pulses of 8.5 ms. After electroporation, the cells were transferred to 20 mL of antibiotic-free RPMI and incubated for 24 h before experimentation.

B.1.12 Determination of mode of cell death

A549-Scramble or A549δPNKPcells were grown on coverslips in complete DMEM/F12 and were either transfected with ASN or SHP-1 siRNA. As a positive control for apoptosis the cell lines were treated with 100 μM 5-(p-bromobenzylidine)-α-isopropyl-4-oxo-2-thioxo-3-thiozolidineacetic acid (BH3I-1, Sigma-Aldrich, Oakville, ON), which is a known apoptosis inducer. The cells were grown under each condition for the indicated length of time before being subjected to a triple stain of Hoechst 33342, Ethidium Homodimer III and Annexin V-FITC as described by the kit manufacturer (Biotium, Hayward, CA).

B.1.13 Single-cell gel electrophoresis

A549-Scramble, A549δPNKP and A549 cells stably depleted of SHP-1 (A549δSHP-1 cells) were grown to confluence in 60-mm plates in complete DMEM/F12. The cells were irradiated with 5 Gy (^{60}Co Gammacell; Atomic Energy of Canada Limited, Ottawa, Canada) and incubated at 37°C for 0, 2, 6, and 24 h for neutral comet assays and 0, 10, 30, 60 or 120 min for the alkaline comet assay. Controls were also included in which cells were not irradiated to give the baseline level of DNA damage present in each cell line. Double and single-strand breaks were then determined by single-cell gel electrophoresis. Cells at each time point were scraped and counted so that 10^5 cells were present on each comet slide. These cells were mixed into 0.1% molten low-melting-point agarose at 42^{o}C in a 1:10 ratio (10 µL cells per 100 µL agarose). 75 µL of the cell:agarose mixture was pipetted onto the comet slide (Trevigen, Gaithersburg, MD) and smoothed over using the side of the pipette tip so that the entire area was covered with agarose. The slides were then kept at 4^{o}C for at least 10 minutes to allow the agarose to solidify. The slides were then submersed in pre-chilled lysis buffer (2.5 M NaCl, 100 M Na_2·EDTA, 10 mM Tris base, 1% SDS, 1% Triton X-100, ph 10) and kept at 4^{o}C for 45 mins in the dark. Excess lysis buffer was then dabbed off the slides, which were then submerged in alkaline solution (200 mM NaOH, 1 mM Na_2·EDTA) for 45 mins at room temperature in the dark.

For the alkaline comet assay, the slides were then placed in an electrophoresis apparatus filled with fresh alkaline solution and run at 1

V/cm and ≈300 mA for 40 mins at 4^{o}C. For the neutral comet assay, the slides were rinsed in TBE after lysis 2X for 5 mins and then placed in an electrophoresis apparatus filled with fresh TBE and run at 1 V/cm and ≈300 mA for 40 mins.

The slides were then washed in 70% ethanol for 5 mins and left to dry overnight. The following morning, the DNA was stained with SYBR Green I (Molecular Probes) and viewed with an AxioScope 2 fluorescence microscope (Zeiss). For each time point, at minimum of 100 random cells were visually analyzed and categorized according to the National Institutes of Health LISTERV (Comet Assay Interest Groups web site; http://cometassay.com/introduction.htm).

B.1.14 γH2AX foci detection

We monitored the level of H2AX phosphorylation before and after γ-radiation as follows. 1 x 10^5 cells (A549-Scramble or A549δSHP-1) were seeded on coverslips in 35 mm dishes with 2 mL DMEM/F12 without antibiotics and left overnight to adhere in a humidified incubator. The dishes were then treated with 5 Gy γ-radiation and left to repair for the indicated time points. Cells were then fixed to the coverslips at room temperature in a 4% paraformaldehyde in PBS solution for 20 minutes. The coverslips were then rinsed with PBS one time and permeabilized in 0.5% Triton X-100 (Sigma-Aldrich) in PBS for 20 minutes at room temperature. The coverslips were then rinsed two times in PBS and incubated with anti-γH2AX primary antibody (Millipore, Billerica, MA) at a dilution of 1:1000 in PBS for 45 minutes at 4^{o}C. The coverslips were then rinsed three times, once in 0.1% Triton X-100:PBS and twice in PBS, respectively, and incubated with Alexa Fluor® 488 secondary antibody (Molecular Probes, Eugene, OR) at a dilution of 1:200 in PBS for 30 minutes at room temperature. The cells were again rinsed three times, once in 0.1% Triton X-100:PBS and twice in PBS, respectively, and mounted on slides with 1 mg/mL p-phenylenediamine and 1 μg/mL DAPI in 90% glycerol in PBS. Phosphorylated H2AX foci were then viewed with a LSM510 laser-scanning confocal microscope (Zeiss) and images were taken with a 20x objective lens using the same microscope settings for each slide. Fluorescence was normalized to background fluorescence and quantified in ImageJ. Error bars represent ± standard error of the mean.

B.1.15 Detection of reactive oxygen species (ROS)

The presence of hydroxyl radicals and peroxynitrite was detected using a commercial kit (Cell Technology, Mountain View, CA), which employs two dyes, aminophenyl fluorescein (APF) and hydroxyphenyl fluorescein (HPF), selective for the detection of these ROS. These dyes are normally non-fluorescent, however, when they encounter ROS, they exhibit fluorescence in a dose dependent manner. Cells were grown in 96-well format and transfected with either ASN or SHP-1 siRNA for 24 h prior to ROS detection. Cells were rinsed twice with modified Hanks balanced salt solution (HBSS) supplemented with 10 mM HEPES, 1 mM $MgCl_2$, 2 mM $CaCl_2$ and 2.7 mM glucose, after which APF or HPF, was diluted to 10 μM in the same modified HBSS and 100 mL applied to the cells for 45 min at 37°C in the dark. The plates were then read using a FLUOstar Optima® plate reader at an excitation wavelength of 488 nm and an emission wavelength of 515 nm. Fluorescence detection was then compared to controls to give the total increase in production of ROS under each condition.

B.1.16 Colony-forming assay

The effect of survival of simultaneous disruption of two proteins was conducted using the clonogenic survival assay. To allow cells time to adhere to the plates, cells were seeded 24 h in advance. Cells were treated with the PNKP inhibitor A12B4C3 for 9-14 consecutive days in triplicate at 0 μM, 0.1 μM, 1 μM, and 10 μM final concentration where 100 cells were plated for the 0 μM, 0.1 μM and 1 μM concentration groups and 300 cells in the 10 μM concentration group. Colonies were then stained with a crystal violet containing 20% methanol for one hour after which the plates were washed in warm water and left to dry overnight. Colonies of 50+ cells were then counted using an automated colony counter (Oxford Optronix, Oxford, UK).

For the indicated colony-forming assays, cells were treated with 0, 1, 2, 4, 6, or 8 Gy of γ-radiation (^{60}Co Gammacell; Atomic Energy of Canada Limited, Ottawa, Canada).

Cells were plated in a colony-forming assay in the presence of increasing concentrations of A12B4C3 with or without the ROS scavenger WR1065 (10 μM). Cells were subjected to these conditions continuously for 10-14 days after which plates were stained with crystal violet and counted. Colonies containing fewer than 30 cells were omitted.

B.1.17 Inhibitors

The PNKP inhibitor, A12B4C3 (2-(1-hydroxyundecyl)-1-(4-nitrophenylamino)-6-phenyl-6,7a-dihydro-1**H**-pyrrolo[3,4-**b**]pyridine-5,7(2**H**,4a**H**)-dione) was diluted to a stock concentration of 1 mM in DMSO. The PARP inhibitor DPQ (3,4-Dihydro-5[4-(1-piperindinyl)butoxy]-1(2H)-isoquinoline) was purchased from Calbiochem and diluted to a stock concentration of 1 mM in DMSO.

B.2 REFERENCES

Hegazy SA, Wang P, Anand M, Ingham RJ, Gelebart P, Lai R (2010) The tyrosine 343 residue of nucleophosmin (NPM)-anaplastic lymphoma kinase (ALK) is important for its interaction with SHP1, a cytoplasmic tyrosine phosphatase with tumour suppressor functions. *J Biol Chem* **285:** 19813-19820

Mendes-Pereira AM, Martin SA, Brough R, McCarthy A, Taylor JR, Kim JS, Waldman T, Lord CJ, Ashworth A (2009) Synthetic lethal targeting of PTEN mutant cells with PARP inhibitors. *EMBO Mol Med* **1:** 315-322

Mereniuk TR, Maranchuk RA, Schindler A, Penner JC, Freschauf GK, Hegazy SA, Lai R, Foley E, Weinfeld M (2012) Genetic screening for synthetic lethal partners of polynucleotide kinase/phosphatase: potential for targeting SHP-1 depleted cancers. *Cancer Research* **Submitted**

Rasouli-Nia A, Karimi-Busheri F, Weinfeld M (2004) Stable down-regulation of human polynucleotide kinase enhances spontaneous mutation frequency and sensitizes cells to genotoxic agents. *Proc Natl Acad Sci U S A* **101:** 6905-6910

Schindler A, Foley E (2010) A functional RNAi screen identifies hexokinase 1 as a modifier of type II apoptosis. *Cell Signal* **22:** 1330-1340